Armando E. Fraire • Philip T. Cagle • Richard S. Irwin •
Dina R. Mody • Armin Ernst • Shanda Blackmon •
Timothy C. Allen • Megan K. Dishop
Editors

Atlas of Neoplastic Pulmonary Disease

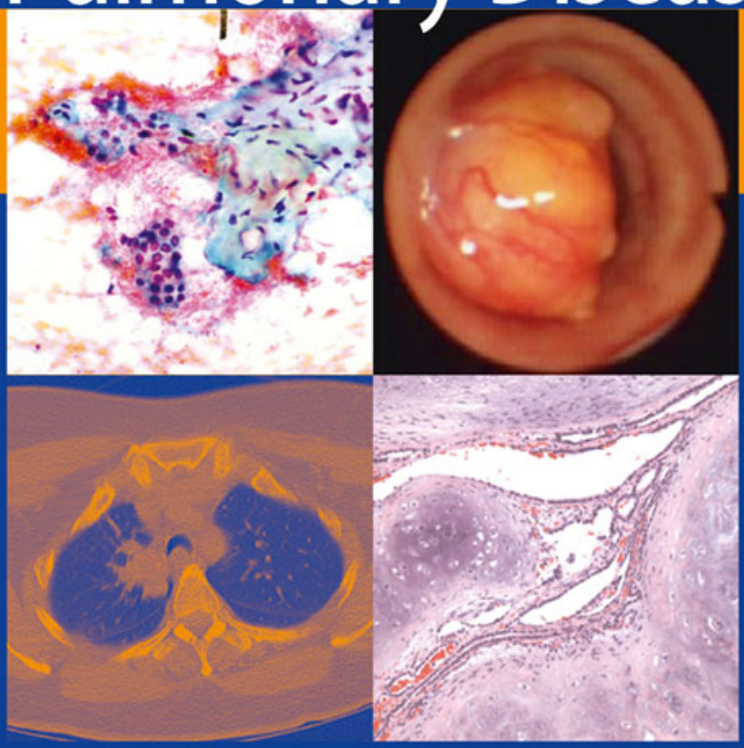

Pathology, Cytology, Endoscopy and Radiology

Springer

ATLAS OF NEOPLASTIC PULMONARY DISEASE

ATLAS OF NEOPLASTIC PULMONARY DISEASE

PATHOLOGY, CYTOLOGY, ENDOSCOPY AND RADIOLOGY

Armando E. Fraire

University of Massachusetts Medical School, Worcester, MA, USA

Philip T. Cagle

Weill Medical College, The Methodist Hospital, Cornell University, Houston, TX, USA

Richard S. Irwin

University of Massachusetts Medical School, Worcester, MA, USA

Dina R. Mody

Weill Medical College, The Methodist Hospital, Cornell University, Houston, TX, USA

Armin Ernst

Harvard Medical School, The Beth Israel Deaconess Medical Center, Boston, MA, USA

Shanda Blackmon

The Methodist Hospital, Houston, TX, USA

Timothy C. Allen

The University of Texas Health Science Center at Tyler, Tyler, TX, USA

Megan K. Dishop

Texas Children's Hospital, Houston, TX, USA

Springer

Editors
Armando E. Fraire
University of Massachusetts
Medical School
Worcester, MA, USA

Dina R. Mody
The Methodist Hospital/
Cornell University/
Weill Medical College
Houston, TX, USA

Timothy C. Allen
The University of Texas
Health Science Center at Tyler
Tyler, Texas, USA

Philip T. Cagle
The Methodist Hospital/
Cornell University/
Weill Medical College
Houston, TX, USA

Armin Ernst
The Beth Israel Deaconess Medical
Center and Harvard
Medical School
Boston, MA, USA

Megan K. Dishop
Texas Children's Hospital
Houston, TX, USA

Richard S. Irwin
University of Massachusetts
Medical School
Worcester, MA, USA

Shanda Blackmon
The Methodist Hospital
Houston, Texas, USA

ISBN 978-0-387-89838-4 e-ISBN 978-0-387-89839-1
DOI 10.1007/978-0-387-89839-1
Springer New York Dordrecht Heidelberg London

Library of Congress Control Number: 2009938107

Printed on acid-free paper

Springer is part of Springer Science+Business Media (www.springer.com)

DEDICATION

To: S. Donald Greenberg, MD

PREFACE

The diagnosis of lung cancer and benign pulmonary tumors can be challenging. This diagnosis can be facilitated by the study of images that allow recognition of patterns of disease, both at the clinical and pathologic levels. Conceptually defined, atlases are specialized books that rely heavily upon images to illustrate any subject matter. Fitting with such a concept, this atlas was developed to fill a void in the approach to diagnosis. In contrast to previous conventional atlases, this atlas is unique in that images from four major disciplines (endoscopy, radiology, histopathology, and cytopathology) involved in the study and diagnosis of lung tumors are brought together in a single volume.

In preparing this work, we had two objectives: (1) to illustrate the common while not ignoring the esoteric by recognizing the need to cover some entities that may only infrequently cross the paths of the practitioner; and (2) to provide a quick, reliable tool that may facilitate diagnosis through recognition of images using an interdisciplinary approach. To achieve these aims, we have selected and put forward images that in our opinion best represent the tumor entities. In some instances, we have recruited the collaboration and materials from other workers in the field.

The atlas is organized into 11 parts containing 41 chapters, closely following the 2004 Classification of Lung Tumors by the World Health Organization (WHO). Accordingly, the chapters represent a wide range of neoplastic lung entities. It begins with tumors of children followed by sections on benign epithelial tumors, salivary gland tumors, mesenchymal neoplasms, lymphoproliferative disorders, cardcinoid tumors, and a section of miscellaneous tumors. The atlas further includes a chapter on WHO-recognized variants of pre-invasive lung disease, major epithelial malignancies, and concludes with a chapter on metastatic lung tumors.

We hope and believe that our efforts during the preparation of this atlas have resulted in a useful, state-of-the-art work that will educate trainees and guide and support the best efforts of practitioners managing lung tumors.

Armando E.Fraire
Philip T. Cagle
Richard S. Irwin
Dina R. Mody
Armin Ernst
Shanda Blackmon
Timothy C. Allen
Megan K. Dishop

ACKNOWLEDGMENTS

We have been fortunate to be able to benefit from archival resources within our own institutions. Many fine individuals have made significant contributions to the writing and production of this atlas and deserve special recognition and thanks. First and foremost are Ms. Karen Balcius whose expert secretarial and administrative assistance helped to coordinate the transcription and organization of the text and Mr. Luigi Piarulli, Digital Multimedia Specialist who helped us to select, process, and reproduce virtually hundreds of endoscopic, radiographic, and histopathologic and cytopathologic images. Recognition is also due to Ms. Karen Barrel and Ms. Cynthia French for their administrative assistance helping us to coordinate our busy professional lives to allow us to make room for the substantial amount of time required to put in this atlas together.

Ms. Melissa Ramondetta, Springer's Executive Editor for Clinical Medicine, and her editorial assistants, Ms. Maureen Tobin and Ms. Dianne Wuori, were a great source of help and encouragement during all phases of the production process and to them we owe a debt of gratitude. Lastly, we are deeply grateful to our many extramural colleagues who contributed images to the various chapters and to the Springer copy editors for the outstanding job they have done editing this atlas.

WORLD HEALTH ORGANIZATION

HISTOLOGICAL CLASSIFICATION OF TUMOURS OF THE LUNG *

Malignant epithelial tumours

Squamous cell carcinoma
- Papillary
- Clear cell
- Small cell
- Basaloid

Small cell carcinoma
- Combined small cell carcinoma

Adenocarcinoma
- Adenocarcinoma, mixed subtype
- Acinar adenocarcinoma
- Papillary adenocarcinoma
- Bronchioloalveolar carcinoma
  - Nonmucinous
  - Mucinous
  - Mixed nonmucinous and mucinous
- Solid adenocarcinoma with mucin production
  - Fetal adenocarcinoma
  - Mucinous ("colloid") carcinoma
  - Mucinous cystadenocarcinoma
  - Signet ring adenocarcinoma
  - Clear cell adenocarcinoma

Large cell carcinoma
- Large cell neuroendocrine carcinoma
  - Combined large cell neuroendocrine carcinoma
- Basaloid carcinoma
- Lymphoepithelioma-like carcinoma
- Clear cell carcinoma
- Large cell carcinoma with rhabdoid phenotype

Adenosquamous carcinoma

Sarcomatoid carcinoma
- Pleomorphic carcinoma
- Spindle cell carcinoma
- Giant cell carcinoma
- Carcinosarcoma
- Pulmonary blastoma

Carcinoid tumours
- Typical carcinoid
- Atypical carcinoid

Salivary gland tumours
- Mucoepidermoid carcinoma
- Adenoid cystic carcinoma
- Epithelial-myoepithelial carcinoma

Preinvasive lesions
- Squamous carcinoma *in situ*
- Atypical adenomatous hyperplasia
- Diffuse idiopathic pulmonary neuroendocrine cell hyperplasia

Mesenchymal tumours
- Angiosarcoma
- Epithelioid haemangioendothelioma
- Pleuropulmonary blastoma
  - Chondroma
  - Congenital peribronchial myofibroblastic tumour
  - Diffuse pulmonary lymphangiomatosis
- Inflammatory myofibroblastic tumour
- Lymphangioleiomyomatosis
- Synovial sarcoma
  - Monophasic
  - Biphasic
- Pulmonary artery sarcoma
- Pulmonary vein sarcoma

Benign epithelial tumours

Papillomas
- Squamous cell papilloma
  - Exophytic
  - Inverted
- Glandular papilloma
- Mixed squamous cell and glandular papilloma

Adenomas
- Alveolar adenoma
- Papillary adenoma
- Adenomas of the salivary gland type
  - Mucous gland adenoma
  - Pleomorphic adenoma
  - Others
- Mucinous cystadenoma

Lymphoproliferative tumours

Marginal zone B-cell lymphoma (MALT type)
- Diffuse large B-cell lymphoma
- Lymphomatoid granulomatosis
- Langerhans cell histiocytosis

Miscellaneous tumours
- Hamartoma
- Sclerosing hemangioma
- Clear Cell tumour
- Germ cell tumours
  - Teratoma, mature
  - Immature
  - Other germ cell tumours
- Intrapulmonary thymoma
- Melanoma

Metastatic Tumours

* Modified from WHO Pathology and Genetics. Tumours of the Lung, Pleura, Thymus and Heart, WD Travis, E. Brambillla, H. Konrad Müller-Hermelink and CC Harris, IARC Press, Lyon, 2004

Contents

CONTRIBUTORS

Issam A. Al-Bozom, M.D. Hamad Medical Corporation, Doha, Qatar

Timothy C. Allen, M.D., J.D. The University of Texas Health Science Center at Tyler, Tyler, TX, USA

Shanda Blackmon, M.D. The Methodist Hospital, Houston, TX, USA

Philip T. Cagle, M.D. Weill Medical College, The Methodist Hospital, Cornell University, Houston, TX, USA

Alberto Cavazza, M.D. Ospedale Santa Maria Nova, Reggio Emilia, Italy

Shylashree Chikkamuniyappa, M.D. University of Texas Health Science Center at San Antonio, San Antonio, TX, USA

Thomas V. Colby, M.D. Mayo Clinic, Scottsdale, Scottsdale, AZ, USA

Megan K. Dishop, M.D. Texas Children's Hospital, Houston, TX, USA

Armin Ernst, M.D. Harvard Medical School, The Beth Israel Deaconess Medical Center, Boston, MA, USA

Carol F. Farver, M.D. The Cleveland Clinic, Cleveland, OH, USA

Armando E. Fraire, M.D. University of Massachusetts Medical School, Worcester, MA, USA

Ana Gimenez, M.D. Hospital de la Santa Creu, i Sant Pau, Barcelona, Spain

Takayuki Haga, M.D. National Highaski Saitama Hospital, Saitama, Japan

Josephine Heim-Hall, M.D. University of Texas Health Science Center at San Antonio, San Antonio, TX, USA

Elise R. Hoff, M.D. University of Pittsburgh Medical Center, Pittsburgh, PA, USA

Richard S. Irwin, M.D. University of Massachusetts Medical School, Worcester, MA, USA

Jaishree Jagirdar, M.D. University of Texas Health Science Center at San Antonio, San Antonio, TX, USA

Toshiaki Kawai, M.D. National Defense Medical College, Saitama, Japan

Keith M. Kerr, MB,ChB, FRCPath Aberdeen University Medical School, Aberdeen, Scotland, UK

Dina R. Mody, M.D. Weill Medical College, The Methodist Hospital, Cornell University, Houston, TX, USA

Nader Morad, M.D., Ph.D. University of Massachusetts Medical School, Worcester, MA, USA

William G. Morice II, M.D., Ph.D. Mayo Clinic Rochester, Rochester, MN, USA

Imaad Bin Mujeeb, M.D. Hamad Medical Corporation, Doha, Qatar

Hassan F. Nadrous, M.D. Critical Care Medicine, Knoxville, TN, USA

Kuniaki Nakanishi, M.D. National Defense Medical College, Saitama, Japan

N. Paul Ohori, M.D. University of Pittsburgh Medical Center, Pittsburgh, PA, USA

Yuichi Ozeki, M.D. National Defense Medical College, Saitama, Japan

Helmut H. Popper, M.D. University of Graz School of Medicine, Graz, Austria

Giulio Rossi, M.D. University de Modena e Reggio Emilia, Modena, Italy

Anjali Saqi, M.D. Columbia University, New York, NY, USA

Seikan Suzuki, Ph.D. Clinical Welfare College, Tokyo, Japan

Tetsu Tsukamoto, M.D. Ebetsu City Hospital, Ebetsu, Japan

CHAPTER 1

Lymphangiomatosis

Megan K. Dishop

Diffuse pulmonary lymphangiomatosis is a rare proliferative process involving pulmonary lymphatic channels, sometimes also involving adjacent mediastinal, retroperitoneal, and thoracic wall tissues. Lymphangiomatosis is typically a sporadic condition, without known familial or genetic predisposition. Age at presentation is most commonly in late childhood, but ranges from infancy to late adulthood. Diagnostic imaging shows diffuse interstitial infiltrates, thickened septal lines and fissures, pleural thickening, and pleural effusions.

Grossly, the pleura may appear opacified and/or fibrotic with accentuation and expansion of interlobular septa. Microscopically, there are increased numbers of endothelial-lined channels along lymphatic routes, expanding the bronchovascular bundles, interlobular septa, and pleura. The lymphatics are complex and anastomosing and vary from large gaping channels with focally muscularized walls to collapsed regions of spindled cells with compact slit-like spaces, the so-called kaposiform variant of lymphangiomatosis.

FIGURE 1.1 Lymphangiomatosis. Diagnostic imaging. **a** Chest X-ray of a 6-year-old boy shows increased septal lines. **b** Concurrent chest CT scan shows thickened interlobar fissures and prominent septal lines.

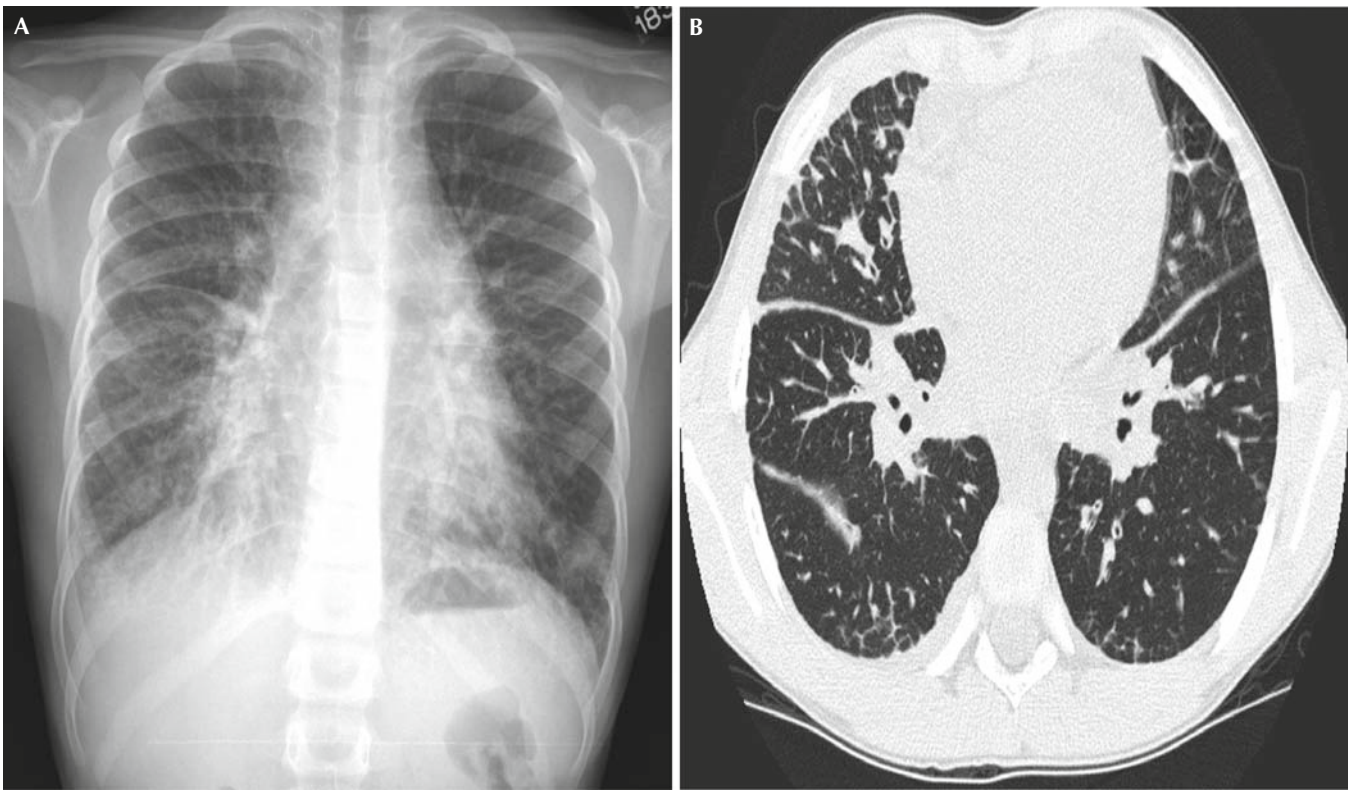

A.E. Fraire et al. (eds.), *Atlas of Neoplastic Pulmonary Disease*,
DOI 10.1007/978-0-387-89839-1_1, © Springer Science+Business Media, LLC 2010

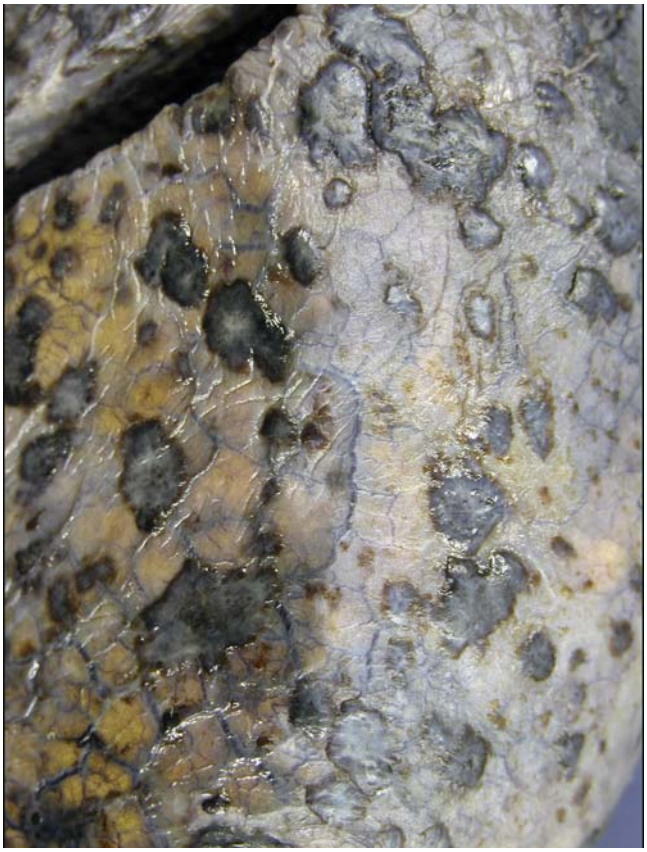

FIGURE 1.2 Lymphangiomatosis. Gross features. Autopsy examination at 8 years of age showed lungs with diffuse mild pleural thickening, accentuation of septal markings, congested vasculature, and scattered irregular dark gray hemorrhagic pleural plaques.

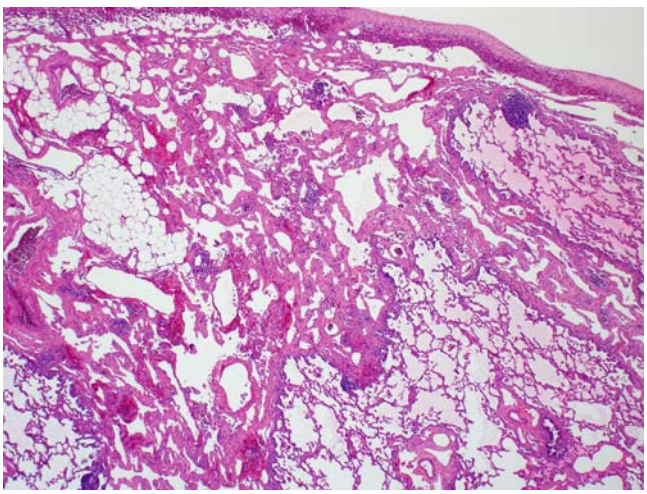

FIGURE 1.3 Lymphangiomatosis. Microscopic features. The peripheral lobules are surrounded by thickened septa and pleura, expanded by a proliferation of dilated lymphatic channels. Hematoxylin and eosin.

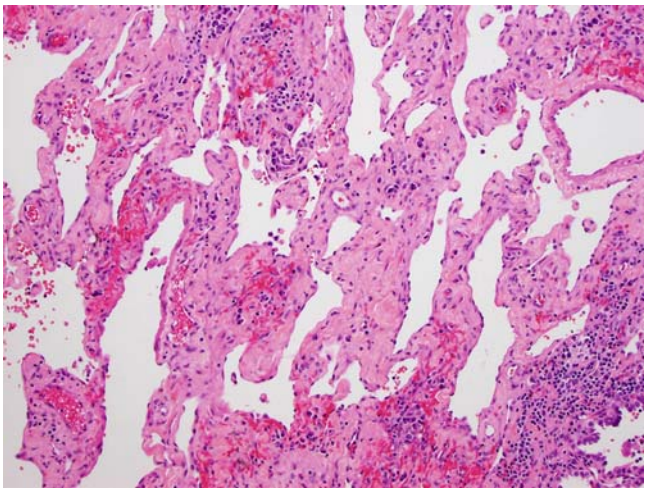

FIGURE 1.4 Lymphangiomatosis. Microscopic features. The lesion is primarily composed of dilated, branching, and anastomosing vascular channels separated by fibroconnective tissue and focally associated with lymphocytic infiltrates. Hematoxylin and eosin.

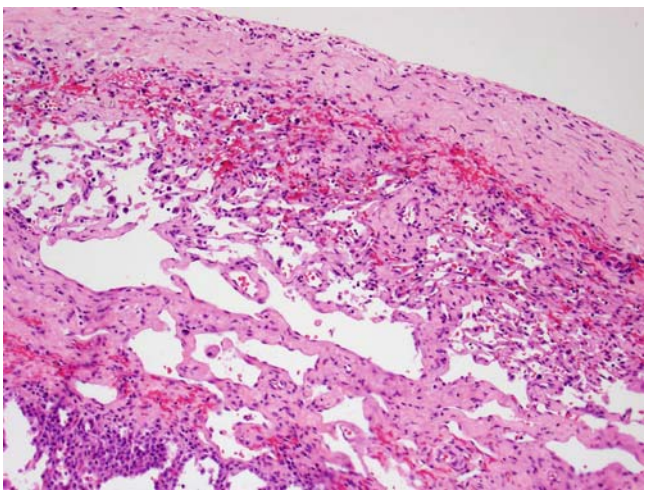

FIGURE 1.5 Lymphangiomatosis. Microscopic features. Hemorrhagic pleural plaques resulted from kaposiform areas of compact slit-like channels, lined by bland spindled cells and containing intraluminal red blood cells. Hematoxylin and eosin.

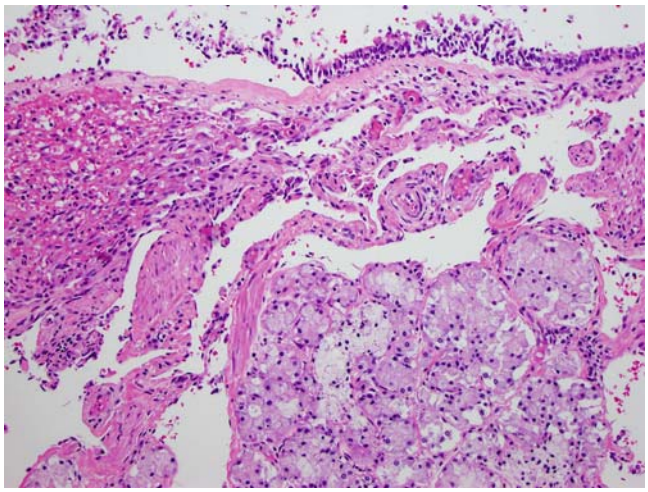

FIGURE 1.6 Lymphangiomatosis. Microscopic features. The lymphatic proliferation extended through the wall of the bronchi, surrounding infiltrating the submucosa and entrapping mucus glands. Hematoxylin and eosin.

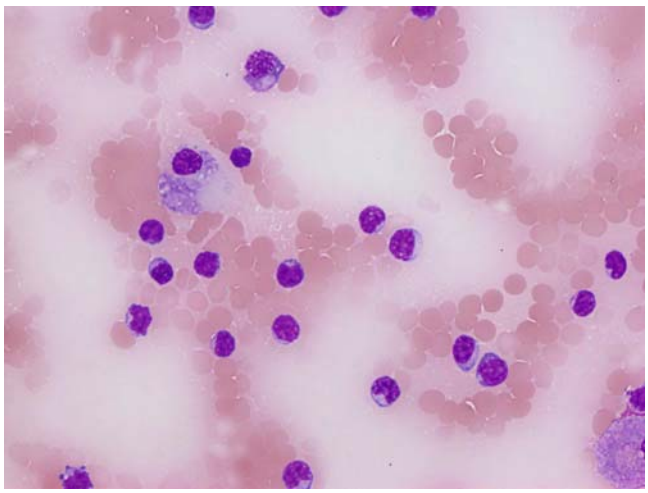

FIGURE 1.7 Lymphangiomatosis. Cytopathologic features. Pleural fluid cytology shows increased lymphocytes, with a background of erythrocytes in this case indicating a hemorrhagic effusion. Giemsa stain.

REFERENCES

- Alvarez OA, Kjellin I, Zuppan CW. Thoracic lymphangiomatosis in a child. *J Pediatr Hematol Oncol*. 2004;26:136–141.
- Faul JL, Berry GJ, Colby TV, et al. Thoracic lymphangiomas, lymphangiectasis, lymphangiomatosis and lymphatic dysplasia syndrome. *Am J Respir Crit Care Med*. 2000;161:1037–1046.
- Takahashi K, Takahashi H, Maeda K, et al. An adult case of lymphangiomatosis of the mediastinum, pulmonary interstitium and retroperitoneum complicated by chronic disseminated intravascular coagulation. *Eur Respir J*. 1995;8:1799–1802.
- Tamay Z, Saribeyoglu E, Ones U, et al. Diffuse thoracic lymphangiomatosis with disseminated intravascular coagulation in a child. *J Pediatr Hematol Oncol*. 2005;27:685–687.
- Tazelaar HD, Kerr D, Yousem SA, et al. Diffuse pulmonary lymphangiomatosis. *Hum Pathol*. 1993;24:1313–1322.

CHAPTER 2

Pleuropulmonary Blastoma

Megan K. Dishop

Although rare, pleuropulmonary blastoma (PPB) is the most common primary malignancy of the lung parenchyma in children. PPB has a spectrum of gross and microscopic morphology, from low-grade cystic lesions to high-grade solid forms. PPB is classified by gross features as type I (cystic), type II (solid and cystic), and type III (solid). PPB is distinguished from adult-type pulmonary blastoma by the absence of malignant epithelial components. The clinical suspicion of malignancy at the time of surgery is often low, as these lesions mimic congenital pulmonary airway malformation by both diagnostic imaging and gross examination.

The International Pleuropulmonary Blastoma Registry (http://www.ppbregistry.org) provides an invaluable resource for physicians, patients, and affected families by providing diagnostic support, therapeutic guidelines, and outcome data for this very rare tumor.

FIGURE 2.1 Pleuropulmonary blastoma, type I. Diagnostic imaging. Lateral chest X-ray shows a circumscribed cystic lesion in the left upper lung field.

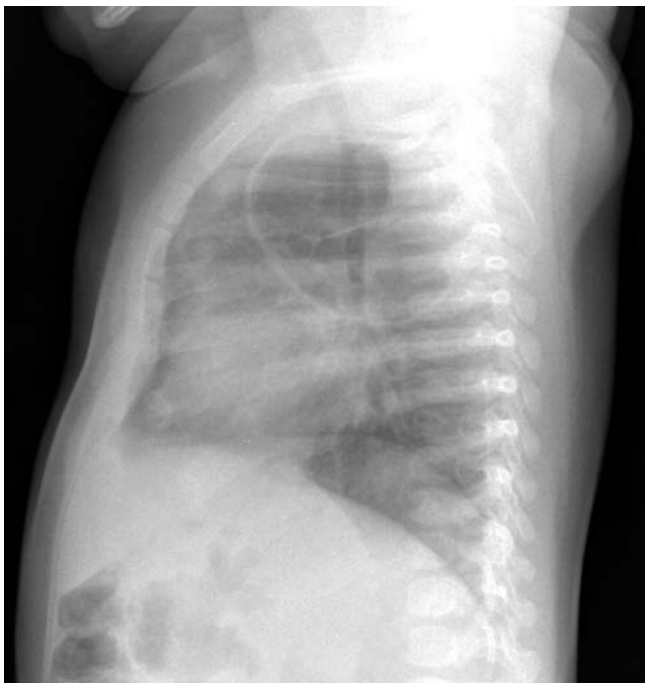

FIGURE 2.2 Pleuropulmonary blastoma, type I. Diagnostic imaging. A CT scan of the chest confirms a left upper lobe circumscribed cystic lesion with a few internal septa.

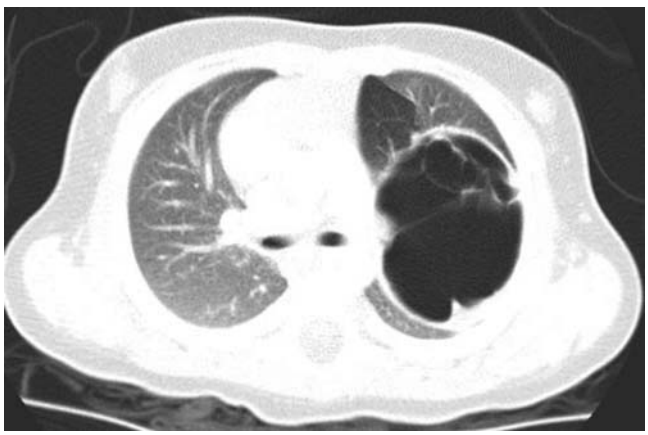

A.E. Fraire et al. (eds.), *Atlas of Neoplastic Pulmonary Disease*,
DOI 10.1007/978-0-387-89839-1_2, © Springer Science+Business Media, LLC 2010

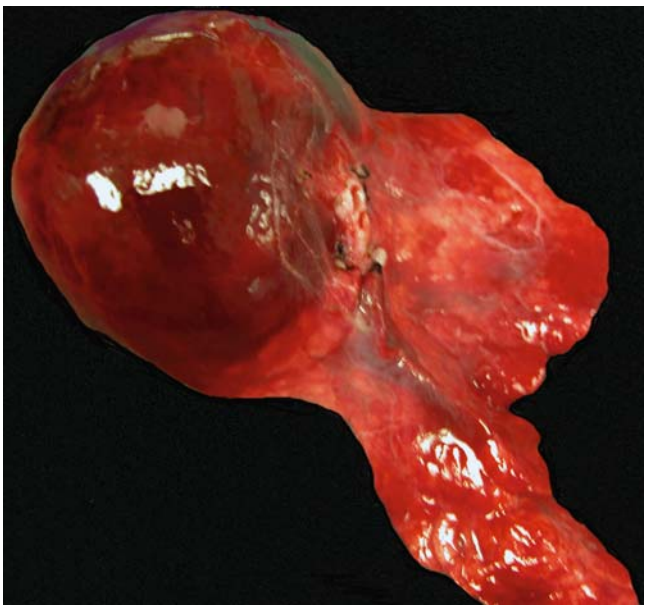

FIGURE 2.3 Pleuropulmonary blastoma, type I. Gross features. Left upper lobectomy specimen. Note large hemorrhagic cystic mass with a smooth shiny outer surface. The mass distends the pleural surface.

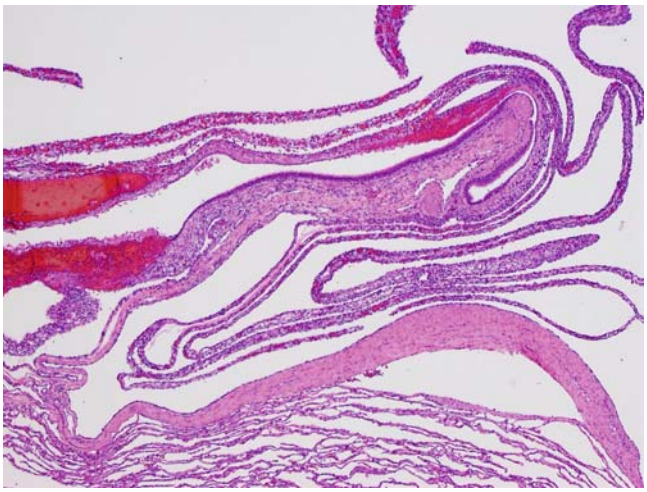

FIGURE 2.4 Pleuropulmonary blastoma, type I. Microscopic features. This low-grade cystic type of pleuropulmonary blastoma is composed of thick and thin septa lined by alveolar-type epithelium in some areas and columnar respiratory epithelium in other areas. The interface with normal lung is sharp in this example. Hematoxylin and eosin.

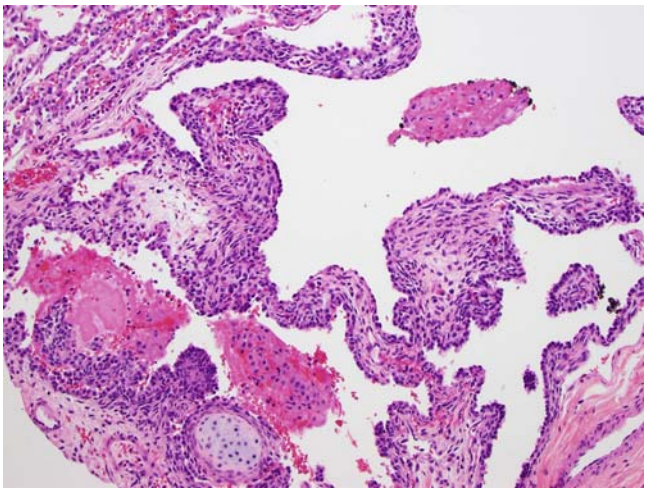

FIGURE 2.5 Pleuropulmonary blastoma, type I microscopic features. Note hypercellular zones of primitive-appearing cells forming a cambium-like layer with fibrous septa. Occasional nodules of immature or mature cartilage are evident. Hematoxylin and eosin.

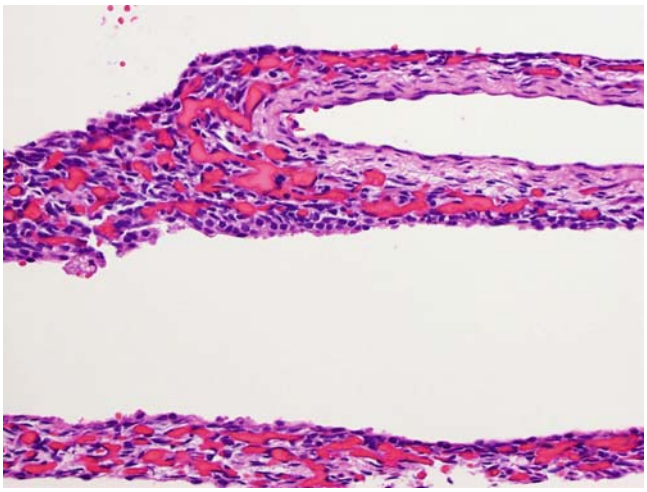

FIGURE 2.6 Pleuropulmonary blastoma, type I. Microscopic features. The hypercellular septa often have a rich capillary network. Hematoxylin and eosin.

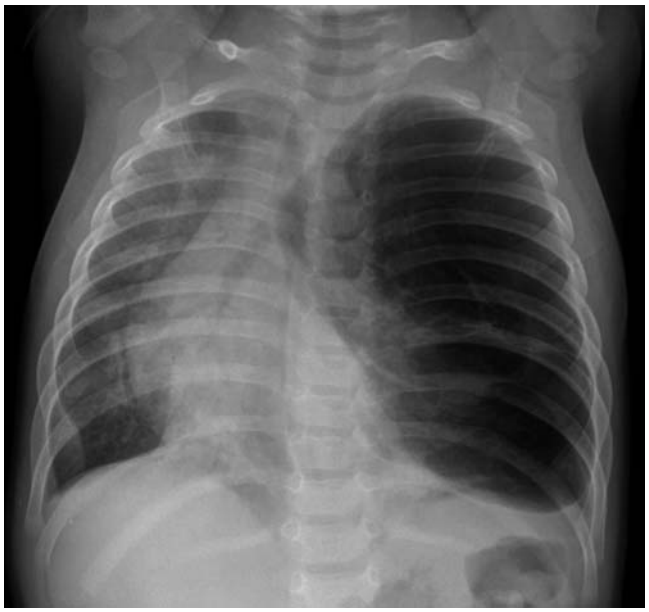

FIGURE 2.7 Pleuropulmonary blastoma, type I. Diagnostic imaging. Chest X-ray shows a large cystic lesion in the left lung field, crossing midline with associated mediastinal shift and tracheal deviation.

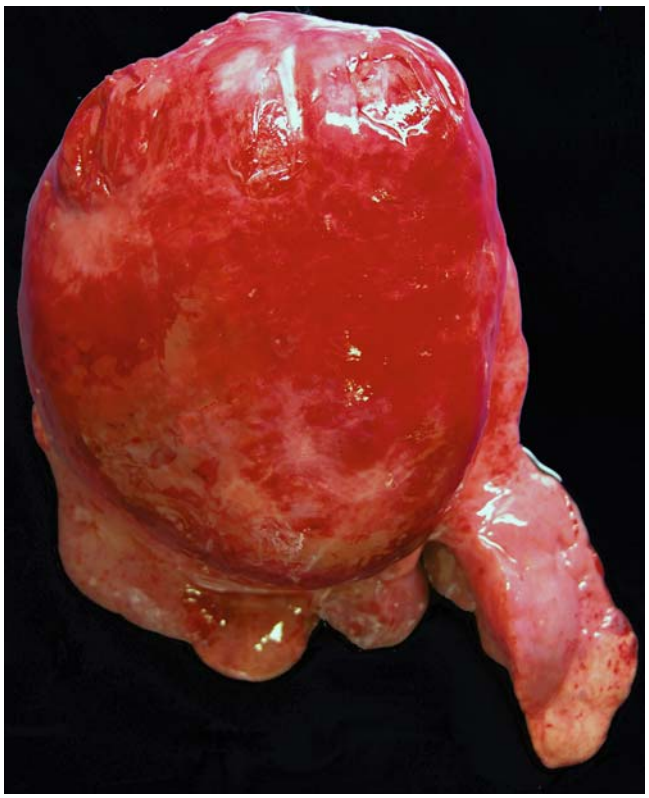

FIGURE 2.8 Pleuropulmonary blastoma, type I. Gross features. This left upper lobectomy specimen shows a large circumscribed mass distending the pleura.

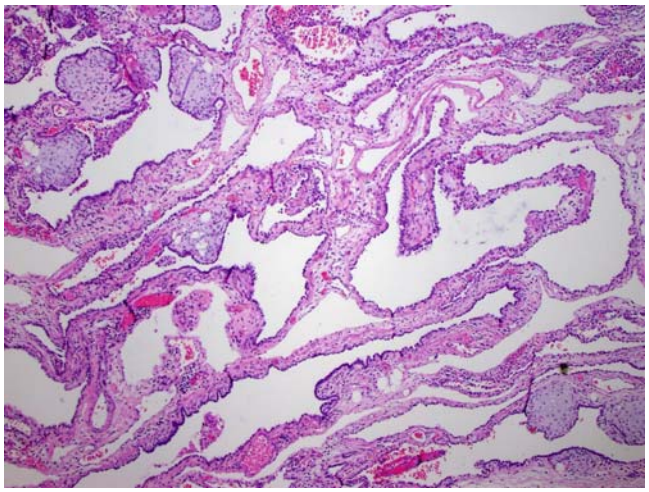

FIGURE 2.9 Pleuropulmonary blastoma, type I. Microscopic features. This lesion shows relatively small cystic spaces surrounded by connective tissue septa lined by both alveolar-type and respiratory-type epithelium. Despite low cellularity overall, the scattered irregular chondroid nodules provide an important clue to the diagnosis of PPB. Hematoxylin and eosin.

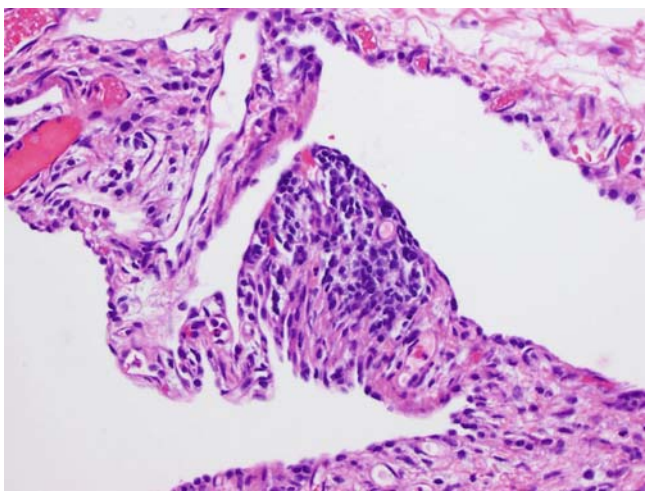

FIGURE 2.10 Pleuropulmonary blastoma, type I. Microscopic features. Extensive search allows identification of rare foci of hyperchromatic primitive-looking cells within the lesion. Hematoxylin and eosin.

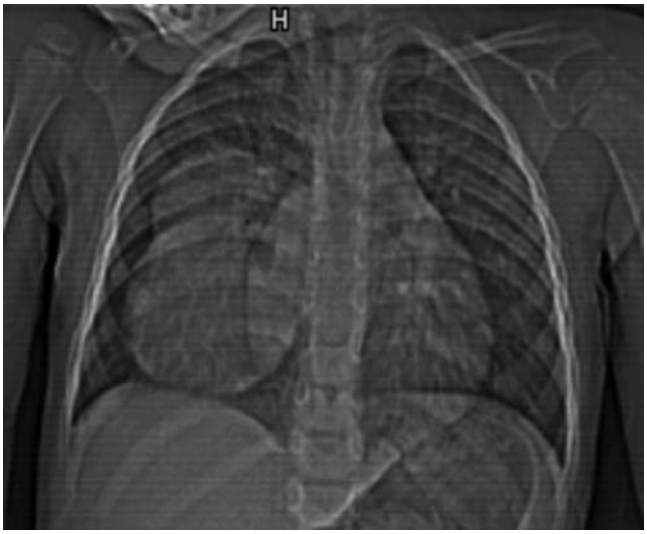

FIGURE 2.11 Pleuropulmonary blastoma, type II. Diagnostic imaging. Scout image from a chest CT of a 3-year-old girl shows a large mass in the right hemithorax. This lesion was recurrent following prior resection of a "congenital cyst" (Courtesy of Dr. L. Samayoa, University of Kentucky, Lexington, KY).

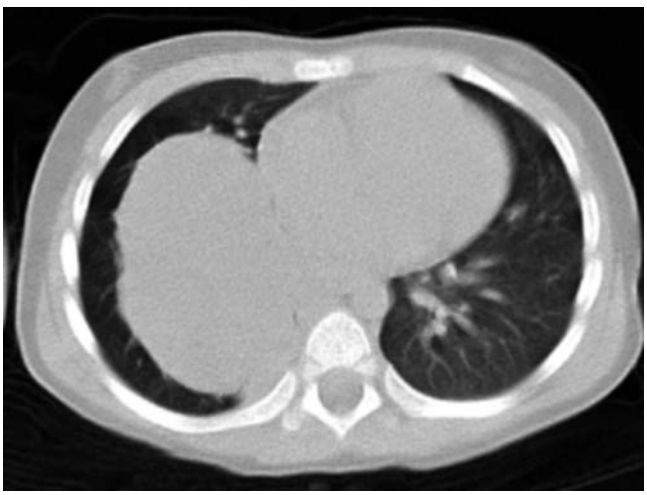

FIGURE 2.12 Pleuropulmonary blastoma, type II. Diagnostic imaging. CT scan of chest. Axial image showing a predominantly solid mass in the right lower hemithorax (Courtesy of Dr. L. Samayoa, University of Kentucky, Lexington, KY).

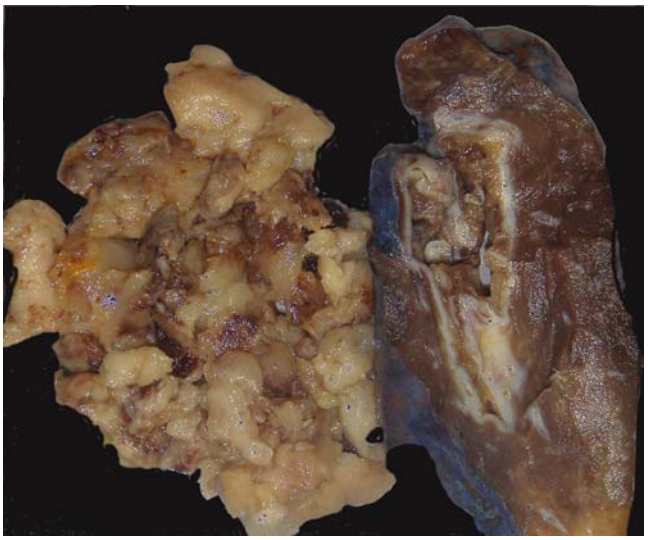

FIGURE 2.13 Pleuropulmonary blastoma, type II. Gross features. Note yellow gray disrupted tumor tissue in both solid and cystic areas. (Courtesy of Dr. L. Samayoa, University of Kentucky, Lexington, KY)

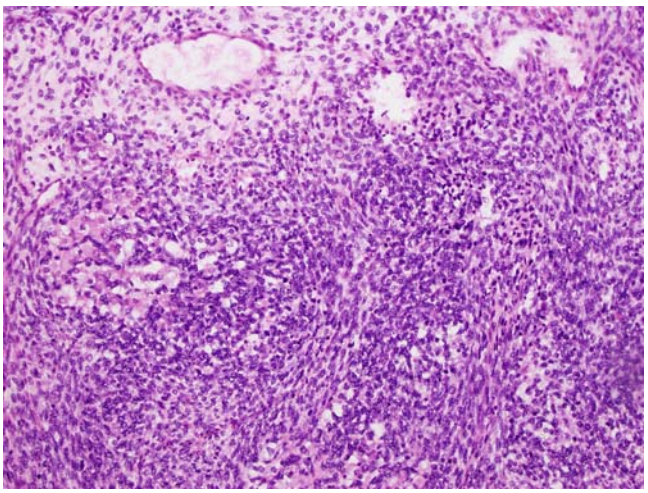

FIGURE 2.14 Pleuropulmonary blastoma, type II. Microscopic features. The solid components in this high-grade pleuropulmonary blastoma consist of compact sheets of small cells with other areas of loose myxoid tissue. Hematoxylin and eosin.

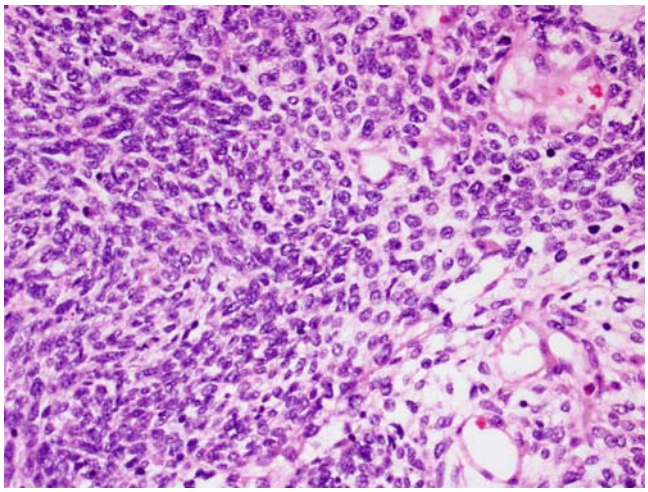

FIGURE 2.15 Pleuropulmonary blastoma, type II. Closer view of microscopic features. In this area, the tumor cells are small and round to spindled with minimal cytoplasm. Hematoxylin and eosin.

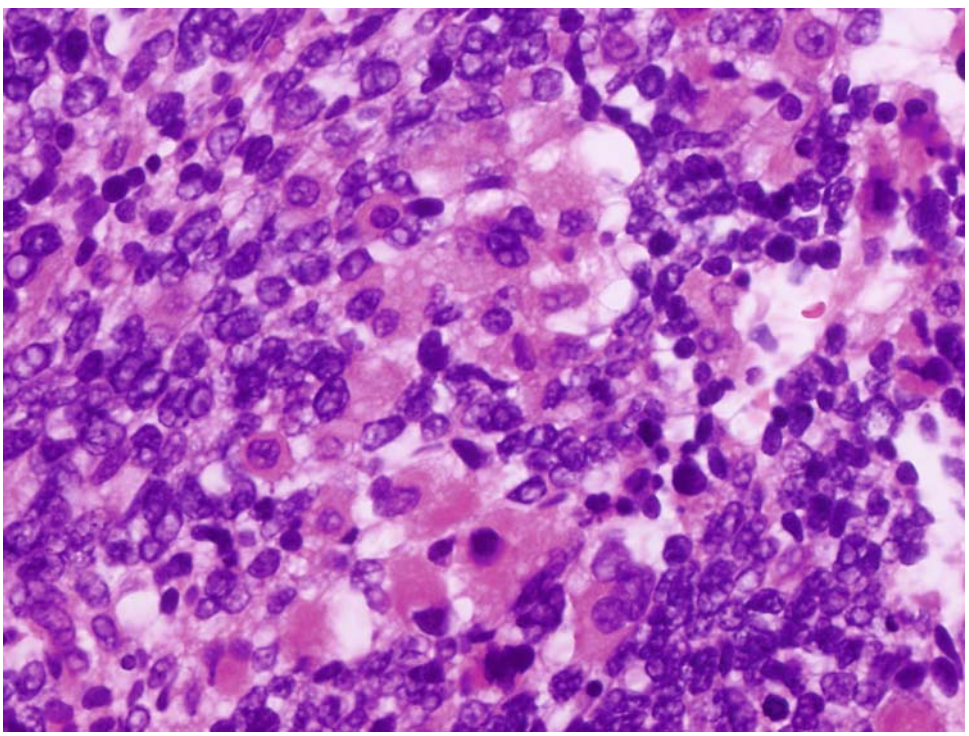

FIGURE 2.16 Pleuropulmonary blastoma, type II. Further closer view of microscopic features. Focal rhabdomyoblast differentiation is a common feature of type II and type III pleuropulmonary blastoma. Hematoxylin and eosin.

REFERENCES

- Boman F, Hill DA, Williams GM, et al. Familial association of pleuropulmonary blastoma with cystic nephroma and other renal tumors: a report from the International Pleuropulmonary Blastoma Registry. *J Pediatr.* 2006;149:850–854.
- Dehner LP, Watterson J, Priest J. Pleuropulmonary blastoma: a unique intrathoracic pulmonary neoplasm of childhood. *Perspect Pediatr Pathol.* 1995;18: 214–226.
- Hill DA, Jarzembowski JA, Priest JR, et al. Type I pleuropulmonary blastoma: Pathology and biology study of 51 cases from the International Pleuropulmonary Blastoma Registry. *Am J Surg Pathol.* 2008;32:282–295.
- Priest JR, Watterson J, Strong L, et al. Pleuropulmonary blastoma: a marker for familial disease. *J Pediatr.* 1996;128:220–224.

CHAPTER 3

Congenital Pulmonary Myofibroblastic Tumor

Megan K. Dishop

Congenital pulmonary myofibroblastic tumor (CPMT) is a very rare benign lung tumor occurring in fetuses and neonates. It typically results in intrauterine fetal demise, hydrops fetalis, or severe respiratory distress at birth. Approximately 10 cases of CPMT have been described in the literature, including cases reported under names such as "bronchopulmonary leiomyosarcoma," "bronchopulmonary fibrosarcoma," and "congenital fibroleiomyosarcoma." The tumor is thought to arise from the pluripotent peribronchial mesenchyme, a precursor to the myofibroblastic phenotype. On chest radiograph, a mass lung lesion causing flattening of the diaphragm and medistinal shift may be seen.

Microscopically, this distinctive tumor is composed of interlacing fascicles of bland spindled cells, surrounding normal lobules of alveolated parenchyma and extending along bronchovascular bundles, interlobular septa, and the pleura. The bronchial cartilage plates entrapped within the spindle cell proliferation are distorted with irregular, enlarged, and elongated forms, a feature which has been described as "cartilaginous metaplasia." The spindled cells have uniform bland cytology with elongated tapered nuclei and eosinophilic fibrillar cytoplasm.

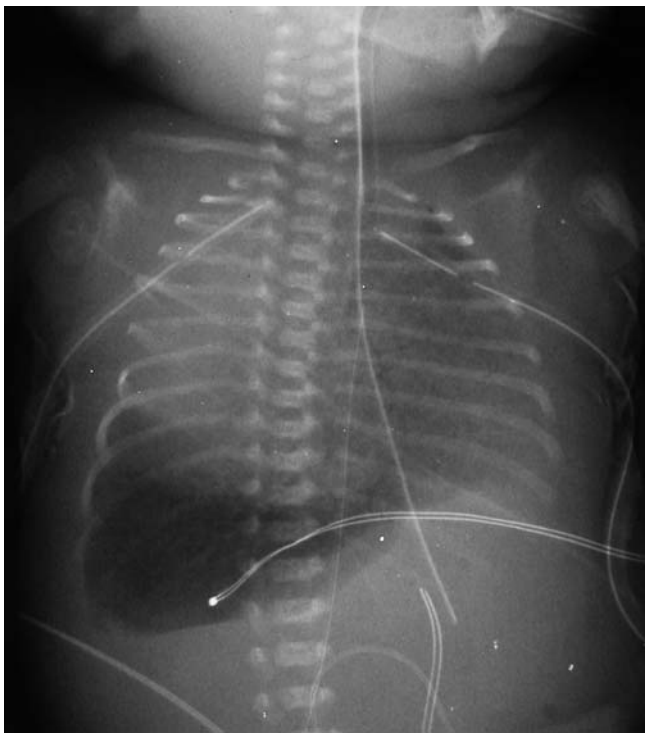

FIGURE 3.1 Congenital pulmonary myofibroblastic tumor. Chest X-ray. This neonate was delivered at 28 weeks gestation and found to have hydrops and respiratory distress at birth. Chest X-ray showed a large mass in the right upper lung field, causing flattening of the right diaphragm, mediastinal shift, and displacement of the heart. He had rapid deterioration despite ventilatory support and died less than 24 h after delivery (Courtesy of Dr. S. Galatzan, Doctors Regional Medical Center, Corpus Christi, TX).

A.E. Fraire et al. (eds.), *Atlas of Neoplastic Pulmonary Disease*,
DOI 10.1007/978-0-387-89839-1_3,

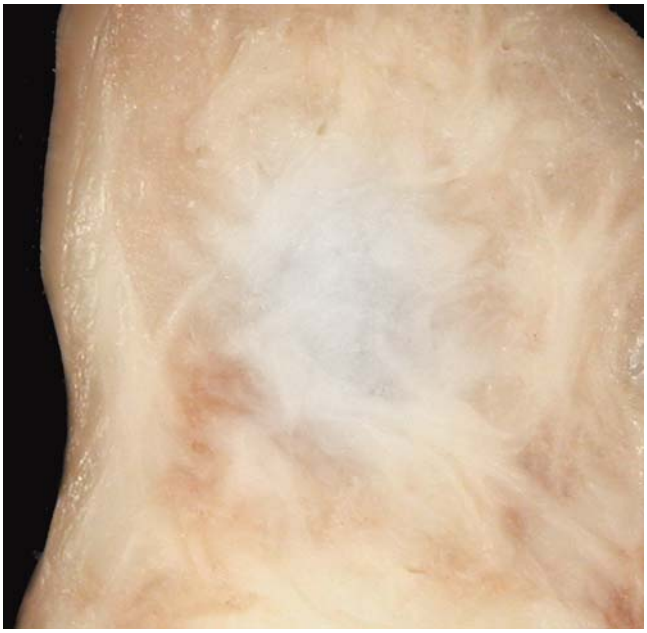

FIGURE 3.2 Congenital pulmonary myofibroblastic tumor. Gross features. At autopsy, cut section of the right lung mass revealed firm pale tan to light brown tissue with a vaguely whorled pattern.

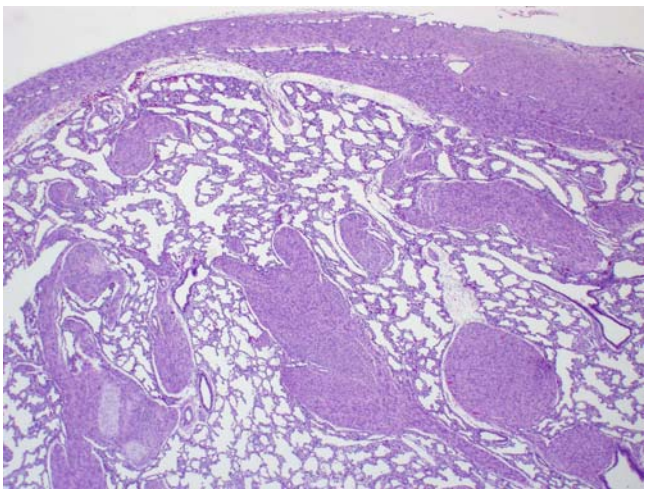

FIGURE 3.3 Congenital pulmonary myofibroblastic tumor. Microscopic features. The tumor is composed of broad bundles and fascicles of bland spindled cells, extending along bronchovascular regions, interlobular septa, and the pleural surface. Hematoxylin and eosin.

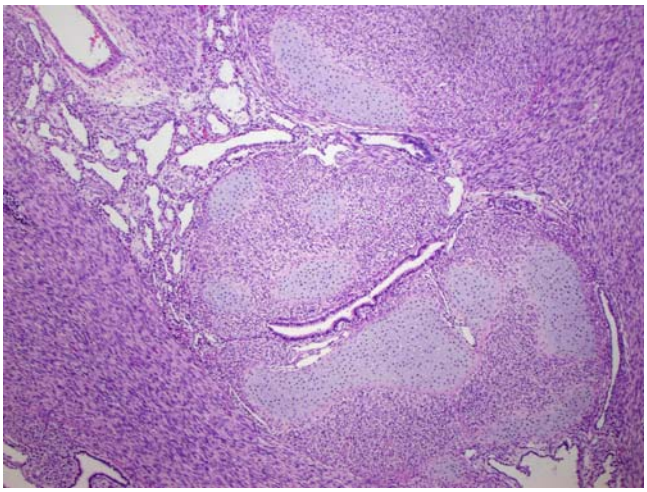

FIGURE 3.4 Congenital pulmonary myofibroblastic tumor. Microscopoic features. Airway contours are distorted and in some areas show irregular proliferation of entrapped cartilage plates. Hematoxylin and eosin.

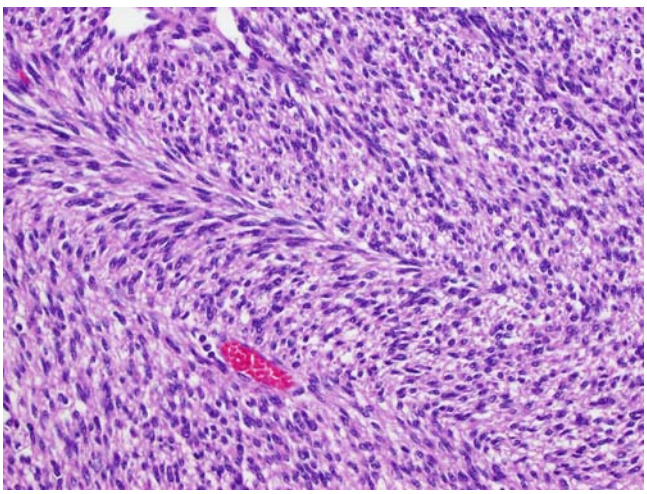

FIGURE 3.5 Congenital pulmonary myofibroblastic tumor. Microscopic features. The tumor shows focal areas with bland fascicles of uniform-looking spindle cells with a herringbone pattern. Hematoxylin and eosin.

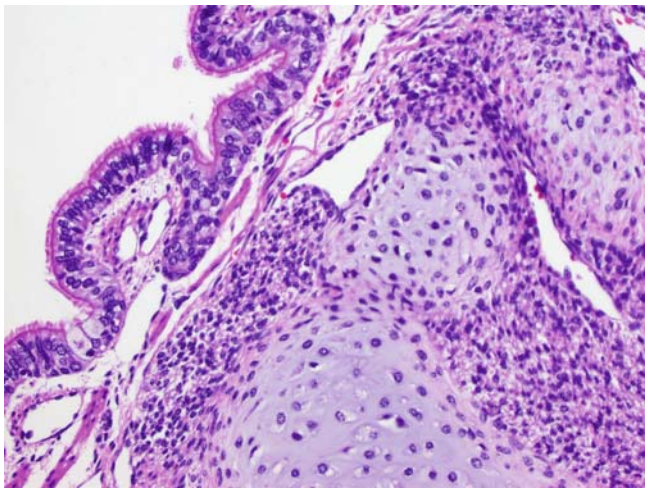

FIGURE 3.6 Congenital pulmonary myofibroblastoma tumor. Microscopic features. The spindled cells infiltrate the submucosa of bronchi and surround malformed cartilage plates. Hematoxylin and eosin.

REFERENCES

- Alobeid B, Beneck D, Sreekantaiah C, et al. Congenital pulmonary myofibroblastic tumor: A case report with cytogenetic analysis and review of the literature. *Am J Surg Path.* 1997;21(5):610–614.
- McGinnis M, Jacobs G, el-Naggar A, et al. Congenital peribronchial myofibroblastic tumor (so-called "congenital leiomyosarcoma"). A distinct neonatal lung lesion associated with nonimmune hydrops fetalis. *Mod Pathol.* 1993;6:487–492.
- Pettinato G, Manivel JC, Saldaña MJ, et al. Primary bronchopulmonary fibrosarcoma of childhood and adolescence: Reassessment of a low-grade malignancy. *Hum Pathol.* 1989;20:463–471.

CHAPTER 4

Alveolar Adenoma

Philip T. Cagle, Timothy C. Allen, and Armando E. Fraire

Under the category of benign adenomas of the lung, the current World Health Organization Classification of Tumors recognizes mucous gland adenoma, mucinous cystadenoma, pleomorphic adenoma, alveolar adenoma, and papillary adenoma. Here we discuss only alveolar adenomas. Alveolar adenomas are rare, benign usually solitary, peripherally located proliferations made of a network of cystic spaces lined by simple cuboidal epithelium, resembling type II pneumocytes. The epithelium in some of these adenomas may become so flattened that it may look like endothelium, closely mimicking vascular proliferations. In these instances, immunostaining for vascular markers such as CD31 or CD34 and epithelial markers such as pancytokeratin or epithelial membrane antigen can help to make the distinction. In one series of six patients with alveolar adenoma, the mean age was 59 years and patients were all asymptomatic. In chest radiographs and CT studies, alveolar adenomas may appear as non-calcified coin lesions in the subpleural zones of the lung. Due to their peripheral location, little is known in terms of their endoscopic appearance or cyotpathologic features.

FIGURE 4.1 Posteroanterior chest radiograph showing a coin lesion in the left mid zone of the lung. This lesion is best visualized in the next image, see Fig. 4.2 (Courtesy of Dr. Ufuk Cagirisi, Ege University Medical Faculty, Izmir, Turkey). With permission from Interact Cardiovasc Thorac Surg, see chapter references for complete citation.

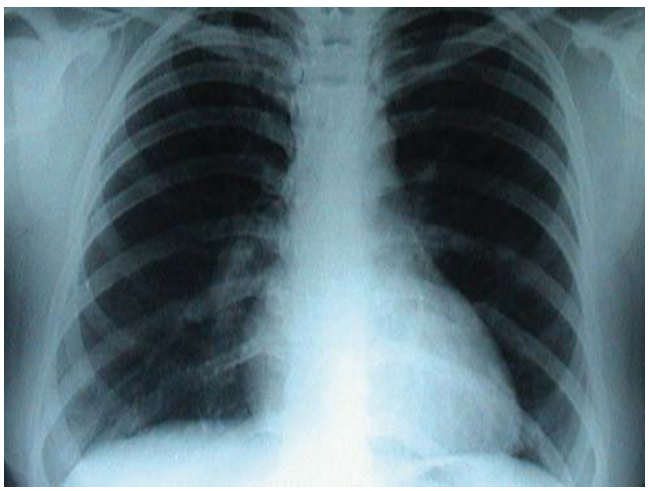

FIGURE 4.2 Spot radiograph showing a coin lesion marked with *arrows* (Courtesy of Dr. Ufuk Cagirisi, Ege University Medical Faculty, Izmir, Turkey). With permission from Interact Cardiovasc Thorac Surg, see chapter references for complete citation.

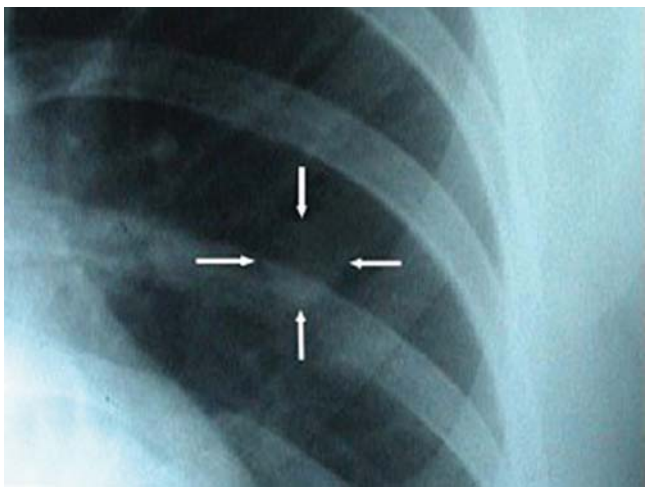

A.E. Fraire et al. (eds.), *Atlas of Neoplastic Pulmonary Disease*,
DOI 10.1007/978-0-387-89839-1_4, © Springer Science+Business Media, LLC 2010

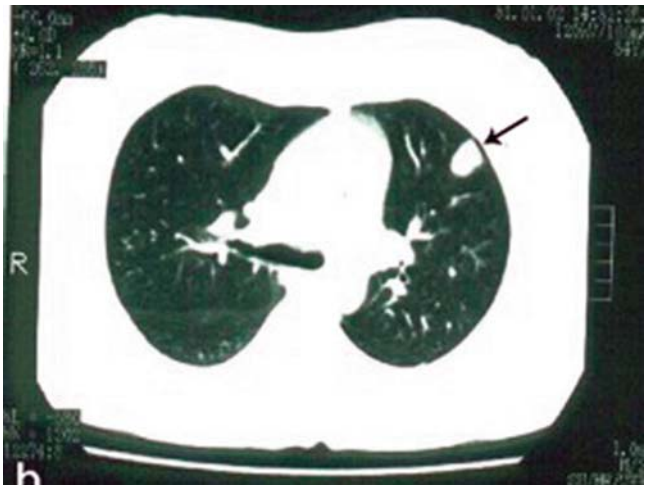

FIGURE 4.3 CT of chest depicting a sharply defined 1.5 cm solitary nodule in the left upper lobe (*arrow*) (Courtesy of Dr. Ufuk Cagirisi, Ege University Medical Faculty, Izmir, Turkey). With permission from Interact Cardiovasc Thorac Surg, see chapter references for complete citation.

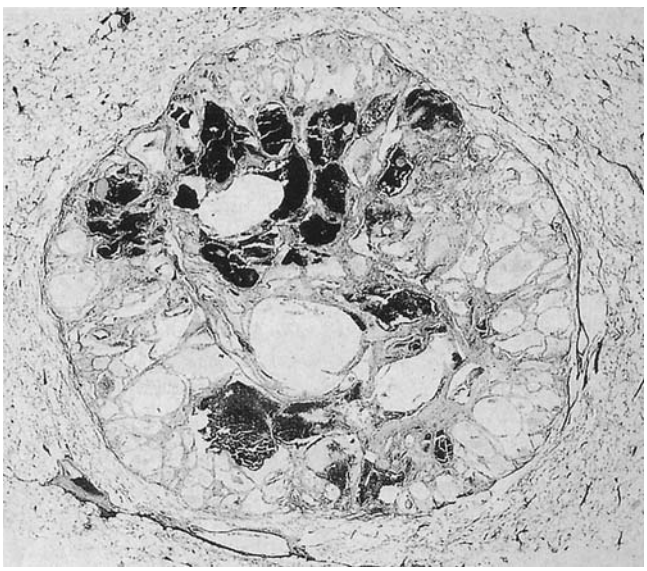

FIGURE 4.4 Lower power view of a circumscribed spheroidal alveolar adenoma showing multiple cystic spaces of variable size and shape. Hematoxylin and eosin. From Tomashefski et al, with permission from Springer (see chapter references for complete citation).

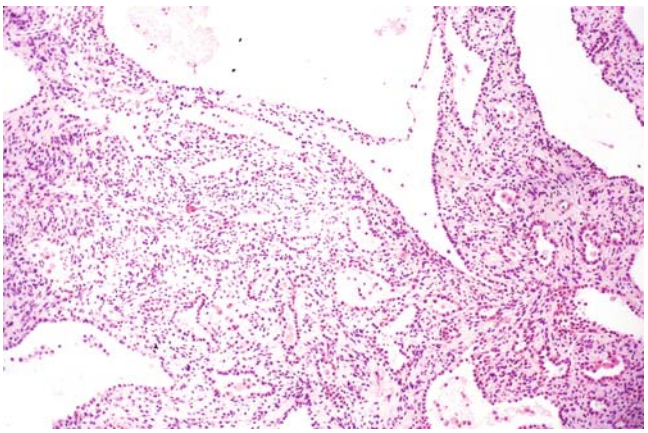

FIGURE 4.5 This medium power view of an alveolar adenoma showing variably sized cystic spaces that are larger toward the center of the lesion. Hematoxylin and eosin. From Tomashefski et al, with permission from Springer (see chapter references for complete citation).

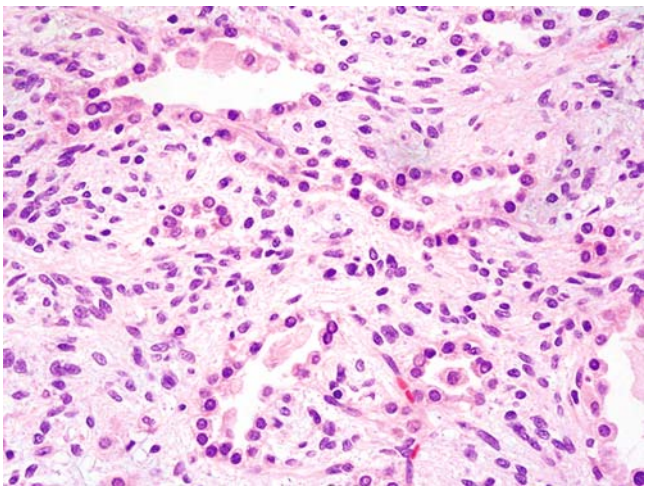

FIGURE 4.6 This high power view of an alveolar adenoma focusing on smaller cystic spaces shows rows of cuboidal, orderly looking type II pneumocytes lining the air spaces. Hematoxylin and eosin. From Tomashefski et al, with permission from Springer (see chapter references for complete citation).

REFERENCES

- Burke LM, Flieder DB. Alveolar adenoma. In: Travis WD, Brambilla E, Müller-Hermelink HK, Harris CC, eds. *World Health Organization Classification of Tumours. Pathology and Genetics of Tumours of the Lung, Pleura, Thymus and Heart*. Lyon: IARC Press; 2004:113–114.
- Burke LM, Rush WI, Khoor A, et al. Alveolar adenoma: a histochemical, immunohistochemical and ultrastructural analysis of 17 cases. *Hum Pathol* 1999;30: 158–167.
- Cakan A, Samancilar O, Nart D, Cagirisi U. Case Report – Pulmonary. Alveolar Adenoma: An unusual lung tumor. *Interact Cardiovasc Thorac Surg*. 2003;2: 343–347.
- Fraire AE, Dail DH. Ch 41. Miscellaneous tumors and tumor-like proliferations of the lung. In: Tomashefski

JF Jr, Cagle PT, Farver CF, Fraire AE, eds. *Dail and Hammar's Pulmonary Pathology*. 3rd ed. Berlin, New York, Heidelberg: Springer-Verlag; 2008:500–541.

- Koppl H, Freudenberg N, Berwanger I, et al. Alveolar adenoma of the lung. Immunohistochemical characterization of type II pneumocytes. *Pathology*. 1996;17: 150–153.
- Yousem SA, Hochholzer L. Alveolar adenoma. *Hum Pathol*. 1986;17:1066–1071.

CHAPTER 5

Uncommon Endobronchial Surface Tumors

Tetsu Tsukamoto, Seikan Suzuki, Armin Ernst, Toshiaki Kawai, Yuichi Ozeki, Philip T. Cagle, Timothy C. Allen and Armando E. Fraire

Under the name "Uncommon Endobronchial Surface Tumors," we consider generally benign epithelial proliferations of the trachea and bronchi whose common denominator is a papillary growth pattern. Currently, the World Health Organization recognizes three major histopathologic types: squamous, glandular, and mixed-type papillomas.

Squamous papillomas can be seen in both children and adults and may be either solitary or multiple. A disseminated form of squamous papilloma known as juvenile tracheo-bronchial papillomatosis is regarded as an aggressive variant and is more likely to occur in younger individuals. Two morphologic growth patterns of squamous papillomas are recognized: exophytic and inverted with exophytic variants being more common. The viral-induced nature of some squamous papillomas is well established. Also known as columnar cell papillomas, glandular papillomas are tumors of the airway lined by ciliated or non-ciliated columnar epithelial cells. They are very rare and may produce symptoms related to airway obstruction. Rarely, columnar or glandular papillomas may also occur at the periphery of the lung or the overlying pleura. In contrast to the squamous papillomas, no etiologic agents have been identified in these lesions. Previously known as transitional papillomas, mixed squamous, and glandular papillomas are also extremely rare tumors featuring connective tissue fronds lined by a mixture of benign squamous cells and benign glandular epithelial cells.

SQUAMOUS PAPILLOMAS

FIGURE 5.1 This endoscopic view of a squamous papilloma of the trachea is from a 31-year-old Chinese woman who presented with increasing shortness of breath over several weeks. Note multi-lobulated mass on the anterior wall of the trachea prior to therapy with argon plasma coagulation.

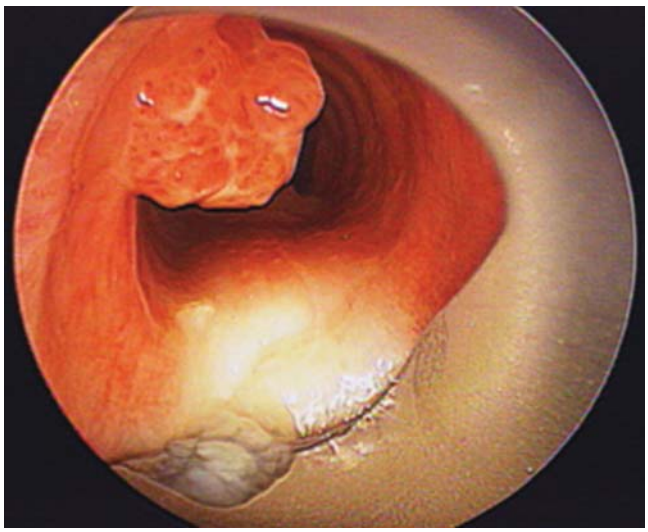

A.E. Fraire et al. (eds.), *Atlas of Neoplastic Pulmonary Disease*,
DOI 10.1007/978-0-387-89839-1_5, © Springer Science+Business Media, LLC 2010

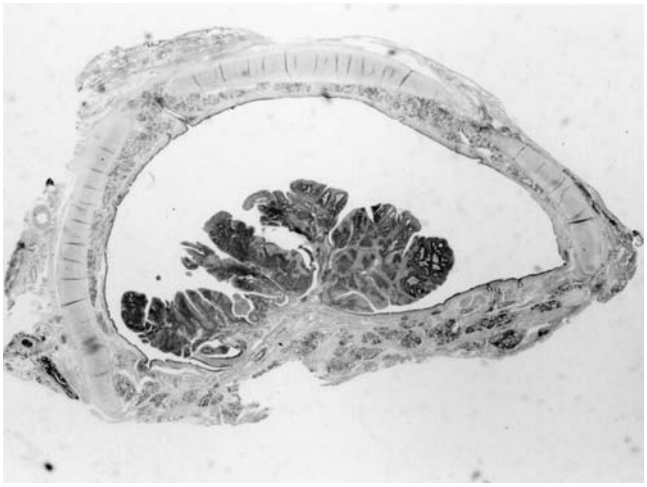

FIGURE 5.2 Subgross mount of a squamous papilloma. Low-power view of a tracheal sessile lesion showing complex arborescent architecture with a wide base of attachment to the posterior wall and partial luminal obstruction (reproduced with permission from Trillo et al).

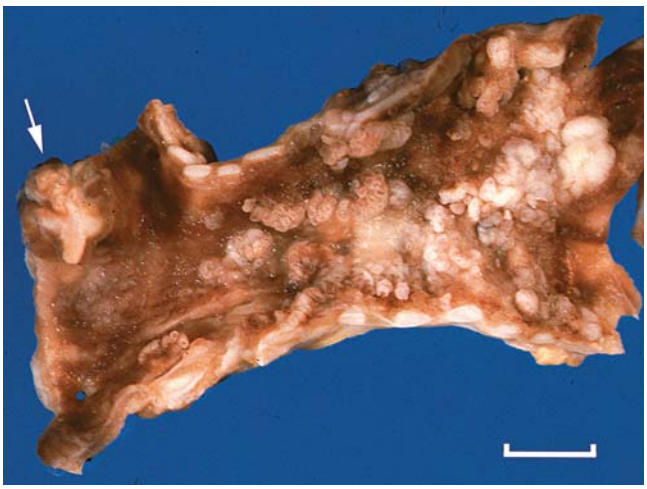

FIGURE 5.3 Gross specimen: Juvenile tracheobronchial papillomatosis. Note numerous squamous papillomatous excrescences distorting the tracheal mucosal surface in this 13-year-old male adolescent. Papillomas extend into the lobar bronchus (Courtesy of Dr. J. Tomashefski, Metrohealth Medical Center, Cleveland, OH) (see chapter references for complete citation).

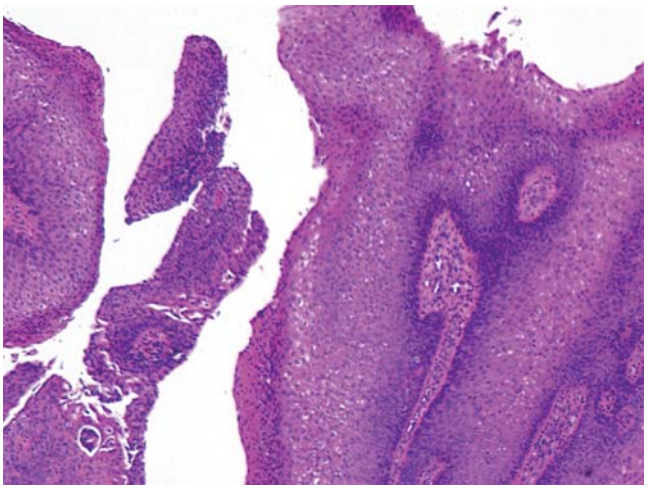

FIGURE 5.4 Microscopic view of a squamous papilloma showing exophytic verrucous extensions of acanthotic squamous epithelium with a hyperplastic basal layer and fibrovascular stalk. Koilocytotic and dysplastic nuclear features are frequently seen in the squamous epithelium of these lesions (Courtesy of Dr. J. Tomashefski, Metrohealth Medical Center, Cleveland, OH) (see chapter references for complete citation).

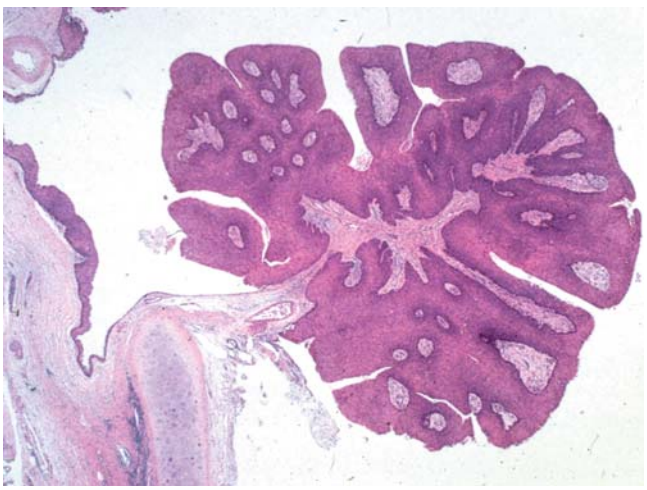

FIGURE 5.5 Subgross mount of another squamous lesion corresponding to a squamous papilloma. Mature squamous epithelial cells line the surface of fibrovascular cores. Note stalk at bottom of the lesion (Courtesy of Dr. Helmut H. Popper, University of Graz, Graz, Austria).

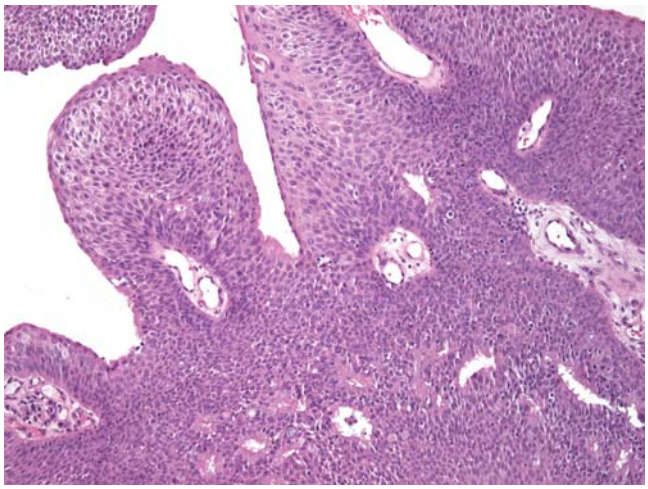

FIGURE 5.6 Squamous papilloma, microscopic view. Note some blunt and some accuminated papillary projections of hyperplastic squamous epithelium with central fibrovascular cores. Hematoxylin and eosin.

GLANDULAR PAPILLOMAS

FIGURE 5.7 Glandular papilloma, chest radiographs showing a poorly defined opacity in the right mid-lung field. Note mild interval change over a near 4-year period of time.

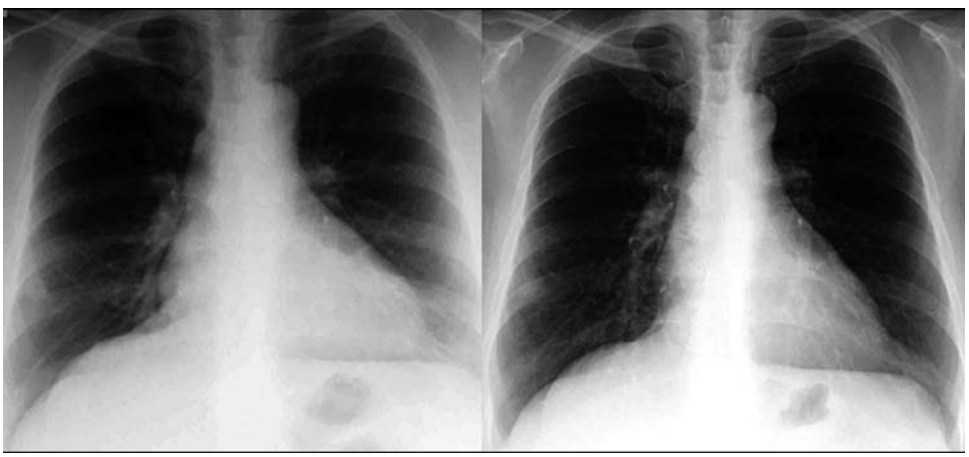

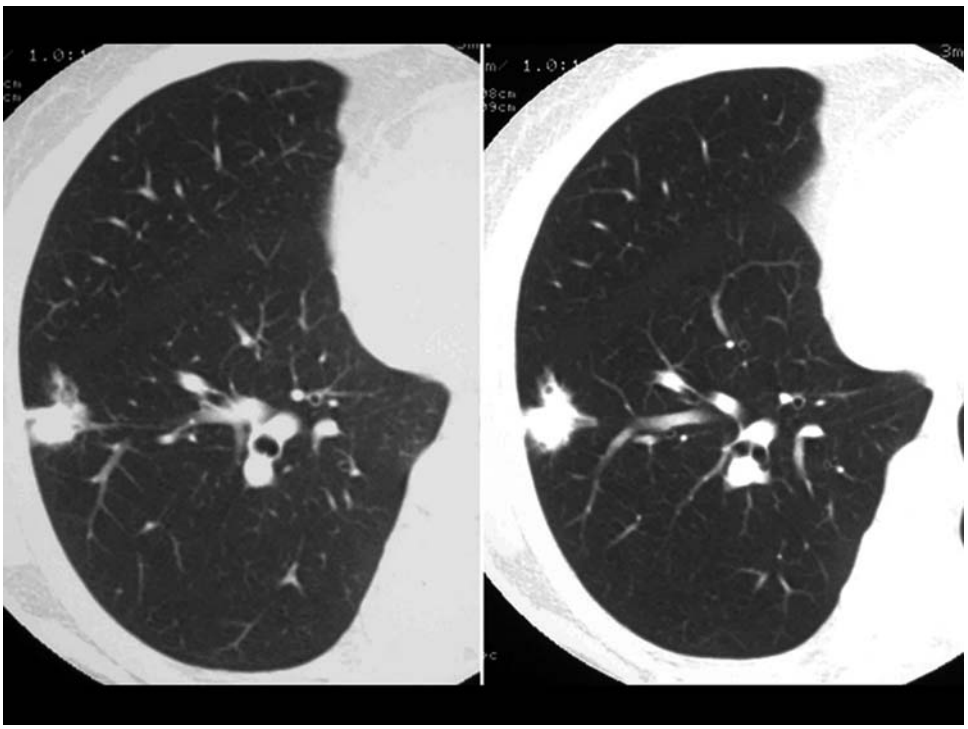

FIGURE 5.8 Glandular papilloma, CT of chest showing an irregular nodular opacity measuring about 1.5 cm, in the right lung.

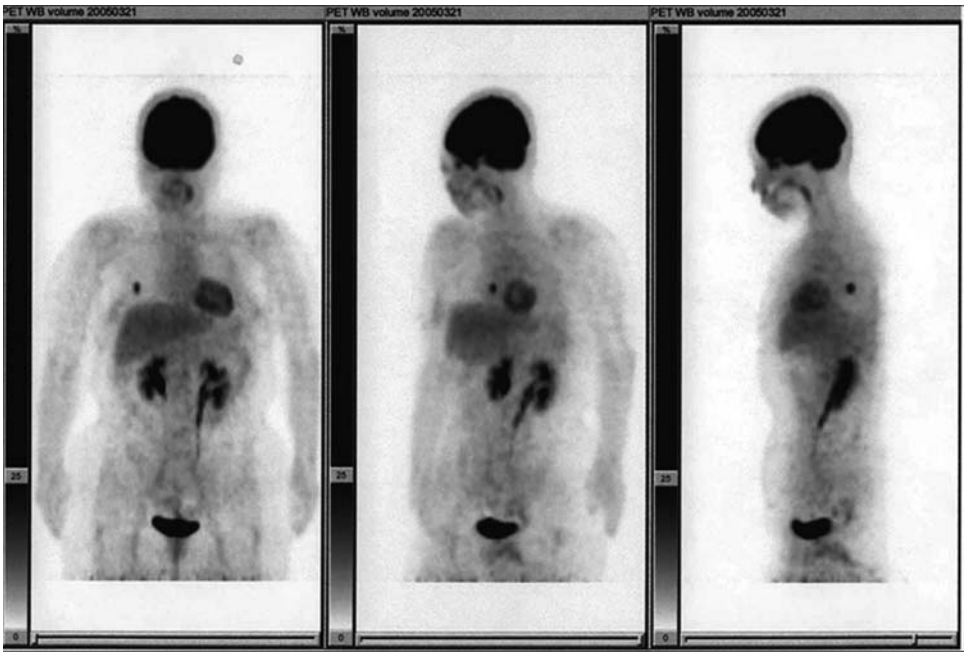

FIGURE 5.9 FDG positron emission tomography of a glandular papilloma showing abnormal uptake of the posteriorly located lung tumor, with a maximal standardized uptake value (SUV max) of 10.8.

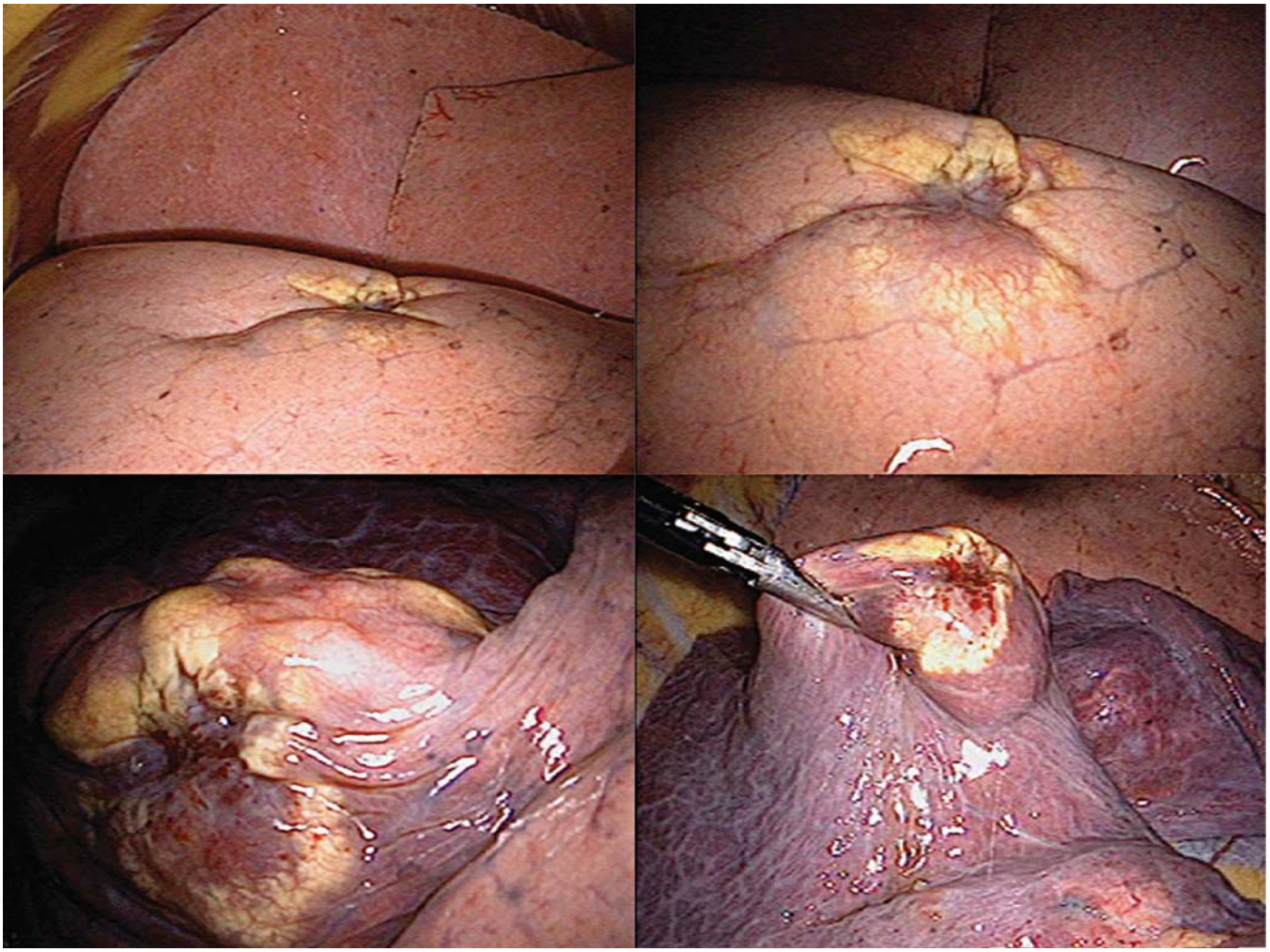

FIGURE 5.10 Pleuroscopic view of a glandular papilloma involving the pleural surface. In this uncommon case, the tumor is manifested as nodular masses puckering the visceral pleural surface.

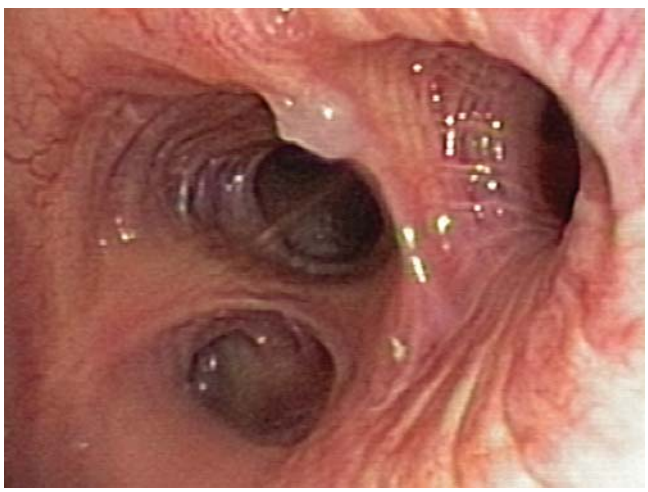

FIGURE 5.11 Endobronchial view of another patient with a glandular papilloma at a secondary carina. Note mucoid appearance of the lesion.

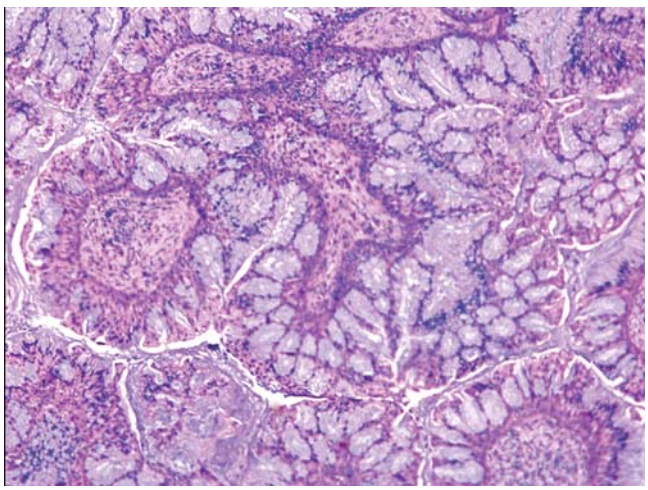

FIGURE 5.12 Glandular papilloma, microscopic view. Note complex glandular structures made up of cells with clear cytoplasm suggestive of mucin production. Hematoxylin and eosin.

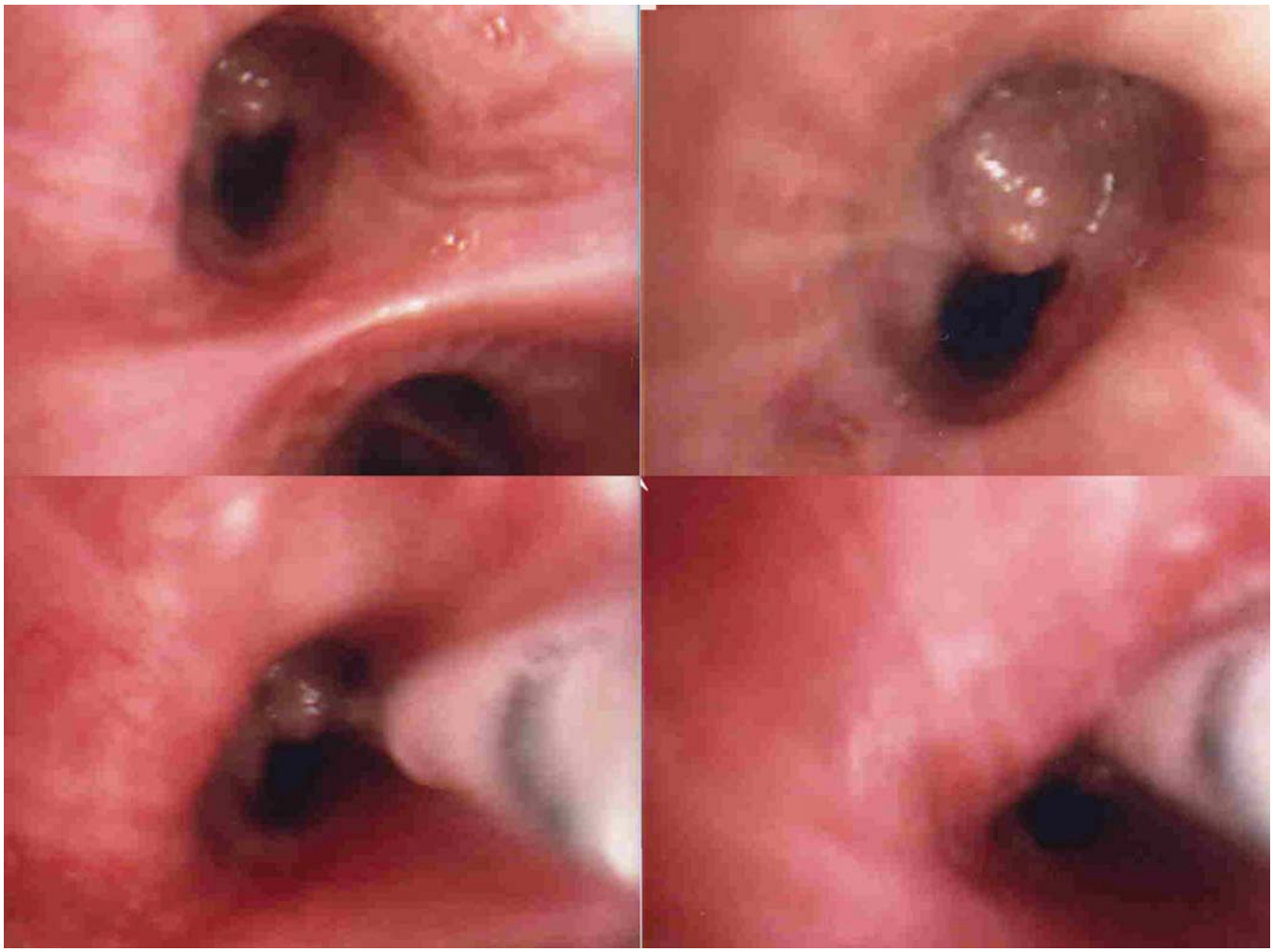

FIGURE 5.13 Endoscopic views showing a tumor of the bronchial mucosa with coarse granular surface (with permission from Bull Tobu Comed Coll, see chapter references for complete citation).

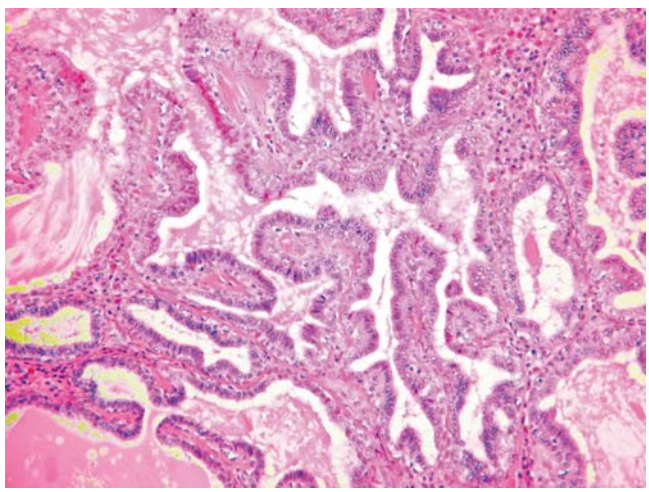

FIGURE 5.14 Microscopic view of the glandular component. Note cords of epithelial cells arranged in a complex papillary fashion. Hematoxylin and eosin (with permission from Bull Tobu Comed Coll, see chapter references for complete citation).

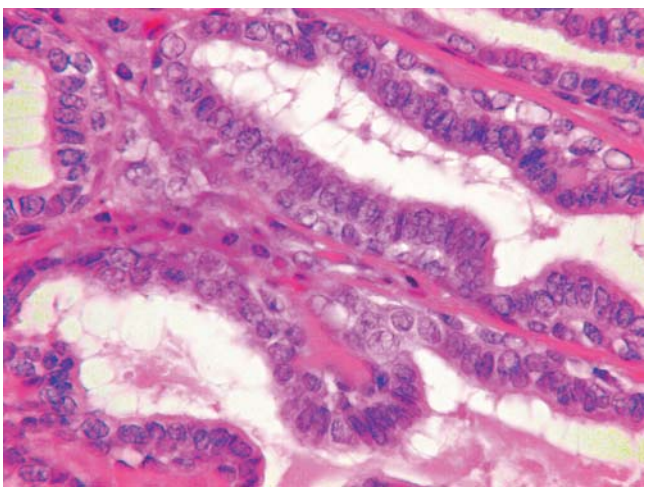

FIGURE 5.15 Closer microscopic view of the glandular component showing tall orderly looking columnar cells lining fibrovascular cores. Hematoxylin and eosin (with permission from Bull Tobu Comed Coll, see chapter references for complete citation).

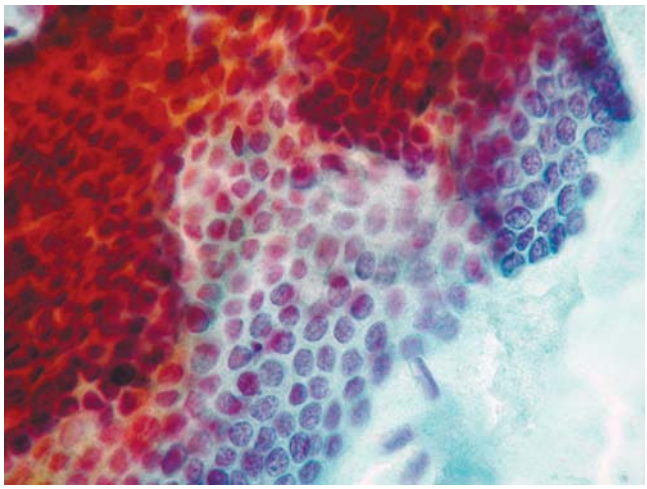

FIGURE 5.16 Cytologic preparation of squamous component showing flat sheets made of squamoid cells with no atypia. Papanicolaou stain (with permission from Bull Tobu Comed Coll, see chapter references for complete citation).

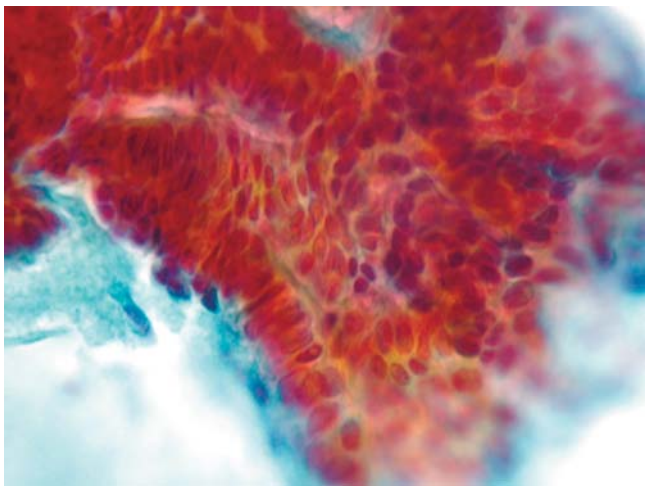

FIGURE 5.17 Closer view of another field of the lesion shown in the previous figure. Note a row of columnar glandular cells in the left lower quadrant. Papanicolaou stain (with permission from Bull Tobu Comed Coll, see chapter references for complete citation).

REFERENCES

- Aida S, Ohara I, Shimazaki H, et al. Solitary peripheral ciliated glandular papillomas of the lung: A report of 3 cases. *Am J Surg Pathol*. 2008;32:1489–1494.
- Basheda S, Gephardt GN, Stoller JK. Columnar papilloma of the bronchus. Case report and literature review. *Am Rev Respir Dis*. 1991;144:1400–1402.
- Clavel CE, Nawrocki B, Boxxeaux B, et al. Detection of human papillomavirus DNA in bronchopulmonary carcinomas by hybrid capture II. A study of 185 tumors. *Cancer*. 2000;88:1347–1352.
- Flieder D, Koss MN, Nicholson A, et al. Solitary pulmonary papillomas in adults: A clinicopathologic and in-situ hybridization study of 14 cases combined with 27 cases in the literature. *Am J Surg Pathol*. 1998;22:1328–1342.
- Fraire AE. Ch 25. Non malignant versus malignant proliferation on lung biopsy. In: Cagle PT, ed. *Diagnostic Pulmonary Pathology*. New York-Basel: Marcel-Dekker, Inc; 2000:525–545.
- Gupta D, Holla J, Layfield L. Topoisomerase alpha II, retinoblastoma gene product and p53: potential relationships with aggressive behavior and malignant transformation in recurrent respiratory papillomatosis. *Appl Immunohistochem Mol Morphol*. 2001;9:86–91.
- Popper HH, El-Shabrawi Y, Wockel W, et al. Prognostic importance of human papillomavirus typing in squamous cell papilloma of the bronchus: comparison of in-situ hybridization and the polymerase chain reaction. *Hum Pathol*. 1994;25:1191–1197.
- Rady PL, Schnadig VJ, Weiss RL, et al. Malignant transformation of recurrent respiratory papillomatosis associated with integrated human papillomavirus type II DNA and mutation of p53. *Laryngoscope*. 1998;108:735–740.
- Trillo A, Guha A. Solitary condylomatous papilloma of the bronchus. *Arch Pathol Lab Med*. 1988;112:731–733.
- Tsukamoto T, Susuki S. Solitary bronchial papilloma of columnar cell type. *Bull Tobu Comed Coll*. 2007;11: 39–45.

CHAPTER 6

Mucous Gland Adenoma

Richard S. Irwin, Philip T. Cagle, Timothy C. Allen,
and Armando E. Fraire

Mucous gland adenomas are rare benign neoplasms believed to arise from minor salivary-type glands of the bronchi. They are usually solitary and their diagnosis is seldom made pre-operatively. Endoscopically, they appear as pink to white sessile polypoid structures with smooth glistening surfaces. Little is known about their radiographic appearance but on CT they have been described as well-demarcated intraluminal masses abutting into the bronchus or presenting with an air-meniscus sign. Others may appear as coin lesions. Grossly the lesions are well circumscribed and, as noted earlier, polypoid in appearance. Microscopically, they are made of multicystic spaces filled with colloid-like material and lined by benign-looking mucin-producing epithelial cells. Some cases are remarkably similar in structure to normal mucous glands of the tracheobronchial tree. Some cases have combined cystic and papillary components while others approach the morphology of low-grade mucoepidermoid tumors. A scant stroma made up of spindle cells with a scattering of lymphocytes may be seen in the background. Mucous gland adenomas with attenuated epithelial lining cells may resemble cystic lymphangiomas. The cytopathology of these tumors has not been described.

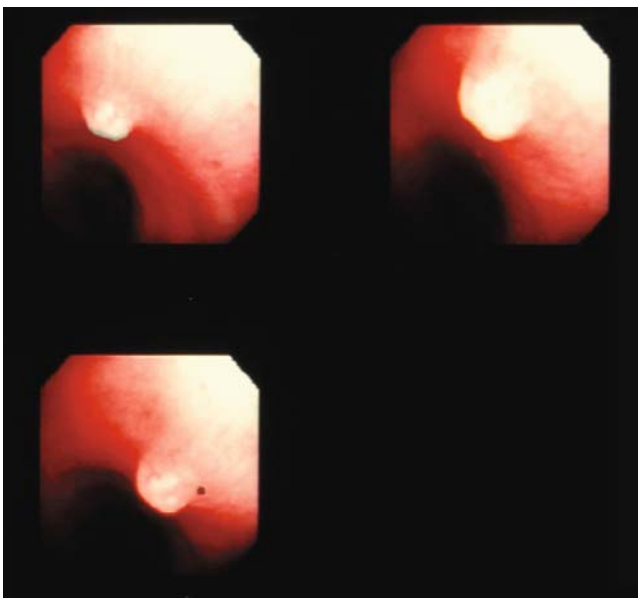

FIGURE 6.1 Endoscopic view of a mucous gland adenoma in the lower trachea, just above the bifurcation. Note small sessile pearly white mound-like structure filled with mucoid material. From Tomashefski et al, with permission from Springer (see chapter references for complete citation).

A.E. Fraire et al. (eds.), *Atlas of Neoplastic Pulmonary Disease*,
DOI 10.1007/978-0-387-89839-1_6, © Springer Science+Business Media, LLC 2010

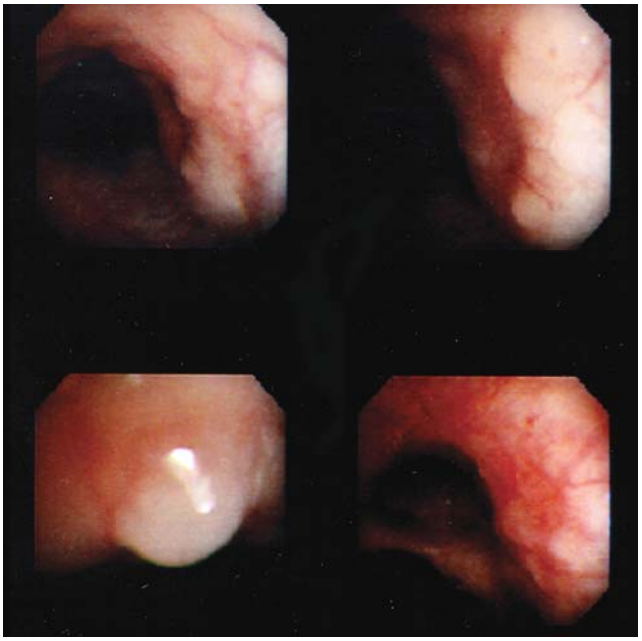

FIGURE 6.2 Endoscopic view of another patient with mucous gland adenoma showing similar characteristics except for a somewhat larger size and less well-defined borders. From Tomashefski et al, with permission from Springer (see chapter references for complete citation).

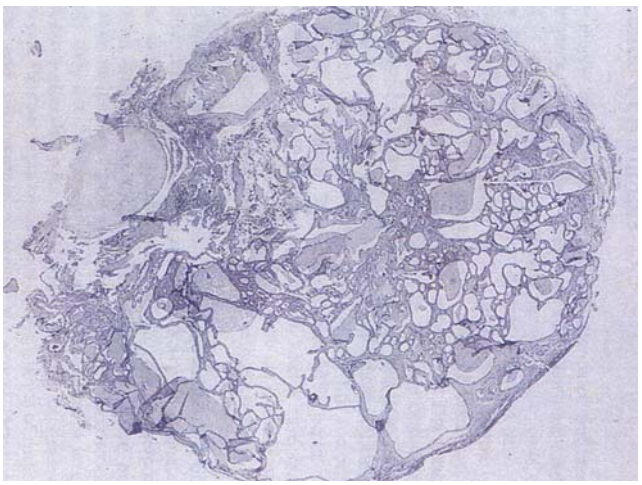

FIGURE 6.3 Subgross (whole mount) view of a mucous gland adenoma showing a predominantly cystic pattern. From Tomashefski et al, with permission from Springer (see chapter references for complete citation).

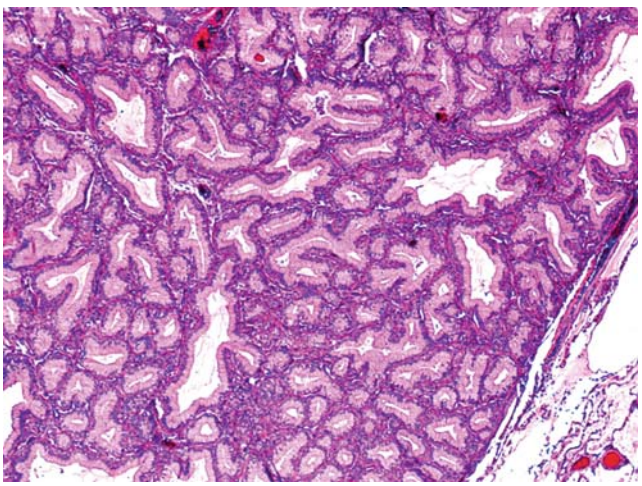

FIGURE 6.4 This microscopic view of another mucous gland adenoma shows an area of the tumor with a non-cystic appearance with irregular glands lined by columnar cells with mucin and a spindle cell stroma. Hematoxylin and eosin (Courtesy of Dr. Bruno Murer, Venice, Italy).

REFERENCES

- England EM, Hochholzer L. Truly benign "bronchial adenoma" Report of 10 cases of mucous gland adenoma with immunohistochemical and ultrastructural findings. *Am J Surg Pathol*. 1995;19:887–899.
- Ferguson CJ, Cleeland JA. Mucous gland adenoma of the trachea: case report and literature review. *J Thorac Cardiovasc Surg*. 1988;95:347–350.
- Flieder DB, Thivolet – Bejui F, Popper H. Mucous gland adenoma. In: Travis WD, Brambilla E, Müller-Hermelink HK, Harris CC, eds. *World Health Organization Classification of Tumours. Pathology and Genetics of Tumours of the Lung, Pleura, Thymus and Heart*. Lyon: IARC Press; 2004:85.
- Fraire AE, Dail DH. Ch 38. Tracheobronchial (salivary type) gland tumors. In: Tomashefski JF, Cagle PT, Farver CF, Fraire AE, eds. *Dail and Hammar Pulmonary Pathology*. 3rd ed. Berlin, New York, Heidelberg: Springer; 2008:398–426.
- Kwon JW, Goo JM, Seo JB, et al. Mucous gland adenoma of the bronchus. CT findings in two patients. *J Comput Assist Tomogr*. 1999;23:758–760.
- Murer B. Mucous gland adenoma. In: Cagle PT, Editor-in-Chief. *Color Atlas and Text of Pulmonary Pathology*. 2nd ed. Philadelphia: Wolters Kluwer/Lippincott Williams and Wilkins; 2008:182.

CHAPTER 7

Pleomorphic Adenoma

Armando E. Fraire, Philip T. Cagle, and Timothy C. Allen

Pleomorphic adenomas are benign neoplasms with mixed epithelial and mesenchymal components that may be endobronchial or parenchymal. They are derived from seromucinous glands of the airway and are similar to those seen in major salivary glands. These tumors are more frequent in men by a factor of about 2:1 with a mean age of 50 years. Productive cough and intermittent dyspnea are manifestations of tracheal tumors. Other symptoms are wheezing, respiratory infection, and rarely hemoptysis. Parenchymal tumors may be clinically silent. Large endobronchial tumors may cause atelectasis, volume loss, or post-obstructive pneumonitis. CT scanning can assist with determination of extension of a tumor from the airways into the pulmonary parenchyma.

Bronchoscopically, these tumors appear polypoid and have a predilection for the postero-lateral portion of the trachea, owing to the greater concentration of glandular elements in this area. The surface varies from gray white to pale pink. These tumors are usually soft to rubbery polypoid nodular masses ranging from 1.5 to 16 cm in diameter. The cut surfaces are gray white and shiny owing to their myxoid content. Pleomorphic adenomas are biphasic tumors containing varying proportions of epithelial and myoepithelial cells mixed with stromal components. The epithelial cells arrange themselves in assorted patterns but tend to preferentially form tubules or stellate-shaped clusters. The stromal components are generally abundant and show myxoid and/or chondroid features. While most pleomorphic adenomas are benign, malignant counterparts do exist but are exceedingly uncommon. Malignant tumors may show focal necrosis, angioinvasion, and increased mitotic activity of up to 10 mitoses per 10 high-power fields. The cytomorphology is similar to that seen in salivary gland tumors. Epithelial or myoepithelial cells with plasmacytolid features are arranged in sheets and syncytia with trabecular and/or ductal arrangements. Typically, a fibrillar chondromyxoid matrix will be evident on the background. When stained with Diff Quick stains, this chondromyxoid matrix will stain in a metachromatic fashion.

FIGURE 7.1 Posteroanterior radiograph of chest. Note intratracheal midline density with lobulated contours. The mass lies proximal to the bifurcation and is better visualized in the CT image (Courtesy of Dr. L. Pasillio, Northampton, MA).

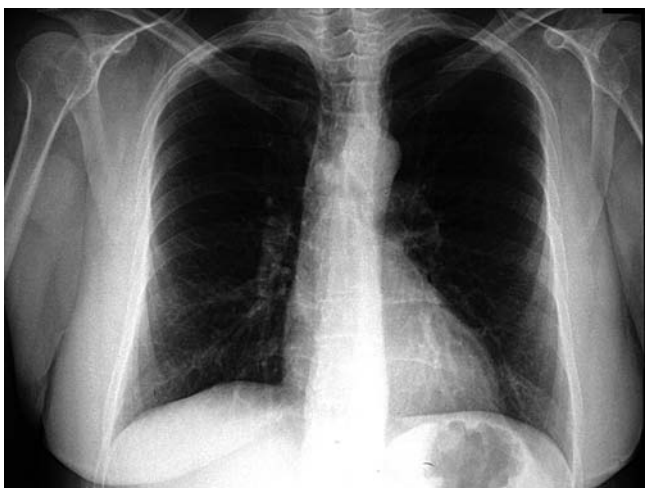

A.E. Fraire et al. (eds.), *Atlas of Neoplastic Pulmonary Disease*,
DOI 10.1007/978-0-387-89839-1_7,

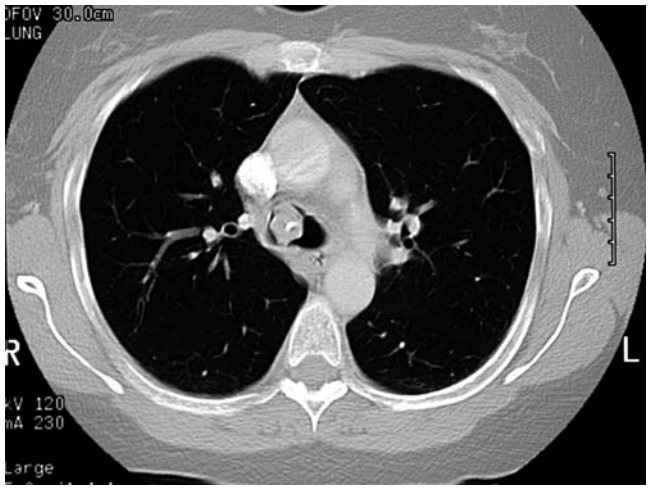

FIGURE 7.2 CT image showing a sessile endotracheal mass with air menisci on both sides. The mass lies just superior to the tracheal bifurcation (Courtesy of Dr. L. Pasillio, Northampton, MA).

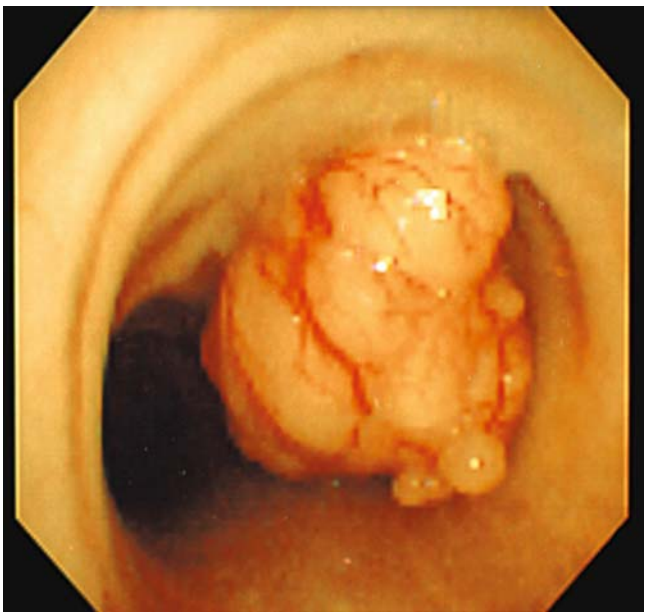

FIGURE 7.3 Endoscopic view of a pleomorphic adenoma of the trachea. Note sessile yellowish tan endotracheal mass showing congested criss-crossing capillaries at its surface (Courtesy of Dr. Jay S. Fleitman, Northampton, MA). From Tomashefski et al, with permission from Springer (see chapter references for complete citation).

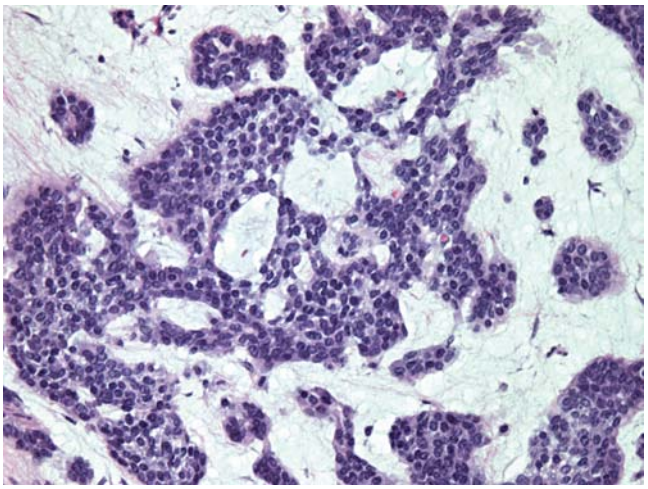

FIGURE 7.4 Histopathologic view of a pleomorphic adenoma showing epithelial-lined tubular structures as well as solid sheets of similar epithelial cells all in a background of amorphous myxoid matrix. Hematoxylin and eosin.

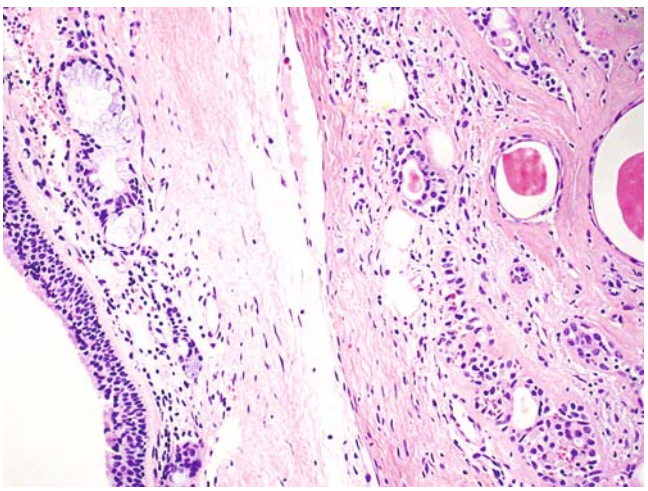

FIGURE 7.5 Histopathologic view of another pleomorphic adenoma impinging upon the bronchial wall. Note respiratory epithelium on the left and tubular structures of the tumor on the right. The tubular structures contain an eosinophilic coagulum. Hematoxylin and eosin. From Tomashefski et al, with permission from Springer (see chapter references for complete citation).

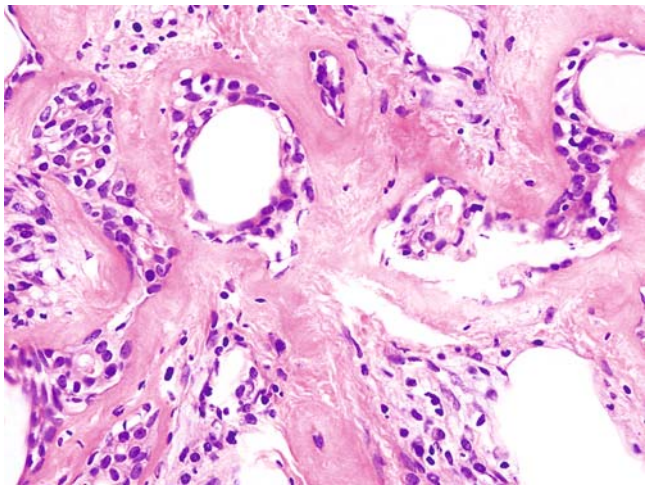

FIGURE 7.6 In this microscopic view of a pleomorphic adenoma, the tubular structures of a pleomorphic adenoma are surrounded by trabecular strands of hypocellular collagenized fibrous stroma. Hematoxylin and eosin. From Tomashefski et al, with permission from Springer (see chapter references for complete citation).

REFERENCES

- Ang KL, Dhannapuneni VR, Morgan WE, et al. Primary pulmonary pleomorphic adenoma. An immunohistochemical study and review of the literature. *Arch Pathol Lab Med*. 2003;127:621–622.
- Duhamel DR. Pleomorphic adenoma. In: Duhamel DR, Harrel JR, eds. *Clinical Atlas of Airway Diseases. Bronchoscopy, Radiology and Pathology*. Philadelphia: Elsevier Saunders; 2005; 104–105.
- Fraire AE, Dail DH. Tracheobronchial tumors of the salivary gland type. In: Cagle PT, Farver C, Fraire AE, eds. *Dail and Hammar's Pulmonary Pathology, Vol II Neoplastic Lung Disease*. 3rd ed. Springer, Berlin, New York: Heidelberg; 2008:398–426.
- Hasleton P. Biphasic pulmonary neoplasms. In: Cagle PT, ed. *Diagnostic Pulmonary Pathology*. New York: Marcel-Dekker Basel; 2000: 665–683.
- Hemmi A, Hirooka H, Mori Y, et al. Malignant pleomorphic adenoma (malignant mixed tumors) of the trachea. Report of a case. *Acta Pathol Jpn*. 1988;38:1215–1226.
- Krane JF, Faquin WC. Ch 10 Salivary Gland. In: Cibas ES, Ducatman BS, eds. *Cytology. Diagnostic Principles and Clinical Correlates*. Edinburgh, London, New York: Saunders; 2003:273–306.
- Moran CA, Suster S, Askin FB, et al. Benign and malignant salivary gland-type mixed tumors of the lung. Clinicopathologic and immunohistochemical study of 8 cases. *Cancer*. 1999;73: 2481–2490.

CHAPTER 8

Mucoepidermoid Tumor

Shanda Blackmon, Armin Ernst, Philip T. Cagle, Dina R. Mody
and Armando E. Fraire

This tumor is a tumor of bronchial ("salivary") gland derivation made of varying proportions of squamous cells, mucin-producing glandular cells, and intermediate cells. The major airways are usually involved but some tumors may be intraparenchymal. The age distribution is wide but generally favors the young, with no clear gender predilection. The symptoms are closely related to any degree of airway obstruction that may be present. Parenchymal lesions may be silent. The chest radiograph may be normal or show early changes of post-obstructive pneumonitis or atelectasis. Some tumors present as solitary nodules. Unilateral hyperlucency in a patient with bronchial asthma has been described in association with these tumors. Those tumors located in the lower trachea or major bronchi are easily accessible to the bronchoscope and show variable degree of obstruction. The tumors arising from the mucosal surface may have a pinkish-red appearance and a prominent vascular engorgement at their mucosal surfaces.

FIGURE 8.1 CT of chest showing a left endobronchial mass originating in the superior segment of the left lower lobe.

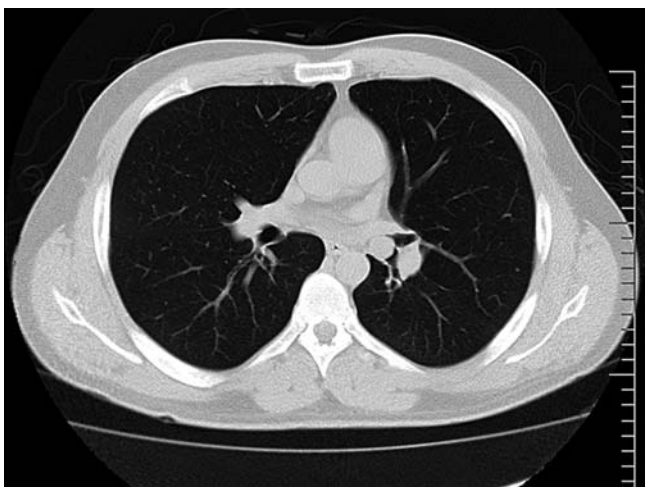

Histopathologically, low-grade and high-grade variants are recognized. The low-grade tumors have abundant mucinous cysts and bland-looking glandular components intermixed with sheets of squamoid cells. The high-grade tumors in contrast have fewer glandular components and comparatively more sheets of squamoid or intermediate cells. Mitoses are frequent and necrosis may be present. The cytomorphology of these tumors mirrors that seen in histological preparations, with varying mixtures of mucinous, squamoid, or intermediate cells. Marked nuclear atypia signifies high-grade variants.

FIGURE 8.2 Radiographic image (tomogram) of a mucoepidermoid tumor of the trachea. The tumor impinges upon the contour of the trachea (Courtesy of Dr. Jerry Balikian, University of Massachusetts Medical School, Worcester, MA). From Tomashefski et al, with permission from Springer (see chapter references for complete citation).

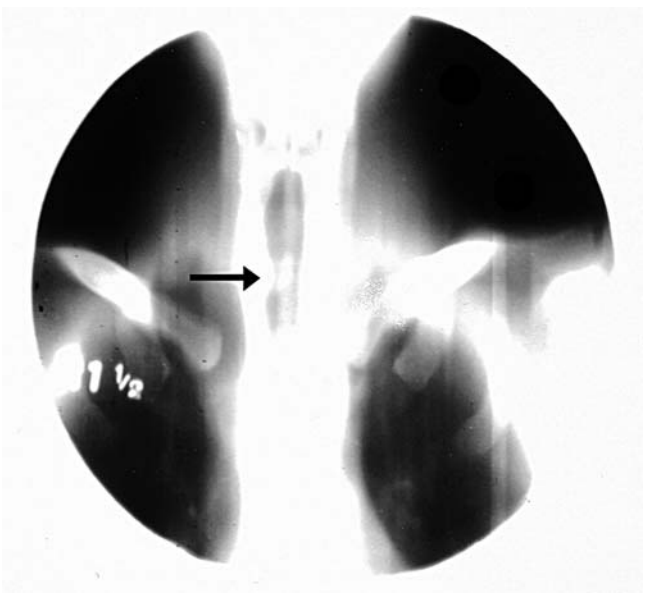

A.E. Fraire et al. (eds.), *Atlas of Neoplastic Pulmonary Disease*,
DOI 10.1007/978-0-387-89839-1_8, © Springer Science+Business Media, LLC 2010

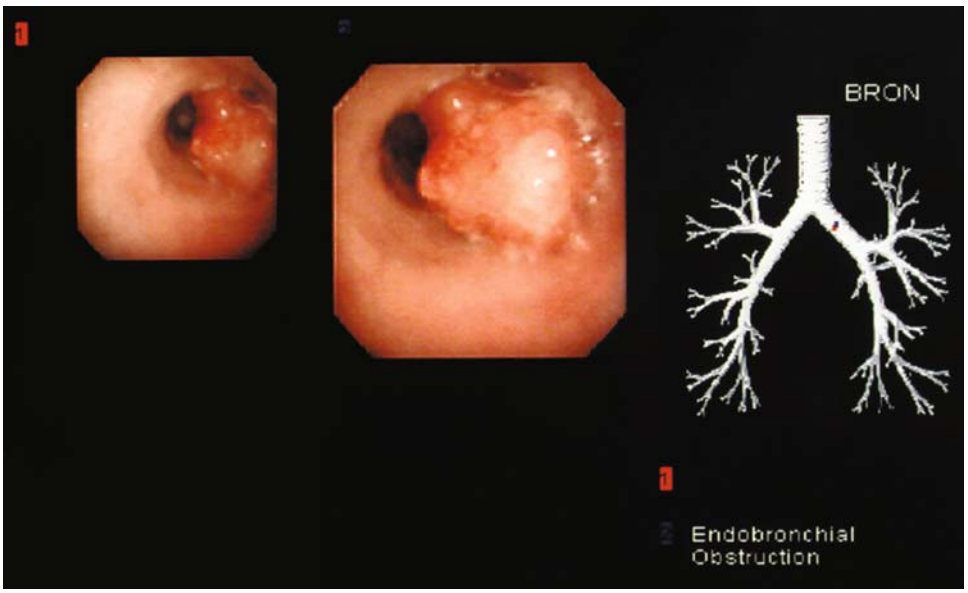

FIGURE 8.3 Endoscopic view of a mucoepidermoid lesion of the left main stem bronchus. Note broadly attached tumor mass with a knobby surface and glistening yellow pink mucosa (Courtesy of Dr. Scott Kopec, University of Massachusetts Medical School, Worcester, MA). From Tomashefski et al, with permission from Springer (see chapter references for complete citation).

FIGURE 8.4 This polypoid non-occlusive reddish tracheal tumor was surgically removed and later found to be a mucoepidermoid tumor (Courtesy of Dr. Andrew Fischer, University of Massachusetts Medical School, Worcester, MA). From Tomashefski et al, with permission from Springer (see chapter references for complete citation).

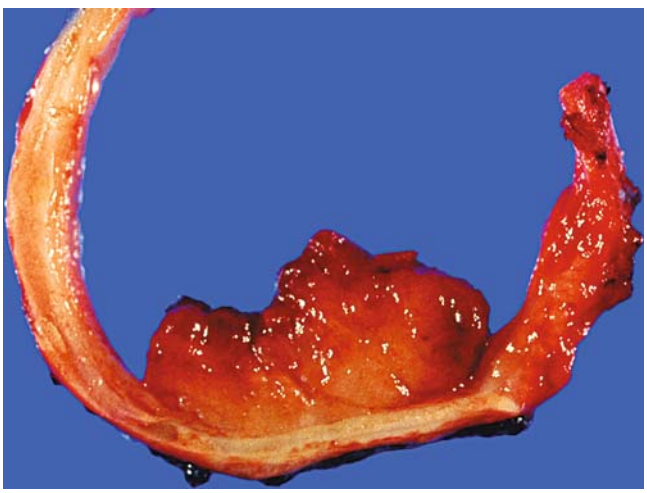

FIGURE 8.5 Histopathology of mucoepidermoid tumor. Note clusters of mucin-filled, goblet-like cells interspersed with well-defined islands of cohesive squamous epithelial cells (hematoxylin and eosin).

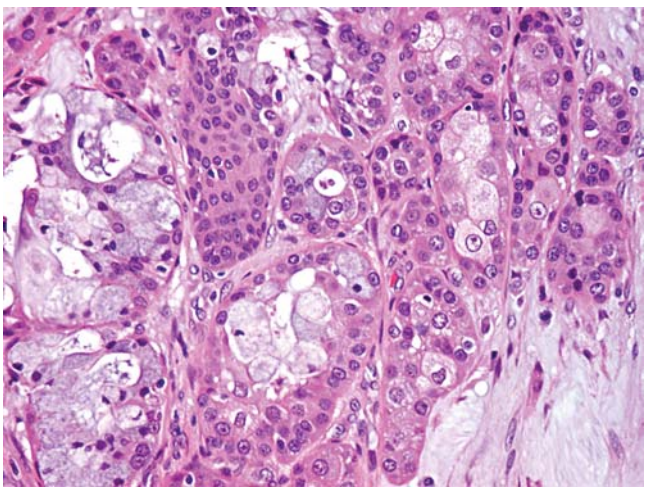

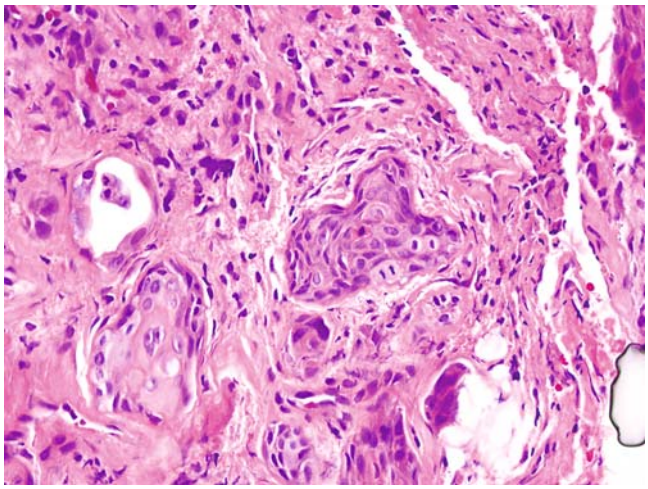

FIGURE 8.6 Another view of a mucoepidermoid tumor showing islands of bland-looking squamous epithelial cells in a fibrocollagenous background (hematoxylin and eosin). From Tomashefski et al, with permission from Springer (see chapter references for complete citation).

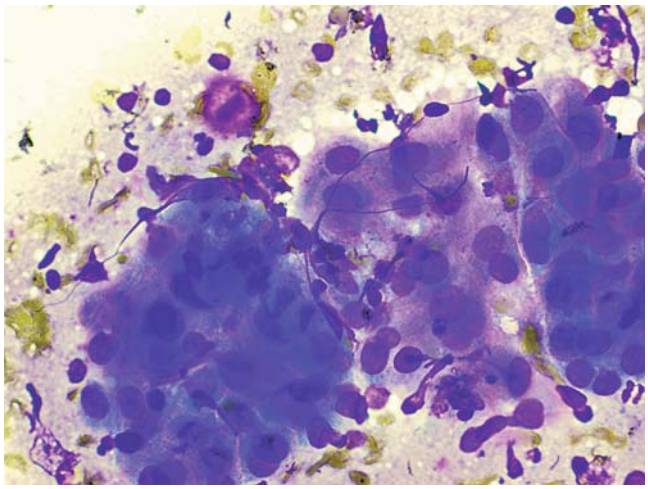

FIGURE 8.8 Mucoepidermoid tumor, cytologic preparation. Note tridimensional groups of epithelial cells with mild atypia (Diff Quick stain).

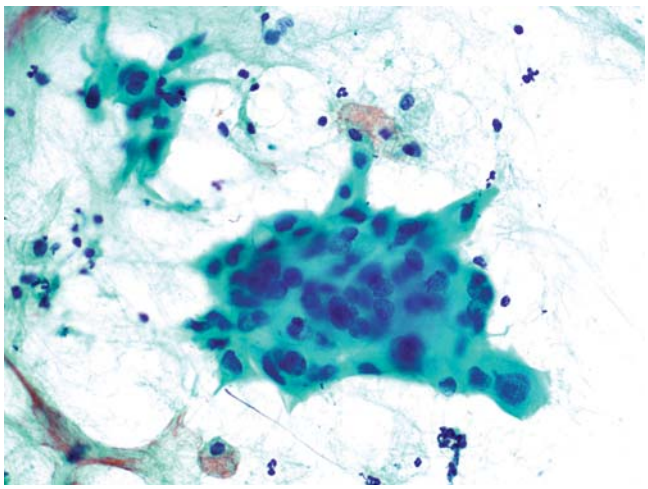

FIGURE 8.7 Mucoepidermoid tumor, cytologic preparation. Note cohesive group of intermediate squamous epithelial cells (Papanicolaou stain).

REFERENCES

- Fraire AE, Dail DH. Tracheobronchial (salivary type) gland tumors. In: Tomashefsky JF, Cagle PT, Farver C, Fraire AE, eds. *Dail and Hammar's Pulmonary Pathology*. 3rd ed. Berlin, New York, Heidelberg: Springer; 2008:398–426.
- French CA. Respiratory tract. In: Cibas ES, Ducataman BS, eds. *Cytology: Diagnostic Principles and Clinical Correlates*. 2nd ed. Saunders: Edinburgh, London, New York; 2003:61–95.
- Hasleton PS. Benign lung tumors and their malignant counterparts. In: PS Hasleton, ed. *Spencer's Pathology of the Lung*. 5th ed. New York, St. Louis, San Francisco: McGraw-Hill; 1996:875–986.
- Patel RG, Norman JR. Unilateral hyperlucency with left lower mass in a patient with bronchial asthma. *Chest*. 1995;107:569–570.
- Yousem SA, Hochholzer L. Mucoepidermoid tumors of the lung. *Cancer*. 1987;60:1346–1352.

CHAPTER 9

Adenoid Cystic Carcinoma

Armin Ernst, Philip T. Cagle, Timothy C. Allen, Dina R. Mody, and Armando E. Fraire

A highly distinctive malignant tumor arising from tracheobronchial glands, adenoid cystic carcinoma is characterized by tubular, cribriform, and solid histopathologic patterns and a propensity for extension along perineural spaces. Asthma-like manifestations with wheezing as a prominent sign can be seen in proximally located lesions. Ulceration of the overlying mucosa may result in blood-tinged sputum or frank hemoptysis while atelectasis is more likely to result from larger obstructing lesions. Tracheal tumors manifest as intraluminal nodules that may have smooth irregular or lobulated margins or as eccentric or circumferential thickening of the tracheal wall with concurrent narrowing of the lumen. Within the trachea, these tumors show a characteristic predilection for the lateral and posterolateral walls at the junction of the cartilaginous tissue and the posterior connective tissue membrane. Growing into the lumen, the tumors may adopt a lobulated, polypoid, or fusiform appearance. The mucosal surfaces may be highly vascularized.

Microscopically, three different growth patterns are recognized (cribriform, tubular, and solid) and it is not uncommon to see them all together. Typically, hyalinized, sclerotic, and/or myxoid PAS-positive matrix material can be seen in the centers of the cribriform or tubular components. A tendency to invade perineural spaces is a well-known feature. The cribriform pattern, often compared to "swiss cheese" is the most distinctive growth pattern. The main cytopathologic findings consist of generally small epithelial cells with high nuclear cytoplasmic ratio with round to oval nuclei. A characteristic finding in cytopathologic bronchial brush preparations is cylinders of bluish hyaline matrix material ringed by the above-cited cells. At times, these cylinders may be translucent on Papanicolaou stains.

FIGURE 9.1 Bronchoscopic image of the right main stem bronchus in a 62-year-old smoking female. A screening CT of chest showed a suspicious airway abnormality and at bronchoscopy a mund-like lesion was found. Endobronchial ultrasound showed significant submucosal extension of the lesion which was eventually diagnosed as an adenoid cystic carcinoma.

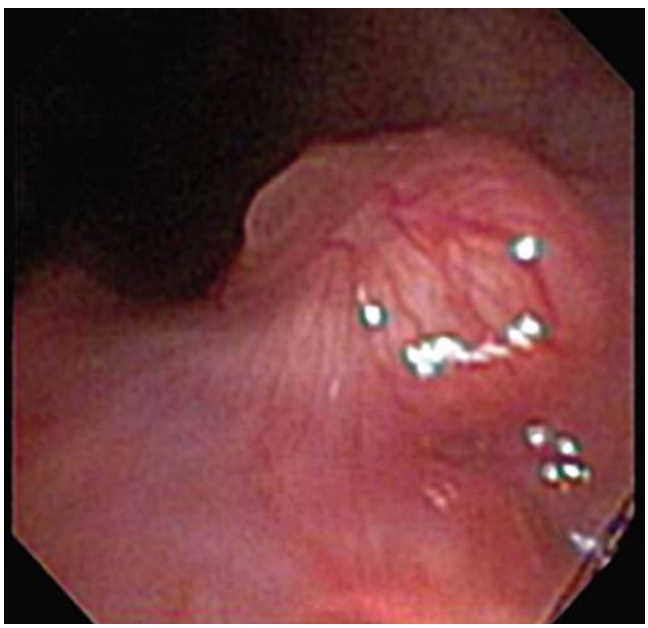

A.E. Fraire et al. (eds.), *Atlas of Neoplastic Pulmonary Disease*,
DOI 10.1007/978-0-387-89839-1_9,

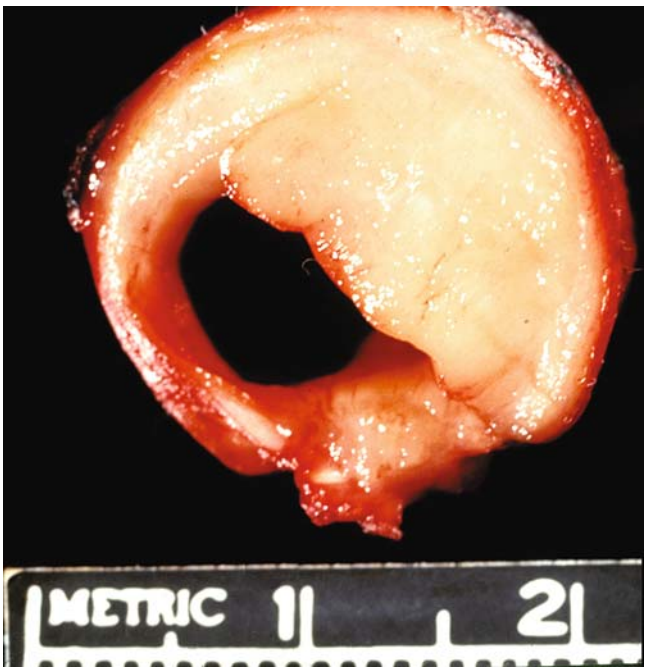

FIGURE 9.2 Gross appearance of an adenoid cystic carcinoma in a major airway. Note significant concentric narrowing of the lumen by an expanding tumor mass showing a pale yellow smooth cut surface (Courtesy of Dr. Eugene J. Mark, Massachusetts General Hospital, Boston, MA). From Tomashefski et al, with permission from Springer (see chapter references for complete citation).

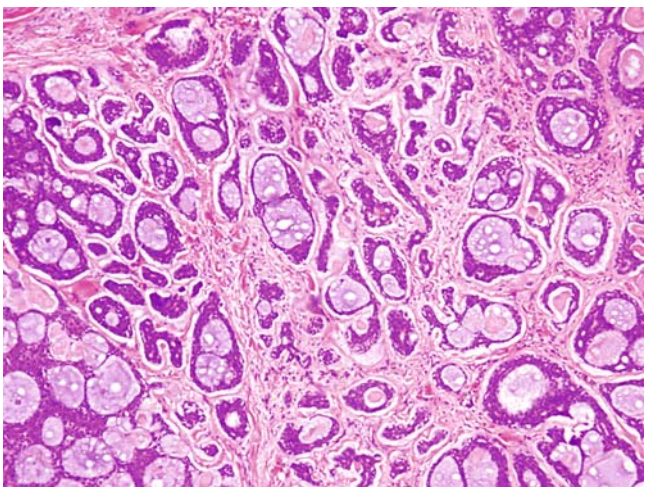

FIGURE 9.3 Adenoid cystic carcinoma, intermediate power microscopic view showing cylinder-shaped mucoid and basement membrane-like material surrounded by small, hyperchromatic, angulated epithelial cells. Hematoxylin and eosin. From Tomashefski et al, with permission from Springer (see chapter references for complete citation).

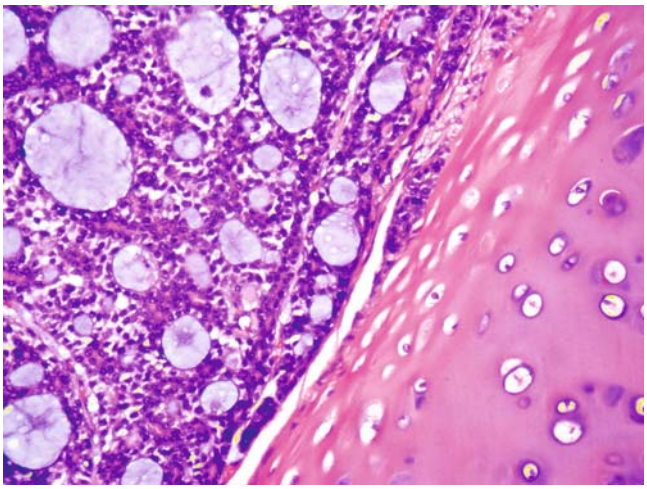

FIGURE 9.4 In this microscopic view, adenoid cystic carcinoma is next to a plate of bronchial cartilage but does not invade it. Hematoxylin and eosin. From Tomashefski et al, with permission from Springer (see chapter references for complete citation).

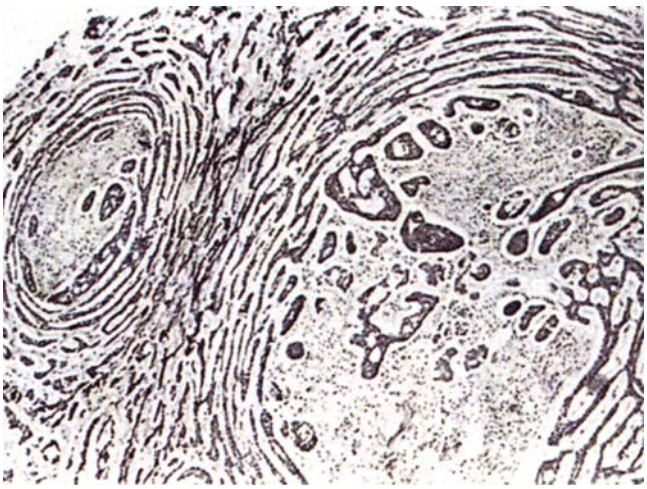

FIGURE 9.5 Microscopic view. Adenoid cystic carcinoma showing typical peri- and intraneural invasion by tumor cells. Hematoxylin and eosin. From Tomashefski et al, with permission from Springer (see chapter references for complete citation).

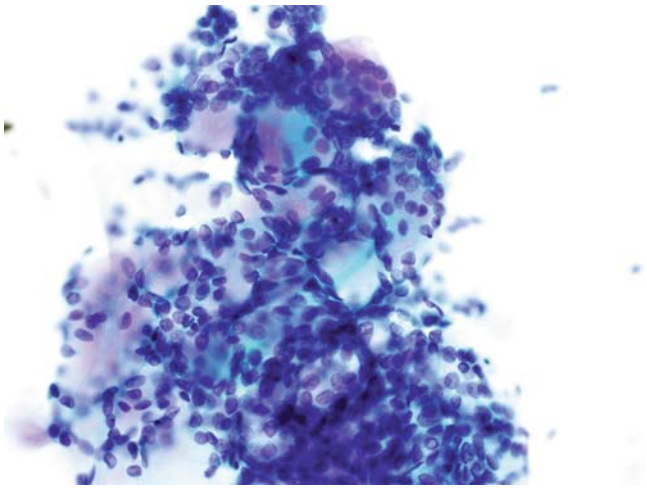

FIGURE 9.6 Adenoid cystic carcinoma, cytologic preparation. Three-dimensional microacinar pattern with pink to pale opaque globules corresponding to basement membrane material. The nuclei are small and round without much nuclear pleomorphism. Papanicolaou stain.

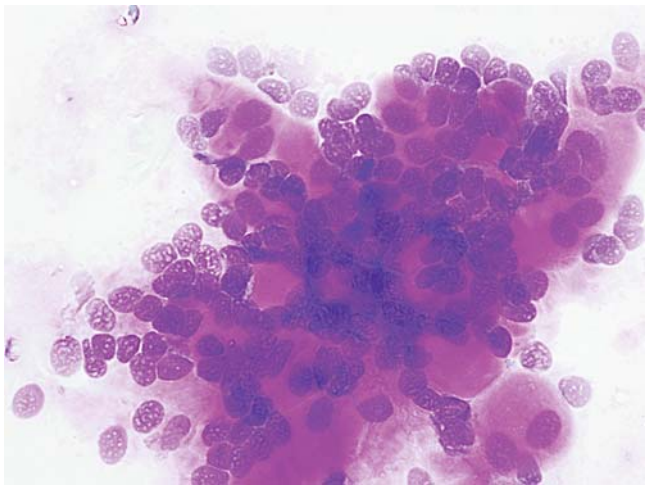

FIGURE 9.7 Adenoid cystic carcinoma, cytologic preparation showing well-rounded magenta-colored globular structures surrounding small cells with blue nuclei and scant cytoplasm. Diff Quick stain.

REFERENCES

- Dennie CJ, Coblentz CL. The trachea: pathologic conditions and trauma. *Can Assoc Radiol J*. 1993;44: 157–167.
- Duhamel DR. Adenoid cystic carcinoma Ch 6. In: Duhamel DR, Hamel JH, eds. *Clinical Atlas of Airways Diseases: Bronchoscopy, Radiology and Pathology*. Philadelphia: Elsevier Saunders; 2005:18–21.
- Fraire AE, Dail DH. Tracheobronchial (salivary type) gland tumors. In: Tomashefski JF Jr, Cagle PT, Farver CF, Fraire AE, eds. *Dail and Hammar's Pulmonary Pathology*. 3rd ed. Springer: Berlin, New York, Heidelberg; 2008:398–426.
- Manninen MP, Paakkala TA, Pukander IS, et al. Diagnosis of tracheal carcinoma at chest radiography. *Acta Radiol*. 1992;33:546–547.
- Fraser RS, Muller NS, Colman N, Pare PD, eds. *Fraser and Paré, Diagnosis of Diseases of the Chest*. 4th ed., Vol 1. Philadelphia, London, Toronto: WB Saunders Co.; 1999:2021–2053.
- Yousem SA, Nicholson AC. Adenoid cystic carcinoma. In: Travis WD, Brambilla E, Müller-Hermelink HK, Harris CC, eds.*World Health Organization Classification of Tumours. Pathology and Genetics of Tumours of the Lung, Pleura, Thymus and Heart*. Lyon: IARC Press; 2004:65–66.

CHAPTER 10

Inflammatory Polyps

Richard S. Irwin and Armando E. Fraire

More common in adults than in children, inflammatory tracheobronchial polyps represent uncommon but distinct non-neoplastic inflammatory lesions secondary to a variety of insults to the airways. These insults include aspiration of foreign bodies, mycobacterial infections, mechanical intubation, chronic smoke injury, and smoldering inflammatory disorders such as cystic fibrosis, bronchial asthma, and chronic tracheobronchitis. Most cases occurring in children are idiopathic. The lesion shown in Fig. 10.1 is solitary but some patients have multiple lesions. Complete collapse of the right lung may be the main chest radiographic findings in children. In children, air bronchograms may show abrupt cut of the right main bronchus unmasking the site of a polypoid-obstructing lesion. CT scan of chest may show volume loss and bronchiectatic changes with mucus plugging of dilated bronchi. Endoscopically, small single polyps may appear innocuous but some are susceptible to bleeding. Massive hemoptysis is an important complication requiring immediate intervention. Acute and chronic inflammation are the histopathologic hallmark of the lesion. Edema, capillary proliferation and squamous metaplasia of the surface epithelium are also seen. Overall, the appearance of these lesions is strikingly similar to granulation tissue. The cytopathology of these lesions is not known.

FIGURE 10.1 Endoscopic view of an inflammatory polyp of the trachea. Note tracheal ring and a small mound-like lesion on the mucosal surface. The surface of the lesion is smooth. From Tomashefski et al, with permission from Springer (see chapter references for complete citation).

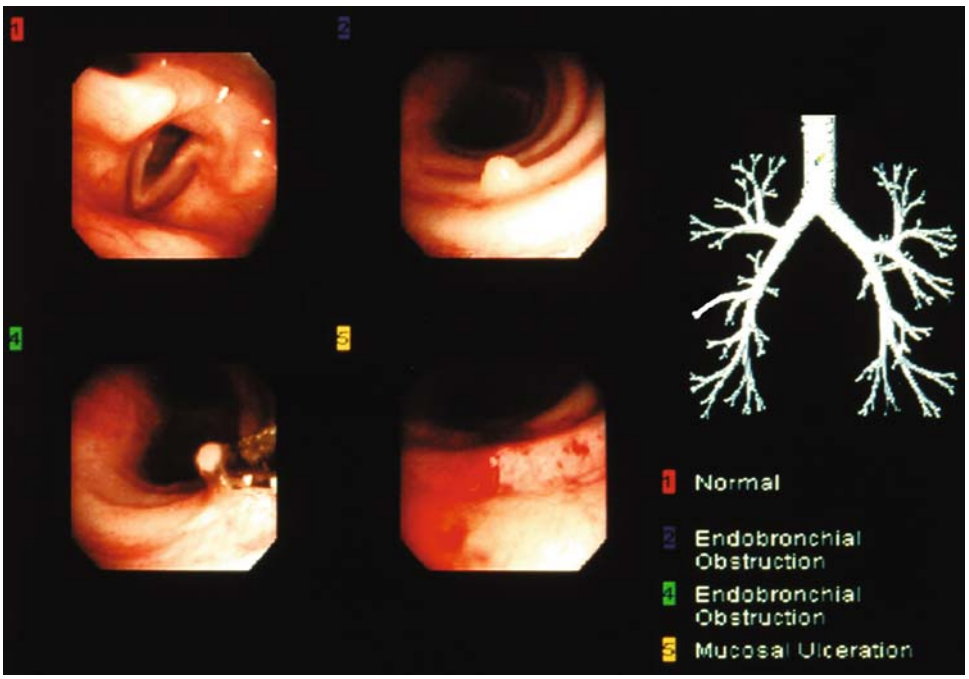

A.E. Fraire et al. (eds.), *Atlas of Neoplastic Pulmonary Disease*,
DOI 10.1007/978-0-387-89839-1_10, © Springer Science+Business Media, LLC 2010

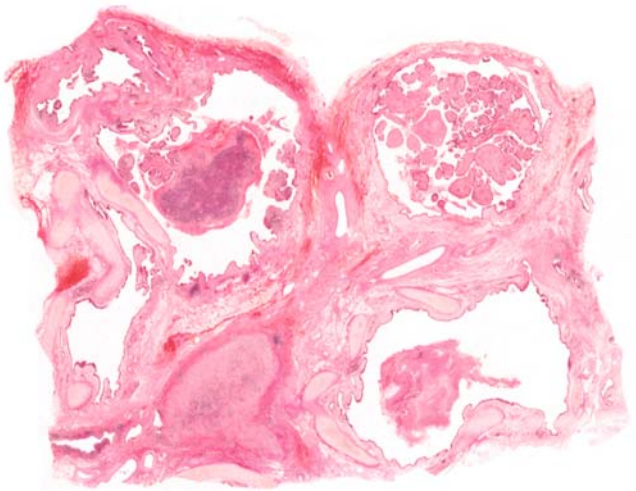

FIGURE 10.2 Subgross appearance of bronchiectatic airways containing multiple arborescent polypoid structures in the setting of bronchiectasis secondary to cystic fibrosis (Courtesy of Dr. Keith M. Kerr, Aberdeen Royal Infirmary, Aberdeen, Scotland). From Tomashefski et al, with permission from Springer (see chapter references for complete citation).

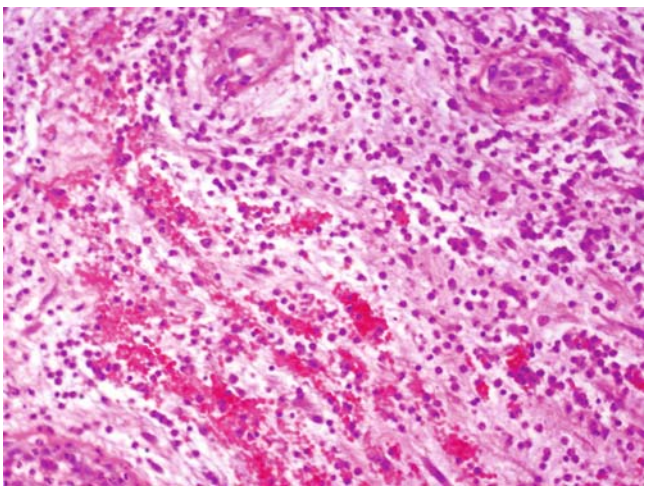

FIGURE 10.3 Microscopic view of an inflammatory polyp showing granulation-like tissue. Hematoxylin and eosin (Courtesy of Dr. Joseph Tomashefski, Jr., MetroHealth Medical Center, Cleveland, OH). From Tomashefski et al, with permission from Springer (see chapter references for complete citation).

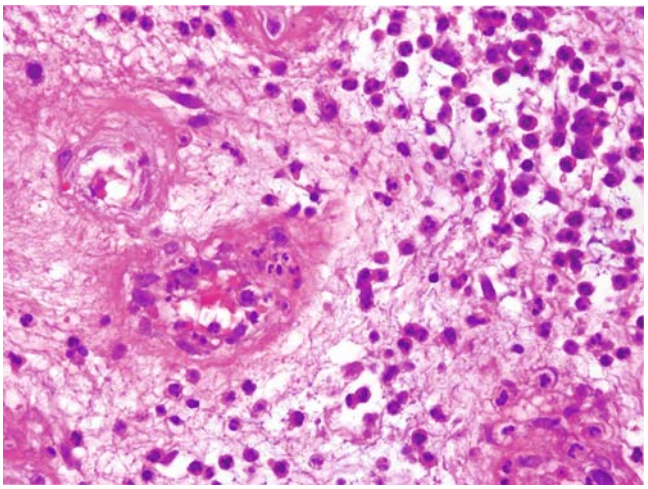

FIGURE 10.4 Microscopic view of an inflammatory polyp showing thick-walled capillaries surrounded by edematous tissue with mononuclear inflammatory cells. Hematoxylin and eosin (Courtesy of Dr. Joseph Tomashefski, Metrohealth Medical Center, Cleveland, OH). From Tomashefski et al, with permission from Springer (see chapter references for complete citation).

REFERENCES

- Fraire AE, Dail DH. Miscellaneous tumors and tumor like proliferations of the lung. In: Tomashefski JF, Cagle PT, Farver C, Fraire AE, eds. *Dail and Hammar's Pulmonary Pathology*. 3rd ed. Berlin, New York, Heidelberg: Springer; 2008:500–541.
- McShane D, Nicholson AG, Goldstraw P, et al. Inflammatory endobronchial polyps in childhood. *Pediatr Pulmonol.* 2002;34:79–84.
- Mittelman M, Fink G, Mor R, et al. Inflammatory bronchial polyps complicated by massive hemoptysis. *Eur J Respir Dis*. 1986;69:63–66.
- Niimi A, Amitami R, Ikeda T, et al. Inflammatory bronchial polyps associated with asthma: resolution with inhaled corticosteroids. *Eur Respir J*. 1995;8:1237–1239.
- Roberts C, Devenny AM, Brooker R, et al. Inflammatory endobronchial polyposis with bronchiectasis in cystic fibrosis. *Eur Respir J*. 2001;18:612–615.
- Snow N, Fratianne RB. Obstructing endobronchial inflammatory polyps: treatment and urgent laser photo ablation. *Trauma.* 2001;150:753–754.
- Yamagishi M, Harada H, Kurihara M, et al. Inflammatory endotracheal polyp resolved after antibiotic treatment. *Respiration*. 1993;60:193–196.

CHAPTER 11

Inflammatory Pseudotumor

Philip T. Cagle, Timothy C. Allen, and Armando E. Fraire

Two variants of this still poorly understood pulmonary lesion are recognized: an adult, most likely non-neoplastic variant, and a variant much more prone to occur in younger individuals, most likely neoplastic. The first variant, illustrated here, is widely believed to be the result of an unresolved inflammatory process similar in some respects to a localized form of organizing pneumonia. Features supporting a neoplastic nature for the second variant are its propensity to involve neighboring structures, cellular atypia, myofibroblastic proliferation, and immunopositivity for ALK-1 and p80. The main histopathologic characteristic of the adult form is the presence of spaces filled by plump fibroblasts without atypia and foamy histiocytes. Radiographic appearances on chest films vary from nodular to diffuse lung lesions. The endoscopic and cytopathologic features of inflammatory pseudotumors are not well defined.

FIGURE 11.1 Inflammatory pseudotumor, gross appearance. Note tumor with a yellow tan discoloration (Courtesy of Dr. Eugene Mark, Massachusetts General Hospital, Boston, MA). From Tomashefski et al, with permission from Springer (see chapter references for complete citation).

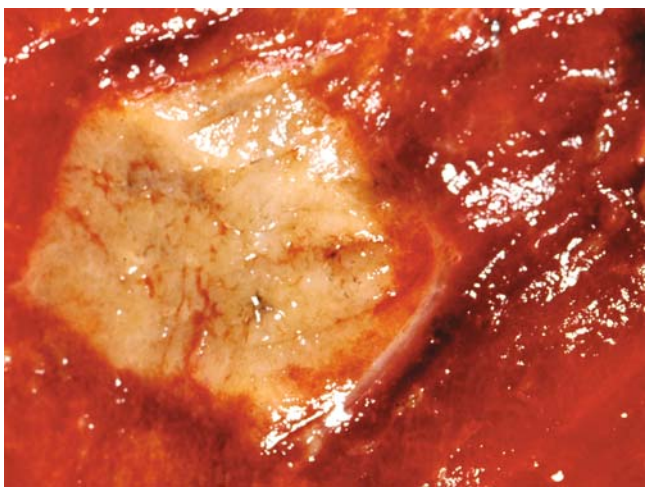

FIGURE 11.2 Inflammatory pseudotumor, microscopic view. Note fibroblastic pattern showing spindle-shaped cells in a collagenized stroma. Hematoxylin and eosin. From Tomashefski et al, with permission from Springer (see chapter references for complete citation).

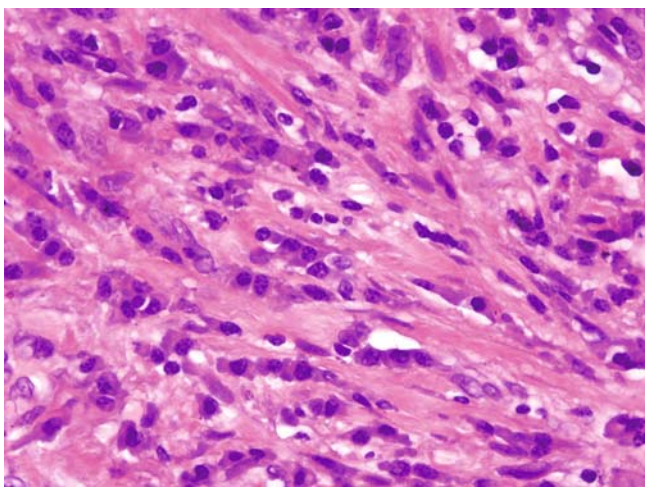

A.E. Fraire et al. (eds.), *Atlas of Neoplastic Pulmonary Disease*,
DOI 10.1007/978-0-387-89839-1_11, © Springer Science+Business Media, LLC 2010

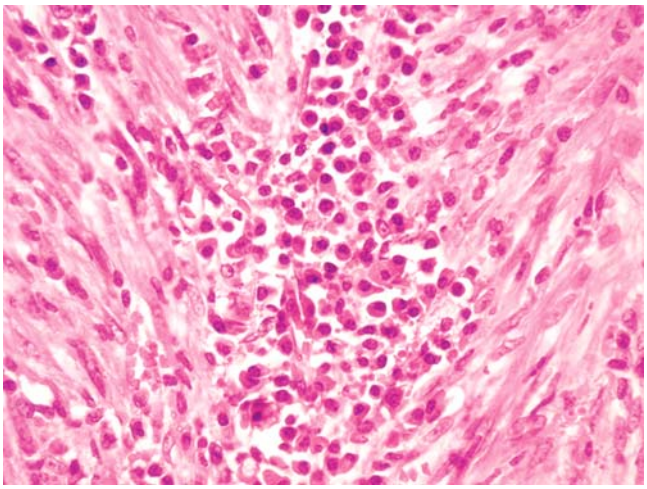

FIGURE 11.3 Inflammatory pseudotumor; microscopic view showing a plasma cell granuloma pattern. In this pattern, small round cells, chiefly lymphocytes, and plasma cells predominate. Hematoxylin and eosin. From Tomashefski et al, with permission from Springer (see chapter references for complete citation).

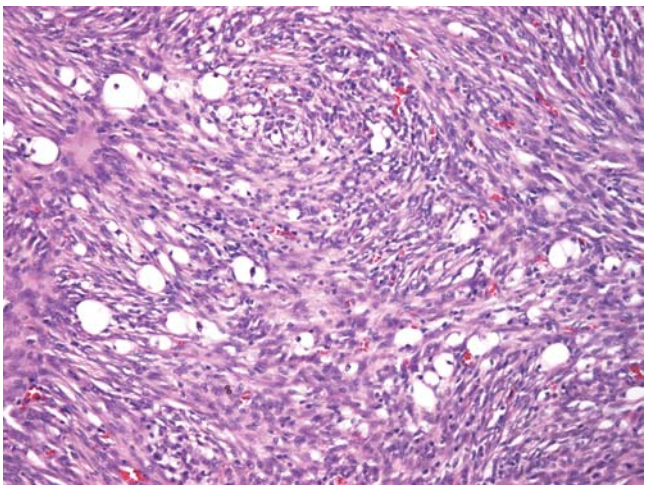

FIGURE 11.4 This microscopic view of an inflammatory pseudotumor shows fascicles of spindle-shaped fibroblastic cells mixed with lymphocytes, foamy macrophages, and plasma cells. This pattern is a mixed form of the patterns shown in the two previous images. Hematoxylin and eosin.

REFERENCES

- Agrons GA, Rosado-de-Christensen, Kirejczyk WM, et al. Pulmonary inflammatory pseudotumor: radiologic features. *Radiology*. 1998;206:511–518.
- Anthony PP. Inflammatory pseudotumor (plasma cell granuloma) of lung, liver and other organs. *Histopathology*. 1993;23:501–503.
- Cerfolio RJ, Allen MS, Nascimento AG, et al. Inflammatory pseudotumors of the lung. *Ann Thorac Surg*. 1999;67:933–936.
- Fraire AE. Non malignant versus malignant proliferations on lung biopsy. In: Cagle PT, ed. *Diagnostic Pulmonary Pathology*. New York: Marcel-Dekker; 2000:525–545.
- Fraire AE, Dail DH. Mesenchymal tumors, Part I: Tumors of fibrous, fibrohistiocytic and muscle origin. In: Tomashefski JF, Cagle PT, Farver C, Fraire AE, eds. *Pulmonary Pathology*. 3rd ed. Berlin, New York, Heidelberg: Springer; 2008:427–461.
- Hedlund GL, Navoy JE, Gallianai CA, et al. Aggressive manifestations of inflammatory pulmonary pseudotumor in children. *Pediatr Radiol*. 1999;29:112–116.
- Ledet SC, Brown RW, Cagle PT. P53 immunostaining in the differentiation of inflammatory pseudotumor involving the lung. *Modern Pathol*. 1995;8:282–286.
- Matsubara O, Mark EJ, Ritter JH. Pseudoneoplastic lesions of the lungs, pleural surfaces and medistinum. In: Wick MR, Humphrey PA, Ritter JH, eds. *Pathology of Pseudoneoplastic Lesions*. Philadelphia: Lippincott-Raven; 1999:97–129.

CHAPTER 12

Pulmonary Chondroma

Armin Ernst, Philip T. Cagle, Timothy C. Allen, and Armando E. Fraire

Chondromas are tumors of the lung and the airways which are made entirely of benign cartilage and by definition, lacking entirely of fat, muscle, or bone. Their true frequency is not known since hamartomas with major cartilaginous components are likely to have been misclassified in the past as chondromas. In addition to the lung, they occur in the larynx, trachea, and major bronchi. Primary chondrosarcomas of the lung do occur but are exceedingly uncommon.

Chondromas are tumors of younger individuals, primarily women, occurring sometimes in the setting of the Carney Triad (pulmonary chondromas, gastrointestinal tumors, and extra-adrenal paragangliomas). Like their closely related hamartomas, chondromas show internal calcific foci that are visible on radiography of the chest. Chondromas of the trachea tend to be small, without compromising the integrity of the wall or limiting the caliber of the airway. As a result, they tend to be minimal or non-symptomatic. Chondromas occurring in the setting of the Carney Triad are said to be sharply circumscribed and in contrast to hamartomas tend to lack internal clefts lined by alveolar epithelium. Cytologic features of chondroma have not been well described but would be expected to include the presence of benign chondrocytes in a hyaline matrix, similar to that seen in hamartomas.

FIGURE 12.1 This endoscopic view of the trachea shows a couple of nodular protuberances on the inner surface of the tracheal wall corresponding to chondromas. Chondromas are generally limited to the tracheal rings and are generally asymptomatic unless they achieve a large size.

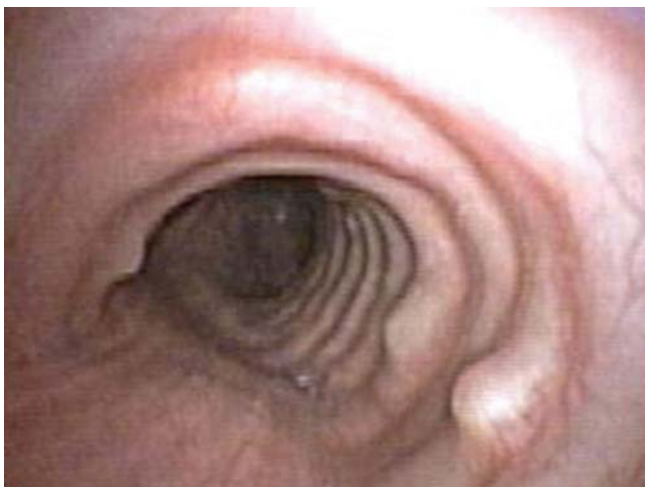

FIGURE 12.2 Chondroma; endobronchial gross appearance of a chondroma within a bronchiectatic airway (Courtesy of Dr. JF Tomashefski, Jr, Metrohealth Medical Center, Cleveland, OH). With permission from Springer (see chapter references for complete citation).

A.E. Fraire et al. (eds.), *Atlas of Neoplastic Pulmonary Disease*,
DOI 10.1007/978-0-387-89839-1_12, © Springer Science+Business Media, LLC 2010

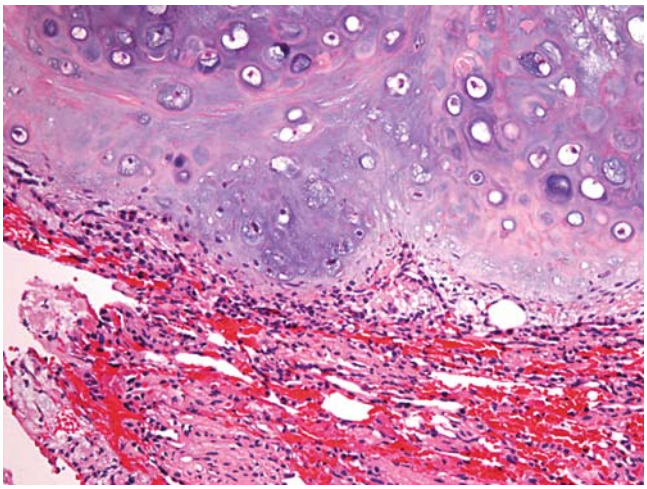

FIGURE 12.3 Chondroma; microscopic view showing demarcated lobules of mature cartilage. Individual chondrocytes lie within lacunar spaces. Next to chondroma is compressed lung parenchyma. Hematoxylin and eosin.

REFERENCES

- Fletcher JA, Longtine J, Wallace K, et al. Cytogenetic and histologic findings in 17 pulmonary chondroid hamartomas. Evidence for a pathogenetic relationship with lipomas and leiomyomas. *Genes Chromosomes Cancer*. 1995;12:220–223.
- Flieder DB. Ch 32 Benign neoplasms of the lungs. In: Zander DS, Farver CF, Chief Editors. *Pulmonary Pathology*. Philadelphia: Churchill, Livingstone, Elsevier; 2008:669–672.
- Fraire AE, Dail DH. Ch 40. Mesenchymal tumors, part II: Tumors of hamartomatous, osteochondromatous, lipomatous, neural and vascular origin. In: Tomashefski JF, Cagle PT, Farver C, Fraire AE, eds. *Dail and Hammars Pulmonary Pathology*. 3rd ed. Berlin, New York, Heidelberg: Springer; 2008:462–499.
- Huang H-Y, Hsieh M-J, Chen W-J, et al. Primary mesenchymal chondrosarcoma of the lung. *Ann Thorac Surg*. 2002;73:1960–1962.
- McDonald JR, Harrington SW, Clagett OT. Hamartoma (often called chondroma) of the lung. *J Thorac Cardiovasc Surg*. 1945;14:128–143.
- Mukensnabl P, Hadravska S. Unusual chondroid hamartoma. *Histopathology*. 2002;41(S1):110.
- Rodriguez FG, Tazelaar HD, Aubry MD, et al. Chondromas in Carney's triad are distinct from pulmonary hamartomas. *Mod Pathol*. 2005;18S:317A.

CHAPTER 13

Pulmonary Hamartoma

Richard S. Irwin, Armin Ernst, Shanda Blackmon, Philip T. Cagle,
Timothy C. Allen, Dina R. Mody, and Armando E. Fraire

Hamartomas are benign mesenchymal neoplasms containing tissues made up of cartilage, smooth muscle, and connective tissue. They occur in the trachea, bronchi, and the lung parenchymal tissues and are said to be the most common benign tumors of the lung. Hamartomas, particularly the intraparenchymal variants, are clinically silent in the majority of cases. However, the endobronchial ones present with varying degree of respiratory distress, depending on the degree of luminal obstruction. They often present on chest radiographs as solitary pulmonary nodules, ranging in size from less than 2 to 5 cm or more. The nodules are frequently calcified and show the typical "popcorn" appearance, owing to their lobulated contours. On computed tomography, fat or fat with calcification can be detected.

Endobronchial lesions may be pedunculated with a tan to pink surface. Luminal narrowing varies considerably but tends to be greater in patients with stridor and/or severe wheezing. Grossly, hamartomas usually present as lesions occurring endobronchially (or endotracheally) in about 10% of the cases and intraparenchymally in the remaining 90%. They generally range from 1 to 3 cm and are gray white in color, rubbery, and firm to palpation. The essential components of a hamartoma are lobulated aggregates of mature cartilage with mixed fat, smooth muscle fibers, and sometimes fibroconnective tissue. Cleft- or slit-like spaces lined by cuboidal to columnar respiratory epithelium may be seen between the cartilaginous lobules. Fine needle aspiration biopsy of pulmonary hamartoma is generally successful with sensitivity and specificity of 78% and 100%, respectively. The single most important cytopathologic feature is the presence of irreg-

FIGURE 13.1 Chest radiograph of pulmonary hamartoma. Note opaque round lesion in right mid-lung field. Three monitor electrode leads are also seen. From Tomashefski et al, with permission from Springer (see chapter references for complete citation).

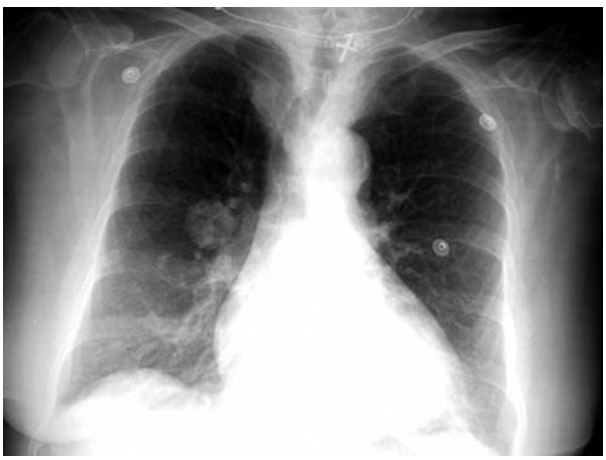

FIGURE 13.2 CT of chest. This centrally located hamartoma is adjacent to the right side of the trachea.

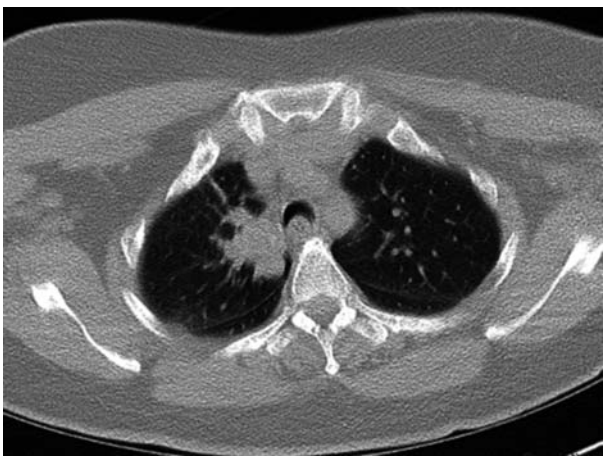

A.E. Fraire et al. (eds.), *Atlas of Neoplastic Pulmonary Disease*,
DOI 10.1007/978-0-387-89839-1_13, © Springer Science+Business Media, LLC 2010

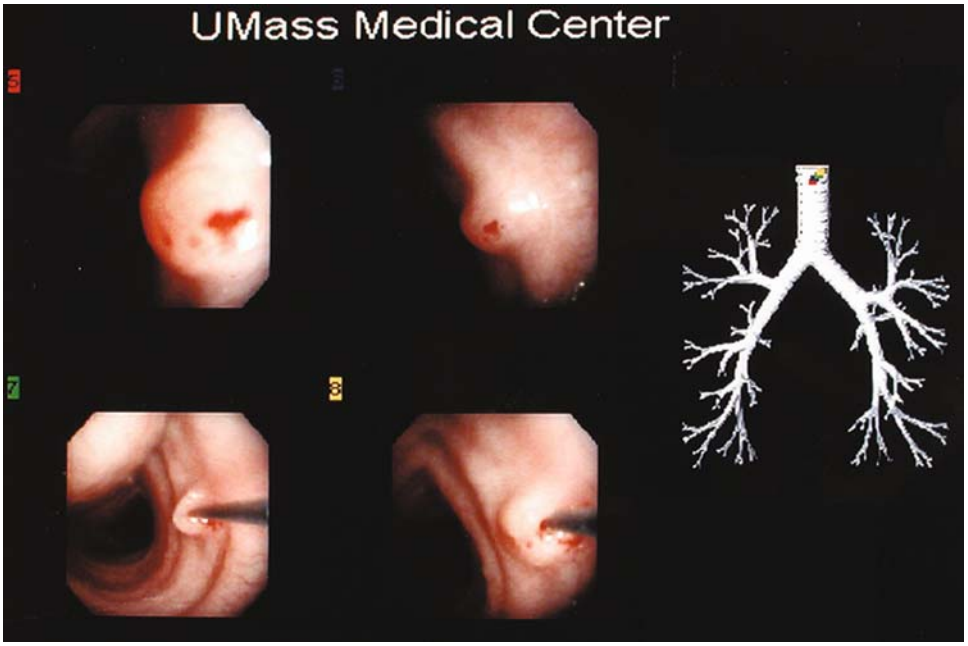

FIGURE 13.3 Endoscopic view of a small, endotracheal, spheroidal lesion covered by intact pinkish red respiratory mucosa. Note tracheal rings adjacent to the lesion. From Tomashefski et al, with permission from Springer (see chapter references for complete citation).

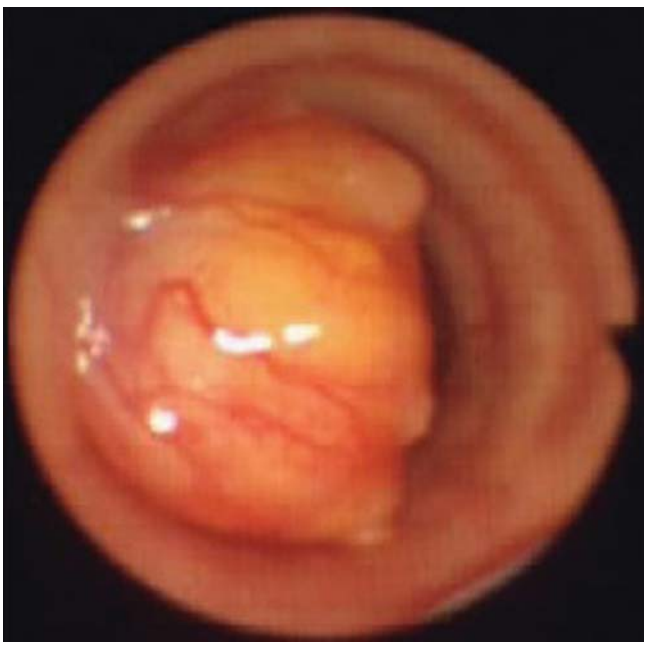

FIGURE 13.4 Endoscopic view of a much larger endotracheal hamartoma projecting into the tracheal lumen in a polypoid fashion. Note prominent tracheal rings adjacent to the lesion. As is the case with most tracheal hamartomas, this lesion was made primarily of mature cartilage.

FIGURE 13.5 This surgically resected parenchymal hamartoma shows a gray-white well-circumscribed mass lesion sharply contrasting with the adjacent brown lung tissue. From Tomashefski et al, with permission from Springer (see chapter references for complete citation).

ular fragments of deeply basophilic purplish blue chondroid/myxoid mesenchyme, at times with well-defined lacunae, containing bland-looking chondrocytes. Other features include bland spindle-shaped cells and equally bland glandular cells. Fat and calcific deposits may also occur but are less common. Cytologically, oval to round epithelial cells in a myxoid background are usually seen.

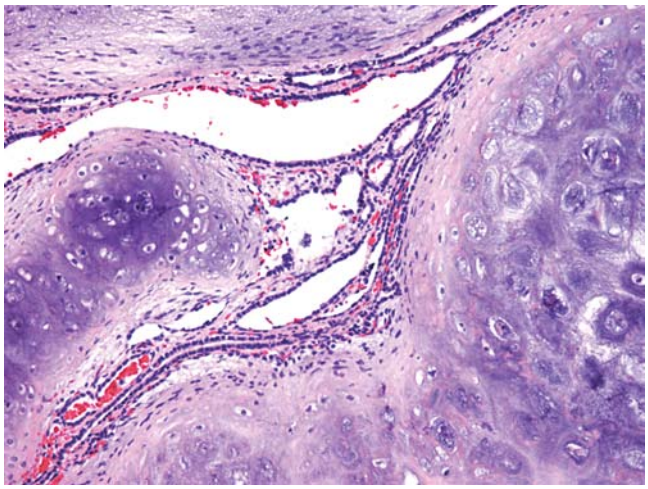

FIGURE 13.6 This microscopic view of a hamartoma shows mature lobules of cartilaginous tissue and epithelial lined clefts. Hematoxylin and eosin.

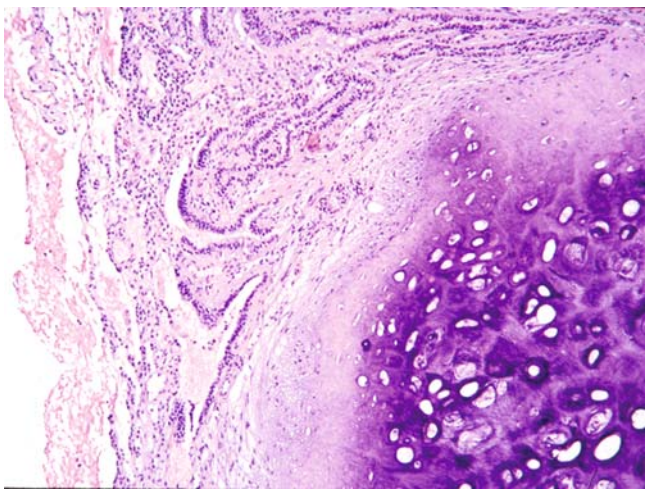

FIGURE 13.7 Another similar microscopic view of hamartoma showing more distinct rows of uniform cuboidal cells lining the epithelial clefts. Hematoxylin and eosin. From Tomashefski et al, with permission from Springer (see chapter references for complete citation).

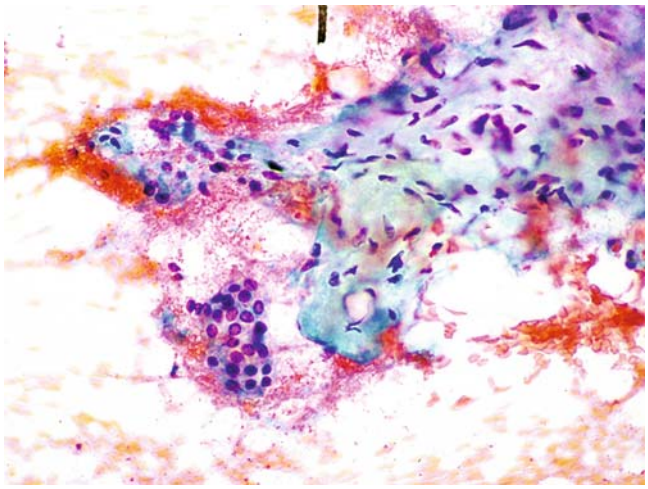

FIGURE 13.8 Cytologic preparation showing myxoid mesenchymal matrix and a group of small round epithelial cells. Papanicolaou stain (Courtesy of Dr. Andrew Fischer, University of Massachusetts Medical School, Worcester, MA). From Tomashefski et al, with permission from Springer (see chapter references for complete citation).

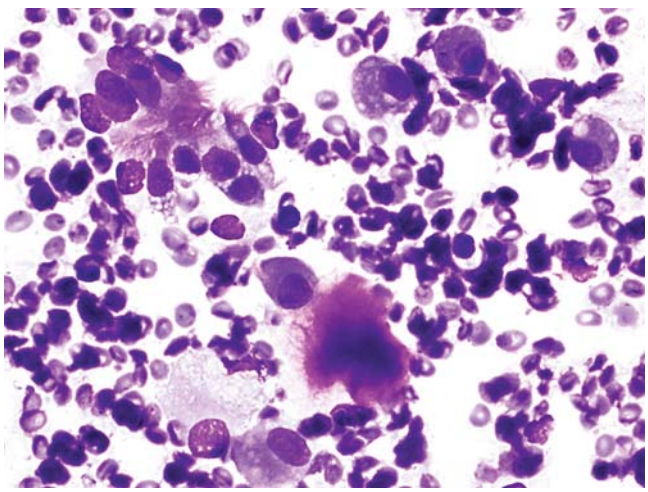

FIGURE 13.9 In this cytologic preparation of a hamartoma, mostly oval to round benign-looking epithelial cell are evident. Diff Quick Stain.

REFERENCES

- Fraire AE, Dail DH. Mesenchymal tumors, Part II: Tumors of hamartomatous Osteochondromatous, lipomatous, neural and vascular origin. In: Tomashefski JF Jr, Cagle PT, Farver CF, Fraire AE, eds. *Dail and Hammar's Pulmonary Pathology.* 3rd Ed. Berlin, New York, Heidelberg: Springer; 2008:462–499.
- French CA. Respiratory tract. In: Cibas ES, Ducataman BS, eds. *Cytology: Diagnostic Principles and Clinical Correlates*. Edinburgh, London, New York: Saunders; 2003:61–95.
- Nicholson AG, Tomashefski JF, Popper H. Hamartoma. In: Travis WD, Brambilla E, Müller-Hermelink HK, Harris CC, eds. *World Health Organization Classification of Tumours. Pathology and Genetics of Tumours of the Lung, Pleura, Thymus and Heart*. Lyon: IARC Press; 2004:113–114.
- Ohori NP. Ch 34. Uncommon endobronchial neoplasms. In: Cagle PT, ed. *Diagnostic Pulmonary*

Pathology. New York-Basel: Marcel Dekker, Inc.; 2000:685–717.
- Prince JS. Ch 24. Hamartoma. In: Duhamell DR, Harrell JH, eds. *Clinical Atlas of Airway Diseases: Bronchoscopy, Radiology and Pathology*. Philadelphia: Elsevier Saunders; 2005:85–86.
- Reittner P, Mueller NL. Tracheal hamartoma: CT findings in two patients. *J Comput Assis Tomogr*. 1999;23:957–958.
- Tomashefski JF. Benign endobronchial mesenchymal tumors. Their relationship to parenchymal hamartomas. *Am J Surg Pathol*. 1982;6:531–540.

CHAPTER 14

Localized Fibrous Tumor

Armin Ernst, Shanda Blackmon, Toshiaki Kawai, and Armando E. Fraire

Formerly believed to be mesotheliomas, localized or solitary fibrous tumors (LFTs) are rare tumors, most common in the pleura but also reported to involve the lung and other parts of the body. Patients with LFTs are usually middle aged but the overall age distribution is wide. Digital clubbing and pleural effusions may be seen. Their size is quite variable ranging from 1 to 2 cm to masses filling an entire hemithorax. This variation in size can be reflected in their radiographic appearance. Tumors larger than 10 cm may behave in a malignant fashion. Calcification occurs in a minority of the cases. Rarely, an LFT will grow into an airway and in those instances it will mimic a tumor of endobronchial or endotracheal origin. Microscopically, a hemangiopericytoma-like pattern and a cellular pattern may co-exist along with the more common "pattern-less" pattern. Fine needle aspirates show scant to variable cellularity, fragments of ropy collagen, and oval to spindly cells with bland-looking oval to round nuclei.

FIGURE 14.1 Localized fibrous tumor. Chest CT view. Note large extraparenchymal soft tissue mass with lobulated contours located in the upper part of the right hemithorax.

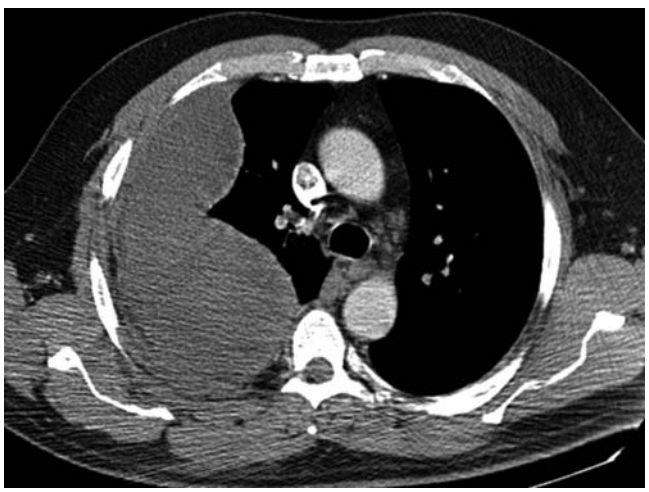

FIGURE 14.2 Localized fibrous tumor, endoscopic view. This 63-year-old non-smoking male presented with recurring right-sided pneumonia. At bronchoscopy an obstructing mass lesion was found in the right main stem bronchus. A biopsy revealed a localized fibrous tumor (Courtesy of Dr. Felix Herthe, Heidelberg, Germany).

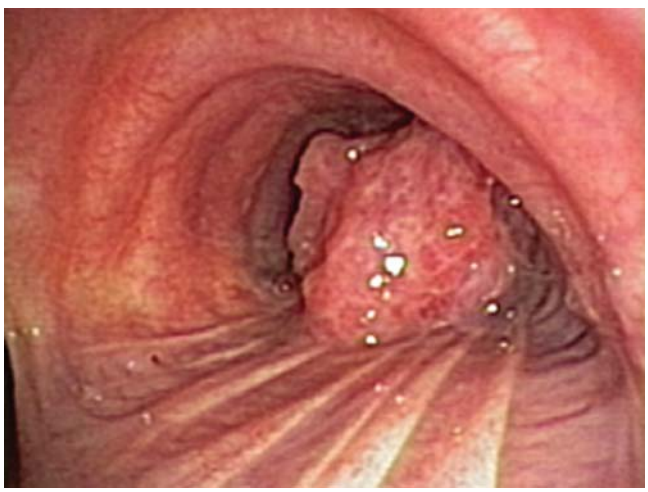

A.E. Fraire et al. (eds.), *Atlas of Neoplastic Pulmonary Disease*,
DOI 10.1007/978-0-387-89839-1_14, © Springer Science+Business Media, LLC 2010

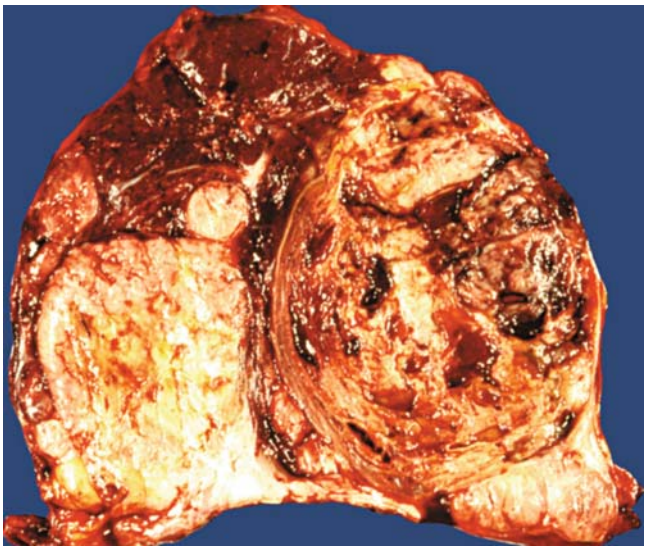

FIGURE 14.3 Localized fibrous tumor. This surgically resected tumor exceeded 10 cms in diameter and was entirely intrapulmonary. The tumor substance was firm but not hard. There was necrosis and hemorrhage within the tumor (From Yousem and Flynn with permission). From Tomashefski et al, with permission from Springer (see chapter references for complete citation).

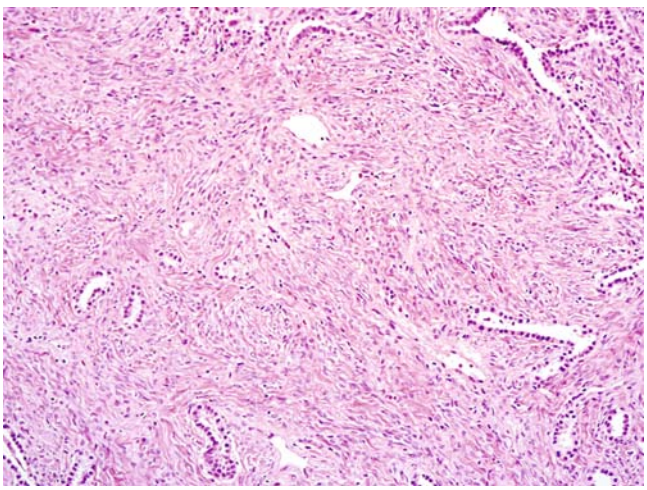

FIGURE 14.4 Localized fibrous tumor, low-power view. Note fibroblastic proliferation and multiple cleft-like spaces representing entrapped bronchiolar epithelium. Hematoxylin and eosin (From Yousem and Flynn with permission). From Tomashefski et al, with permission from Springer (see chapter references for complete citation).

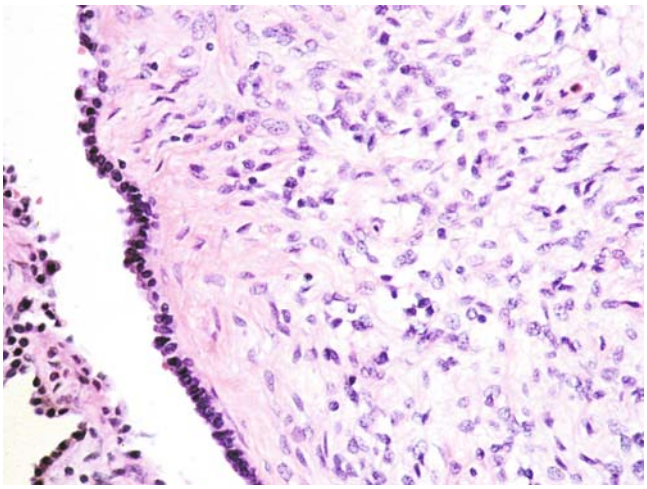

Figure 14.5 Localized fibrous tumor, closer view showing bronchiolar-like spaces within a fibroblastic proliferation showing the typical pattern-less pattern. Hematoxylin and eosin (From Yousem and Flynn with permission). From Tomashefski et al, with permission from Springer (see chapter references for complete citation).

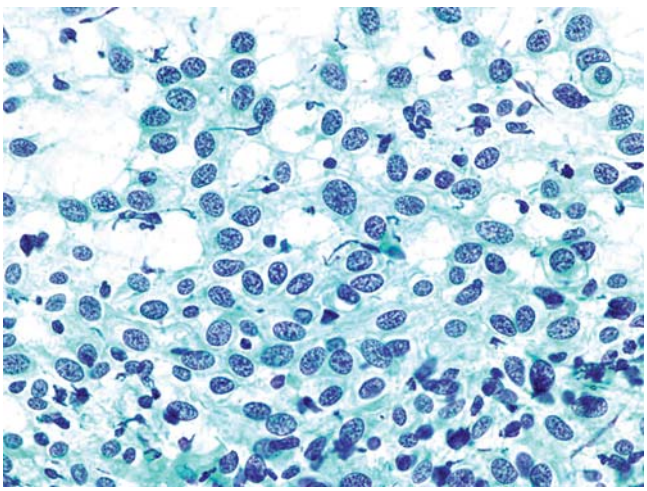

Figure 14.6 Localized fibrous tumor. Fine needle aspirate cytologic preparation. Note moderate cellularity, with bland-looking cells showing round to oval nuclei and a fair amount of cytoplasm. Papanicolaou stain.

REFERENCES

- Brunneman RB, Ro JY, Ordonez NG, et al. Extrapleural solitary fibrous tumor: a clinicopathologic study of 24 cases. *Mod Pathol*. 1999;12:1034–1042.
- Caruso RA, La Spada F, Gaeta M. Report of an intrapulmonary fibrous tumor: Fine needle aspiration cytologic findings, clinicopathological and immunohistochemical features. *Diagn Cytopathol*. 1996;14: 64–67.
- Fraire AE, Dail DH. Mesenchymal tumors, Part I: Tumors of fibrous, fibrohistiocytic and muscle origin. In: Tomashefski JF, Cagle PT, Farver CF, Fraire AE, eds. *Dail and Hammar's Pulmonary Pathology*. 3rd ed. Berlin, New York, Heidelberg: Springer; 2008:427–461.
- Guillou L, Fletcher JA, Fletcher CDM, et al. Extrapleural solitary fibrous tumour and hemangiopericytoma. In: Fletcher CDM, Unni KK, Mertens F, eds. *World Health Organization classification of Tumours. Pathology and Genetics. Tumors of Soft Tissue and Bone*. Lyon: IARC Press; 2002:86–90.
- Hasegawa T, Matsuno Y, Shimoda T, et al. Extrathoracic solitary fibrous tumors: their histological variability and potentially aggressive behavior. *Hum Pathol*. 1999;30:1464–1473.
- Laga AC, Allen TC, Cagle PT. Solitary fibrous tumor. In: Cagle PT, Editor-in-Chief. *Color Atlas and Text of Pulmonary Pathology*. 2nd ed. Philadelphia, Baltimore, New York: Wolters Kluwer Lippincott Williams and Wilkins; 2008:170–171.
- Okiki N, Bernatz PE, Woolner LB. Localized mesothelioma of the pleura. *J Thorac Cardiovasc Surg*. 1978;75:363–372.
- Van de Rijn M, Lombard CM, Rouse RV, et al. Expression of CD34 by solitary fibrous tumors of the pleura, mediastinum and lung. *Am J Surg Pathol*. 1994;18:814–820.
- Wick MR, Mills SE. Benign and borderline tumors of the lungs and pleura. In: Leslie KO, Wick MR, eds. *Practical Pulmonary Pathology*. Philadelphia, Edinburgh, London: Churchill Livingstone; 2005: 706–713.
- Yousem SA, Flynn SD. Intrapulmonary localized fibrous tumor (so-called localized fibrous tumor). *Am J Clin Pathol*. 1988;89:365–369.

CHAPTER 15

Lipomas and Liposarcomas

Richard S. Irwin, Ana Gimenez, and Armando E. Fraire

In contrast to lipomas of soft tissue, lipomas of the lung are distinctly rare. Most are endobronchial and few are parenchymal. About 100 cases have been described up to the mid-1990s. Lipomas occur primarily in men over the age of 40. If sufficiently large a lipoma may cause atelectasis or obstructive pneumonitis. The density of lipomas is about the same as water and this becomes manifest on CT of chest. Microscopically, the main constituent is mature fat. This may be lobulated. Cellular atypia is not commonly seen. As in the case of soft tissue lipomas, lesions with prominent vascular components (angiolipomas) do occur in the lung. One must be careful not to diagnose lipoma in a hamartoma showing an excess of mature fat. One excellent review of lipomas is provided by Moran et al. A unique case of a pulmonary liposarcoma was reported by one of us. In that case, the tumor tissue was lobulated and yellowish in color. Microscopically, bizarre gigantic lipoblasts with nuclear and cytoplasmic vacuolation were evident. Lipomas are usually resectable and their prognosis is favorable. Liposarcomas are malignant tumors and their outcome depends to a large degree on histologic grade and the extent of the tumor. The cytopathologic characteristic of fatty tumors of the lung is not known but is likely to be similar to that of fatty tumors occurring elsewhere.

Figure 15.1 Lipoma, endoscopic view. Note single smooth-surfaced pink-white sessile polypoid lesion. From Tomashefski et al, with permission from Springer (see chapter references for complete citation).

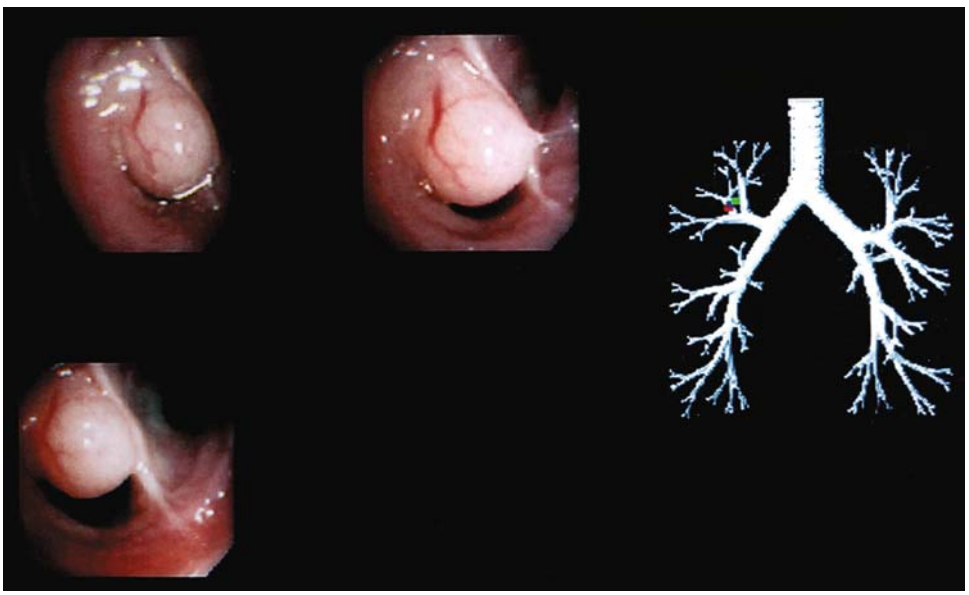

A.E. Fraire et al. (eds.), *Atlas of Neoplastic Pulmonary Disease*,
DOI 10.1007/978-0-387-89839-1_15, © Springer Science+Business Media, LLC 2010

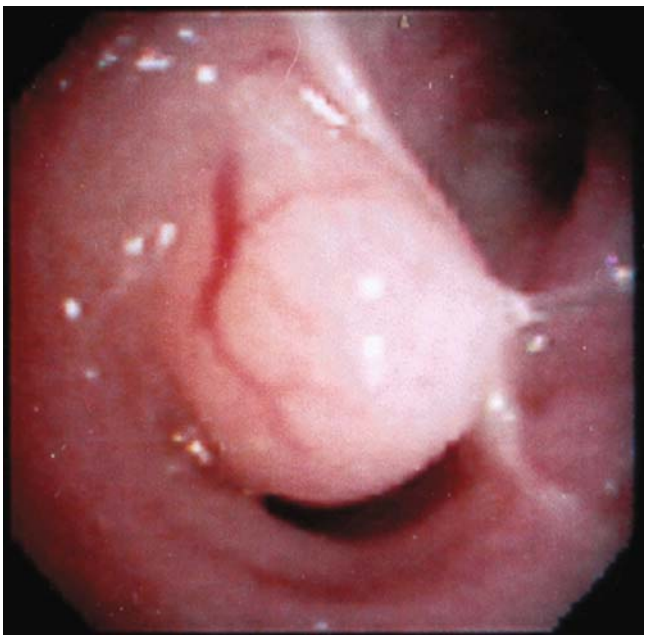

Figure 15.2 Closer endoscopic view of the lipoma shown in the preceding illustration. In areas, the lesion is nearly translucent. From Tomashefski et al, with permission from Springer (see chapter references for complete citation).

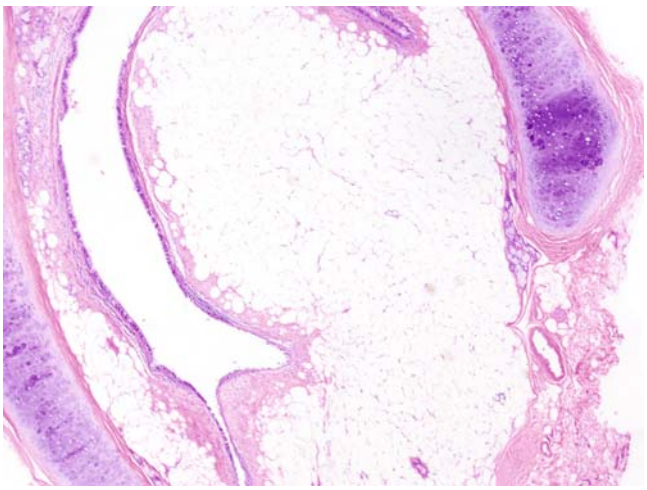

Figure 15.3 Microscopic view of an endobronchial lipoma. Note polypoid lesion projecting into the lumen. The lesion is entirely made of mature fat and is covered by respiratory mucosa. Hematoxylin and eosin. From Tomashefski et al, with permission from Springer (see chapter references for complete citation).

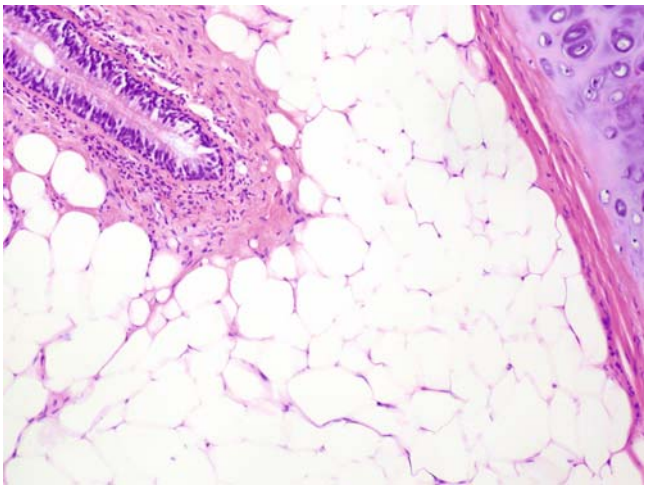

Figure 15.4 Closer microscopic view of the preceding lipoma. Note mature quality of the adipocytes. Hematoxylin and eosin. From Tomashefski et al, with permission from Springer (see chapter references for complete citation).

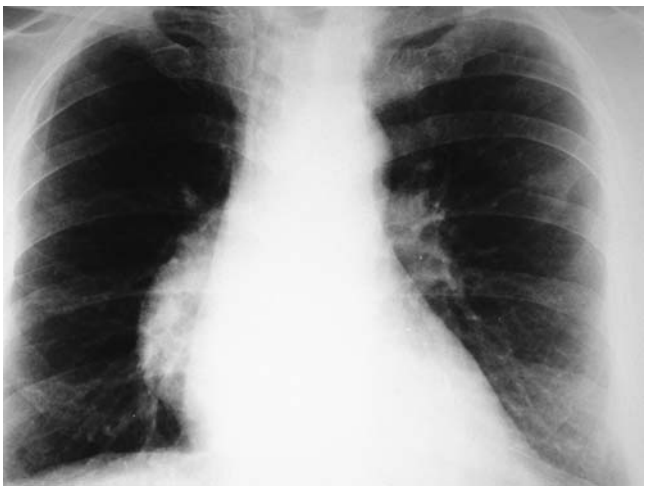

Figure 15.5 Liposarcoma. Posteroanterior radiographic view of chest showing a large mass in the right lower lobe (Reproduced with permission from Radiographics).

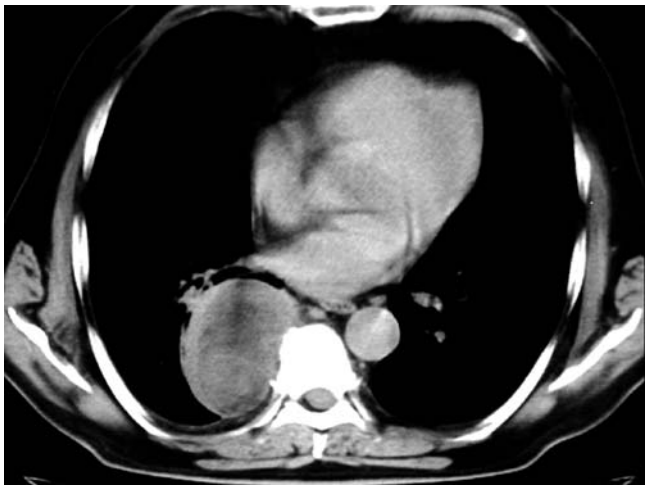

Figure 15.6 Liposarcoma. CT image showing heterogenous right tumor mass with areas of attenuation (Reproduced with permission from Radiographics).

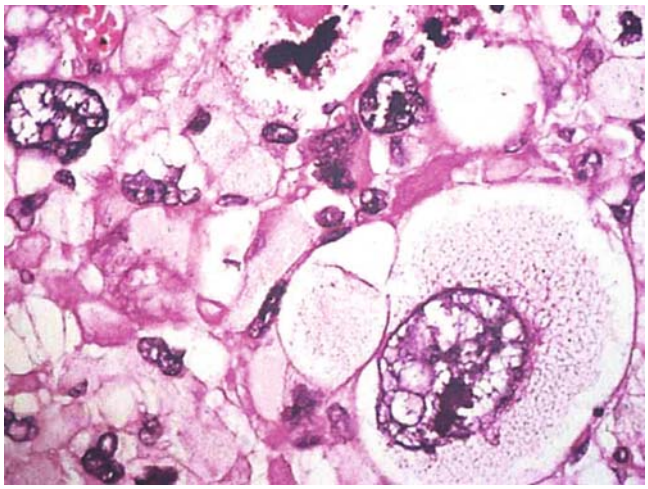

Figure 15.8 Liposarcoma. Microscopic view. Note bizarre gigantic lipoblasts with nuclear and cytoplasmic vacuolization. Hematoxylin and eosin (Reproduced with permission from Radiographics).

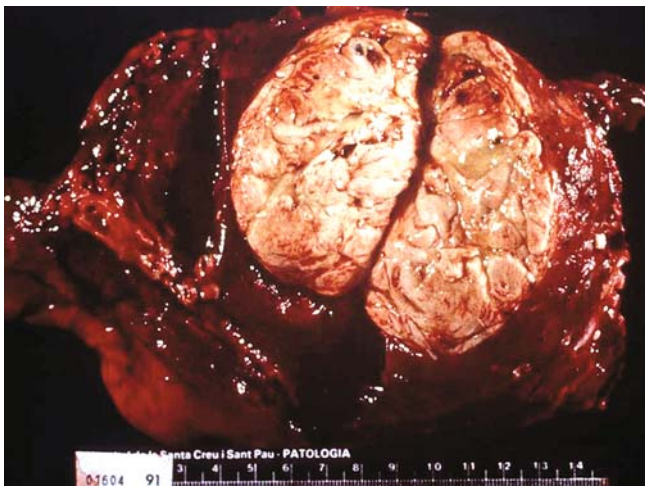

Figure 15.7 Liposarcoma. Surgically resected mass showing a yellowish lobulated cut surface reflecting high fat content (Reproduced with permission from Radiographics).

REFERENCES

- Bango A, Colubs L, Molinos L, et al. Endobronchial lipomas. *Respiration*. 1993;60:297–301.
- Fraire AE, Dail DH. Mesenchymal tumors, Part II: Tumors of hamartomatous, osteochondromatous, lipomatous, neural and vascular origin. In: Tomashefski J, Cagle PT, Farver C, Fraire AE, eds. *Pulmonary Pathology*. 3rd ed. Berlin, New York, Heidelberg: Springer-Verlag; 2008:462–499.
- Fraser RS, Müller NL, Colman N, Paré PD, eds. *Fraser and Paré's Diagnosis of Diseases of the Chest*. 4th ed. Philadelphia, London, Toronto: WB Saunders Co; 1999:386.
- Gimenez A, Franquet T, Prats R, et al. Unusual primary lung tumors: A radiologic-pathologic overview. *Radiographics*. 2002;22:601–619.
- Guinee DG, Thornberry DS, Azumi N, et al. Unique pulmonary presentation of an angiolipoma. Analysis of clinical, radiographic and histopathologic features. *Amer J Surg Pathol*. 1995;19:476–480.
- Moran CA, Suster S, Koss MN. Endobronchial lipomas: A clinicopathologic study of four cases. *Mod Pathol*. 1994;7:212–214.
- Palvio D, Egeblad K, Paulsen SM. Atypical lipomatous hamartoma of the lung. *Virchows Arch* [*Pathol Anat*]. 1985;405:253–261.
- Politis J, Funahashi A, Gehisen J, et al. Intrathoracic lipomas: Report of three cases and review of the literature with emphasis on endobronchial lipomas. *J Thorac Cardiovasc Surg*. 1979;77:550–556.
- Schraufnagel DE, Morin JE, Wang NS. Endobronchial lipoma. *Chest*. 1979;75:97–99.

CHAPTER 16

Cystic Lymphangioma

Shylashree Chikkamuniyappa, Josephine Heim-Hall, Jaishree Jagirdar, and Armando E. Fraire

Although not strictly a neoplasm, cystic lymphangiomas of the lung present as space-occupying tumor masses causing symptoms related to displacement of normal structures and/or obstruction of the airways or chylothorax secondary to blockage of lymphatic channels. Lymphangiomas are more common in the neck where they are known as cystic hygromas. On CT of the chest, they present as well-defined nodular densities. While lymphangiomas may also occur in the airways, their endoscopic features have not been well characterized.

Grossly, the lesion illustrated in this chapter had a bluish glistening cut surface. The main microscopic feature is cystic spaces of variable size lined by flat endothelial linings. Vascular markers such as CD31 and CD34 and cytokeratin are helpful in separating cystic lymphangiomas from bronchogenic cysts or other epithelial-lined cystic lesions of the lung. Cytopathology does not appear to play a role in the diagnosis of these lesions, although parenchymal lesions impinging on large airways may be accessible to the bronchoscope and brush or wash cytologic techniques. The prognosis is favorable. Surgical resection and/or sclerotherapy are said to be curative.

FIGURE 16.1 Lymphangioma. CT of chest showing well-defined homogeneous nodular density in the posterior segment of the lower lobe of the right lung (Reproduced with permission from the Scientific World Journal).

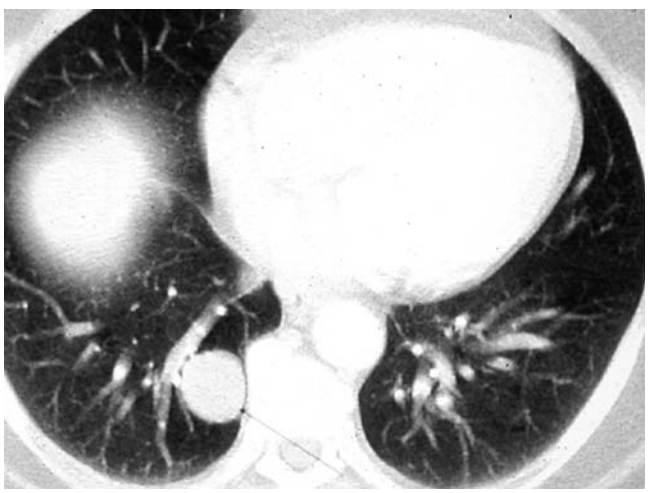

FIGURE 16.2 Lymphangioma. Gross specimen of surgically resected mass lesion. On cut surface, the lesion was well demarcated and had a dark bluish glistening appearance. The surrounding lung is not remarkable (Reproduced with permission from the Scientific World Journal).

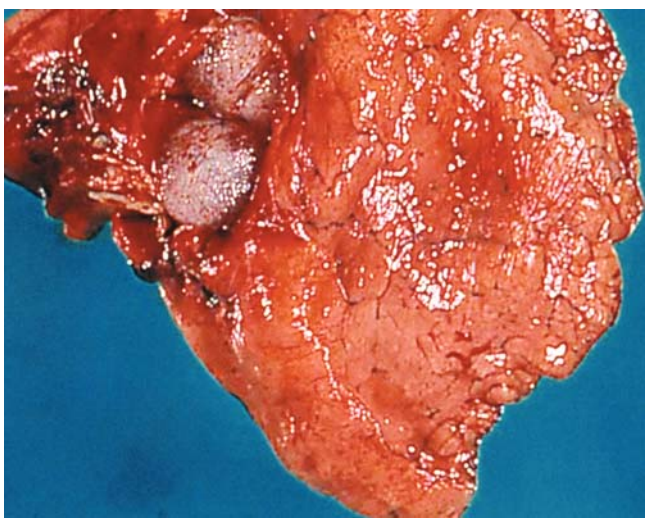

A.E. Fraire et al. (eds.), *Atlas of Neoplastic Pulmonary Disease*,
DOI 10.1007/978-0-387-89839-1_16, © Springer Science+Business Media, LLC 2010

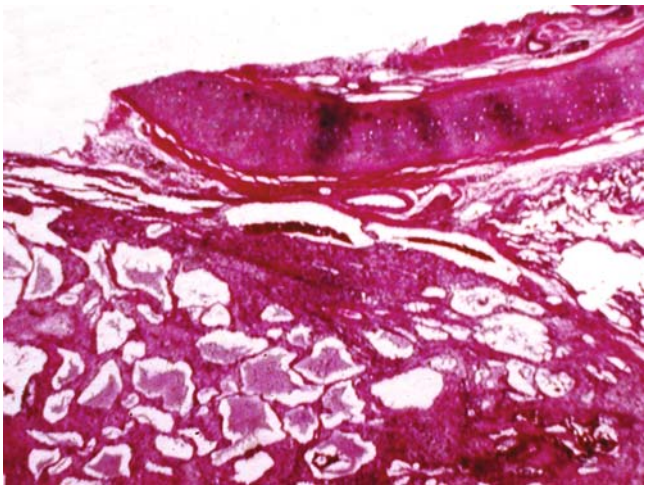

FIGURE 16.3 Lymphangioma. Microscopic view showing cystic spaces of variable size separated from one another by thin fibrous bands. Hematoxylin and eosin (Reproduced with permission from the Scientific World Journal).

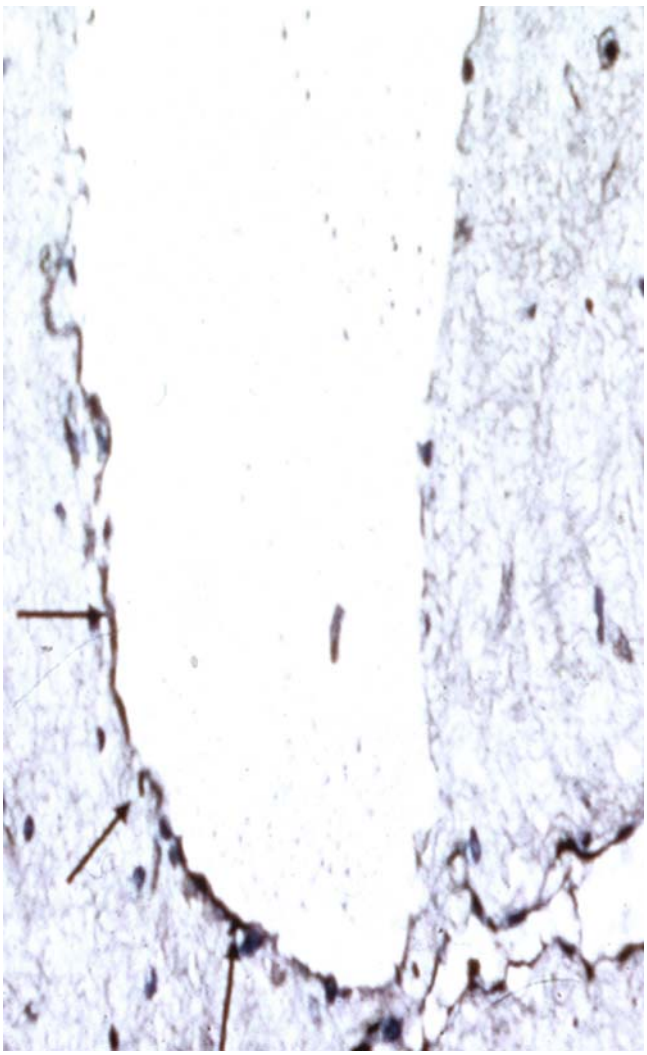

FIGURE 16.4 Lymphangioma. Immunostain for CD31 showing flat endothelial cells with positive immunoreactivity (*arrows*) (Reproduced with permission from the Scientific World Journal).

REFERENCES

- Brown M, Pysher T, Coffin CM. Lymphangioma and congenital pulmonary lymphangiectasis: A histologic, immunohistochemical and clinicopathologic comparison. *Mod Pathol.* 1999;12:569–575.
- Chikkamuniyappa S, Heim-Hall J, Jajirdar J. Solitary endobronchial lymphangioma: A case report and review of the literature. *Scientific World Journal.* 2005;5:103–108.
- Fraire AE, Dail DH. Mesenchymal tumors, Part II: Tumors of hamartomatous, osteochondromatous, lipomatous, neural and vascular origin. In: Tomashefski J, Cagle PT, Farver C, Fraire AE, eds. *Pulmonary Pathology*. 3rd ed. Berlin, New York, Heidelberg: Springer-Verlag; 2008:462–499.
- Kim WS, Lee KS, Kim I, et al. Cystic intrapulmonary lymphangioma: HRCT findings. *Pediatr Radiol.* 1995;25:206–207.
- Langer JC, Fitzgerald PG, Desa D, et al. Cervical cystic hygroma in the fetus: Clinical spectrum and outcome. *J Pediatr Surg.* 1990;25:58–61.
- Sanlialp I, Karnak I, Tanyel FC, et al. Sclerotherapy for lymphangioma in children. *Int J Pediatr Otorhinolaryngol.* 2003;67:795–800.
- Takahara T, Morisaki Y, Torigoe T, et al. Intrapulmonary cystic lymphangioma: report of a case. *Surg Today.* 1998;28:1310–1312.

CHAPTER 17

Lymphangioleiomyomatosis

Helmut H. Popper, Nader Morad, Issam A. Al-Bozom, Imaad Bin Mujeeb, and Armando E. Fraire

A unique disorder, lymphangioleiomyomatosis (LAM) is characterized by proliferation of small myoid cells with formation of numerous cystic spaces that greatly distort the normal architecture of the lung. Currently, LAM is regarded as a member of the family of PEComas (tumors derived from perivascular epithelial cells) and is closely associated with tuberous sclerosis, multifocal micronodular pneumocyte hyperplasia, and angiomyolipomas of the kidney.

LAM is essentially a disease of women with only rare cases reported in men. Clinical presentation is insidious with increasing shortness of breath, cough, episodes of pneumothorax, and, in some patients, chylothorax. The radiological hallmark of the disease is a striking cystic change of the lungs, a change that reflects gross architectural distortion of the lung parenchyma. Microscopically, multiple haphazardly distributed groups of small spindle cells representing smooth muscle cells are seen in combination with cystically dilated spaces of varying sizes. These lesional cells are also known as myoid or LAM cells. The myoid cells are usually seen around bronchioles and lymphocytes but also in the pleura and interlobular septa. A prognostic score based on the extent of cysts and groups of myoid cells has been devised. The cells are immunoreactive for estrogen receptor and HMB-45, a marker of melanocytic differentiation. LAM can be diagnosed cytopathologically. The main cytopathologic findings on fine needle aspirates are cohesive clusters of myoid cells in a lymphocyte-rich background.

FIGURE 17.1 Lymphangioleiomyomatosis in tuberous sclerosis. High-resolution computed tomographs of chest. Note numerous cysts throughout both lungs (Reproduced with permission from the Radiological Society of North America).

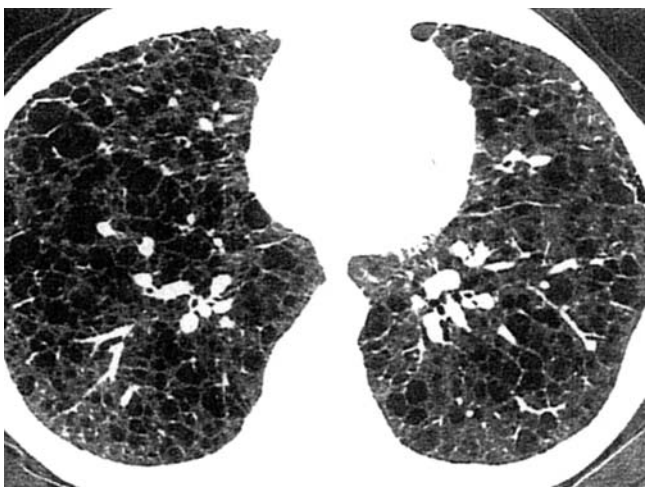

FIGURE 17.2 Lymphangioleiomyomatosis. Video thorascopic view of visceral pleura. Note cobblestoned appearance of the pleural surface due to subpleural air cysts and dilated lymphatic channels (Courtesy of Drs. Angelina Bautista and J.F. Tomashefski, Jr, Cleveland, OH). With permission from Springer (see chapter references for complete citation).

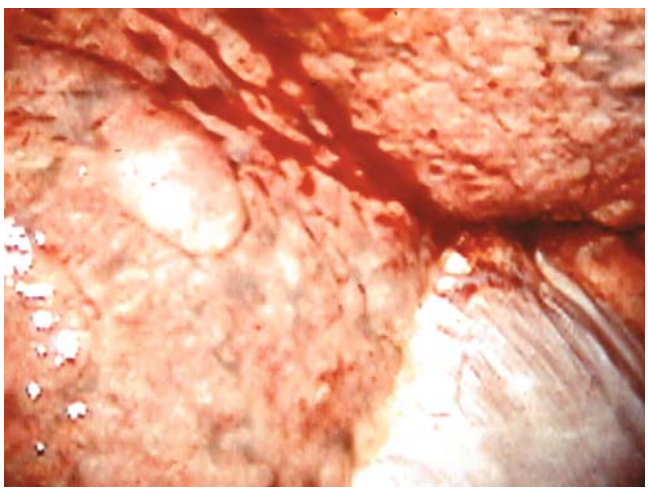

A.E. Fraire et al. (eds.), *Atlas of Neoplastic Pulmonary Disease*,
DOI 10.1007/978-0-387-89839-1_17, © Springer Science+Business Media, LLC 2010

FIGURE 17.3 Lymphangioleiomyomatosis. Gross appearance of lung affected by LAM. Note rigid fibrous walls separating cysts of varying sizes. From Tomashefski et al, with permission from Springer (see chapter references for complete citation).

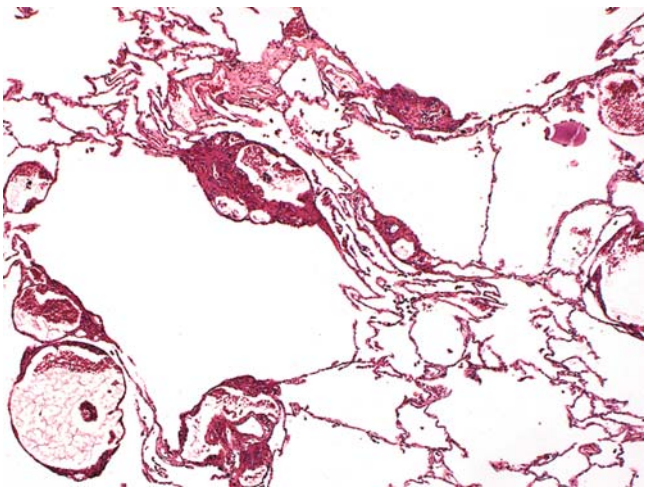

FIGURE 17.4 Lymphangioleiomyomatosis. Low-power microscopic view. Note dense hypercellular aggregates of proliferating myoid cells near cystic spaces. Hematoxylin and eosin. From Tomashefski et al, with permission from Springer (see chapter references for complete citation).

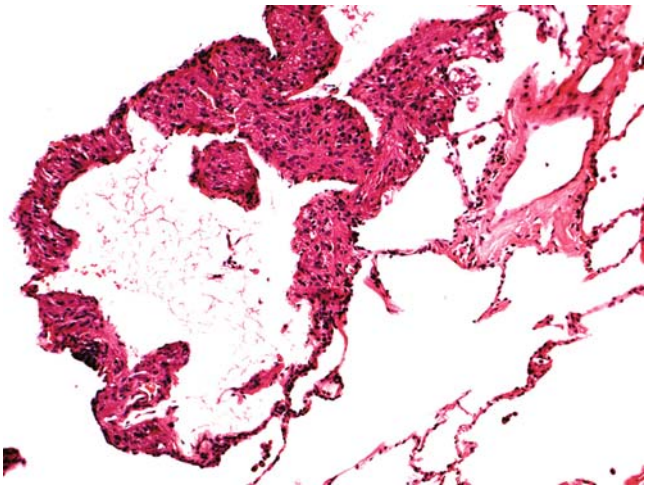

FIGURE 17.5 Lymphangioleiomyomatosis. Intermediate microscopic power view. Note compact aggregates of small spindly looking myoid cells, the so-called LAM cells. Hematoxylin and eosin. From Tomashefski et al, with permission from Springer (see chapter references for complete citation).

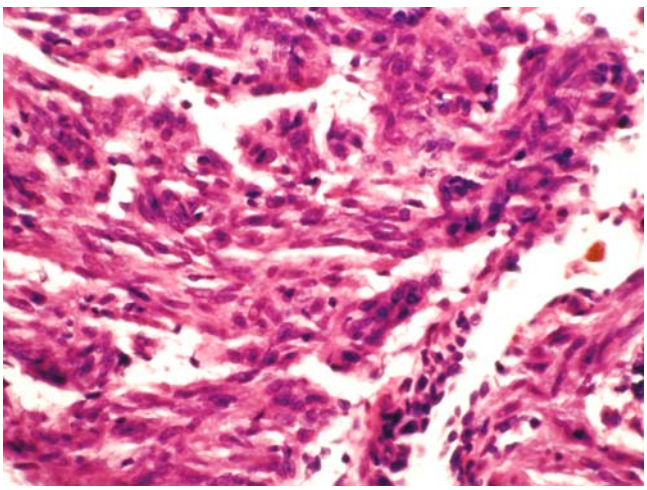

FIGURE 17.6 Lymphangioleiomyomatosis. High-power microscopic view showing smooth muscle appearance of the LAM cells. Hematoxylin and eosin. From Tomashefski et al, with permission from Springer (see chapter references for complete citation).

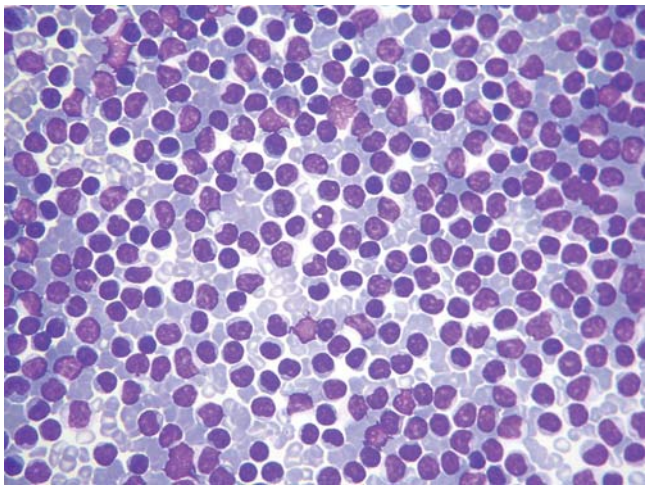

FIGURE 17.7 Lymphangioleiomyomatosis. Cytological preparation showing background mixed population of reactive mature-looking lymphocytes. Diff-Quick stain (Reproduced with permission from Acta Cytologica).

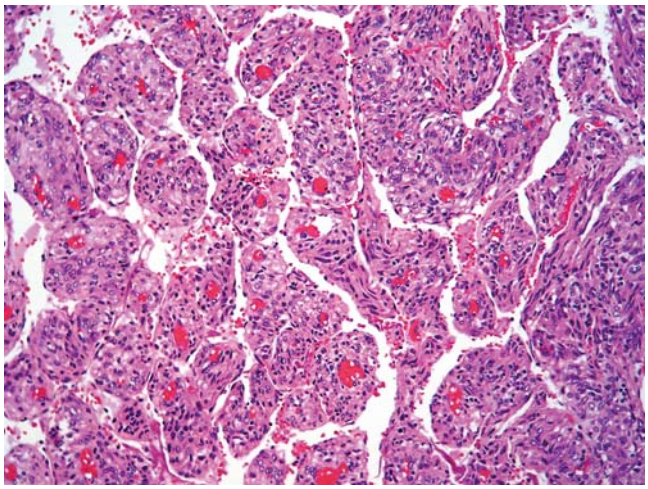

FIGURE 17.9 Lymphangioleiomyomatosis. Microscopic examination revealing anastomosing channels surrounded by specialized smooth muscle cells (myoid cells). Hematoxylin and eosin (Reproduced with permission from Acta Cytologica).

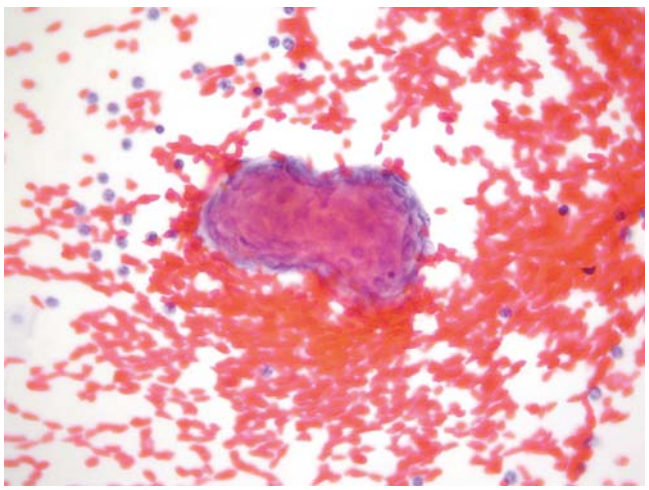

FIGURE 17.8 Lymphangioleiomyomatosis. Cytological preparation showing tridimensional cohesive clusters of epithelioid cells, note the presence of few mature lymphocytes in the background. Papanicolaou stain (Reproduced with permission from Acta Cytologica).

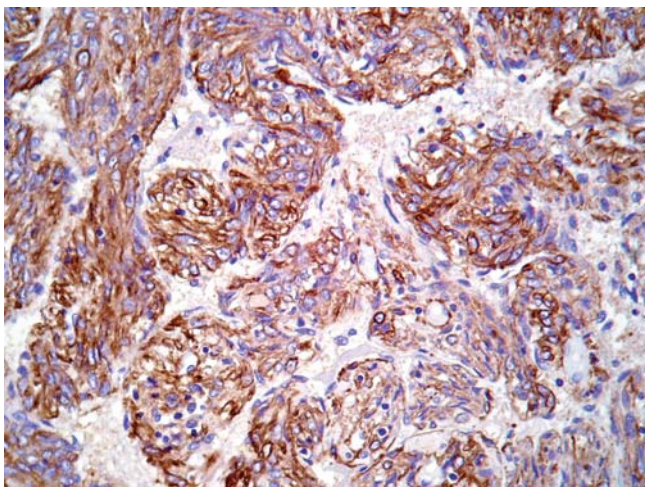

FIGURE 17.10 Lymphangioleiomyomatosis. Tumor cells in this preparation are immunoreactive for HMB-45, a marker of melanocytic differentiation (HMB-45 immunostain) (Reproduced with permission from Acta Cytologica).

REFERENCES

- Al-Bozom IA, Mujeeb IB, Murad N. Retroperitoneal lymphangioleiomyomatosis diagnosed by fine needle aspiration. *Acta Cytologica*. 2007;51:594–596.
- Corrin B, Liebow A, Friedman PJ. Pulmonary lymphangiomyomatosis: a review. *Am J Pathol*. 1975;79:347–382.
- Folpe AL. Neoplasms with perivascular epithelioid cell differentiation (PEComas). In: Travis WD, Brambilla E, Müller-Hermelink HK, Harris CC, eds. *World Health Organization Classification of Tumours. Pathology and Genetics. Tumours of the Lung, Pleura, Thymus and Heart*. Lyon: IARC Press; 2004:221–222.
- Fraire AE, Dail DH. Mesenchymal tumors, Part I: Tumors of fibrous, fibrohistiocytic and muscle origin. In: Tomashefski JF, Cagle PT, Farver C, Fraire AE, eds. *Dail and Hammar Pulmonary Pathology*. 3rd ed. Berlin, New York, Heidelberg: Springer-Verlag; 2008: 427–461.
- Lenoir S, Grenier P, Brauner MW, et al. Pulmonary lymphangiomyomatosis and tuberous sclerosis: comparison and radiographic and thin-section CT findings. *Radiology* 1990;175:329–334.
- Matsui K, Beasley MB, Nelson WK, et al. Prognostic significance of pulmonary lymphangioleiomyomatosis histologic score. *Am J Surg Pathol*. 2001;25:479–484.
- Matsui K, Takeda K, Yu Z-X, et al. Down regulation of estrogen and progesterone receptors in the abnormal smooth muscle cells in pulmonary lymphangioleiomyomatosis following therapy. *Am J Respir Crit Care Med*. 2000;161:1002–1009.
- Popper HH, Juettner-Smolle FM, Pontgratz MG. Micronodular hyperplasia of type II pneumocytes a new lung lesion associated with tuberous sclerosis. *Histopathology*. 1991;16:347–354.
- Stern EJ, Webb WR, Golden JA, et al. Cystic lung disease associated with eosinophilic granuloma and tuberous sclerosis. Air trapping at dynamic ultrafast high-resolution CT. *Radiology*. 1992;182:325–329.

CHAPTER 18

Epithelioid Hemangioendothelioma

Toshiaki Kawai, Armin Ernst, Carol F. Farver, Armando E. Fraire, and Anjali Saqi

This unique vascular tumor is not exclusive to the lung. It can also be seen in liver, bone, pleura, and other anatomical sites. Its prognosis is unpredictable with life expectancies ranging widely from 1 to 15 years after diagnosis. Epithelioid hemangioendothelioma (EHE) has a distinct predilection for younger females, with 80% of cases occurring in women, before the age of 40. Typically, multiple bilateral nodules are seen on chest radiographs, although cases presenting as solitary masses have also been described. Epithelioid hemangioendothelioma involving the pleura may mimic mesothelioma on chest radiographs and CT scans. The endoscopic features of EHE are not well known. In the case shown here, the tumor was exophytic and multinodular. Some patients with EHE present clinically with hemoptysis. At gross inspection, tumors are well-defined gray tan in color. Microscopically the tumor presents as multiple nodules that may be necrotic or calcified. The nodules typically grow in a micropolypoid growth pattern filling the alveoli. The tumor cells forming the nodules are small, round to oval and show intracytoplasmic vacuoles. These vacuoles are believed to represent primitive vascular lumina and are required for diagnosis. On cytologic preparations, cells of EHE may arrange themselves around central cores of amorphous metachromatic material in a "ship-wheel" fashion. Individually, the cells retain their epithelioid plump morphology and may at times present with rhabdoid features.

FIGURE 18.1 Epithelioid hemangioendothelioma. Chest radiograph showing two nodular densities in the right mid-lung field. The peripheral density is near the pleura while the more centrally located density overlies the hilum.

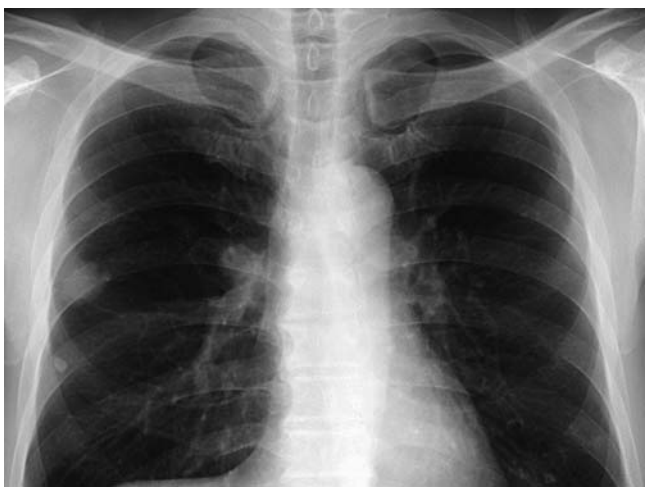

FIGURE 18.2 Epithelioid hemangioendothelioma. CT of chest showing a larger laterally located density with central calcification in the right lower lobe as well as a more central lesion near the hilar area.

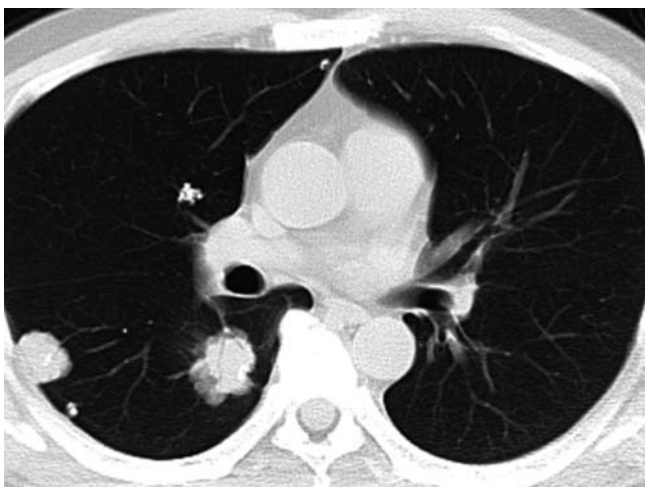

A.E. Fraire et al. (eds.), *Atlas of Neoplastic Pulmonary Disease*,
DOI 10.1007/978-0-387-89839-1_18, © Springer Science+Business Media, LLC 2010

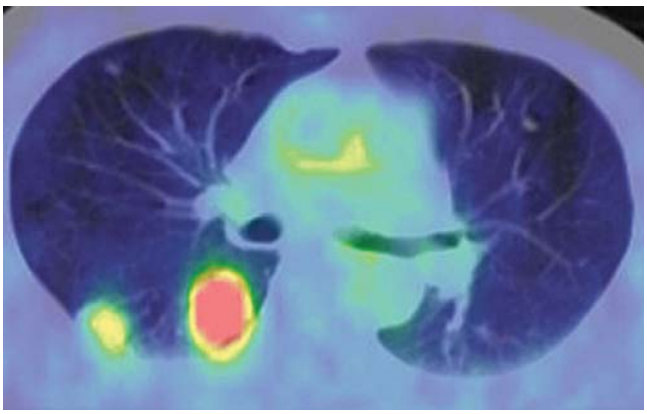

FIGURE 18.3 Epithelioid hemangioendothelioma. PET–CT fusion image showing increased metabolic activity in both a medially located and a central nodular lesion of the right lung.

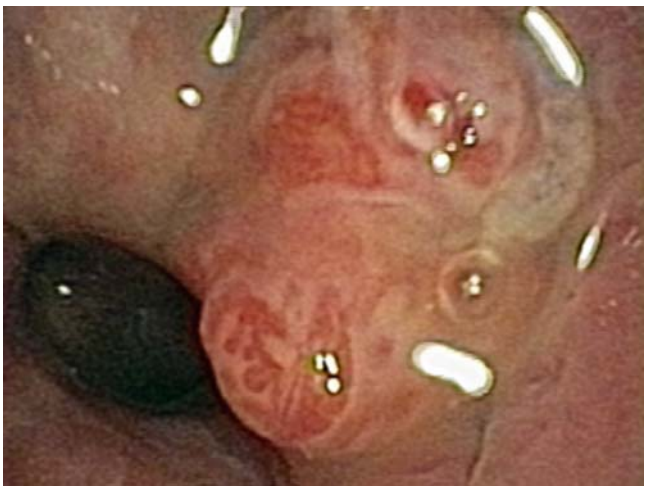

FIGURE 18.4 Endoscopic view of a malignant vascular tumor. Close up of an exophytic multinodular lesion from a 32-year-old woman who initially presented with hemoptysis. Biopsy confirmed the diagnosis (Courtesy of Dr. Felix Herth, University of Heidelberg, Heidelberg, Germany).

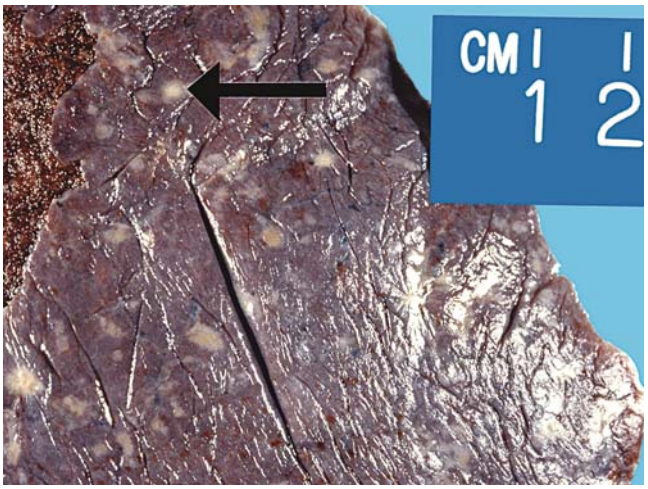

FIGURE 18.5 Epithelioid hemangioendothelioma. Gross appearance. Small subpleural whitish nodules on pleural surface. From Tomashefski et al, with permission from Springer (see chapter references for complete citation).

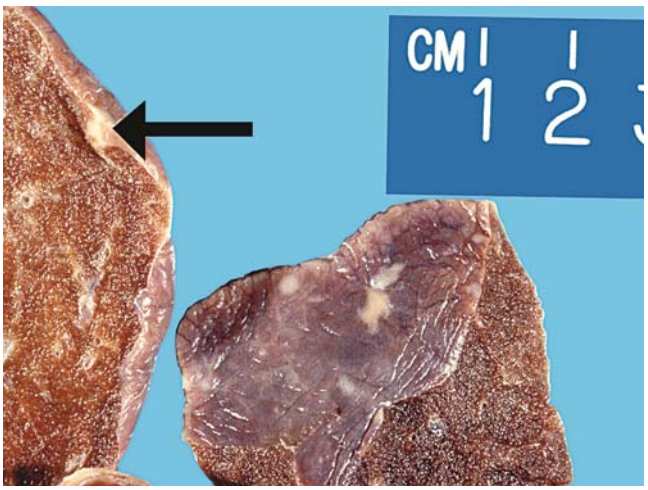

FIGURE 18.6 Epithelioid hemangioendothelioma. Gross appearance. Note nodules on cut surfaces of lung (*arrow*). From Tomashefski et al, with permission from Springer (see chapter references for complete citation).

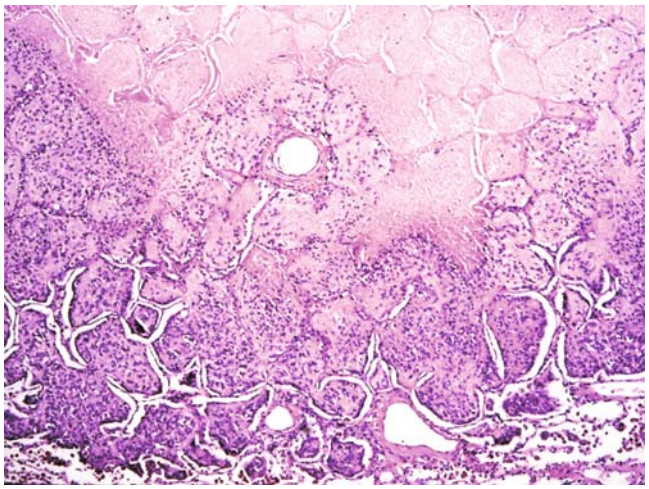

FIGURE 18.7 Epithelioid hemangioendothelioma. Microscopic view. Note advancing micropolypoid tumoral pattern growth with coagulative necrosis on central areas. Hematoxylin and eosin. From Tomashefski et al, with permission from Springer (see chapter references for complete citation).

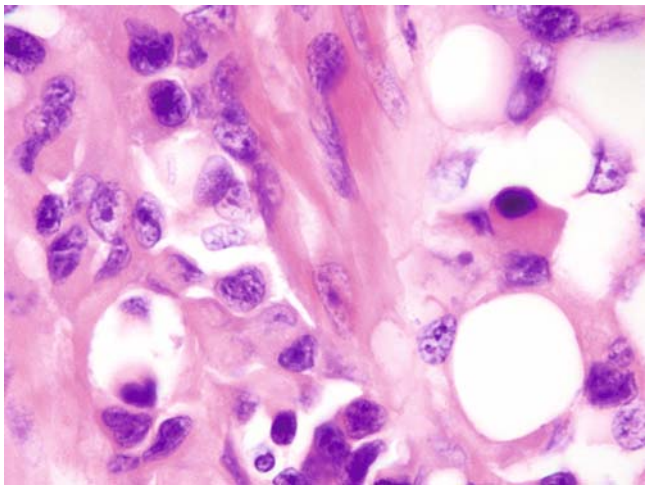

FIGURE 18.9 Epithelioid hemangioendothelioma. Microscopic view. Note cells with cytoplasmic vacuoles representing primitive vascular lumina. Hematoxylin and eosin. From Tomashefski et al, with permission from Springer (see chapter references for complete citation).

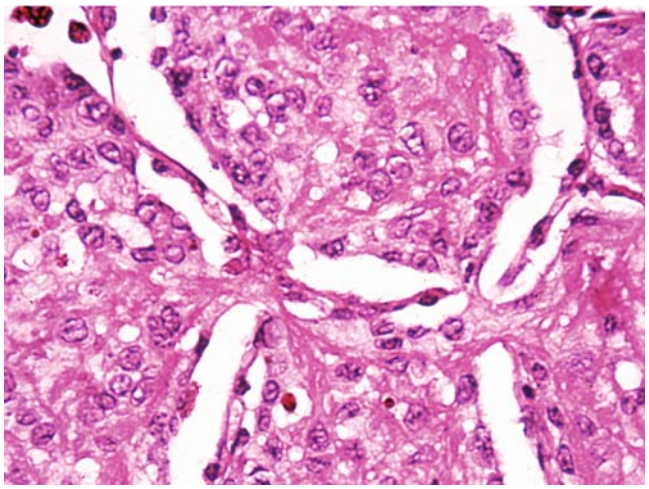

FIGURE 18.8 Epithelioid hemangioendothelioma. Microscopic view. Note extension of tumor cells through pores of Kohn into adjacent alveolar spaces. Hematoxylin and eosin. From Tomashefski et al, with permission from Springer (see chapter references for complete citation).

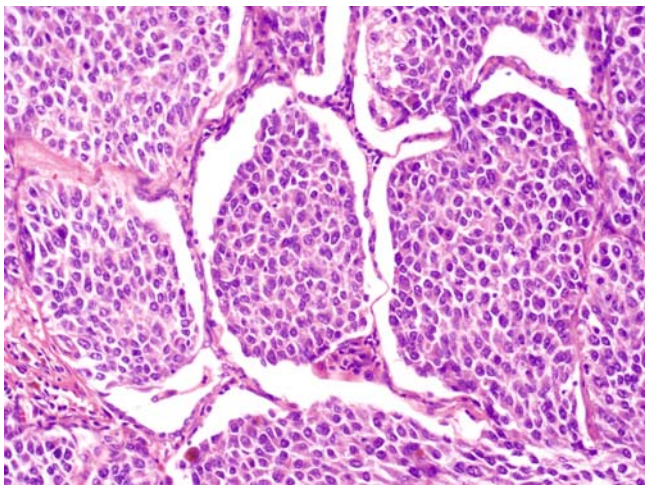

FIGURE 18.10 Large cell carcinoma of lung. Microscopic view. Micropolypoid intraalveolar growth pattern is not exclusive of epithelioid hemangioendothelioma. This large cell carcinoma was seen extending from one alveolar space to the next through the pores of Kohn. Hematoxylin and eosin. From Tomashefski et al, with permission from Springer (see chapter references for complete citation).

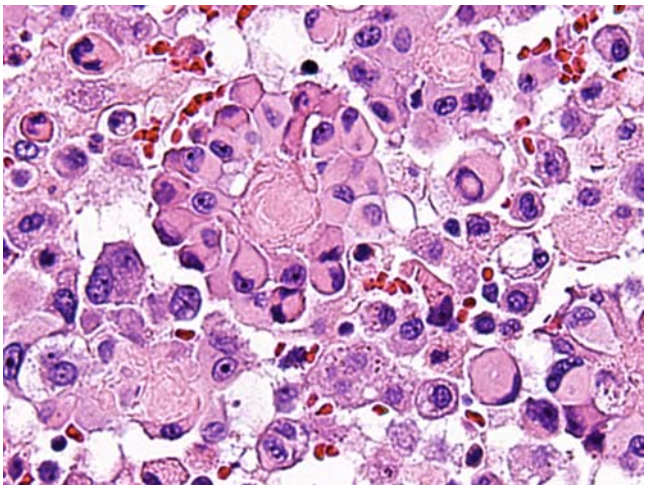

FIGURE 18.11 Epithelioid hemangioendothelioma. Cytologic preparation showing loosely cohesive clusters of cells with eccentric, displaced nuclei resembling plasmacytoid cells. Note also these cells are arranged around a centrally located core of amorphous acellular material. Cell block preparation. Hematoxylin and eosin.

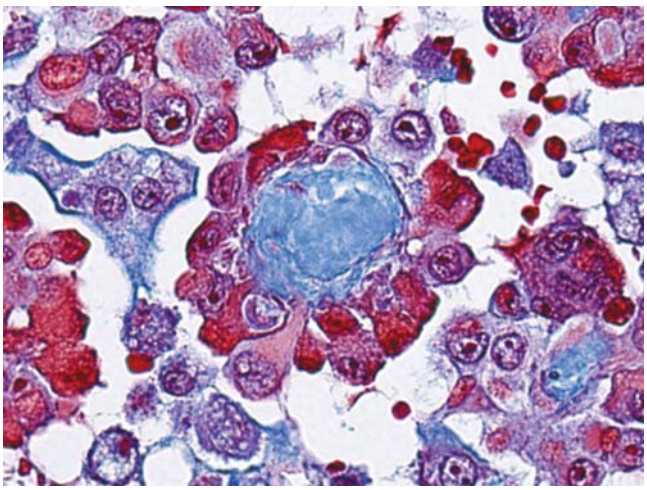

FIGURE 18.12 Epithelioid hemangioendothelioma. Cytologic preparation showing epithelioid cells around a central acellular core with a "ship-wheel" configuration. Cell block preparation. Trichrome stain.

REFERENCES

- Abati A, Cajigas A, Hijazi Y. Metastatic epithelioid hemangioendothelioma in a pleural effusion: diagnosis by cytology. *Diagn Cytopathol*. 1994;11:64–67.
- Boudousquie A, Lawce H, Sherman R, et al. Complex translocation (7;22) identified in an epithelioid hemangioendothelioma. *Cancer Genet Cytogenet*. 1996;92:116–121.
- Buggage R, Soudi N, Olson J, et al. Epithelioid hemangioendothelioma of the lung: pleural effusion cytology, ultrastructure, and brief literature review. *Diagn Cytopathol*. 1995;13:54–60.
- Dail D, Liebow A, Gmelick J, et al. Intravascular, bronchiolar and alveolar tumor of the lung (IVBAT). An analysis of twenty cases of a peculiar sclerosing endothelial tumor. *Cancer*. 1983;51:452–464.
- Dean P, Haggitt R, O'hara C. Malignant epithelioid hemangioendothelioma of the liver in young women. Relationship to oral contraceptive use. *Am J Surg Pathol*. 1985;9:695–704.
- Fraire AE, Dail DH. Mesenchymal tumors, part II: Tumors of hamartomatous, osteochondromatous, lipomatous, neural and vascular origin. In: Tomashefski JF, Cagle PT, Farver CF, Fraire AE, eds. *Dail and Hammar's Pulmonary Pathology*. 3rd ed. Springer: Berlin, New York, Heidelberg; 2008: 462–499.
- Murer B, Gruber-Mösenbacher, Popper HH. Unusual primary malignant lung neoplasms. In: Zander DS, Farver CF, eds. *Pulmonary Pathology, a Volume in the Series of Foundations in Diagnostic Pathology*. Philadelphia: Churchill Livingstone Elsevier; 2008:606–608.
- Saqi A, Nishet L, Gagneta P, et al. Primary pleural epithelioid hemangioendothelioma with rhabdoid phenotype: Report and review of the literature. *Diagn Cytopathol*. 2007;35:203–208.
- Yousem S, Hochholzer L. Unusual thoracic manifestations of epithelioid hemangioendothelioma. *Arch Pathol Lab Med*. 1987;111:459–463.

CHAPTER 19

Pulmonary Artery Sarcoma

Philip T. Cagle, Timothy C. Allen, and Armando E. Fraire

This type of pulmonary vascular tumor differs primarily from epithelioid hemangioendothelioma and angiosarcoma on account of its intravascular location and fibroblastic or leiomyomatous nature. Clinically, pulmonary artery sarcoma may present as a single large pulmonary embolus or multiple smaller emboli. Some may present with symptoms and signs right sided cardiac failure. CT tomography, MRI and angiography are of great value in the detection of these tumors but even with these technologies a premortem diagnosis is only made in half of the cases. Intraluminal masses can be detected by pulmonary angiography showing smooth tapering of pulmonary arteries and "to and fro" motion of pedunculated or lobulated tumors. By virtue of their intravascular location, endoscopy does not contribute much to the visualization of these tumors unless they have directly spread in the lumen of the airways.

On gross inspection, pulmonary artery sarcomas can have a distinct multinodular appearance made up of nodules kept together by thin or broad connecting bridges, ultimately assuming the appearance of an intravascular cast with prominent branching. Most vascular sarcomas are intraarterial and a minority intravenous. The arterial variants tend to be poorly differentiated with fibroblastic or myofibroblastic differentiation while the venous variants are likely to be leiomyosarcomas of intermediate or high grade of differentiation.

FIGURE 19.1 Axial CT of chest showing pulmonary artery sarcoma. The sarcoma forms a large mass (*arrow*) outlined by contrast material straddling the bifurcation of the pulmonary artery and extending into the left lower lobe (*dashed arrow*) (Courtesy of Dr. ES Yi, Mayo Clinic, Rochester, MN). With permission from Cardiology Clinics (see chapter references for complete citation).

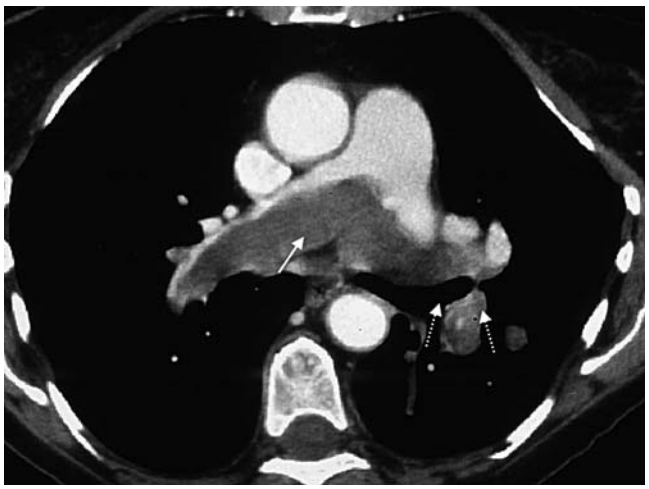

FIGURE 19.2 Gross photograph of pulmonary artery sarcoma revealed by pulmonary thromboendarterectomy procedure (R: right pulmonary artery; L: left pulmonary artery) (Courtesy of Dr. ES Yi, Mayo Clinic, Rochester, MN). With permission from Cardiology Clinics (see chapter references for complete citation).

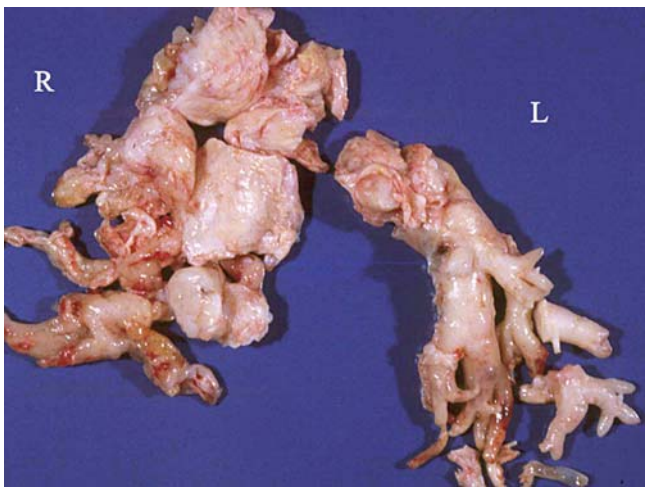

A.E. Fraire et al. (eds.), *Atlas of Neoplastic Pulmonary Disease*,
DOI 10.1007/978-0-387-89839-1_19, © Springer Science+Business Media, LLC 2010

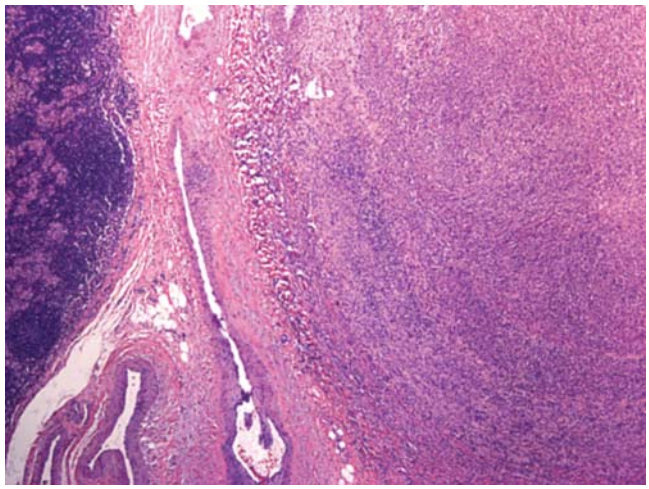

FIGURE 19.3 Pulmonary Artery Sarcoma. This low power microscopic view of a pulmonary artery sarcoma shows a dense cellular proliferation filling the vessel's lumen. A curved band of pink-colored tissue on the left represents the vascular wall. Further on the left there is an epithelial cleft and cartilage. Hematoxylin and eosin.

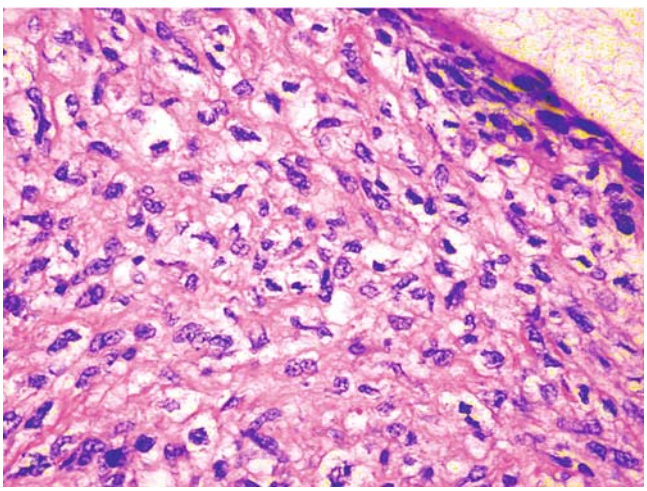

FIGURE 19.4 Pulmonary Artery Sarcoma. Close microscopic view of a pulmonary artery sarcoma showing hypercellularity and pleomorphism. Hematoxylin and eosin (Courtesy of Dr. Maria Moliner; Tufts University School of Medicine, Boston, MA). From Tomashefski et al, with permission from Springer (see chapter references for complete citation).

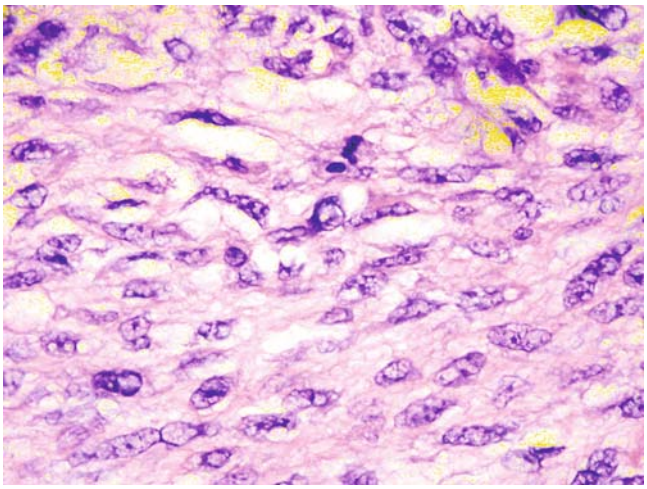

FIGURE 19.5 Pulmonary Artery Sarcoma. Closer microscopic view of tumor in the preceding image showing spindle cell morphology and some mitotic figures. Hematoxylin and eosin (Courtesy of Dr. Maria Moliner, Tufts University School of Medicine, Boston, MA). From Tomashefski et al, with permission from Springer (see chapter references for complete citation).

REFERENCES

- Burke AP, Virmani R. Sarcomas of the great vessels. A clinicopathologic study. *Cancer*. 1993;71:1761–1773.
- Cox JE, Chiles C, Aquino SL, et al. Pulmonary artery sarcomas: a review of clinical and radiology features. *J Comput Assist Tomogr*. 1997;21:750–755.
- Devendra G, Mo M, Kerr KM, et al. Pulmonary artery sarcomas: the UCSD experience. *Am J Respir Crit Car Med*. 2002;165:A24.
- Fraire AE, Dail DH. Mesenchymal tumors, Part II: Tumors of hamartomatous, osteochondromatous, lipomatous, neural, and vascular origin. In: Tomashefski JF, Cagle PT, Farver CF, Fraire AE, eds. *Dail and Hammar's Pulmonary Pathology.* 2nd ed. Berlin, New York, Heidelberg: Springer; 2008:462–499.
- Murer B, Gruber-Mösenbacher U, Popper HH. Unusual primary malignant lung neoplasms. In: Zander DS, Farver CF, eds. *Pulmonary Pathology, a Volume in the Series of Foundations in Diagnostic Pathology*. Philadelphia: Churchill Livingston Elsevier; 2008:608–612.

- Okuno T, Matsuda K, Ueyama K, et al. Leiomyosarcoma of the pulmonary vein. *Pathol Int*. 2000; 50:839–846.
- Oliai BR, Tazelaar HD, Lloyd RV, et al. Leiomyosarcoma of the pulmonary veins. *Am J Surg Pathol*. 1999;23:1082–1088.
- Yamaguchi T, Suzuki K, Asamura H, et al. Lung carcinoma with polypoid growth in the main pulmonary artery: report of two cases. *Jpn J Clin Oncol*. 2000;30:358–361.
- Yi ES. Tumors of the pulmonary vasculature. *Cardiol Clin*. 2004;22:431–440.

CHAPTER 20

Synovial Sarcoma

Shanda Blackmon, Philip T. Cagle, Timothy C. Allen, Dina R. Mody, and Armando E. Fraire

Synovial sarcomas are uncommon malignant tumors of uncertain histogenesis made primarily of spindle cells displaying variable epithelial components. In the respiratory tract, synovial sarcomas preferentially arise from the pleura and secondarily from the parenchymal tissue of the lung. The SYT-SSX fusion gene is characteristic of this sarcoma. Synovial sarcomas show no significant gender distribution and affect individuals with a wide age range. Symptoms are chiefly related to the effect of a space-occupying mass. Those tumors that occur in the pleura may present with effusions. In one series, conventional chest radiographs showed ill-defined thoracic lesions that computed tomographic scans subsequently helped to delineate. In that series, heterogeneous enhancement and an absence of calcifications were noted. Most if not all synovial sarcomas are inaccessible to the flexible bronchoscope. Therefore, data pertaining to their endoscopic appearance is very limited.

The gross appearance of these tumors is not characteristic. Tumor nodules vary in size from less than 1.0 cm to 15–20 cm. The tumor nodules are soft to rubbery with areas of necrosis, hemorrhage and some with cystic change. Microscopically, synovial sarcoma can be biphasic or monophasic. Most intrapulmonary cases are monophasic and are characterized by solid sheets of atypical spindle cells. Biphasic tumors contain epithelial clusters, sometimes with a gland-like appearance, that are positive on immunostains for pan-cytokeratin. Cytopathologic experience with this neoplasm is based only in rare individual case reports. One report called attention to a primary pleuropulmonary synovial sarcoma confirmed by cytogenetics. An FNA showed highly cellular, dispersed "small round blue cells" in a hemorrhagic background. In another report, a metastatic synovial sarcoma to the pleura (from the leg) showed fibrous spindle-shaped cells as well as epithelioid cells arranged in gland-like structures.

FIGURE 20.1 CT scan of a synovial sarcoma located in the right lower lobe. Note irregular lobulated contour of the tumor mass.

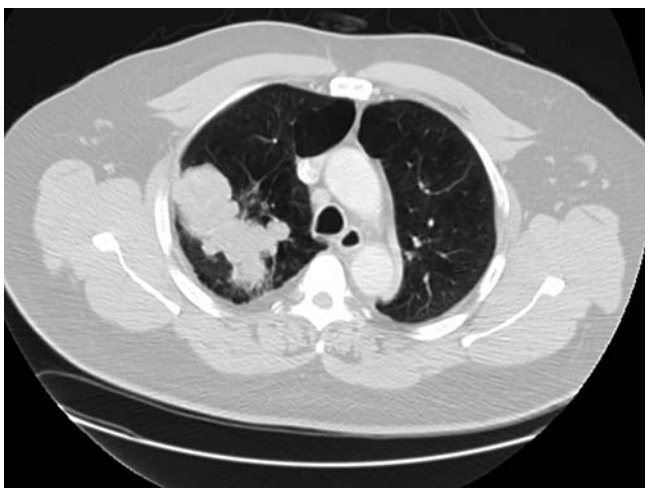

A.E. Fraire et al. (eds.), *Atlas of Neoplastic Pulmonary Disease*,
DOI 10.1007/978-0-387-89839-1_20,

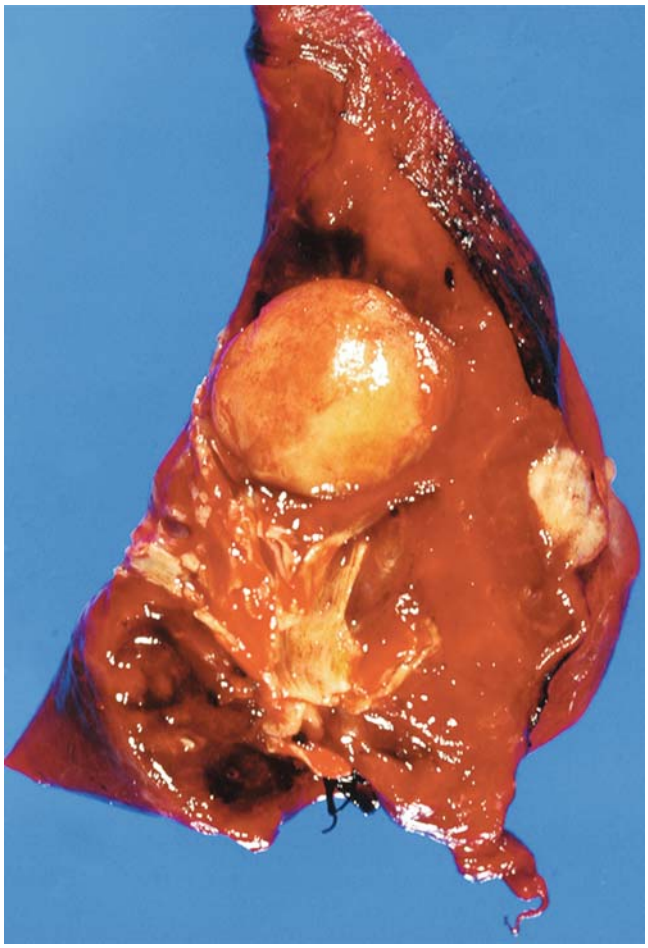

FIGURE 20.2 Synovial sarcoma. Gross appearance. Note large spheroidal tumor mass with a smooth yellow pink surface and a smaller mass on the right (Courtesy of Dr. Andrew Fischer, University of Massachusetts Medical School, Worcester, MA). From Tomashefski et al, with permission from Springer (see chapter references for complete citation).

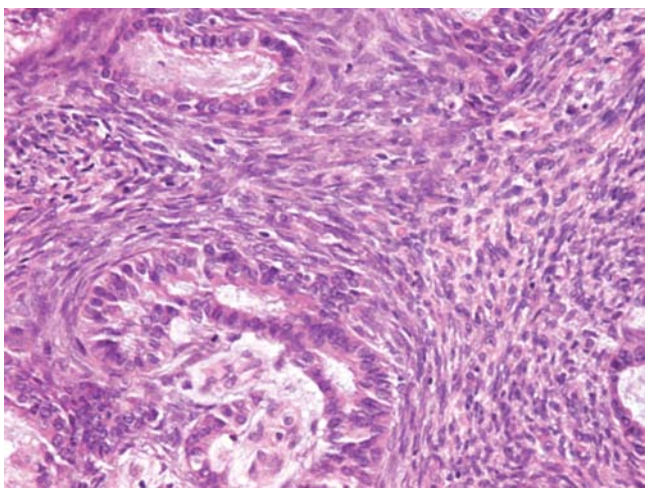

FIGURE 20.3 Microscopically, this biphasic synovial sarcoma shows spindle cells with some gland-like structures lined by orderly looking cuboidal cells. Hematoxylin and eosin.

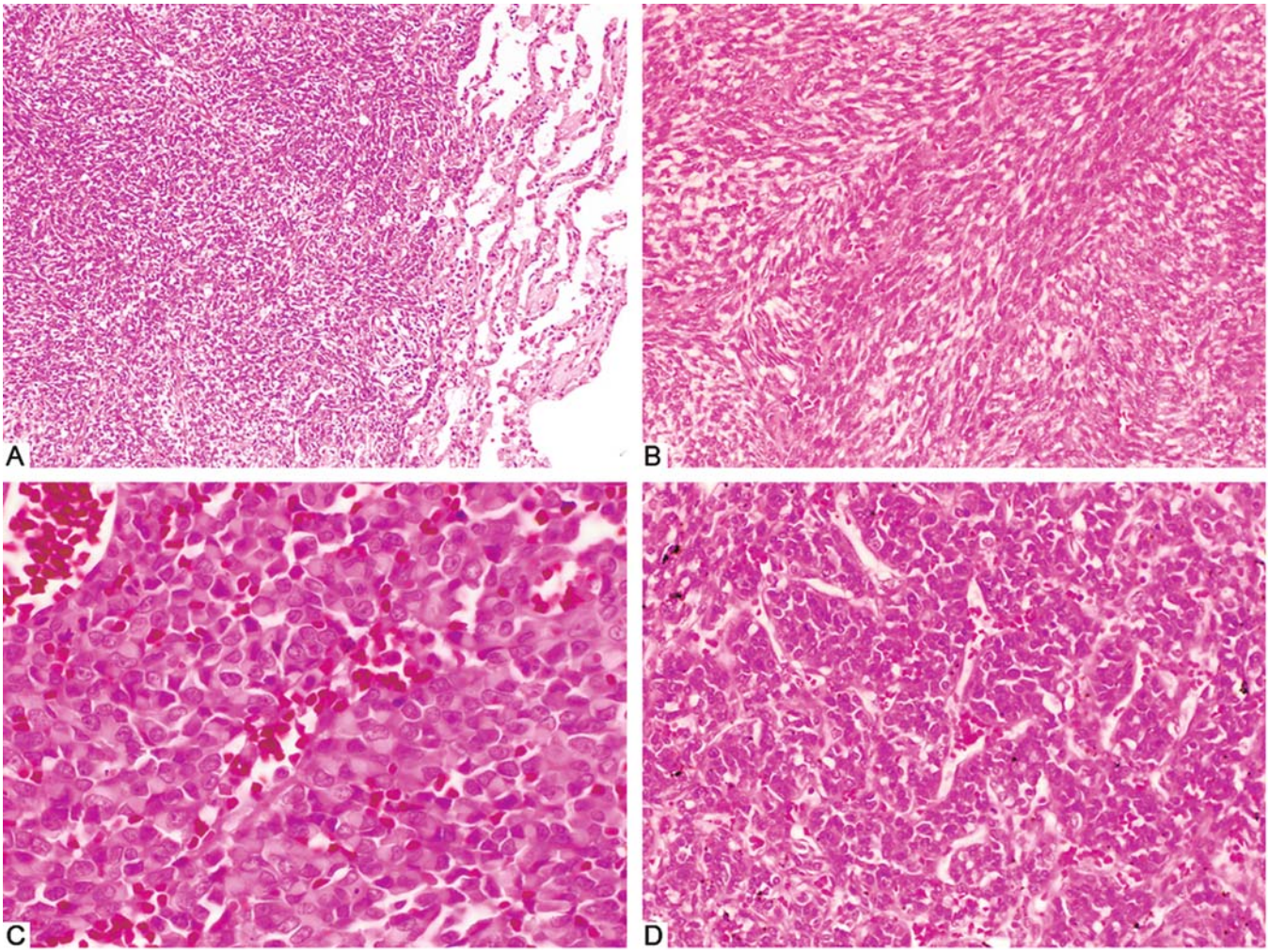

FIGURE 20.4 Microscopic view of another synovial sarcoma. **a** Monophasic fibrous synovial sarcoma. Note solid proliferation of spindle cells and uninvolved lung tissue on the right. **b** Closer view of same. **c** In this area, rhabdoid features are present. **d** Less well-differentiated tumor showing rounded cells and a hemangiopericytomatous vascular pattern. Hematoxylin and eosin (Courtesy of Dr. S. Okamoto and Dr. H. Hashimoto, University of Occupational and Environmental Health, Kitaki-Ushu, Japan). With permission from Histopathology (see chapter references for complete citation).

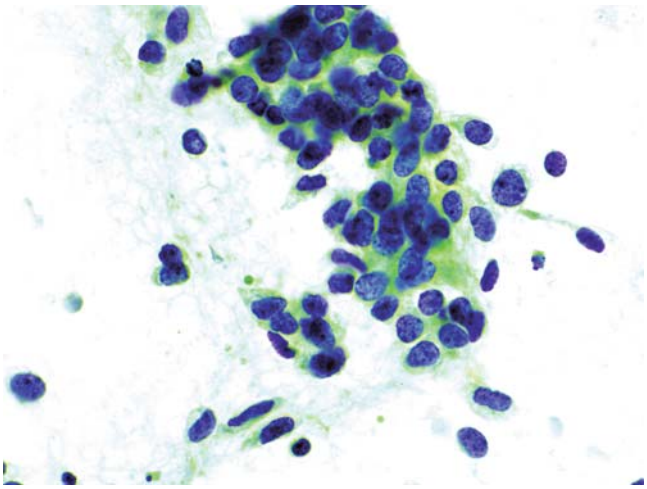

FIGURE 20.5 Cytologic preparation of a monophasic synovial sarcoma showing round and oval to spindle-shaped cells. Papanicolaou stain.

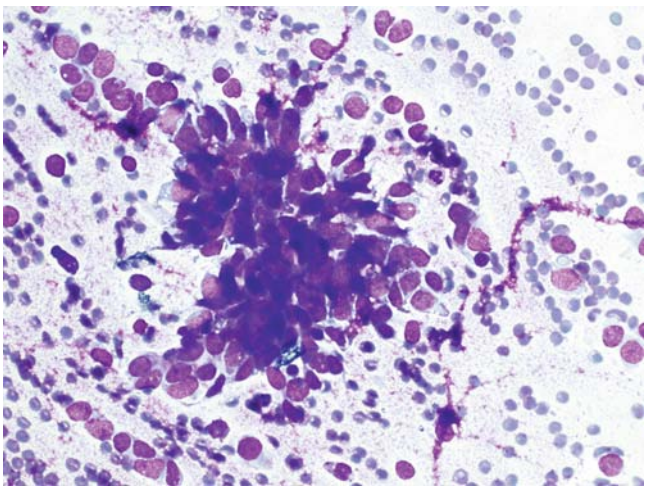

FIGURE 20.6 Cytologic preparation of the sarcoma shown in Fig. 20.5. In this air-dried preparation, the tumor cells are more cohesive and fusiform. Diff Quick stain.

REFERENCES

- Aubry MC, Suster S, Tazelaar HD, et al. Pulmonary synovial sarcoma. In: Travis WD, Brambilla E, Müller-Hermelink HK, Harris CC, eds. *World Health Organization Classification of Tumours. Pathology and Genetics of Tumours of the Lung, Pleura, Thymus and Heart*. Lyon: IARC Press; 2004:111–112.
- Fraire AE, Dail DH. Ch 41. Miscellaneous tumors and tumor-like proliferations of the lung. In: Tomashefski JF Jr, Cagle PT, Farver CF, Fraire AE, eds. *Dail and Hammar's Pulmonary Pathology.* 3rd ed. Berlin, New York, Heidelberg: Springer;2008:500–541.
- Gaertuer E, Zeren EH, Fleming MV, et al. Biphasic synovial sarcoma arising in the pleural cavity. A clinicopathologic study of five cases. *Amer J Surg Pathol.* 1996;20:36–45.
- Hammar SP. Lung and pleural neoplasms. In: Dabbs DJ, ed. *Diagnostic Immunohistochemistry*. Philadelphia: Churchill Livingstone; 2002:267–312.
- Hisaoka M, Hashimoto H, Iwamasa T, et al. Primary synovial sarcoma of the lung: report of two cases confirmed by molecular detection of SYT-SSX fusion gene transcripts. *Histopathology.* 1999;34:205–210.
- Nguyen GK, Jeannot A. Cytology of synovial sarcoma metastases in pleural fluid. *Acta Cytol.* 1982;26: 517–520.
- Roberts CA, Seemayer TA, Neff JR. Translocation (X;18) in primary synovial sarcoma of the lung. *Cancer Genet Cytogenet.* 1996;88:49–52.
- Rosenberg AE. Bone, joints and soft tissue tumors. In: Kumar V, Abbas AK, Fausto N, eds. *Robbins and Cotran Pathologic Basis of Disease*. 7th ed. Philadelphia: Elsevier-Saunders; 2005:1273–1324.
- Taylor CA, Barnhart A, Pettenati MJ, et al. Primary pleuropulmonary synovial sarcoma diagnosed by fine needle aspiration with cytogenetic confirmation: A case report. *Acta Cytol.* 2005;49:673–676.
- Zeren H, Moran CA, Suster S. Primary pulmonary sarcomas with features of monophasic synovial sarcoma. A clinico-pathologic study of 25 cases. *Hum Pathol.* 1995;26:474–480.

CHAPTER 21

Marginal Zone B-Cell Lymphoma (Maltoma)

Shanda Blackmon, Philip T. Cagle, Timothy C. Allen, N. Paul Ohori, Elise R. Hoff, and Armando E. Fraire

A low-grade lymphoma, maltoma, represents a form of marginal zone lymphoma arising from mucosal (bronchial) associated lymphoid tissue. Maltomas may arise de novo or be preceded by autoimmune disorders of the lung. Radiographically, maltoma may present as single or multiple nodular masses involving one or both lungs. Airways are usually not affected by these tumors and are likely to remain intact, appearing as air bronchograms on high-resolution CT of the chest. Although not readily visualized endoscopically, a rare maltoma may be diagnosed by endoscopic or transbronchial biopsy. The main histopathologic constituents of maltoma are lymphoid cells resembling small lymphocytes, centrocytes, monocytoid B cells, and lymphoplasmacytic cells, generally with a low level of cellular atypia. An important histopathologic feature of these lesions is involvement of airway epithelium by lymphoid cells, the so-called lymphoepithelial lesion. Cytologically, a mixture of small and large lymphocytes with low level of cellular atypia may be seen.

Over time, some maltomas may progress to large diffuse B-cell lymphomas.

FIGURE 21.1 CT of chest showing a large irregularly shaped consolidation corresponding to marginal zone B-cell lymphoma (maltoma). The lesion primarily involves the left upper lobe, adjacent to the hilar area.

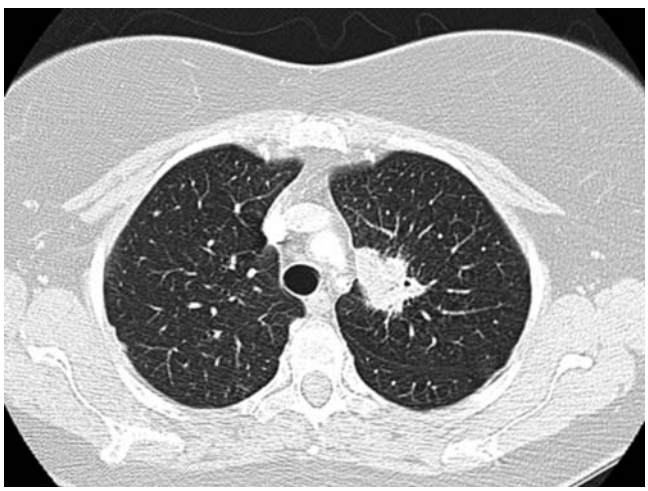

A.E. Fraire et al. (eds.), *Atlas of Neoplastic Pulmonary Disease*,
DOI 10.1007/978-0-387-89839-1_21, © Springer Science+Business Media, LLC 2010

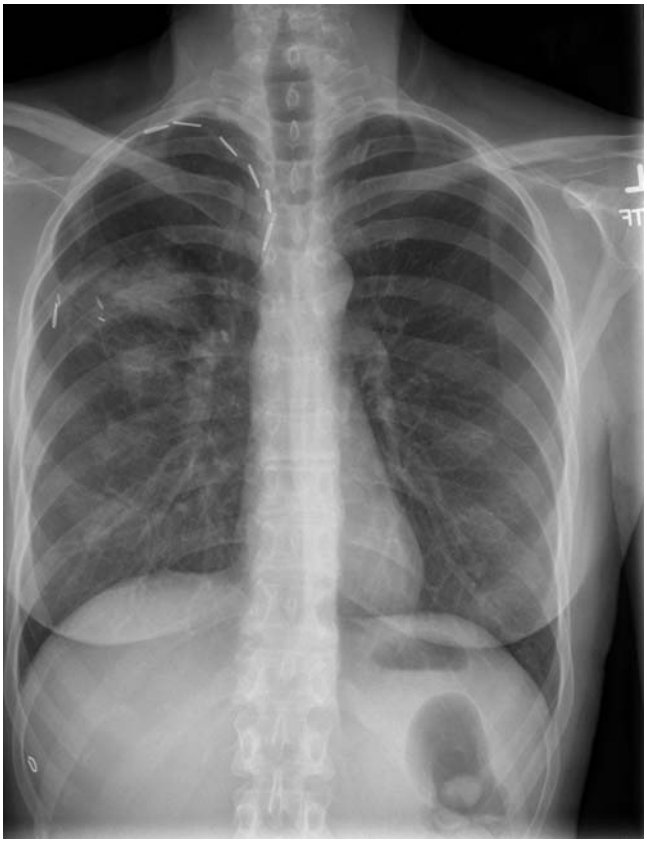

FIGURE 21.2 Chest radiograph showing air space consolidation in the right upper lobe. The lesion was initially interpreted as lymphoid nodular hyperplasia but eventually diagnosed as a marginal zone B-cell lymphoma.

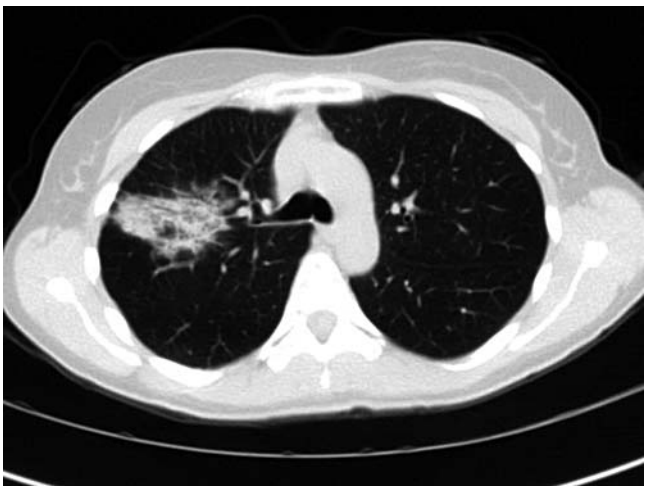

FIGURE 21.3 CT of chest corresponding to chest radiograph shown in Fig. 21.2. Note a large area of air space consolidation in the right upper lobe spilling into the right middle lobe. The lesion measured about 3.5 × 2.4 cm.

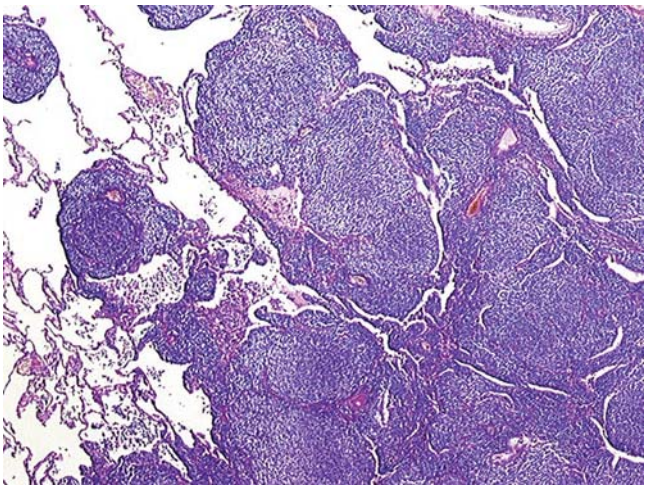

FIGURE 21.4 Marginal zone B-cell lymphoma, histopathologic features. Note dense nodular aggregates of basophilic lymphoid aggregates filling alveolar spaces. Uninvolved lung tissue can be seen in he left lower corner. Hematoxylin and eosin.

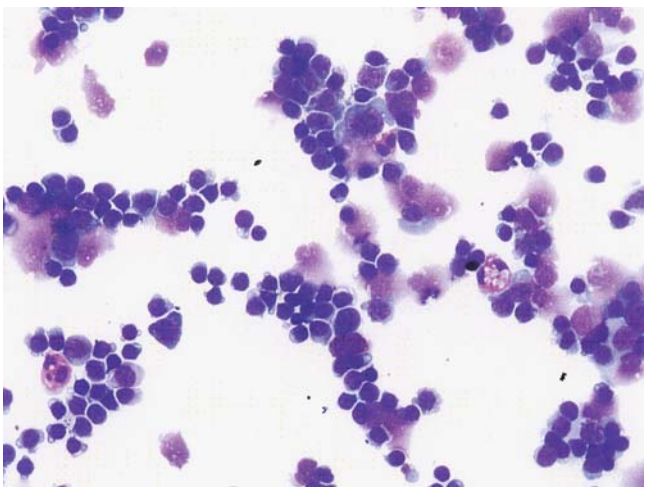

FIGURE 21.5 Marginal zone B-cell lymphoma, cytopathologic features. Note lymphoid population of round intermediate-size lymphocytes with some plasmacytoid appearance (Diff-Quick Stain). From Tomashefski et al, with permission from Springer (see chapter references for complete citation).

REFERENCES

- Fiche M, Caprons F, Berger F, et al. Primary pulmonary non-Hodgkins lymphoma. *Histopathology*. 1995;26:529–537.
- Greenberg SD, Heisler JG, Gyorkey F, et al. Pulmonary lymphoma versus pseudolymphoma, a perplexing problem. *South Med J*. 1972;65:775–784.
- Koss MN. Pulmonary lymphoid disorders. *Semin Diagn Pathol*. 1995;12:158–171.

- Li G, Hansmann ML, Zwingers T, et al. Primary lymphomas of the lung: Morphological, immunohistochemical and clinical features. *Histopathology.* 1990;16:519–531.
- Morice WG, Colby TV. Ch 32. Lymphoproliferative diseases. In: Tomashefski JF Jr., Cagle PT, Farver CF, Fraire AE, eds. *Dail and Hammar's Pulmonary Pathology*. 3rd ed. Berlin, New York, Heidelberg: Springer; 2008:1–46.
- Nicholson AG, Harris NL. Marginal zone B-cell lymphoma of the mucosal associated lymphoid tissue (Malt type). In: Travis WD, Brambilla E, Müller-Hermelink HK, Harris CC, eds. *World Health Organization Classification of Tumours. Pathology and Genetics of Tumours of the lung, Pleura, Thymus and Heart*. Lyon:IARC Press; 2004:88–90.
- Ohori NP, Hoff ER. Ch 45. Cytopathology of pulmonary neoplasia. In: Tomashefski JF, Cagle PT, Farver CF, Fraire AE, eds. *Dail and Hammar's Pulmonary Pathology.* 3rd ed., Vol II. Springer: Berlin, Heidelberg, New York; 2008:767–795.

CHAPTER 22

Diffuse Large B-Cell Lymphoma

Shanda Blackmon, Armin Ernst, Philip T. Cagle, Timothy C. Allen,
N. Paul Ohori, Elise R. Hoff, and Armando E. Fraire

The high-grade non-Hodgkin lymphoma is characterized by a diffuse proliferation of large neoplastic B cells, typically showing nuclear size equal to or greater than the size of a normal macrophage. It is the second most common pulmonary lymphoma after maltoma. It occurs in a wide age range from children to adults. Patients are usually symptomatic. Grossly, the lesions are nodular in configuration and show no lobar predilection. Histopathologically, the process is highly distinctive involving both the pleura and the vascular system of the lung, features that can also be observed in imaging studies of the chest. The underlying lung architecture is usually obliterated, often with necrosis. In some cases, the neoplastic lymphoma cells occupy the alveolar spaces, a pneumonic-like process that has been termed tumoral pneumonia. The cytopathology of this lesion has not been well studied but the lymphoid nature of the cells can be ascertained in both papanicolaou and hematoxylin and eosin-stained preparations and greatly enhanced by the judicious use of lymphoid markers such as CD3, CD5, CD20, and CD23 and/or flow cytometry. Caution should be exercised however since a false negative flow cytometry may be obtained because of necrosis. In difficult or borderline case, gene analysis can be of help.

FIGURE 22.1 Diffuse large B-cell lymphoma. CT scan of chest of a diffuse large B-cell lymphoma presenting as an anterior mediastinal mass.

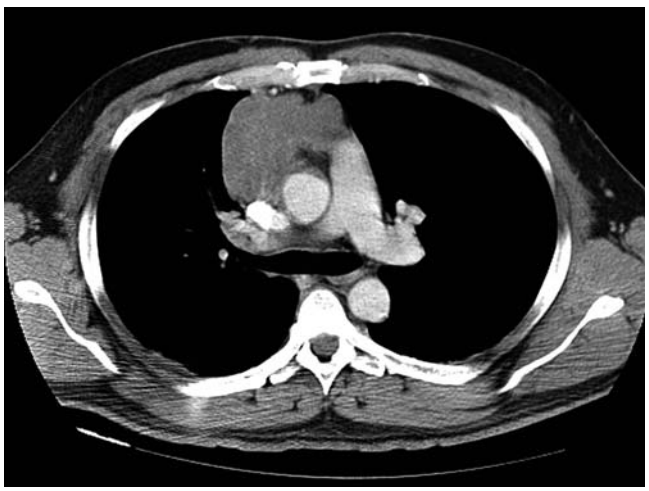

FIGURE 22.2 Diffuse large B-cell lymphoma. Endoscopic image of a pulmonary lymphoma protruding into the lumen of an airway as a polypoid pink red mass.

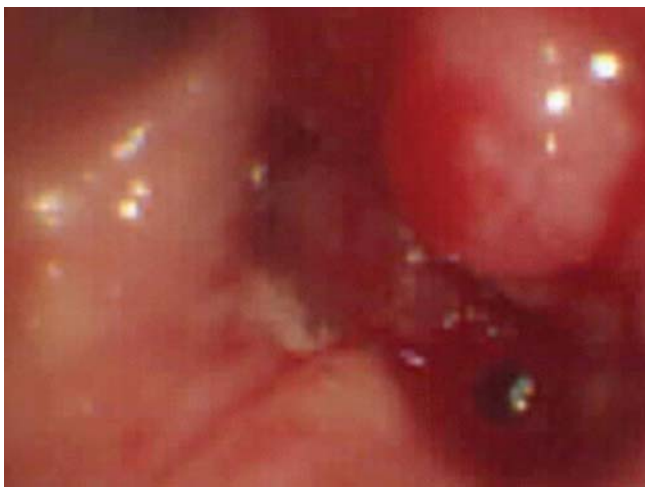

A.E. Fraire et al. (eds.), *Atlas of Neoplastic Pulmonary Disease*,
DOI 10.1007/978-0-387-89839-1_22,

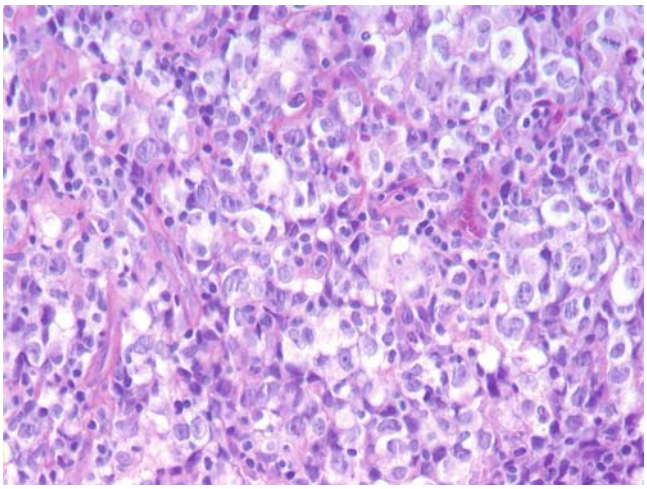

FIGURE 22.3 Diffuse Large B - Cell lymphoma, histopathologic view. Note sheets of large lymphoid cells that are larger than smaller darker background normal lymphocytes. These sheets of cells efface the underlying alveolar architecture of the lung. Hematoxylin and eosin.

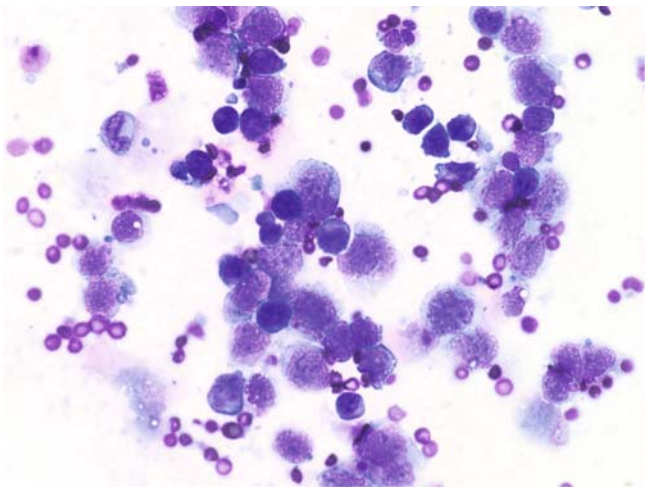

FIGURE 22.4 Diffuse large B-cell lymphoma, cytopathologic view. Note cellular population of large lymphoid cells with nuclear membrane irregularity and coarse chromatin. Diff Quick stain. From Tomashefski et al, with permission from Springer (see chapter references for complete citation).

REFERENCES

- Cordier JF, Chailleux E, Lauque D, et al. Primary pulmonary lymphoma. A clinical study of 70 cases in non-immunocompromised patients. *Chest*. 1993;103: 201–208.
- Hertzman ER. Pulmonary neoplastic and lymphoproliferative disease in AIDS. A review. *Radiology*. 1990;177:347–351.
- Jorgensen JL. Primary large B-cell lymphoma In: Cagle PT, Editor in Chief. *Color Atlas of Pulmonary Pathology*. 2nd ed. Philadelphia, Baltimore, New York: The Wolters Kluwer Co; 2008:104–105.
- Morice WG, Colby TV. Lymphoproliferative disorders. In: Tomashefski JF Jr., Cagle PT, Farver CF, Fraire AE, eds. *Dail and Hammar's Pulmonary Pathology*. 3rd ed. Berlin, New York, Heidelberg: Springer; 2008:462–499.
- Nicholson AG, Harris NL. Primary pulmonary diffuse large B-cell lymphoma. In: Travis WD, Brambilla E, Müller-Hermelink HK, Harris CC, eds. *World Health Organization Classification of Tumours. Pathology and Genetics of Tumours of the Lung, Pleura, Thymus and Heart*. Lyon:IARC Press; 2004:113–114.
- Nicholson AG, Wotherspoon AC, Diss TC, et al. Pulmonary B cell non Hodgkin lymphomas. The value of immunohistochemistry and gene analysis in diagnosis. *Histopathology*. 1995;26:395–403.
- Ohori NP, Hoff ER. Ch 45. Cytopathology of pulmonary neoplasia. In: Tomashefski JF, Cagle PT, Farver CF, Fraire AE, eds. *Dail and Hammar's Pulmonary Pathology*. 3rd ed., Vol II. Springer: Berlin, Heidelberg, New York; 2008:767–795.

CHAPTER 23

Lymphomatoid Granulomatosis

Thomas V. Colby, William G. Morice, and Armando E. Fraire

First described in the 1970's by Liebow et al., lymphomatoid granulomatosis (LYG) is currently defined by the World Health Organization Classification of Tumors as an extranodal angiocentric and angiodestructive lymphoproliferative disorder associated with infection by the Epstein-Barr virus (EBV) and/or immunodeficiency states. Lymphomatoid granulomatosis is more common in adults and has a preference for males. Patients are usually symptomatic and some may have concurrent extrapulmonary disease in the skin, central nervous system, and other anatomical sites. Lung lesions on chest radiographs and/or CT scans are nodular with or without cavitation. In some patients, the lesions may be reticulonodular. The gross anatomical features of LYG closely parallel the radiographic findings, consisting of nodular masses histologically composed of atypical B lymphoid cells permeating vascular walls with associated necrosis. Essentially, LYG is a T-cell rich, large B-cell lymphoma in which the B cells are positive for EBV. In situ hybridization on paraffin sections for EBV-expressed RNAs (EBER)

FIGURE 23.1 Lymphomatoid granulomatosis. Typical radiographic findings in a CT of chest. Note numerous bilateral lung nodules, some showing cavitation. From Tomashefski et al, with permission from Springer (see chapter references for complete citation).

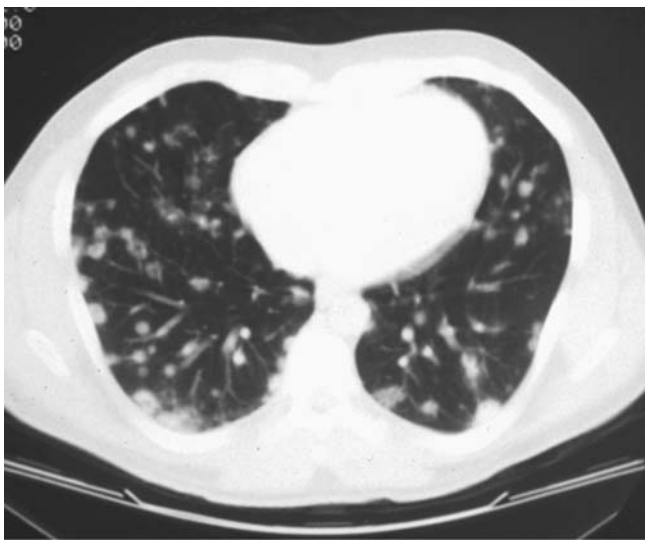

FIGURE 23.2 Lymphomatoid granulomatosis. Gross appearance of lung tissue. Note bulging fish-flesh-like nodules replacing much of the pulmonary substance. From Tomashefski et al, with permission from Springer (see chapter references for complete citation).

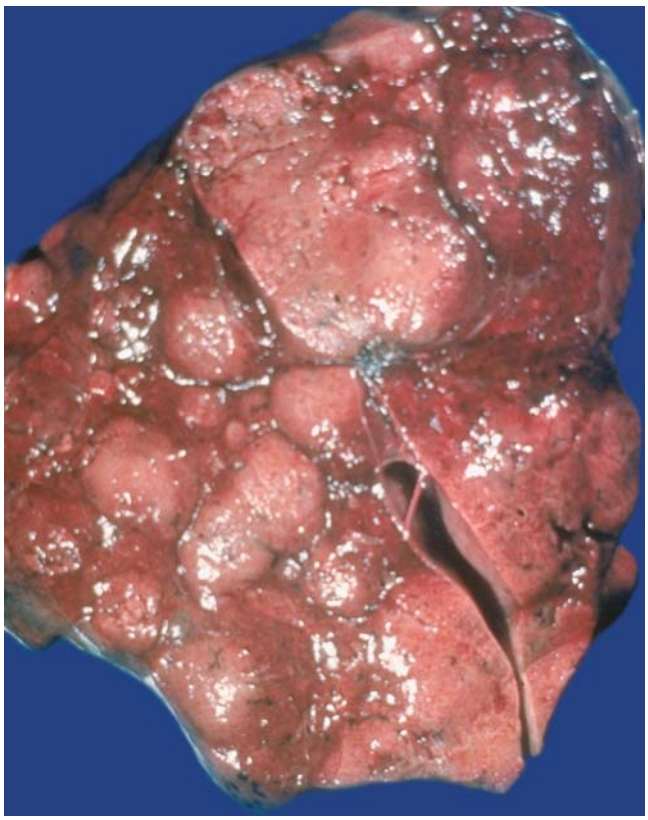

A.E. Fraire et al. (eds.), *Atlas of Neoplastic Pulmonary Disease*,
DOI 10.1007/978-0-387-89839-1_23, © Springer Science+Business Media, LLC 2010

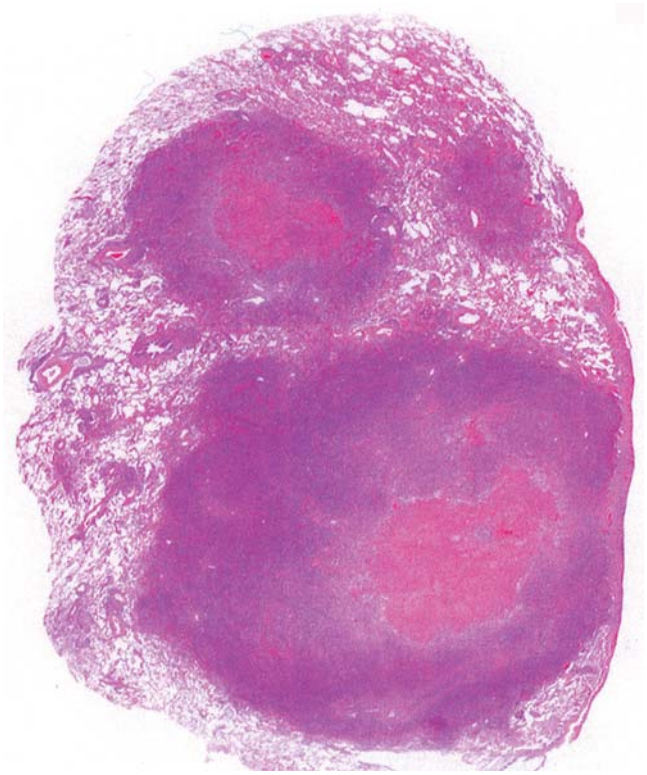

FIGURE 23.3 Lymphomatoid granulomatosis. Whole mount of histologic slide showing nodular lesions with central necrosis. The necrosis is "tumor-like" rather than wedge-shaped as it would be in conventional lung infarcts. From Tomashefski et al, with permission from Springer (see chapter references for complete citation).

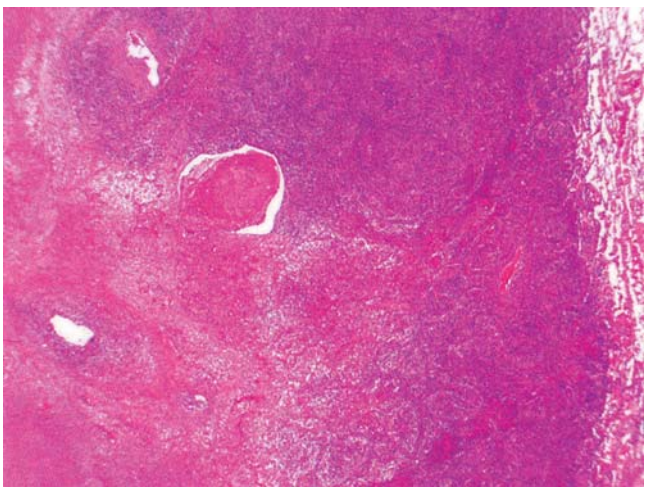

FIGURE 23.4 Lymphomatoid granulomatosis. Microscopic view showing vascular infiltration within a necrotic area seen at the 11.00 o'clock position. Hematoxylin and eosin. From Tomashefski et al, with permission from Springer (see chapter references for complete citation).

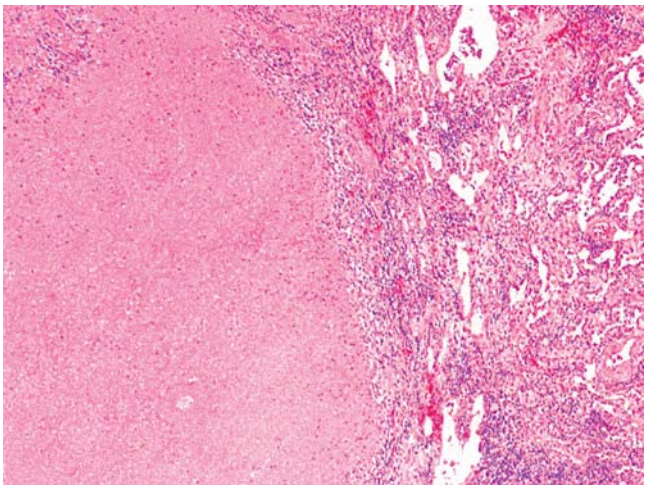

FIGURE 23.5 Lymphomatoid granulomatosis, closer microscopic view showing a transition between the necrotic and non-necrotic areas. Within the necrotic areas, there were some CD20 positive cells suggesting the B cells had become necrotic. Hematoxylin and eosin. From Tomashefski et al, with permission from Springer (see chapter references for complete citation).

is a useful and sensitive tool not only for diagnosis but also for grading of the lesion. Cytologically, some of the lymphoid cells may not be atypical, resembling small mature lymphocytes. Low- and high-grade lesions of LYG have been described, the latter clinically approaching the level of diffuse large cell lymphoma, in terms of clinical presentation and management.

REFERENCES

- Guinee D, Jaffe E, Kingma D, et al. Pulmonary lymphomatoid granulomatosis. Evidence for a proliferation of Epstein-Barr virus infected B-lymphocytes with a prominent T-cell component and vasculitis. *Am J Surg Pathol*. 1994;18:753–764.
- Jorgensen JL. Lymphomatoid granulomatosis In: Cagle PT, Editor-in-Chief. *Color Atlas and Text of Pulmonary Pathology*. 2nd ed. Philadelphia, Baltimore, New York: The Wolters Kluwer Co.; 2008:106–107.
- Koss MN, Harris NL. Lymphomatoid granulomatosis. In: Travis WD, Brambilla E, Müller-Hermelink HK, Harris CC, eds. *World Health Organization Classification of Tumours. Pathology and Genetics of Tumours of the Lung, Pleura, Thymus and Heart*. Lyon: IARC press; 2004:92–94.
- Morice WG, Colby TV. Ch 32, Lymphoproliferative diseases. In: Tomashefski JF Jr., Cagle PT, Farver CF, Fraire AE, eds. *Dail and Hammar's Pulmonary Pathology*. 3rd ed. Berlin, New York, Heidelberg:Springer; 2008:1–45.

- Morice WG, Kurtin PJ, Myers JL. Express of cytologic lymphocyte-associate in pulmonary lymphomatoid granulomatosis. *Am J Clin Pathol*. 2002;118: 391–398.
- Saldaña MJ, Patchesfky AS, Israel HI, et al. Pulmonary angiitis and granulomatosis. The relationship between histological features, organ involvement and response to treatment. *Human Pathol*. 1977;8:391–409.

CHAPTER 24

Langerhans Cell Histiocytosis

Timothy C. Allen, Philip T. Cagle, Dina R. Mody, and Armando E. Fraire

Langerhans cell histiocytosis (LCH) formerly known as pulmonary eosinophilic granuloma is currently regarded by the World Health Organization as a clonal neoplastic proliferation of histiocytes. However, adult variants may represent reactive processes, usually associated with cigarette smoking. Most patients with LCH are either current or former smokers. Radiographically, LCH shows a predilection for the mid to upper lung zones, presenting on high-resolution CT of the chest as nodular lesions, with or without cystic change. Rarely, regional lymph nodes may be affected by the diseases process. The histopathological hallmark of the disease are star-shaped fibrotic lesions containing Langerhans histiocytes. These cells are cells with abundant pale cytoplasm and a distinctively folded or grooved nuclei. Typically, these cells will stain positively with CD1a and the S-100 protein. Cytoplasmic racket-shaped Birbeck granules are present by electron microscopy. A secondary feature that may be focally prominent is the presence of eosinophils. Eosinophils tend to be sparse on older lesions and are not required for diagnosis. Their presence is however valuable since it may clue the observer to the possibility of LCH. An association with other lymphoid malignancies particularly Hodgkin's disease of the lung has been reported. Rarely, a definite cytopathologic diagnosis of LCH can be made in pulmonary secretions or fluid material from bronchoalveolar lavage procedures. The presence and recognition of eosinophils, in bronchoalveolar lavage fluid material may however alert the clinician to consider the diagnosis.

A.E. Fraire et al. (eds.), *Atlas of Neoplastic Pulmonary Disease*,
DOI 10.1007/978-0-387-89839-1_24,

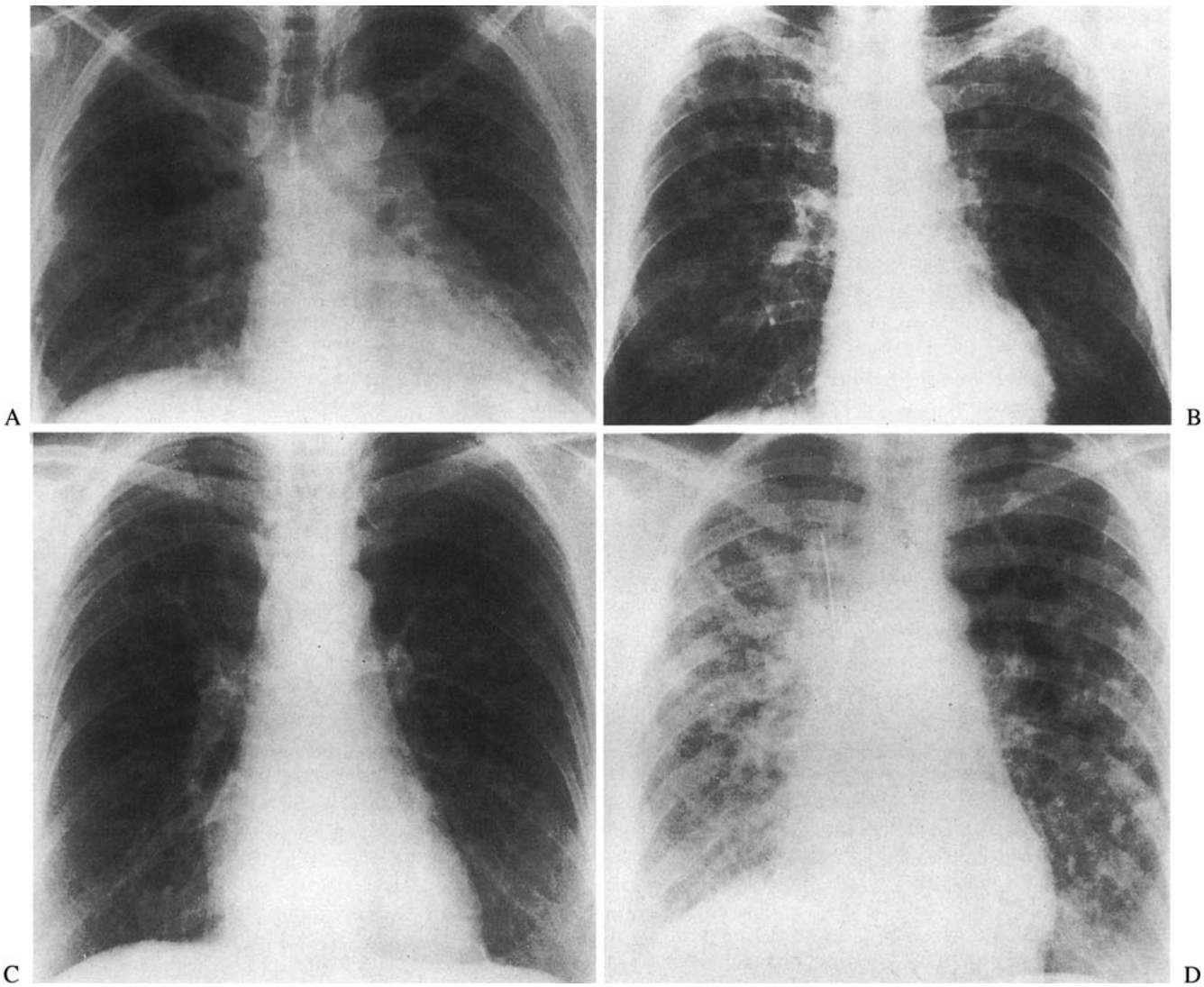

FIGURE 24.1 Chest radiographs from four patients with varying modalities of pulmonary Langerhans cell histiocytosis. (**a**) Diffuse reticulonodualr infiltrates. (**b**) Bilateral infiltrates with sparing of costophrenic angles. (**c**) Bilateral micronodular infiltrates. (**d**) Bilateral macronodular infiltrates that can be mistakenly interpreted as evidence of metastatic disease (Courtesy of Drs. S.P. Hammar and Timothy C. Allen). From Tomashefski et al, with permission from Springer (see chapter references for complete citation).

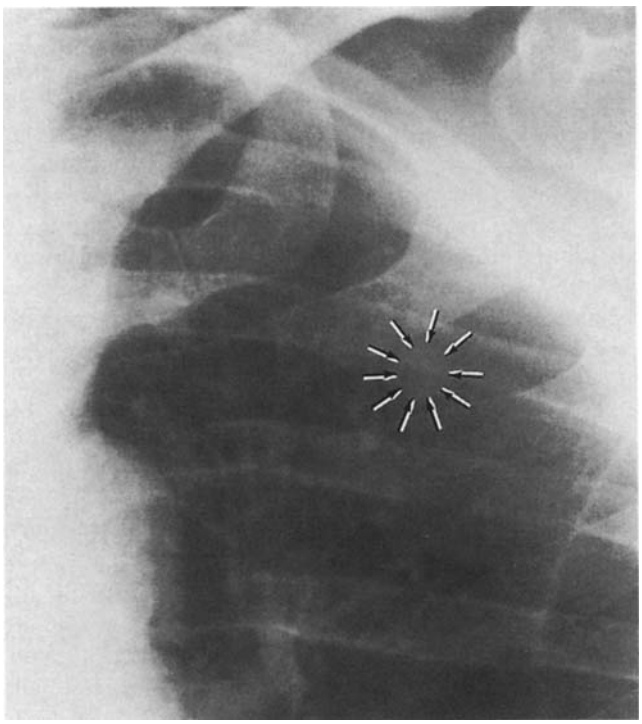

FIGURE 24.2 Chest radiographs of a 65-year-old man with isolated left upper lobe nodule (*star*) that on biopsy was found to represent pulmonary Langerhans cell histiocytosis (Courtesy of Drs. S.P. Hammar and Timothy C. Allen). From Tomashefski et al, with permission from Springer (see chapter references for complete citation).

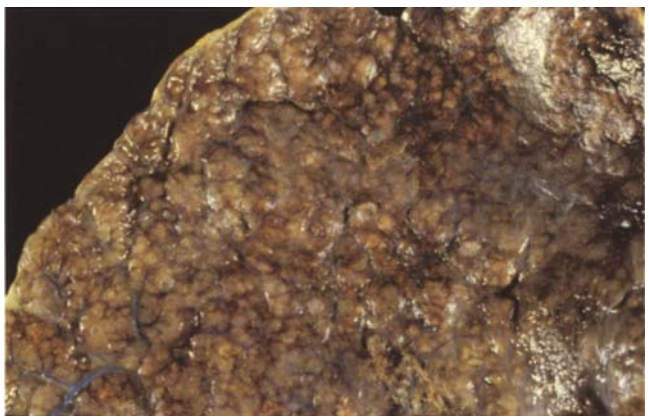

FIGURE 24.3 Gross appearance of lung in a patient with advanced pulmonary Langerhans cell histiocytosis. Note scarred nodular pleural surface with honeycombing (Courtesy of Drs. S.P. Hammar and Timothy C. Allen). From Tomashefski et al, with permission from Springer (see chapter references for complete citation).

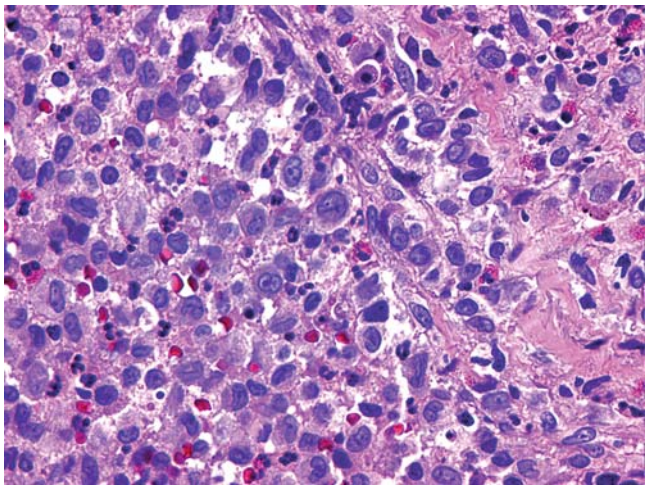

FIGURE 24.4 Microscopic appearance of pulmonary Langerhans cell histiocytosis. Note histiocytes with typical features of Langerhans cells in association with eosinophils, round lymphocytes, and scattered fibroblasts (Hematoxylin and eosin).

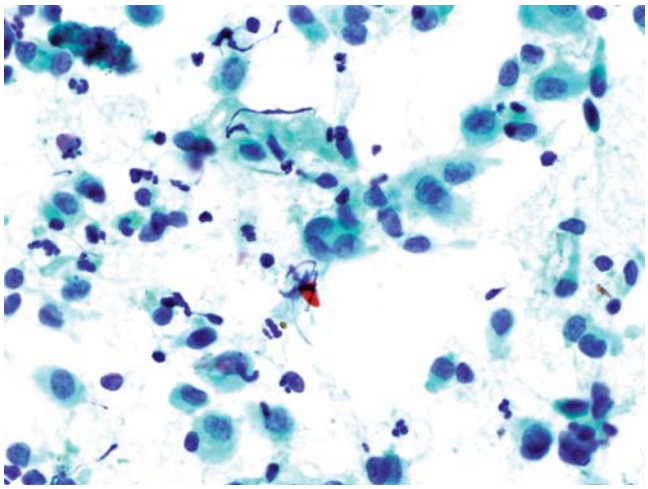

FIGURE 24.5 Cytologic appearance of pulmonary Langerhans cell histiocytosis. Note discohesive histiocytic cells with bean-shaped nuclei (Papanicolaou stain).

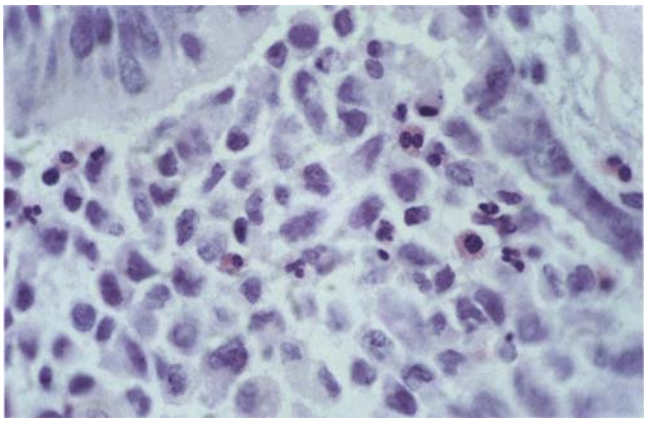

FIGURE 24.6 This cytologic preparation from bronchiolar lumen shows numerous Langerhans histiocytosis cells mixed with other inflammatory cells (Courtesy of Drs. S.P. Hammar and Timothy C. Allen). From Tomashefski et al, with permission from Springer (see chapter references for complete citation).

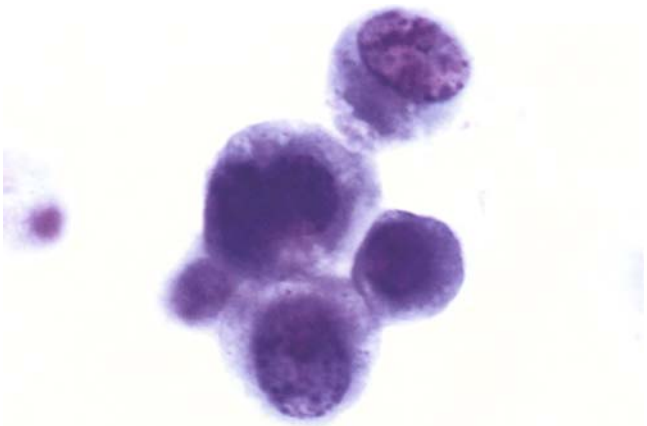

FIGURE 24.7 In sputum preparations, cells other than Langerhans cell histiocytes can be seen. The image represents a group of highly atypical alveolar epithelial cells (Courtesy of Drs. S.P. Hammar and Timothy C. Allen). From Tomashefski et al, with permission from Springer (see chapter references for complete citation).

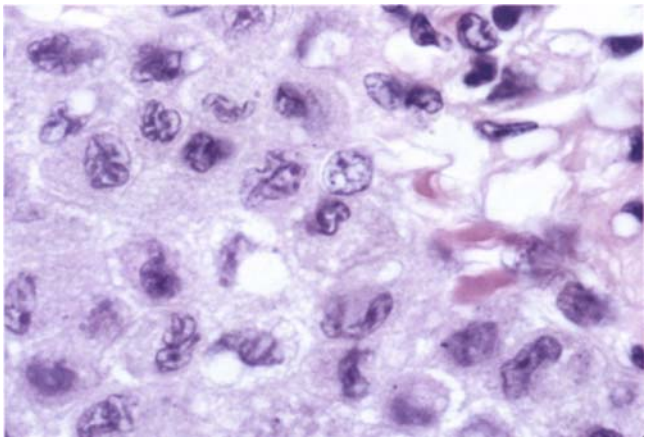

FIGURE 24.8 An additional preparation of cellular material identified within the lumen of a respiratory bronchiole shows an accumulation of histiocytes some of which have an appearance consistent with Langerhans histiocytosis cells (Courtesy of Drs. S.P. Hammar and Timothy C. Allen). From Tomashefski et al, with permission from Springer (see chapter references for complete citation).

REFERENCES

- Agostini C, Alberas C, Bariffo F, et al. First report of Italian register for diffuse infiltrative lung disorders. *Monaldi Arch Chest Dis*. 2001;56:367–368.
- Colby TV, Travis WD. Pulmonary langerhans cell histiocytosis. In: Travis WD, Brambilla E, Müller-Hermelink HK, Harris CC, eds. *World Health Organization Classification of Tumours. Pathology and Genetics of Tumours of the Lung, Pleura, Thymus and Heart*. Lyon: IARC Press; 2004: 95–96.
- Hammar SP, Allen TC. Ch 16. Histiocytosis and storage diseases. In: Tomashefski JF Jr., Cagle PT, Farver CF, Fraire AE, eds. *Dail and Hammar's Pulmonary Pathology*. 3rd ed. Berlin, Springer: New York, Heidelberg; 2008:600–649.
- Jaffe ES, Harris NL, Stain H, et al. *WHO Classification of Tumours of Haemapoeitic and Lymphoid Tissues*. 1st ed. Lyon: IARC Press; 2001.
- Shaker KG, Umali CB, Fraire AE. Langerhans cell histiocytosis of the lung in association with mediastinal adenopathy. *Pathol Int*. 1995;45:762–766.
- Vassallo R, Ryu JH, Colby TV, et al. Pulmonary langerhans cell histiocytosis. *N Engl J Med*. 2000;342:1969–1978.
- Yousem SA, Colby TV, Chen YY, et al. Pulmonary langerhans cell histiocytosis: Molecular analysis of clonality. *Am J Surg Pathol*. 2001;25:630–636.

CHAPTER 25

Typical and Atypical Carcinoids

Shanda Blackmon, Richard S. Irwin, Armin Ernst, Philip T. Cagle, Timothy C. Allen, N. Paul Ohori, Elise R. Hoff, Dina R. Mody, and Armando E. Fraire

Primarily occurring in the airways, carcinoids tumors may also arise peripherally within the lung. Their histopathologic hallmark is a growth pattern that suggests neuroendocrine differentiation (organoid, trabecular, insular, etc.). Two major variants of carcinoid tumors are recognized: typical and atypical. Some carcinoid tumors, particularly the ones that are peripherally located, may be clinically silent. Fever, cough, expectoration, chest pain, and hemoptysis occur in a substantial number of centrally located cases. The most common radiologic manifestation, seen in about 80–85% of cases, is evidence of bronchial obstruction, owing to the majority of these tumors occupying a central endobronchial location. Bronchial obstruction is revealed as atelectasis or obstructive pneumonitis. Peripheral carcinoids, often the spindle cell variant, occur as solitary pulmonary nodules manifested as well-defined homogenous densities, usually up to 3 cm in diameter. Rarely bone within these tumors may become evident on chest radiograph or computed tomography. The latter may also show marked vascular enhancement in contrast studies. Tumorlets are essentially small carcinoid tumors, 5 mm or less by convention, usually intraparenchymal, not accessible by bronchoscopy, and difficult to distinguish from other small pulmonary tumors by CT of chest and are not discussed here.

At bronchoscopy, carcinoids may appear as smooth ball-like growths that may partially or totally obstruct the airways. Some may be pedunculated, others sessile. Interpretive caution may be needed when the adjacent mucosa is thickened as this may represent inflammation related to obstruction and not necessarily infiltration by tumor. Carcinoid tumors are highly vascularized tumors and caution is advised when planning to perform endoscopic biopsy since bleeding may be copious. Endoscopy offers an optional therapeutic approach for endobronchial tumor that are deemed removable by this modality. The gross appearance of these tumors recapitulates that seen at endoscopy. The endoluminal variants tend to be smaller than the pure parenchymal forms. The so-called iceberg tumors are mixed forms of tumors with ultraluminal and parenchymal components. The cut surface of these tumors is often yellow and without evidence of necrosis.

Major microscopic features of both typical and atypical carcinoids include a classic growth pattern, namely organoid, trabecular, or rosette-forming. However, in some tumors a solid growth pattern is seen. Individual cells have uniform round nuclei, finely granular cytoplasm, and variable but generally scant amount of cytoplasm. Clear, granular, plasmacytoid, oncocytic, and

FIGURE 25.1 CT of chest showing two nodular lesions, one on the left and one on the right side. The right-sided nodule was diagnosed as typical carcinoid.

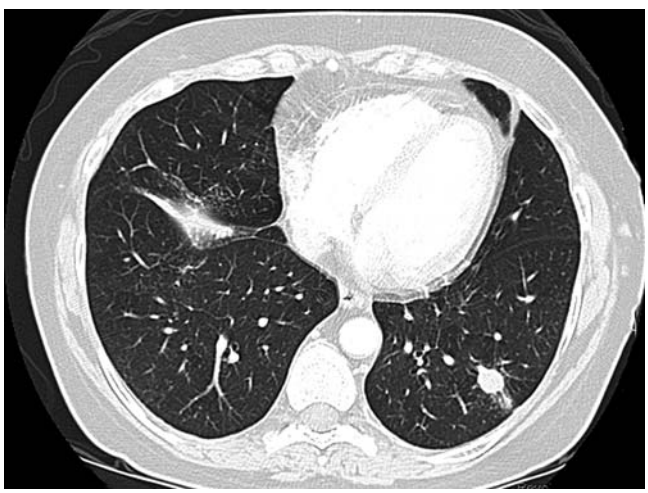

A.E. Fraire et al. (eds.), *Atlas of Neoplastic Pulmonary Disease*,
DOI 10.1007/978-0-387-89839-1_25,

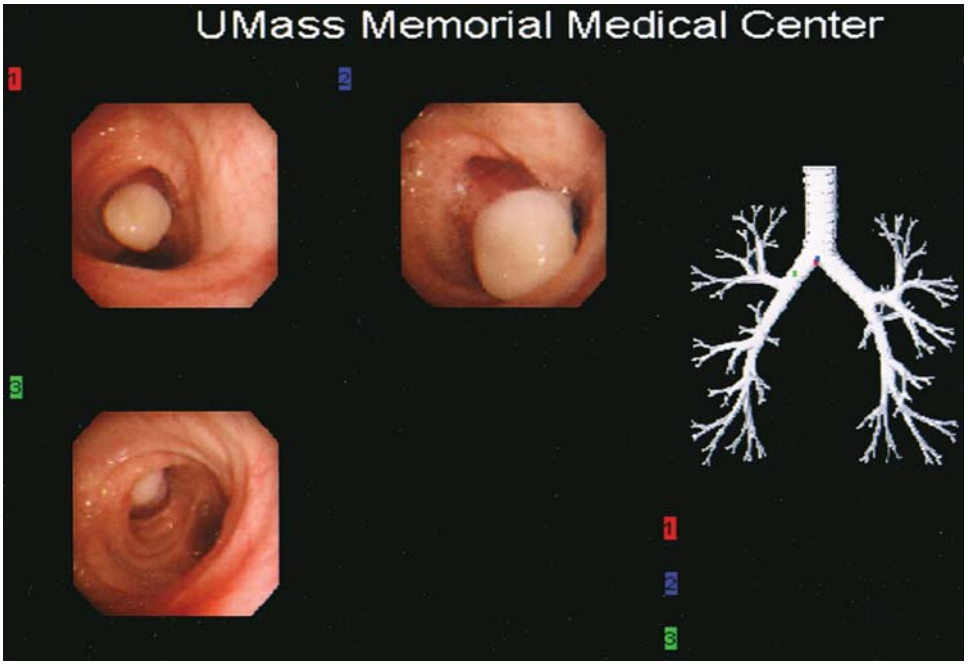

FIGURE 25.2 Typical carcinoid. Endoscopic view showing a grayish white globoid lesion with a smooth outer surface nearly occluding the airway lumen.

melanotic variants are recognized. The presence of necrosis and mitosis (0–2 per 10 HPF's for the typical forms and 3–10 for the atypical ones) helps to separate these variants. Cellular atypia more prominent in the atypical variants is a subjective criterion and not generally regarded as helpful in the differential diagnosis.

The mucosal surface of these tumors is often intact and as a result sputum cytology is often negative. In bronchial brush cytologic preparations, typical carcinoids may show tight clusters of cells with moderately abundant cytoplasm and round nuclei with moderately granular chromatin. In contrast, the cells of the atypical variants tend to be pleomorphic and to arrange themselves in loose clusters of cells with scant cytoplasm and round nuclei with coarsely granular chromatin.

FIGURE 25.3 Typical carcinoid. Microscopic appearance of a carcinoid tumor showing uniform tumor cells arranged in an organoid pattern. Respiratory epithelium is on the right. Hematoxylin and eosin.

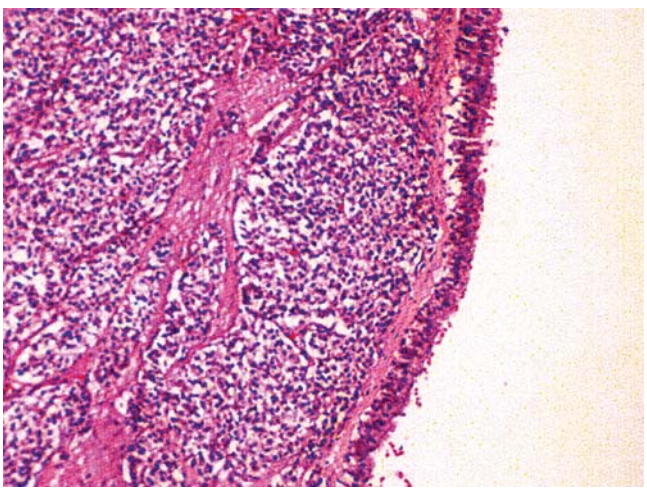

FIGURE 25.4 Typical carcinoid. In this cytopathologic preparation of a typical carcinoid, the tumor cells show uniformity of size and shape. The stippled nuclear chromatin gives some of the tumor cells a plasmacytoid appearance. Papanicolaou stain.

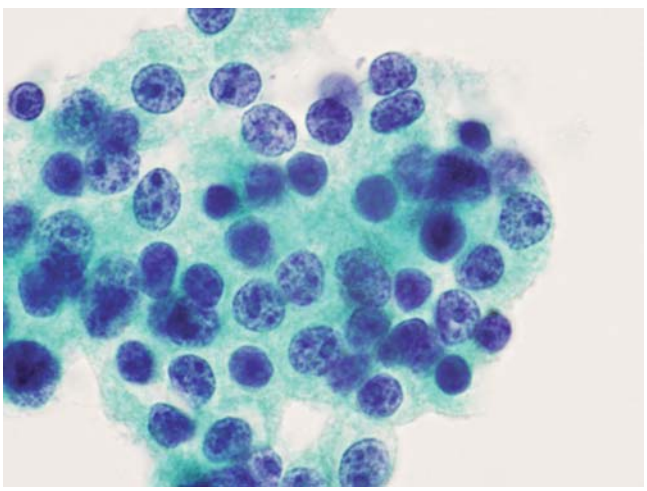

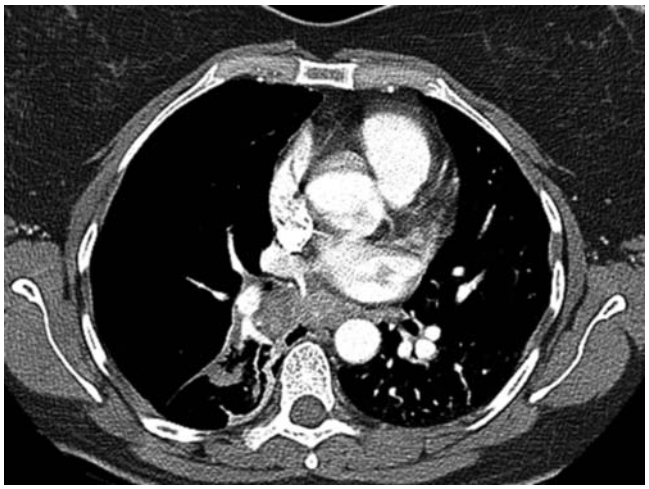

FIGURE 25.5 Atypical carcinoid. CT scan of chest showing a tracheal mass at the bifurcation site with near total obliteration of its lumen. There is also distal atelectasis of the superior segment of the right lower lobe. Biopsy showed atypical carcinoid.

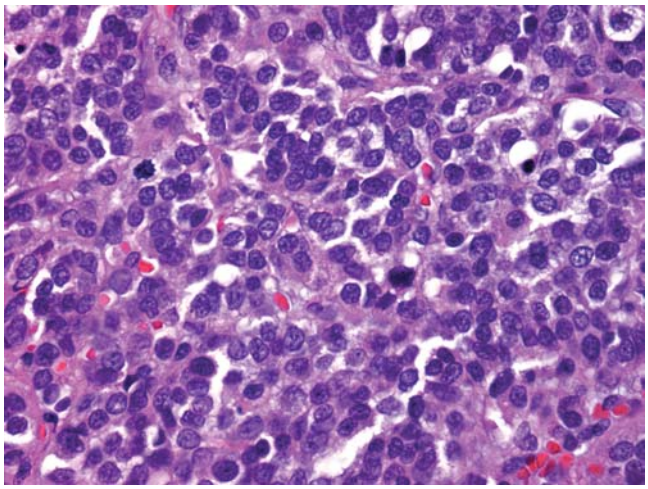

FIGURE 25.7 Atypical carcinoid, microscopic appearance showing cellular crowding with cells having no distinct organoid pattern. Hematoxylin and eosin.

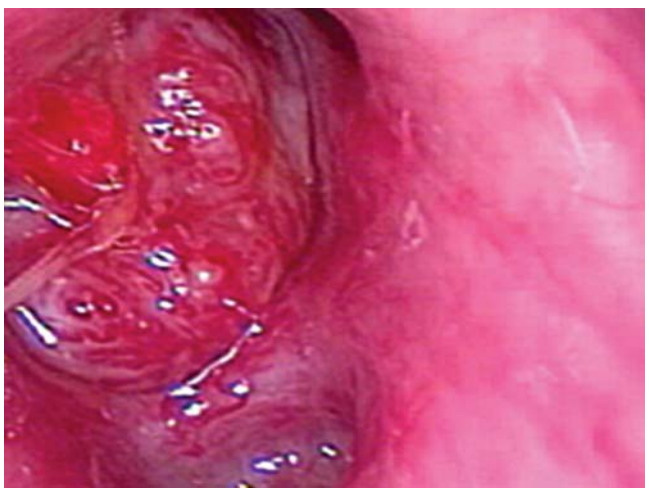

FIGURE 25.6 Atypical carcinoid. Endoscopic view of a mass lesion in the distal left main stem bronchus. The surface of the mass lesion is relatively smooth similar to that of the surrounding mucosa but much more reddish in color. Biopsy showed atypical carcinoid.

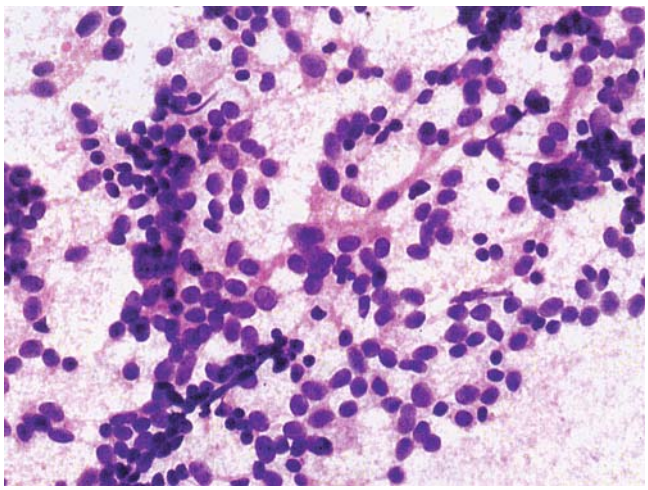

FIGURE 25.8 Atypical carcinoid. Cytopathologic preparation showing cellular pleomorphism. However, cellular pleomorphism is not a reliable criterion for diagnosis. The most useful distinguishing features – mitotic figures and punctate necrosis – are often not reliably identified on cytology specimens. Diff Quick Stain. From Tomashefski et al, with permission from Springer (see chapter references for complete citation).

REFERENCES

- Beasley MB et al. Carcinoid tumour In: Travis WD, Brambilla E, Müller-Hermelink HK, Harris CC, eds. *Pathology and Genetics. Tumours of the Lung, Pleura, Thymus and Heart. The World Health Organization Classification of Tumors*. Lyon: IARC Press; 2004:59–62.
- CA French. Ch 2. Respiratory tract In: Cibas ES, Ducatman BS, eds. *Cytology. Diagnostic Principles and Clinical Correlates*. Edinburgh, London, New York: Saunders; 2003:83–85.
- Hapole DH Jr, Feldman JM, Buchanan S, et al: Bronchial carcinoid tumors: A retrospective analysis of 126 patients. *Ann Thorac Surg*. 1992;54:50–55.
- Iser G, Pfohl M, Dorr U, et al: Ectopic ACTH secretion due to a bronchopulmonary carcinoid localized by somatostatin receptor scintigraphy. *Clin Invest*. 1994;72:887–891.
- Magid D, Siegelman SS, Eggleston JC, et al: Pulmonary carcinoid tumors: CT assessment. *J Comput Assist Tomogr*. 1989;13:244–247.

- Ohori NP, Hoff ER. Ch 45. Cytopathology of pulmonary neoplasia. In: Tomashefski JF, Cagle PT, Farver CF, Fraire AE, eds. *Dail and Hammar's Pulmonary Pathology*. Vol II. Springer: Berlin, Heidelberg, New York; 2008:767–795.
- Soga J, Yakuwa Y: Bronchopulmonary carcinoids: An analysis of 1875 reported cases with special reference to a comparison between typical carcinoids and atypical varieties. *Ann Thorac Cardiovasc Surg*. 1999;5: 211–219.
- Todd TR, Cooper JD, Weissberg D, et al: Bronchial carcinoid tumors. *J Thorac Cardiovasc Surg*. 1980;79: 532–536.
- Travis WD, Linnoila RI, Tsokos MG, et al. Neuroendocrine tumors of the lung with proposed criteria for large cell neuroendocrine carcinoma: An ultrastructural, immunohistochemical and flow cytometric study of 35 cases. Am J Surg Pathol. 1991;15:529–553.

CHAPTER 26

Teratoma

Shanda Blackmon, Philip T. Cagle, Timothy C. Allen,
and Armando E. Fraire

Teratomas are neoplasms derived from two or more germ cell lines that may be either mature or immature. Teratomas occur in individuals aged 19–68 years old but some occur in younger individuals. The presenting symptoms are those of an intrapulmonary mass. Rarely, trichoptysis (literally, the expectoration of hair) has been described in some cases. Teratomas are slow-growing tumors, and slow growth of radiologically documented cases by CT will be suggestive of the diagnosis, particularly in cases showing associated fat, cavitation, and calcification. Lucencies within densities are said to be pathognomonic but not characteristic.

Grossly, teratomas present as solid masses that vary in texture and appearance. Cystic change within the tumors may occur and in these instances granular, watery, or flaky yellow debris can be observed within the cystic cavity. Teratomas of the lung resemble those occurring in other anatomical sites but differ in that complex well-developed structures such as dental pieces are seldom found. Microscopically, all three germinal layers are represented with dermal elements such as skin and skin appendages being common. Fat, thymic, and pancreatic tissues have been reported as have muscle, bone, cartilage, and neural tissues. Malignant teratomas may present with metastasis to lymph nodes. It is absolutely necessary to exclude a gonadal teratoma or an extra-gonadal teratoma in a non-pulmonary site before a diagnosis of primary teratoma of lung is made with confidence.

FIGURE 26.1 Teratoma. CT of chest. Note well-circumscribed tumor mass in the superior segment of the right lower lobe.

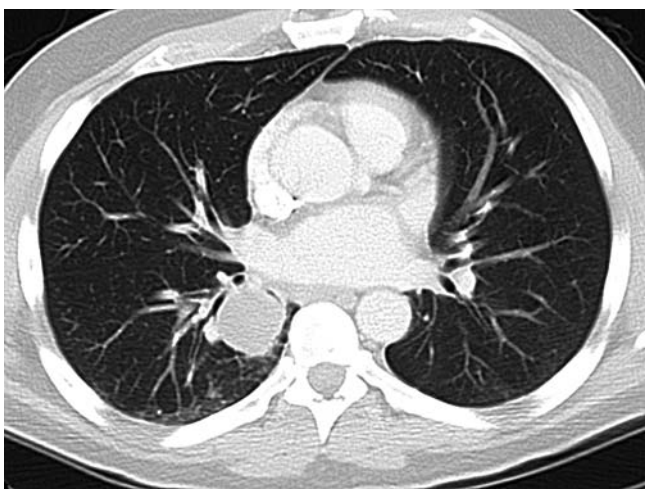

FIGURE 26.2 Teratoma. At left is bronchus; at right is epidermis with appendages. Fat is in the middle lower part. Hematoxylin and eosin. From Tomashefski et al, with permission from Springer (see chapter references for complete citation).

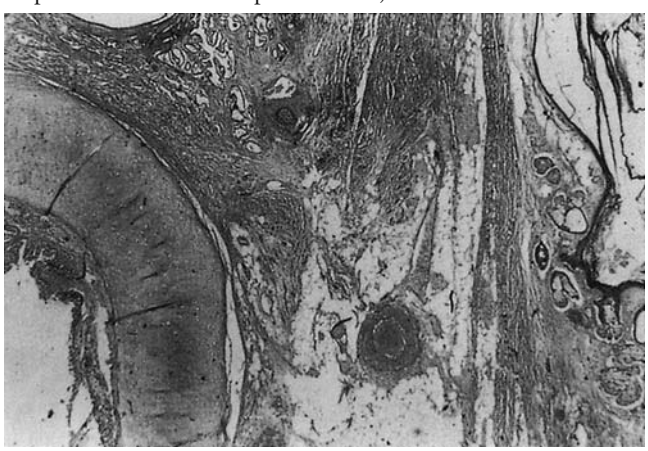

A.E. Fraire et al. (eds.), *Atlas of Neoplastic Pulmonary Disease*,
DOI 10.1007/978-0-387-89839-1_26,

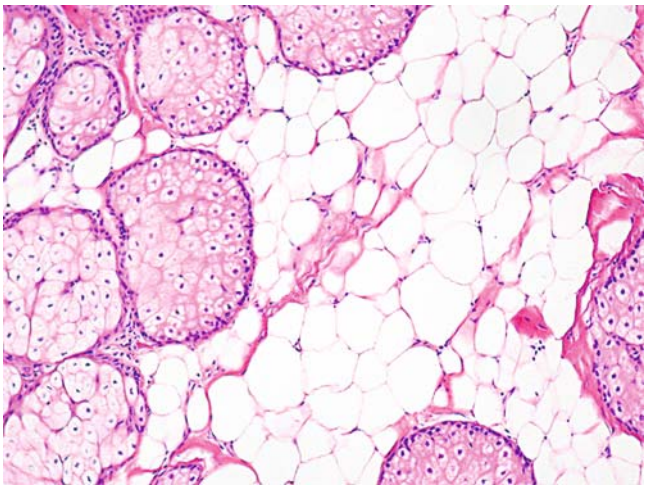

FIGURE 26.3 Teratoma, microscopic view showing mature adipose tissue (fat) and sebaceous glands. Hematoxylin and eosin. From Tomashefski et al, with permission from Springer (see chapter references for complete citation).

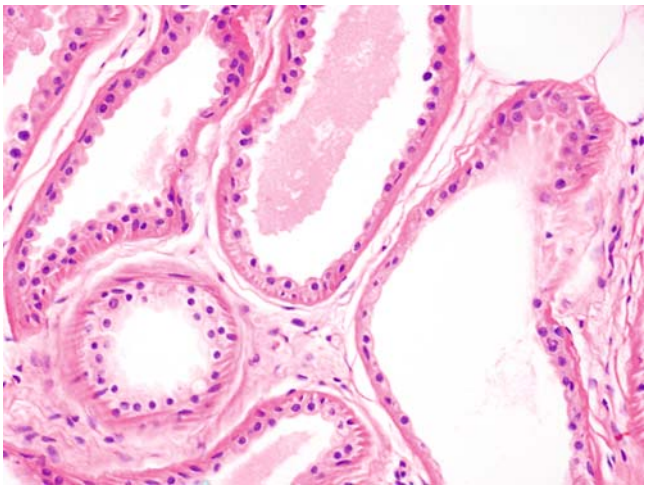

FIGURE 26.4 Teratoma. Close view of another area of a teratoma showing tissues of ectodermal (sebaceous glands) and mesodermal (mature fat) derivation. Hematoxylin and eosin. From Tomashefski et al, with permission from Springer (see chapter references for complete citation).

REFERENCES

- Fraire AE, Dail DH. Ch 41. Miscellaneous tumors and tumor-like proliferations of the lung. In: Tomashefsky JF, Cagle PT, Farver CA, Fraire AE, eds. *Dail and Hammar Pulmonary Pathology*. 3rd ed. Berlin, New York, Heidelberg: Springer; 2008:500–541.
- Kayser K, Gabius HJ, Hagemeyer O. Malignant teratoma of lung with lymph node metastasis of the ectodermal component. *Anal Cell Pathol.* 1993;5: 31–37.
- Morgan DE, Sanders C, McElvein RB. Intrapulmonary teratoma: a case report and review of the literature. *J. Thorac Imaging*. 1992;7:70–77.
- Nicholson AG. Teratoma. In: Travis WD, Brambilla E, Müller-Hermelink HK, Harris CC, eds. *WHO Tumours of the Lung, Pleura, Thymus and Heart*. Lyon: IARC Press; 2004:119.

CHAPTER 27

Melanoma

Toshiaki Kawai, Philip T. Cagle, Timothy C. Allen, Takayuki Haga,
Kuniaki Nakanishi, and Armando E. Fraire

Primary melanomas of the lung are rare malignant tumors of uncertain histogenesis believed by some to arise from melanocytic metaplasia of the bronchial respiratory epithelium or from primitive displaced melanocytic cells from the foregut, during the process of embryogenesis. Melanomas show no gender predilection and most occur between the ages of 29 and 80 years. Clinical symptoms are related to obstruction with dyspnea or hemoptysis predominating. Little is known about the radiographic appearance of primary melanomas of lung. Some present as pleural effusions of unknown origin. Metastatic melanoma usually presents as multiple tumor masses but may on occasion be single.

Endoscopy may reveal pigmentation of the airway mucosa in combination with a mass lesion. The pigmentation should be differentiated from that due to anthracosis. Centrally located melanomas are made up of polypoid endoluminal masses of fleshy brown to black tissue. More peripherally located melanomas do occur but are even rarer than the central ones. Tumor cells are similar to those of melanomas occurring elsewhere, namely they are apt to be large, polygonal, discohesive cells with prominent nucleoli and variable degree of pigmentation. Some, however, may totally lack pigmentation. To our knowledge, the cytopathologic features of melanoma have not been well characterized but would be expected to show features similar to those of melanomas occurring elsewhere.

FIGURE 27.1 Radiograph of chest showing massive right pleural effusion. Reproduced with permission from Acta Medica Okayama, see chapter references for complete citation.

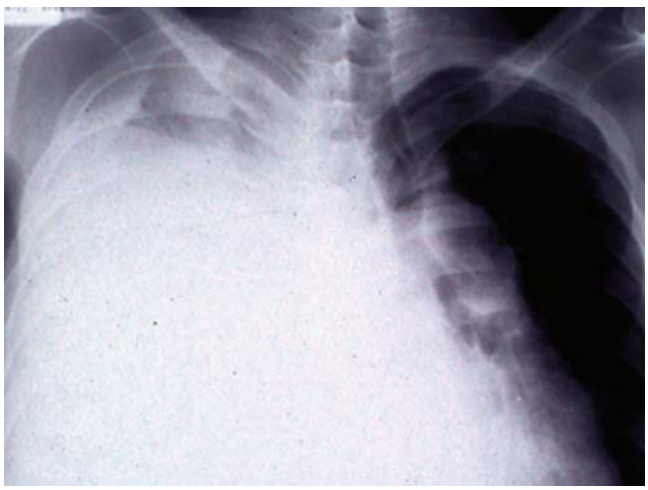

A.E. Fraire et al. (eds.), *Atlas of Neoplastic Pulmonary Disease*,
DOI 10.1007/978-0-387-89839-1_27,

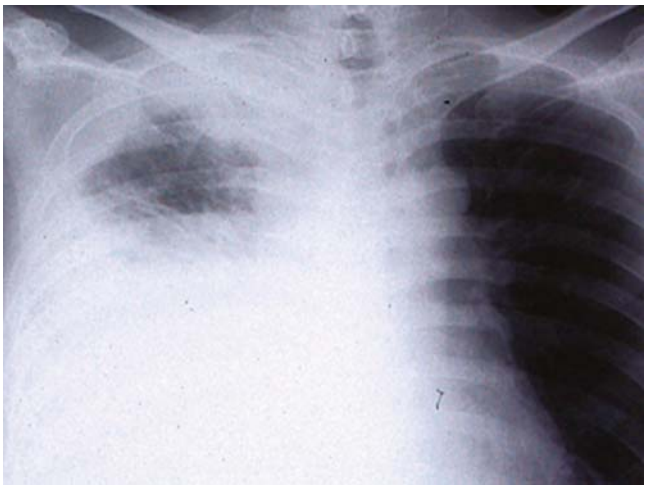

FIGURE 27.2 Radiograph of chest showing partial re-expansion of the right lung following drainage of the pleural effusion. Reproduced with permission from Acta Medica Okayama, see chapter references for complete citation.

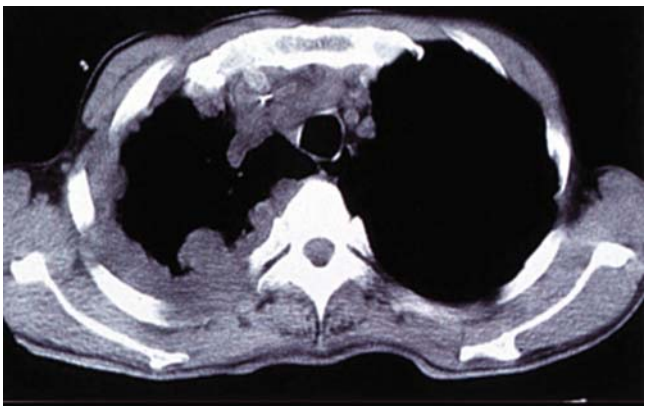

FIGURE 27.3 CT of chest showing irregularly shaped pleural-based tumor mass following the contour of the chest wall. Reproduced with permission from Acta Medica Okayama, see chapter references for complete citation.

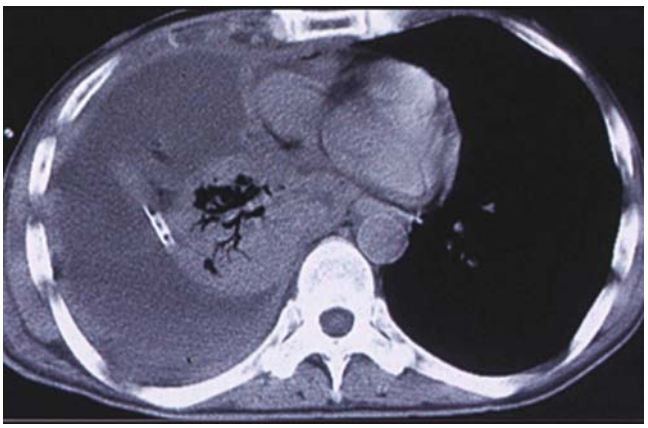

FIGURE 27.4 CT of chest showing tumor extension from the pleura into the chest wall. Reproduced with permission from Acta Medica Okayama, see chapter references for complete citation.

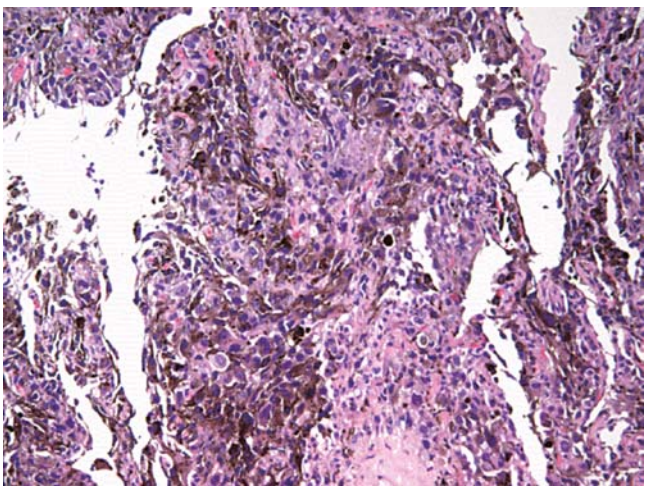

FIGURE 27.5 This histopathologic image of an intrapulmonary melanoma shows a cellular proliferation with heavy melanin pigmentation in some of the melanoma cells. Hematoxylin and eosin.

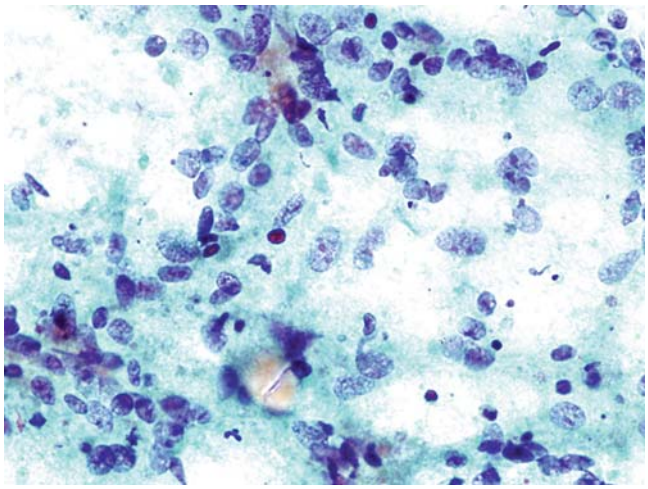

FIGURE 27.6 This cytologic preparation of a metastatic subcutaneous right chest mass represents melanoma from a pleuropulmonary primary. Note non-pigmented large cells with high nuclear cytoplasmic ratio and multiple nucleoli. Papanicolaou stain. Reproduced with permission from Acta Medica Okayama, see chapter references for complete citation.

REFERENCES

- Cagle P, Mace ML, Judge DM, et al. Pulmonary melanoma: primary vs metastatic. *Chest*. 1982;85:125–126.
- Duhamel DR. Ch 18. Metastatic melanoma In: Duhamel DR, Hanell JH, eds. *Clinical Atlas of Airway Diseases: Bronchoscopy, Radiology and Pathology*. Philadelphia: Elsevier Saunders; 2005:18–19.
- Jennings TA, Axiotis CA, Kreiss Y, et al. Primary malignant melanoma of the lower respiratory tract. Report of a case and review of the literature. *Am J Clin Pathol*. 1990;94:649–655.
- Kawai T, Haga T, Nakanishi K. Primary malignant melanoma of the pleura. Report of an autopsy case. *Arch Pathol Lab Med*. 2008;132:285–286A.
- Kawai T, Takayuki H, Nakanishi K. Malignant melanoma of the pleura. *Acta Medica Okayama*. 2009;75:1234–1235.
- Littman CD. Metastatic melanoma mimicking primary bronchial melanoma. *Histopathology*. 1991;18:561–563.
- Nicholson AG. Melanoma. In: Travis WD, Brambilla E, Müller-Hermelink HK, Harris CC, eds. *World Health Organization Classification of Tumours. Pathology and Genetics. Tumours of the Lung, Pleura, Thymus and Heart*. Lyon: IARC Press; 2004:121.
- Ost D, Sogoloff H, Menezes G. Primary pulmonary melanoma: case report and literature review. *Mayo Clin Proc*. 1999;74:62–66.

CHAPTER 28

Thymoma

Shanda Blackmon, Richard S. Irwin, Philip T. Cagle,
Timothy C. Allen, Dina R. Mody, and Armando E. Fraire

This is a rare neoplasm believed to arise from ectopic or aberrant thymic tissue in either lung or pleura, with histologic features resembling those of thymomas occurring in the thymus gland. The clinical manifestations are nonspecific including cough, chest pain, and fever. Tumors located near the pleura may be associated with effusions. Rare cases associated with myasthenia gravis have been reported. Radiologic findings refer to the presence of a mass lesion and are said to be nonspecific. An important consideration when considering a tumor solely on basis of chest radiograph and/or gallium^{67} studies is the scanning of any possible extension of a mediastinal thymoma into the lung tissue, mimicking a primary lung tumor. In such instances, CT scanning can, in some cases, correctly identify a connecting pedicle, tracing the tumor back into the mediastinum.

As is the case with radiographic techniques, bronchoscopic evaluation of any histologically proven thymoma requires exclusion of a primary mediastinal thymoma extending into the lung. A report has been described of a woman with chest CT evidence of a well-defined mass with focal calcification in the anterior mediastinum with associated coin lesions in the lungs. At bronchoscopy, a polypoid endobronchial tumor was identified. Biopsy revealed a thymoma. On further resection, a primary mediastinal thymoma with extension into lung and bronchi was documented. We have encountered a similar patient with extension of thymoma into the airway.

Thymomas vary widely in size, ranging up to 12 cm and are usually circumscribed encapsulated masses with lobulated cut surfaces and focal cystic changes. The histopathology of primary pleural and pulmonary thymomas resembles that of thymomas arising in the thymus gland. They have prominent lymphoid components and a lobulated architecture with lobules separated from one another by fibrous septae. Admixed with the lymphoid cells, epithelioid components can be seen. The epithelial cells can form nests, trabeculae as well as rosettes and are cytokeratin-positive. A helpful cytopathologic feature is the presence of epithelial cells in a background of lymphoid cells.

FIGURE 28.1 CT scan of an intrapulmonary thymoma presenting as an anterior mediastinal mass adjacent to the anterior left trunk of the pulmonary artery.

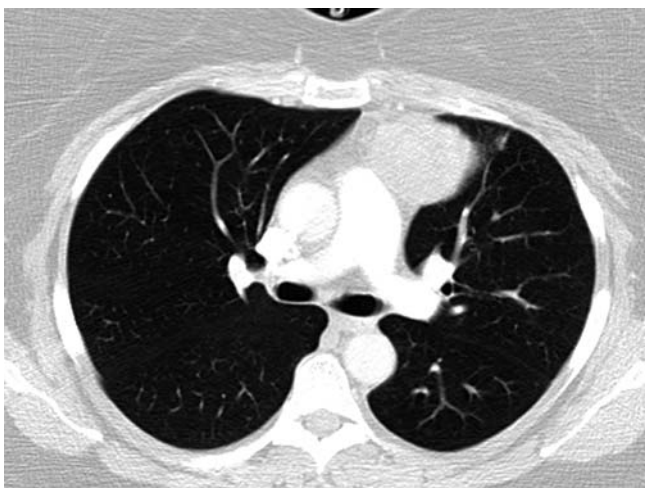

A.E. Fraire et al. (eds.), *Atlas of Neoplastic Pulmonary Disease*,
DOI 10.1007/978-0-387-89839-1_28, © Springer Science+Business Media, LLC 2010

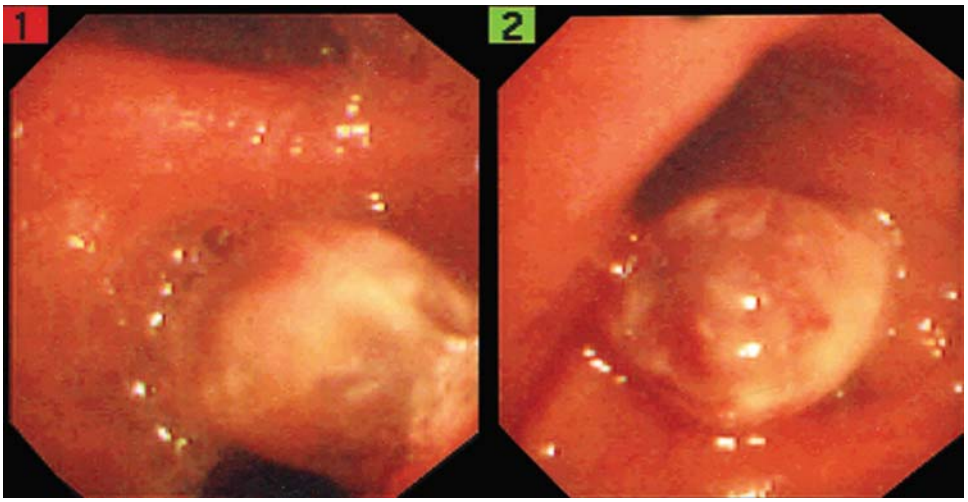

FIGURE 28.2 Gross appearance: this thymoma presented as a protruding mass into the lumen of a major airway, in a polypoid fashion. Note smooth, non-ulcerated yellow red surface.

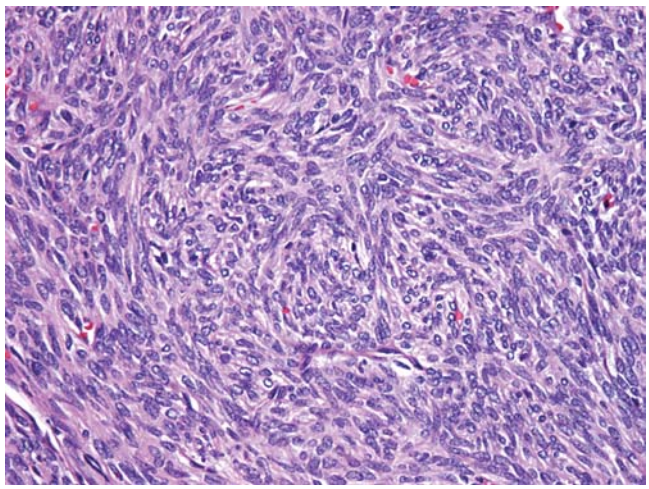

FIGURE 28.3 This high-power histopathologic view of an epithelial thymoma of lung shows multiple fascicles of uniform-looking spindle-shaped cells with nuclear hyperchromatism. Hematoxlyin and eosin.

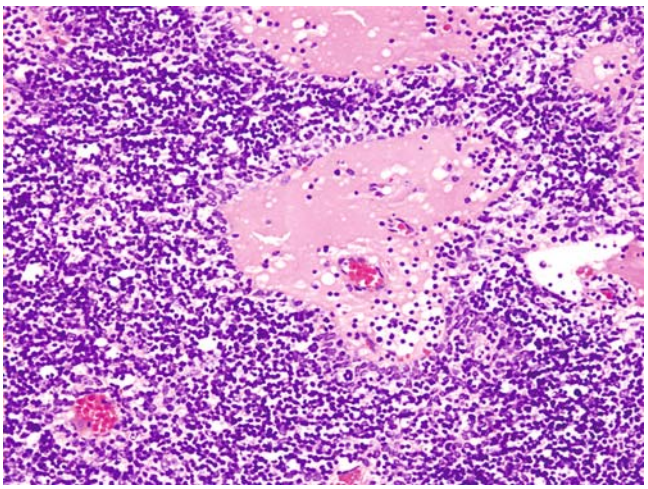

FIGURE 28.4 Thymoma. Histopathologic appearance: this mediastinal thymoma shows small spindle cells overwhelmed by a population of small lymphocytes. Hematoxylin and eosin (Courtesy of Dr. Peter Wu, University of Massachusetts Medical School, Worcester, MA). From Tomashefski et al, with permission from Springer (see chapter references for complete citation).

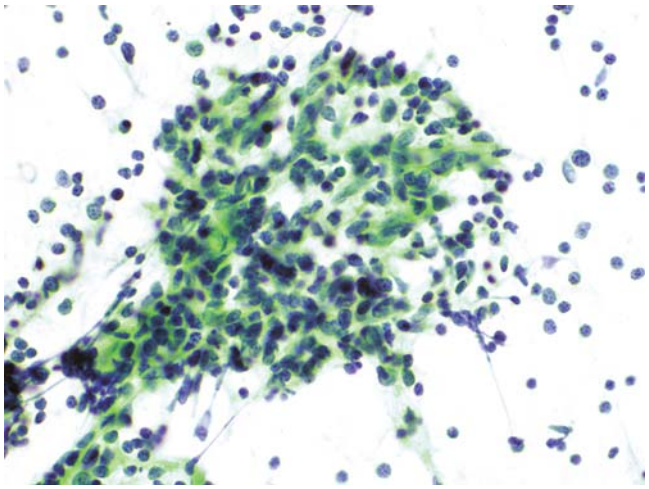

FIGURE 28.5 This cyotpathologic preparation of a thymoma shows a bi-modal cell population consisting of small dark lymphocytes and larger pale spindly epithelial cells. Papanicolaou stain.

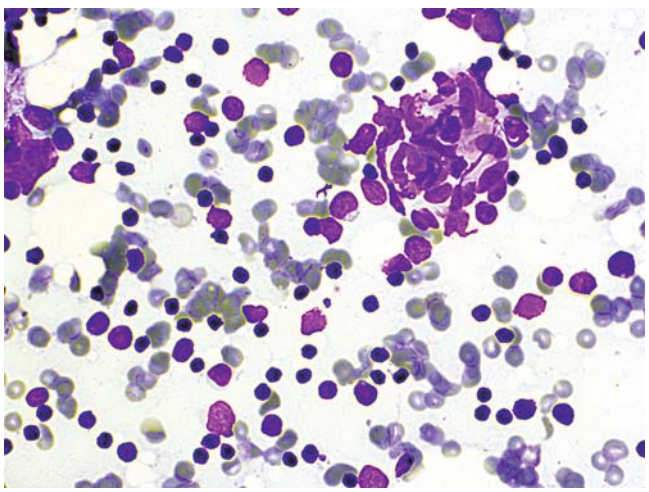

FIGURE 28.6 Thymoma. Cytopathology: This cytopathologic preparation shows predominant lymphoid cells of varying sizes. Diff-quick stain.

REFERENCES

- Fraire AE, Dail DH. Ch 41. Miscellaneous tumors and tumor-like proliferations of the lung. In: Tomashefski JF Jr., Cagle PT, Farver CF, Fraire AE, eds. *Dail and Hammar's Pulmonary Pathology*. 3rd ed. Berlin, New York, Heidelberg: Springer; 2008:500–541.
- Hasleton PS. Ch 34. Pleural disease. In: Hasleton PS, ed. *Spencer's Pathology of the Lung*. 5th ed. New York, St. Louis, San Francisco: McGraw-Hill; 1996: 1131–1210.
- Kaplan IL, Swayne LC, Widmann WD, et al. CT demonstration of "ectopic" thymoma. *J Comput Assist Tomogr*. 1988;12:1037–1038.
- Moran CA, Suster S, Fishback NF, et al. Primary intrapulmonary thymoma. A clinicopathologic and immunohistochemical study of 8 cases. *Am J Surg Pathol*. 1995;19:304–312.
- Moran CA, Travis WD, Rosado-de-Christensen M, et al. Thymomas presenting as pleural tumors: Report of 8 cases. *Am J Surg Pathol*. 1992;16:138–144.
- Neoplasms of uncertain histogenesis and nonneoplastic tumors. In: Fraser RS, Müller NL, Colman N, Paré PD, eds. *Fraser and Paré's Diagnosis of Diseases of the Chest*. Philadelphia, Long, Toronto: WB Saunders Co; 1999:1363–1380.
- Nicholson AG, Moran C. Intrapulmonary thymoma. In: Travis WD, Brambilla E, Müller-Hermelink HK, Harris CC, eds. *World Health Organization Classification of Tumours of the Lung, Pleura, Thymus and Heart*. Lyon: IARC Press; 2004:120.
- Sakuraba M, Sagara Y, Tamura A, et al. A case of invasive thymoma with endobronchial growth. *Ann Thorac Cardiovasc Surg*. 2005;11:114–116.

CHAPTER 29

Glomus Tumor of the Lung

Hassan F. Nadrous and Armando E. Fraire

Glomus tumors are distinctly uncommon in the lung and the trachea. Outside the lung and trachea, glomus tumors are seen in the extremities, particularly around the nail beds and internally in bone, stomach, colon, and small intestine and other sites. They are said to be derived from the glomus apparatus and thought to regulate blood flow, particularly in the extremities. Their true frequency is not known since some cases may have been reported as angiomatous tumors. Glomus tumors are regarded as vascular tumors and those that have a more prominent vascular network are known as glomangiomas. An oncocytic variant has been described. Glomangiosarcomas are also seen but are exceptionally rare. The age of patients with tracheal glomus tumors range from 34 to 74 years and show a distinct male predominance. Presenting symptoms are dyspnea, cough, and hemoptysis. Most are located in the posterior (membranous) wall of the trachea and protrude into its lumen causing the above-cited symptoms and signs. In the respiratory tract, computed tomography and interactive virtual bronchoscopy have proven useful in diagnosis and outlining the extent of these tumors. The main microscopic feature is groups of uniform-looking cells surrounded by irregularly shaped vascular channels. The tumor cells are smooth muscle actin positive and negative for CD34, S100 protein, and cytokeratin. The main differential diagnosis is with carcinoid tumors and localized fibrous tumors. Immunostains for neuroendocrine markers (chomogranin synaptophysin) and vascular markers (CD34 and CD31) can assist in distinguishing these tumors from neuroendocrine neoplasms. The cytopathologic features of glomus tumors have not been well documented.

A.E. Fraire et al. (eds.), *Atlas of Neoplastic Pulmonary Disease*,
DOI 10.1007/978-0-387-89839-1_29,

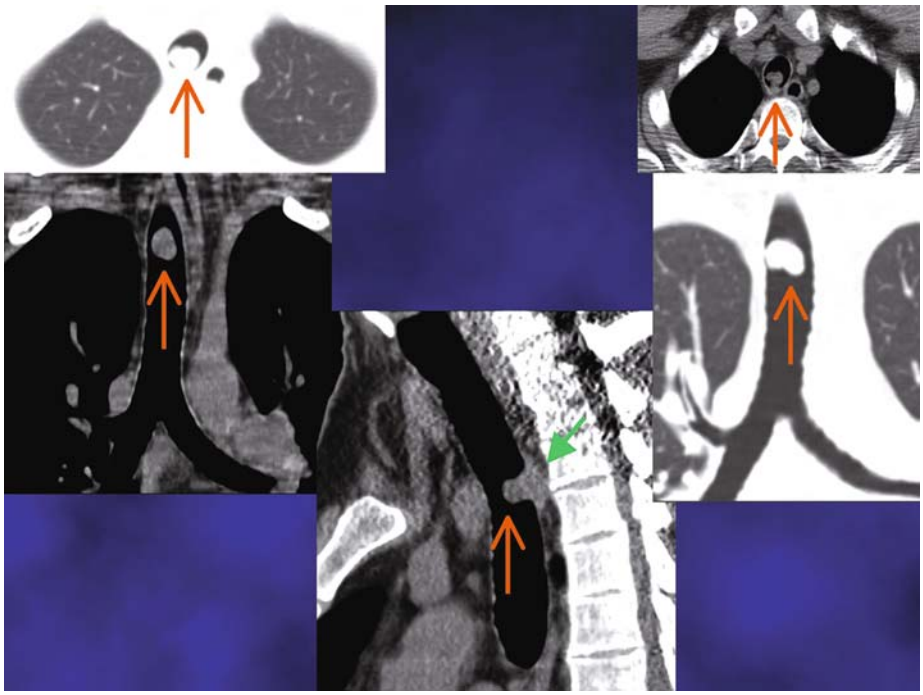

Figure 29.1 Glomus tumors of the trachea. Computed tomography images showing endoluminal and extramural extent ofthe tumor (from Nadrous et al., with permission). See chapter reference for complete citation.

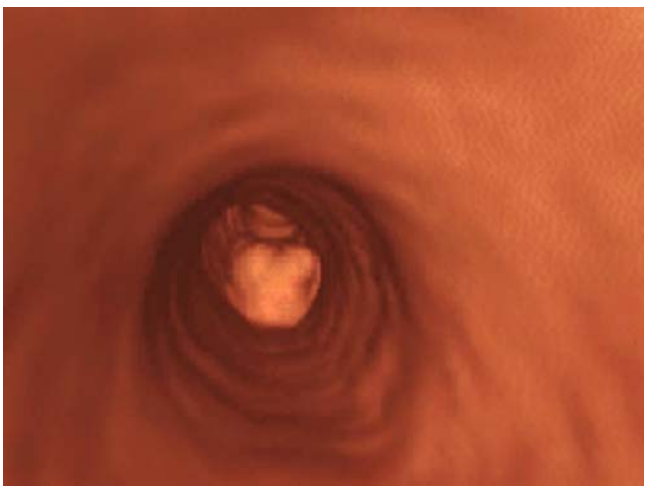

Figure 29.2 Glomus tumors of the trachea. Bronchoscopic view. Highly detailed interactive virtual bronchoscopy showing a lobulated tumor in the posterior wall (from Nadrous et al., with permission). See chapter reference for complete citation.

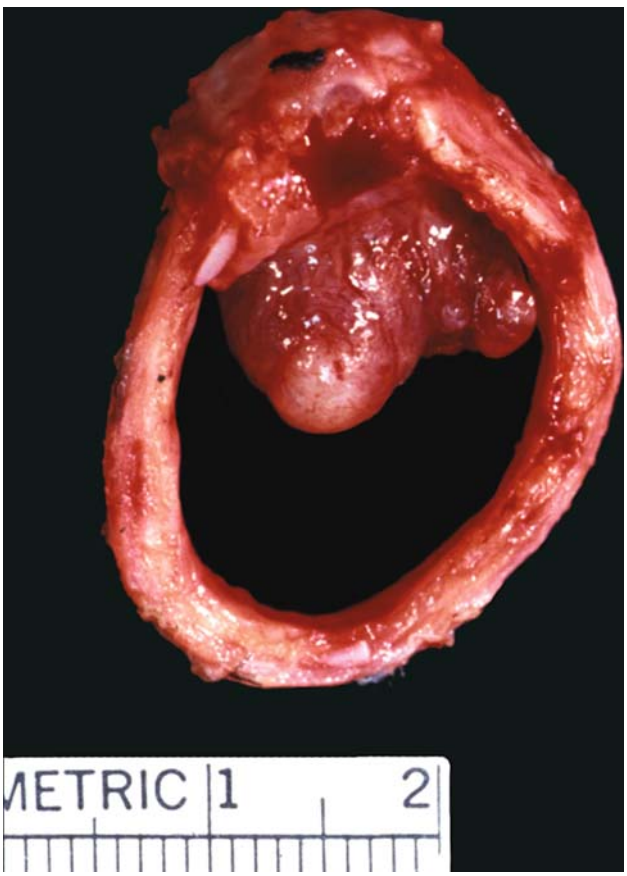

Figure 29.3 Glomus tumor of the trachea. Gross appearance of a surgically resected specimen. Note polypoid mass arising from the posterior membranous wall (from Nadrous et al., with permission). See chapter reference for complete citation.

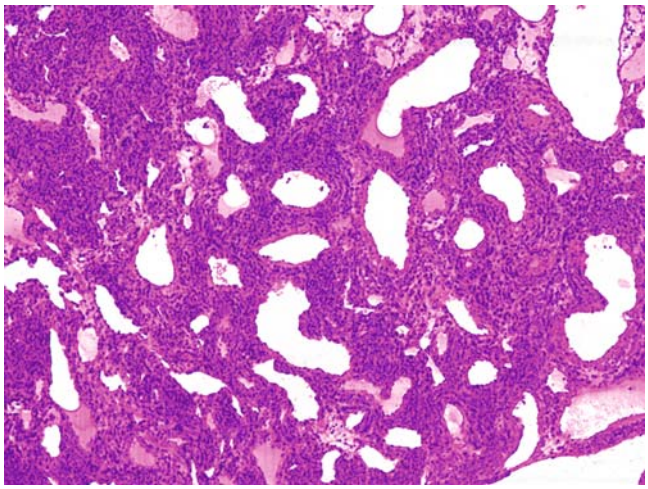

Figure 29.4 Glomus tumor of the trachea. Histopathology: note sheets and trabeculae made up of uniform-looking cells surrounding dilated vascular channels. Hematoxlyin and eosin (from Nadrous et al., with permission).

REFERENCES

- Altorjay A, Arató G, Adame M, et al. Synchronous multiple glomus tumors of the esophagus and lung. *Hepatogastroenterology.* 2003;50:687–690.
- Folpe AL. Glomus Tumours. In: Fletcher CDM, Unni K, Mertens F, eds. *World Health Organization Classification of Tumors. Pathology and Genetics. Tumors of soft Tissue and Bone*. Lyon: IARC Press, 2002;136–137.
- Fraire AE, Dail DH. Mesenchymal tumors, Part I: Tumors of fibrous, fibrohistiocytic and muscle origin. In: Tomashefsky JF, Cagle PT, Farver C, Fraire AE, eds. *Pulmonary Pathology*. 3rd ed. Berlin, New York, Heidelberg, Springer; 2008:427–461.
- Hishida T, Hasegawa T, Asamura H, et al. Malignant glomus tumor of the lung. *Pathol Int*. 2003;52:632–636.
- Koss MN, Hochholzer L, Moran CA. Primary pulmonary glomus tumor: a clinicopathologic and immunohistochemical study of two cases. *Mod Pathol*. 1998;11:253–258.
- Nadrous HF, Allen MS, Bartholomas BJ, et al. Glomus tumor of the trachea: value of multidetector computed tomographic virtual bronchoscopy. *Mayo Clin Proc*. 2004;79:237–240.

CHAPTER 30

Sclerosing Hemangioma

Armando E. Fraire, Giulio Rossi, Alberto Cavazza, and Dina R. Mody

Sclerosing hemangioma is an uncommon lung tumor believed to be derived from primitive respiratory epithelium. The tumor cells consist of two basic cell populations: surface cuboidal cells and deeper polygonal stromal cells. These tumors show a distinct female predilection and some series have been exclusively female. Among females, nonsmoking, middle-age Asian women appear to be at greater risk. The mean age at presentation is about 45 years but age varies widely from adolescence to mid-eighties. Up to 90% of the patients are said to be asymptomatic. Rare patients will present with vague chest pain or discomfort. Chest radiographs show nodular lesions that may gradually enlarge over time. There is no preference for any lobe of the lung but most are juxtapleural. Calcification can be appreciated on computed tomography and while cavitation does not occur, some cases may have a positive air-meniscus sign.

Endoscopy does not play a major role in the recognition or identification of sclerosing hemangioma because the majority of sclerosing hemangiomas are subpleural in location. Rare tumors, however, may be visible endoscopically and in those instances they may present as polypoid masses protruding into the airway. These lesions are circumscribed and easily freed up (shelled out) from the adjacent lung parenchyma. They may be gray-white or tan yellow or, in some other instances, dark red. On cut surfaces, the tumor substance may be spongy and filled with blood. These tumors are made up of the above-cited basic cell populations (surface cuboidal and deeper polygonals) that may be arranged in four different histopathologic patterns: solid, papillary, hemorrhagic, and sclerotic. Within areas displaying a papillary pattern, aggregates of foamy cells are often seen amidst the papillae. Given the subpleural location of these tumors, a transthoracic approach for FNA cytologic diagnosis is most often needed. Cytopathologically, papillary arrangements of bland-looking epithelial cells may be seen.

FIGURE 30.1 Bronchoscopic view of a sclerosing hemangioma nearly filling the bronchial lumen. Note smooth non-ulcerated pink mucosal surface.

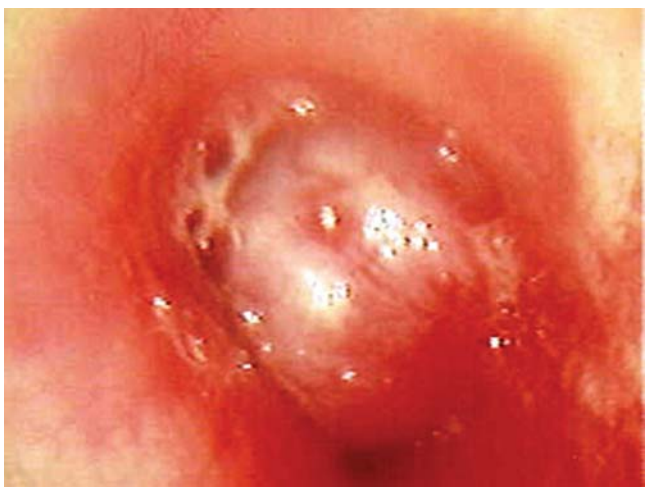

A.E. Fraire et al. (eds.), *Atlas of Neoplastic Pulmonary Disease*,
DOI 10.1007/978-0-387-89839-1_30, © Springer Science+Business Media, LLC 2010

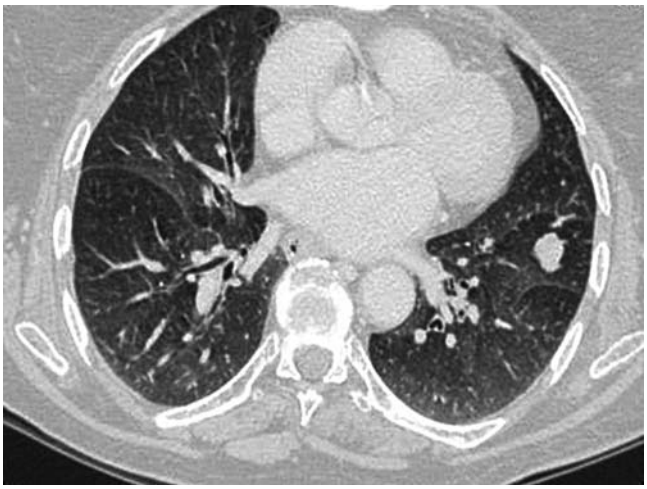

FIGURE 30.2 CT scan of chest, lung windows. Note peripherally located nodular lesion in the left lower lung zone. The lesion is away from the pleura.

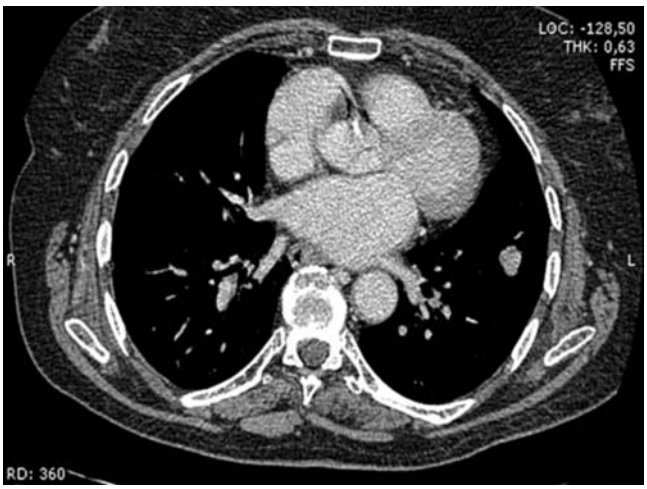

FIGURE 30.3 CT scan of chest, mediastinal window. Note same nodular lesion shown in Fig. 30.2 with no pleural attachment.

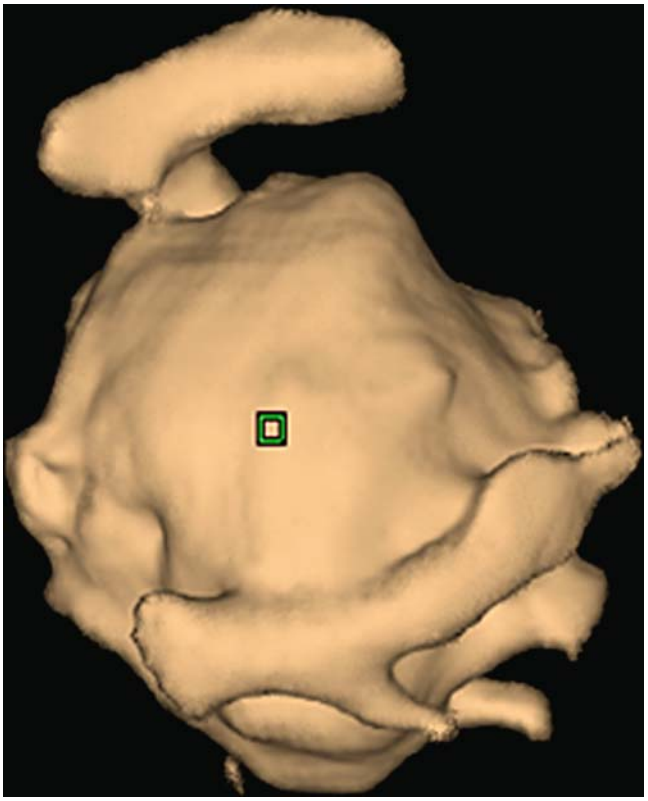

FIGURE 30.4 Sclerosing hemangioma. Digital tridimensional reconstruction of the nodular lesion shown in Figs. 30.2 and 30.3. While maintaining its nodular appearance, the lesion is now found to have tubular- and appendage-like extensions superiorly and along its equator.

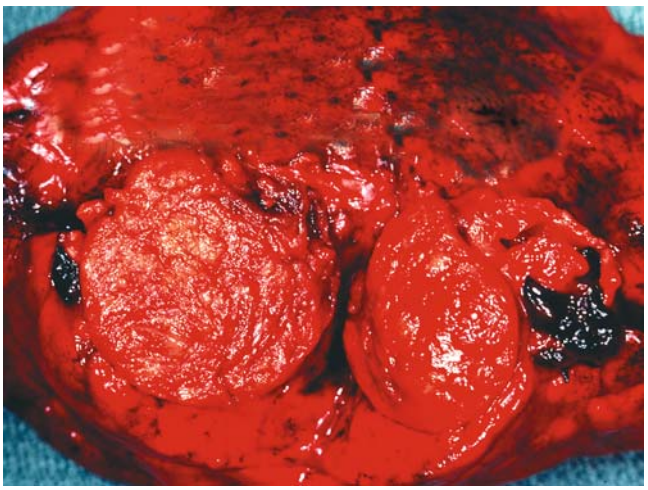

FIGURE 30.5 Sclerosing hemangioma. Gross appearance in the fresh state. Note bisected hemorrhagic-looking nodular mass (Courtesy of Dr. Eugene Mark, Massachusetts General Hospital, Boston, MA). Reproduced with permission from Tomashefski et al. See chapter references for complete citation.

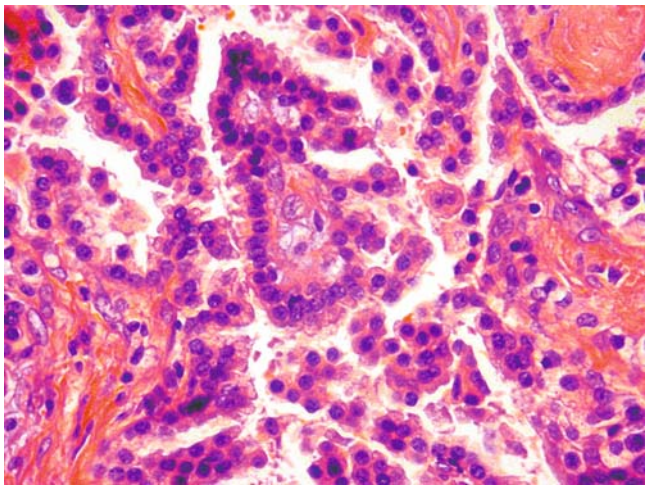

FIGURE 30.6 Sclerosing hemangioma. Note papillary fronds with distinctly separate darker cells lining the surface of the papillae. Hematoxylin and eosin. Reproduced with permission from Tomashefski et al. See chapter references for complete citation.

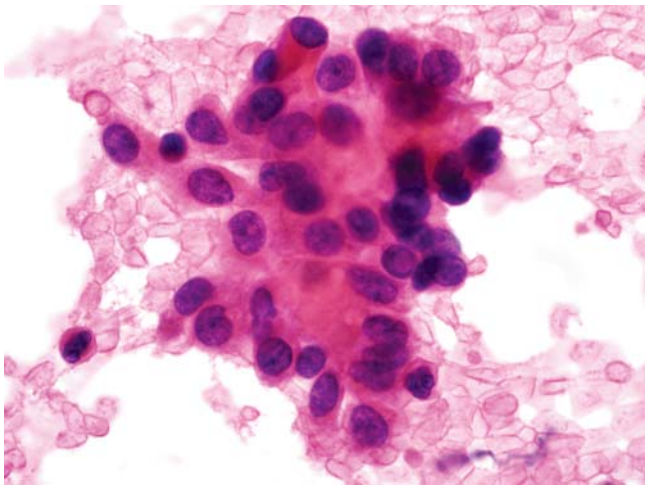

FIGURE 30.8 Cytopathology of sclerosing hemangioma, cell block. Note cluster of dark oval to round epithelial cells resembling surface cells. Hematoxylin and eosin.

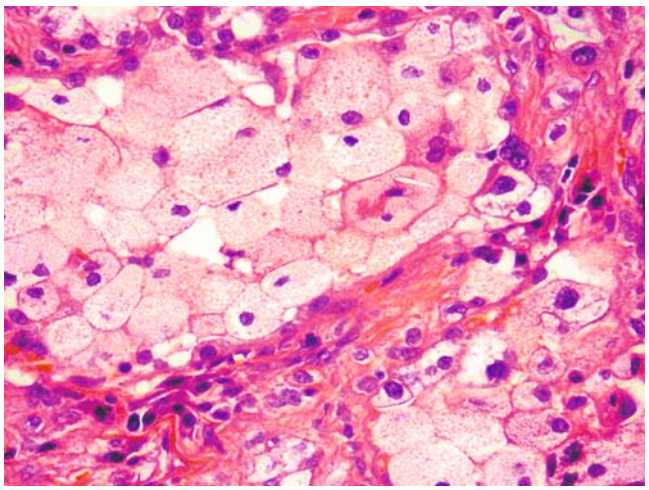

FIGURE 30.7 Sclerosing hemangioma, showing one aggregate of foam cells. Hematoxylin and eosin. Reproduced with permission from Tomashefski et al. See chapter references for complete citation.

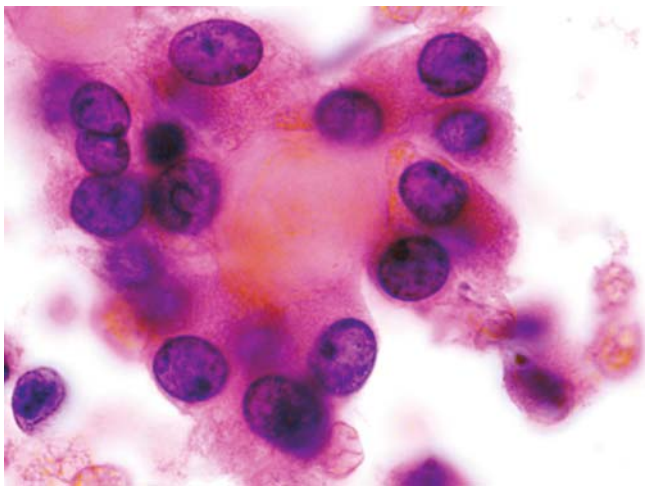

FIGURE 30.9 Cytopathology of sclerosing hemangioma, cell block. A closer view showing a papillary structure with dark uniform-looking epithelial cells at its surface. Hematoxylin and eosin.

REFERENCES

- Chan ACL, Chan JKC. Pulmonary sclerosing hemangioma consistently expresses thyroid transcription factor-1 (TTF-1). A new clue to histogenesis. *Am J Surg Path*. 2000;24:1531–1536.
- Devoussoux-Shisheboran M, Hayashi T, Linnoila RI, et al. A clinicopathologic study of 100 cases of pulmonary sclerosing hemangioma with immunohistochemical studies. *Am J Surg Pathol*. 2000;24:906–916.
- Devouassoux-Shisheboran M, Nicholson AG, Leslie K, et al. Sclerosing hemangioma. In: Travis WD, Brambilla E, Müller- Hermelink HK, Harris CC, eds. *World Health Organization Classification of Tumours. Pathology and Genetics of Tumours of the Lung, Pleura, Thymus and Heart*. Lyon: IARC Press; 2004:115–117.
- Fraire AE, Dail DH. Ch 41. Miscellaneous Tumors and Tumor-Like Proliferations of the lung. In: Tomsashefski JF Jr., Cagle PT, Farver CF, Fraire AE, eds. *Dail and Hammar's Pulmonary Pathology*. 3rd ed. Berlin, New York, Heidelberg: Springer; 2008:462–499.
- Fraser RS, Muller NL, Colman N, Paré PD, eds. *Fraser and Pare's Diagnosis of Diseases of the Chest*. 4th ed. Philadelphia, London, Toronto: WB Saunders Co.; 1999:1365.

- Nicholson AG, Magkou C, Snead D, et al. Unusual sclerosing hemangiomas and sclerosing hemangioma-like lesions, and the value of TTF-1 in making the diagnosis. *Histopathology*. 2002;41:404–413.
- Sartori G, Bettelli S, Schirosi L, et al. Microsattelite and EGFR, HER2 and K-ras analyses in sclerosing hemangioma of the lung. *Am J Surg Pathol*. 2007;31: 1512–1520.
- Wang E, Lin D, Wang Y, et al. Immunohistochemical and ultrastructural markers suggest different origins for cuboidal and polygonal cells in pulmonary sclerosing hemangioma. *Hum Pathol*. 2004;35:503–508.

CHAPTER 31

Preinvasive Disease

Keith M. Kerr, Dina R. Mody, and Armando E. Fraire

Under preinvasive disease, we consider three WHO (World Health Organization) recognized lesions of the lungs: squamous dysplasia (SD) as a precursor of squamous cell carcinoma, atypical adenomatous hyperplasia (AAH) as a precursor of adenocarcinoma, and diffuse idiopathic pulmonary neuroendocrine hyperplasia (DIPNECH) as a possible precursor of tumorlets and carcinoid tumors.

The existence of central airway SD and its association to tobacco smoke has been documented for decades, primarily through the combined use of serial sputum cytology and fluorescent bronchoscopy. However, knowledge concerning AAH and DIPNECH is comparatively much more recent. In contrast to SD which can be visualized and monitored through bronchoscopy and serial sputum cytology or serial bronchial biopsies, the diagnosis and surveillance of AAH and DIPNECH remains difficult. This is due in part to the small size of the lesions and in part to their deep location and inaccessibility within the lung parenchyma. Nonetheless, the detection of AAH and DIPNECH has been greatly enhanced on account of awareness and increased use of modern technologies such as spiral CT and high-resolution CT of the chest.

A.E. Fraire et al. (eds.), *Atlas of Neoplastic Pulmonary Disease*,
DOI 10.1007/978-0-387-89839-1_31, © Springer Science+Business Media, LLC 2010

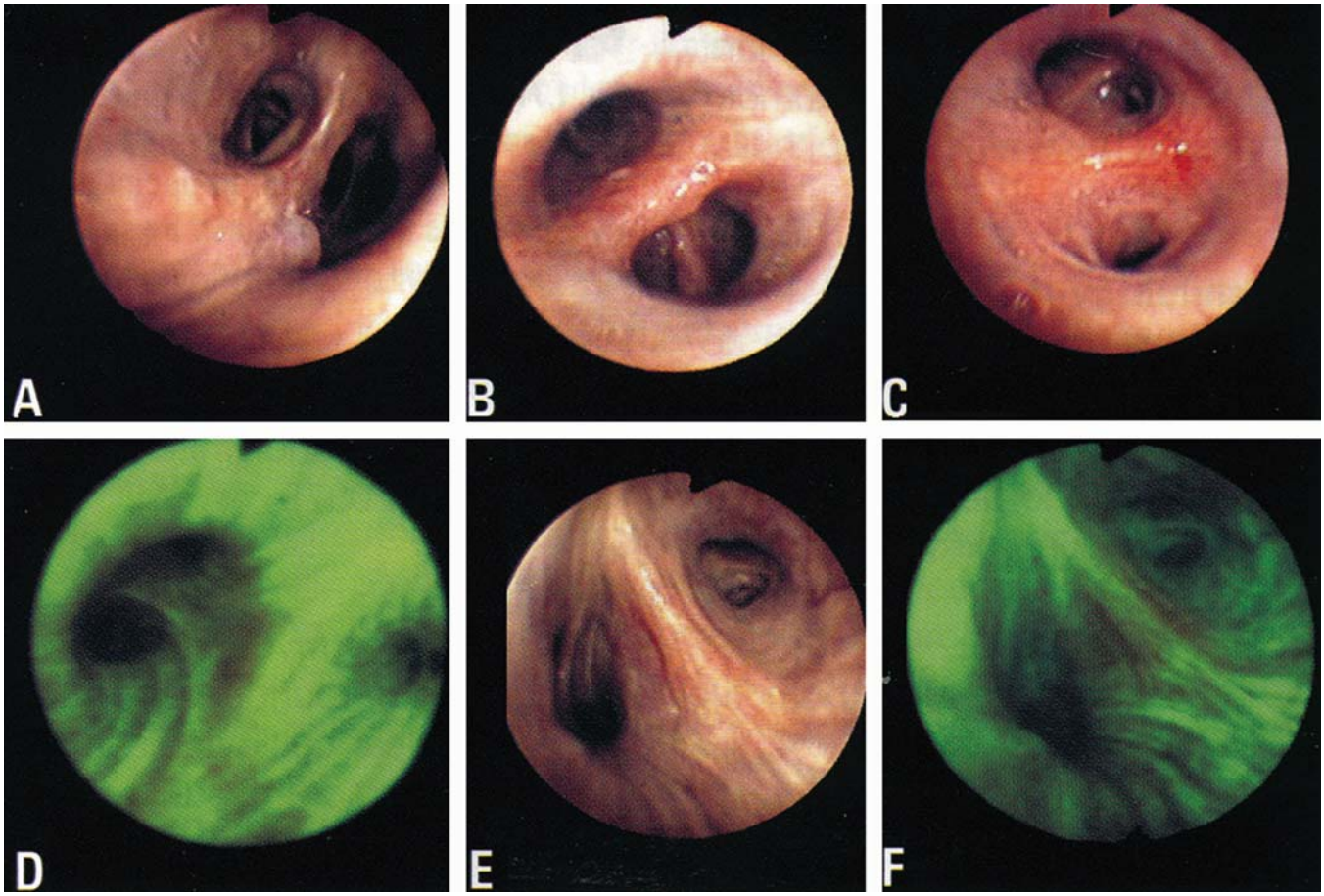

FIGURE 31.1 Bronchoscopy images of squamous dysplasia and carcinoma in situ. **a** Nodular carcinoma in situ of the *left lower* lobe. White-light image. **b** Carcinoma in situ *right upper* lobe with focal thickening of the bronchial bifurcation and slight irregularity of the bronchial mucosa. **c** Carcinoma in situ upper divisional bronchus, *left upper* lobe. Focal increase in vascularity was observed under white-light bronchoscopy. **d** Carcinoma in situ *left upper* lobe. The lesion is visible as an area of reddish-brown fluorescence under autofluorescence bronchoscopy, using the LIFE-Lung Device. **e** Severe dysplasia *left upper* lobe. No abnormality under white-light bronchoscopy. **f** Same case as (**e**). The dysplastic lesion is visible as an area of reddish fluorescence under autofluorescence bronchoscopy, using the Onco-LIFE Device (Xillix Technologies Inc., Vancouver, Canada) (Courtesy of W.A. Franklin and Associates).

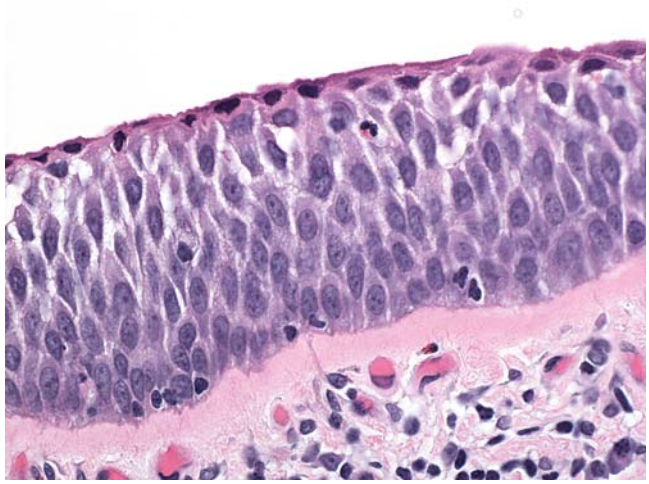

FIGURE 31.2 Squamous epithelium with basal cell hyperplasia. Note orderly arrangement of basal epithelial cells with evidence of some intercellular bridges. Hematoxylin and eosin.

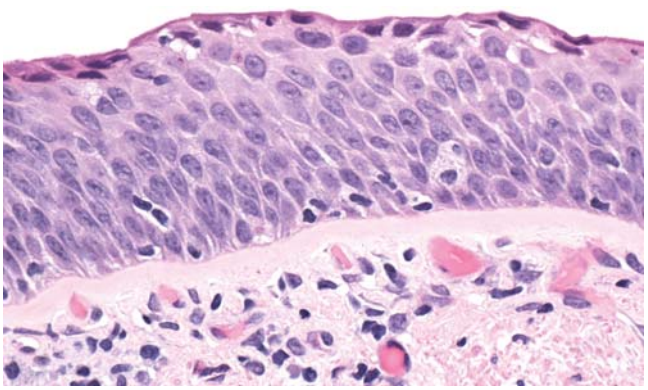

FIGURE 31.3 Squamous epithelium with squamous metaplasia arising from squamous differentiation developing in a background of basal cell hyperplasia. Hematoxylin and eosin.

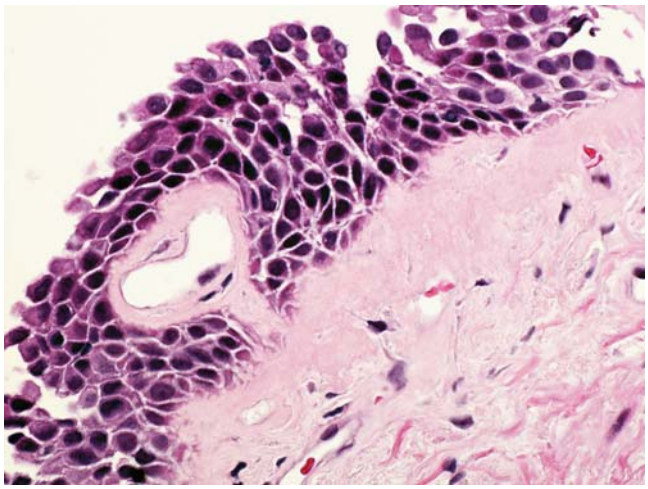

FIGURE 31.4 Squamous epithelium with angiogenic squamous dysplasia. This is characterized by atypical squamous epithelial cells covering capillary vascular buds often surrounded by eosinophilic basement membrane material. Hematoxylin and eosin.

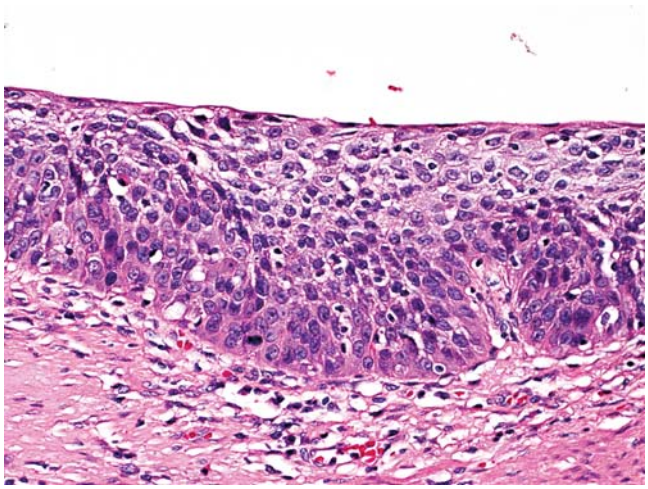

FIGURE 31.6 Squamous epithelium with moderate dysplasia. Note basal mitotic activity and maturation of upper third. Hematoxylin and eosin.

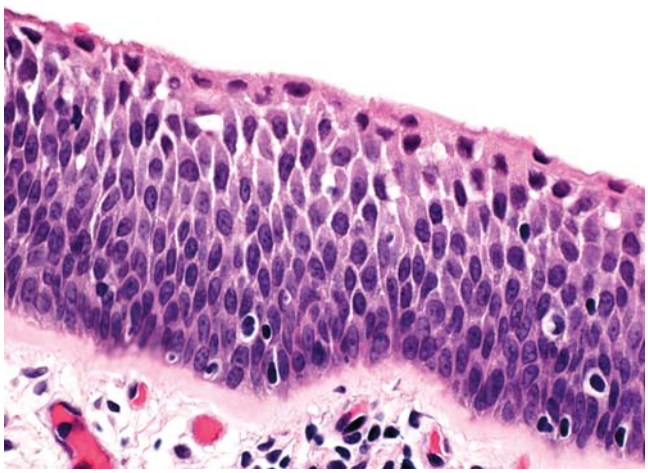

FIGURE 31.5 Mild squamous dysplasia characterized by minimal atypic and crowding of basal cells with vertically oriented nuclei. Hematoxylin and eosin.

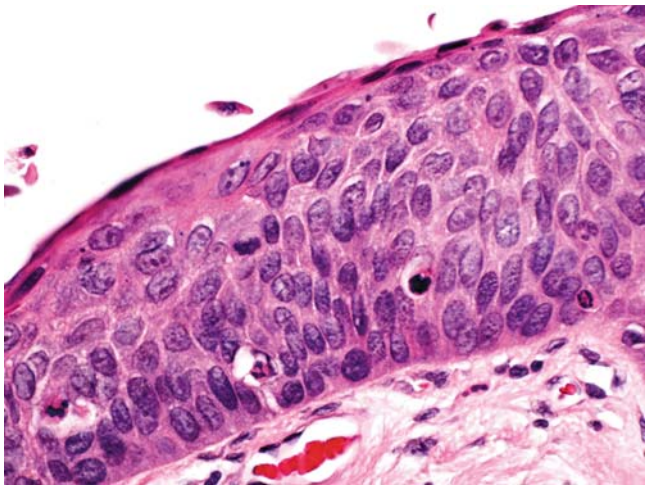

FIGURE 31.7 Severe squamous dysplasia. Note epithelium with minimal surface maturation and mitotic activity which reaches the middle third. Hematoxylin and eosin.

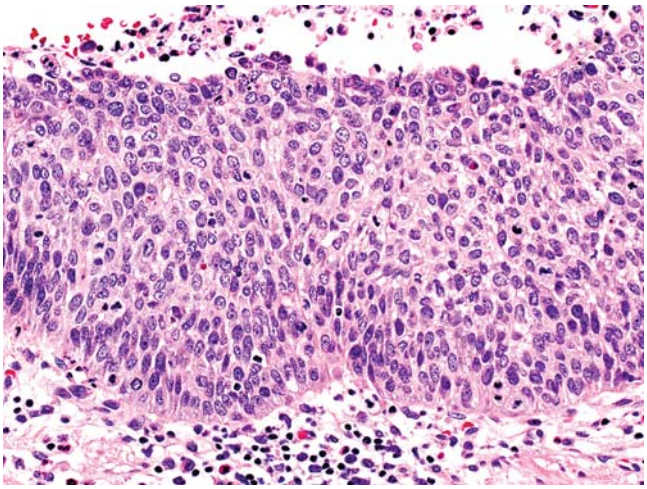

FIGURE 31.8 Squamous cell carcinoma in situ. If inverted, this epithelium, which lacks (surface) maturation would look the same. Note marked cellular crowding, cytologic atypia, and mitotic activity throughout. Hematoxylin and eosin.

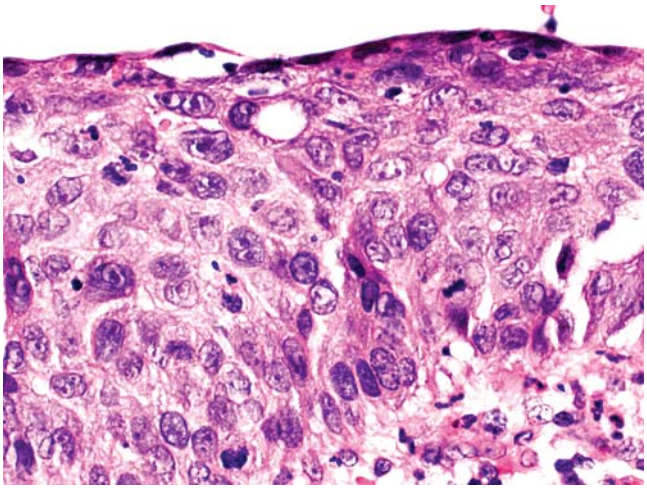

FIGURE 31.9 Squamous cell carcinoma in situ seen at a magnification greater than that of Fig. 31.8. Note near total lack of cellular orientation, nuclear hyperchromatism, and mitoses in all three thirds of the epithelium. Hematoxylin and eosin.

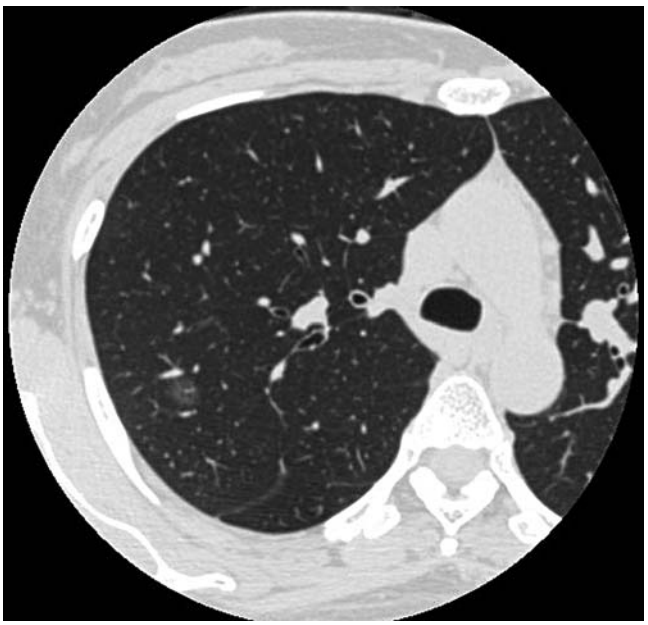

FIGURE 31.10 Atypical adenomatous hyperplasia. Spiral high-resolution CT scan of chest. Note small non-solid "ground glass opacity" detected during a lung cancer screening program. When resected, this lesion proved to be (an unusually large) focus of atypical adenomatous hyperplasia (Contributed by Dr. Hironobu Ohmatsu, National Cancer Center Hospital East, through the courtesy of Dr. Ryutaro Kakinuma, Research Center for Cancer Prevention and Screening, National Cancer Center, Tokyo, Japan).

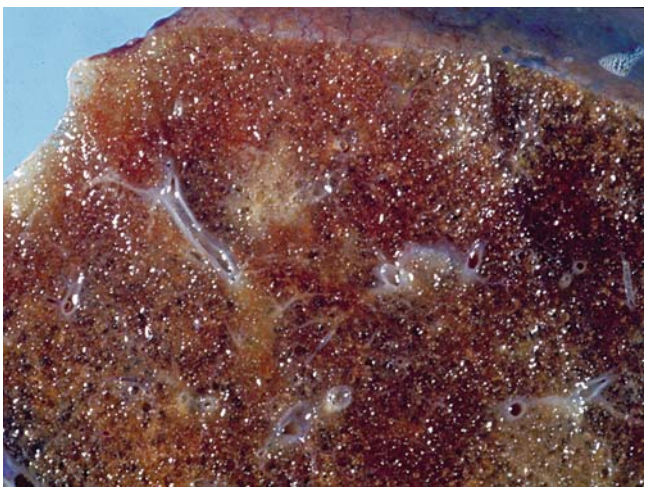

FIGURE 31.11 Atypical adenomatous hyperplasia; gross appearance. Note tiny whitish focus, 1–2 mm in diameter in the subpleural region of the lung. Individual alveoli can be seen within the lesion. Hematoxylin and eosin.

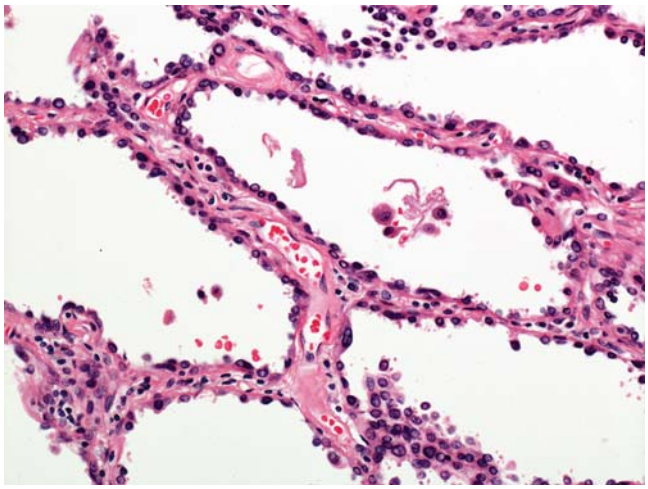

FIGURE 31.12 Atypical adenomatous hyperplasia microscopic view. Note cellular crowding, nuclear hyperchromasia, and occasional giant nuclei. Hematoxylin and eosin.

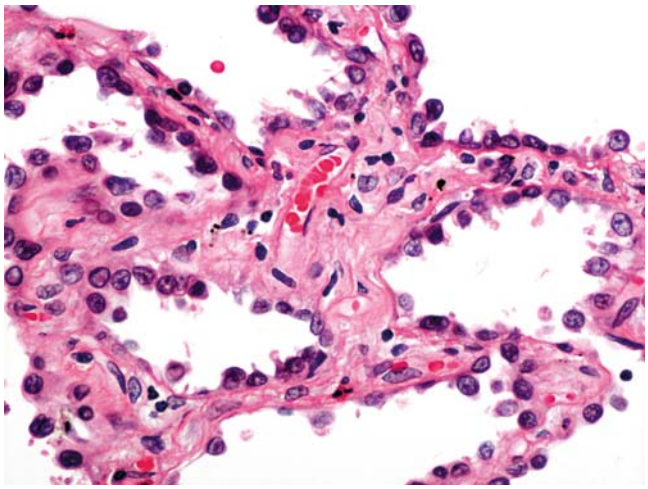

FIGURE 31.13 Atypical adenomatous hyperplasia. In this high power view of an AAH lesion, a greater degree of interstitial expansion due to fibrosis is noted. Also note moderate cellular crowding and cells protruding in a hobnail fashion into the air spaces. Hematoxylin and eosin.

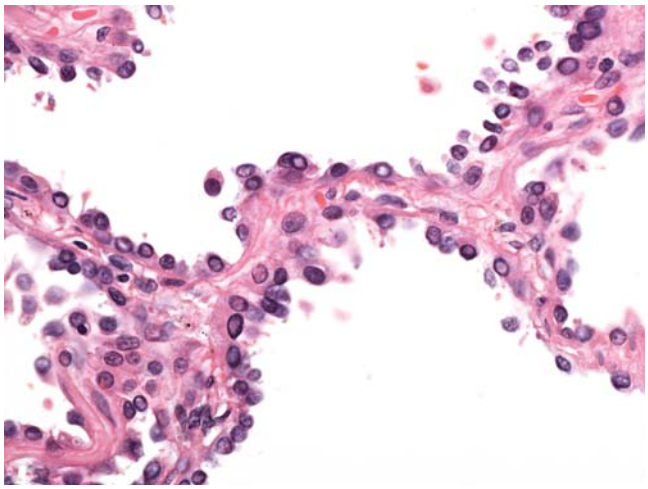

FIGURE 31.14 Atypical adenomatous hyperplasia. In this area of an AAH lesion, a single interalveolar septum displays interstitial thickening, some cells with double nuclei as well as nuclear inclusions. Nuclear inclusions are not uncommon in AAH. Hematoxylin and eosin.

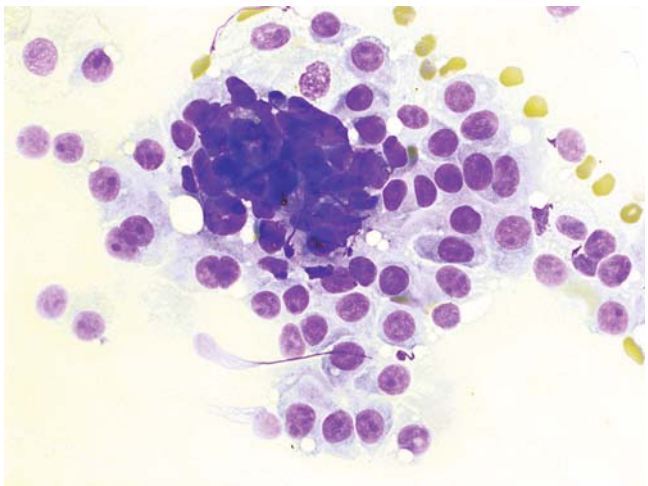

FIGURE 31.15 Atypical adenomatous hyperplasia. Cytopathologic features – it is not possible to make a cytologic diagnosis of atypical adenomatous hyperplasia. However, the diagnosis can be suspected. Note the loose acinar arrangement of relatively bland-appearing enlarged cells without much variation from one cell to another. The nuclear cytoplasmic ratio is increased but without much nuclear pleomorphism. The bland features in the case tend to favor AAH. Diff Quick Stain.

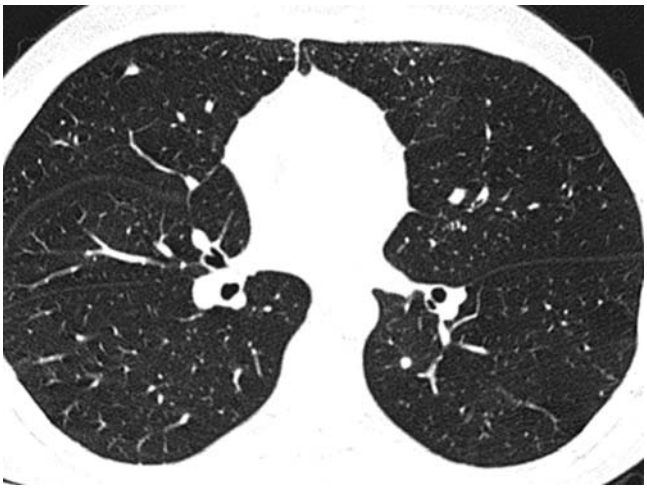

FIGURE 31.16 Diffuse neuroendocrine cell hyperplasia. High-resolution CT scan from patient with DIPNECH. Small parenchymal nodules are seen in both lungs. A mild degree of mosaicism reflects differential air-trapping in some lobules due to small airway obstruction (Image courtesy of Prof. D.M. Hansell, Royal Brompton Hospital, London).

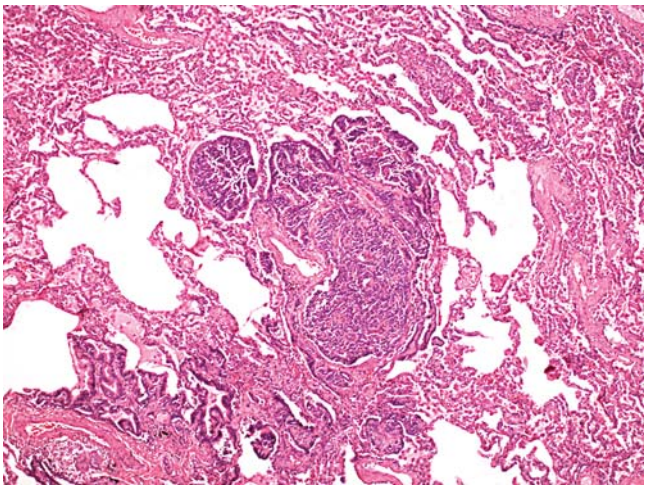

FIGURE 31.17 Neuroendocrine lesion: lower power view of a carcinoid tumorlet associated with DIPNECH. In this lesion, the airway lumen is obliterated by proliferating neuroendocrine cells. Hematoxylin and eosin.

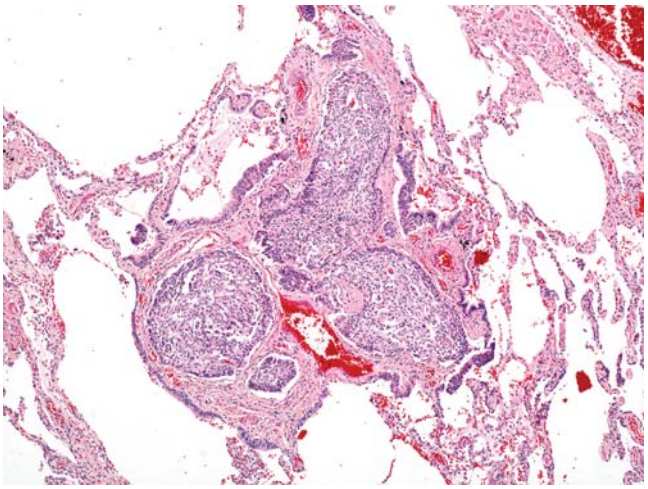

FIGURE 31.18 Neuroendocrine lesion; note carcinoid tumorlet and peribronchiolar metaplasia signifying structural/morphologic alteration of surrounding small airways. Hematoxylin and eosin.

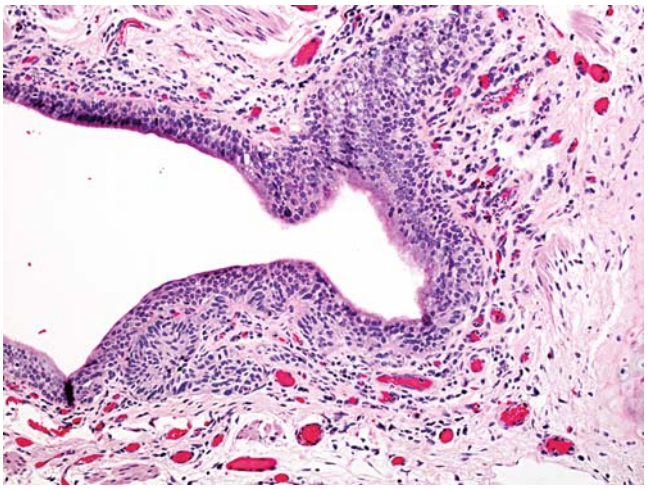

FIGURE 31.19 Neuroendocrine lesion: bronchiole with a nest of peribronchiolar hyperplasia of pulmonary neuroendocrine cells. This is characteristic of DIPNECH. Hematoxylin and eosin.

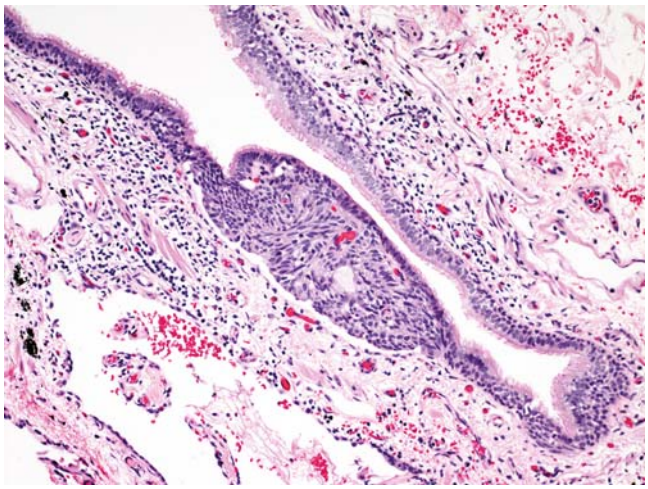

FIGURE 31.20 Neuroendocrine lesion: this bronchiole shows a nodule of neuroendocrine cells (neuroendocrine body) protruding into its lumen. Hematoxylin and eosin.

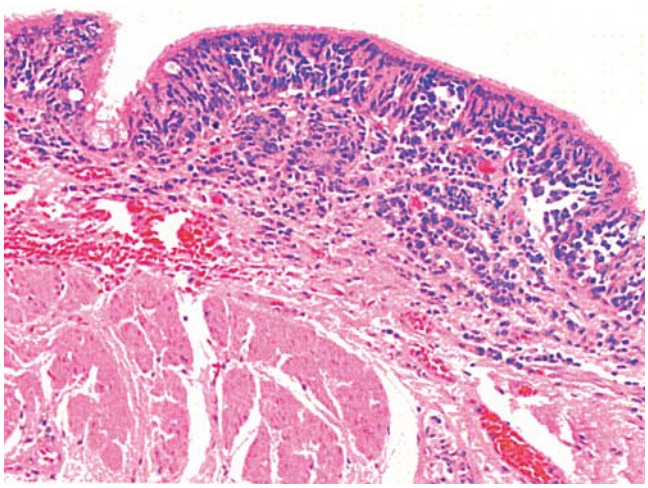

FIGURE 31.21 Small cell carcinoma of lung may develop de novo. This tiny plaque-like lesion was found incidentally in bronchial mucosa during routine microscopic examination of a lung resected for squamous cell carcinoma. Hematoxylin and eosin. From Tomashefski et al, with permission from Springer (see chapter references for complete citation).

REFERENCES

- Aguayo SM, Miller YE, Waldron JA, et al. Idiopathic diffuse hyperplasia of pulmonary neuroendocrine cells and airway disease. *N Engl J Med*. 1992;327:1285–1288.
- Chapman AD, Kerr KM. The association between atypical adenomatous hyperplasia and primary lung cancer. *Br J Cancer*. 2000;83:632–636.
- Franklin WA, Wistuba II, Geisinger KR, et al. Squamous dysplasia and carcinoma in situ. In: Travis WD, Brambilla E, Muller-Hermelink HK, et al., eds. *World Health Organization Classification of Tumours. Pathology and Genetics of Tumours of the Lung, Pleura, Thymus and Heart*. Lyon: IARC Press; 2004:68–72.
- Keith RL, Miller YE, Gemmill RM, et al. Angiogenic squamous dysplasia in bronchi of individuals at high risk for lung cancer. *Clin Cancer Res*. 2000;6:1616–1625.
- Kerr KM, Fraire AE. Ch 34. Preinvasive disease. In: Tomashefski J, Cagle PT, Farver C, Fraire AE, eds. *Dail and Hammar Pathology of the Lung*. 3rd ed. Vol 2, Neoplastic Disease. Berlin, New York, Heidelberg: Springer; 2008:158–215.
- Kerr KM, Fraire AE, Pugatch B, et al. Atypical adenomatous hyperplasia. In: Travis WD, Brambilla E, Muller-Hermelink HK, et al, eds. *World Health Organization Classification of Tumours. Pathology and Genetics of Tumours of the Lung, Pleura, Thymus and Heart*. Lyon: IARC Press; 2004:73–75.
- Kerr KM. Morphology and genetics of preinvasive pulmonary disease. *Curr Diag Pathol*. 2004;10:259–268.
- Lee JS, Brown KK, Cool C, et al. Diffuse pulmonary neuroendocrine cell hyperplasia: Radiologic and clinical features. *J Comput Assist Tomogr*. 2002;26:180–184.
- Miller RR. Bronchioloalveolar cell adenomas. *Am J Surg Pathol*. 1990;14:904–912.
- Miller RR, Muller NL. Neuroendocrine cell hyperplasia and obliterative bronchiolitis in patients with peripheral carcinoid tumours. *Am J Surg Pathol*. 1995;19:653–658.
- Travis WD, Colby TV, Corrin B, et al., eds. *Histological Typing of Lung and Pleural Tumours. WHO International Histological Classification of Tumours*. 3rd ed. Berlin: Springer; 1999.

CHAPTER 32

Squamous Cell Carcinoma

Shanda Blackmon, Armin Ernst, Philip T. Cagle, Timothy C. Allen, Dina R. Mody, N. Paul Ohori, Elise R. Hoff, and Armando E. Fraire

A major type of non-small cell lung cancer, squamous cell carcinoma was for many years the leading cell type in terms of frequency. Currently, it ranks second to adenocarcinoma but remains a major cause of morbidity and mortality. As is the case with small cell cancers, squamous cell carcinomas are centrally located, near the hilum and prone to present with hemoptysis and/or early symptoms related to bronchial obstruction. Owing to their central location, squamous cell carcinomas are also accessible to the bronchoscope and are apt to be diagnosed early by means of biopsy and/or exfoliative and sputum cytology. Often achieving a large size and due to extensive necrosis, squamous cell carcinomas frequently cavitate, presenting as abscess-like masses, radiographically. Other types of carcinomas may also cavitate but to a lesser degree and frequency.

Major histopathologic features of squamous cell carcinomas are keratinization of individual cells, squamous pearls, and intercellular bridges. These features, however, may not be present in poorly differentiated tumors. Histopathologic variants of squamous cell carcinoma include clear cell, papillary, basaloid, and a small cell variant mimicking small cell carcinoma. Cytopathologic features helpful in diagnosis are single cells and small clusters in sputum, sheets of cells ("fish in stream") in bronchial brushings as well as very dark nuclei ("lump of coal" or "inkblot blot" nuclei) in sputum preparations.

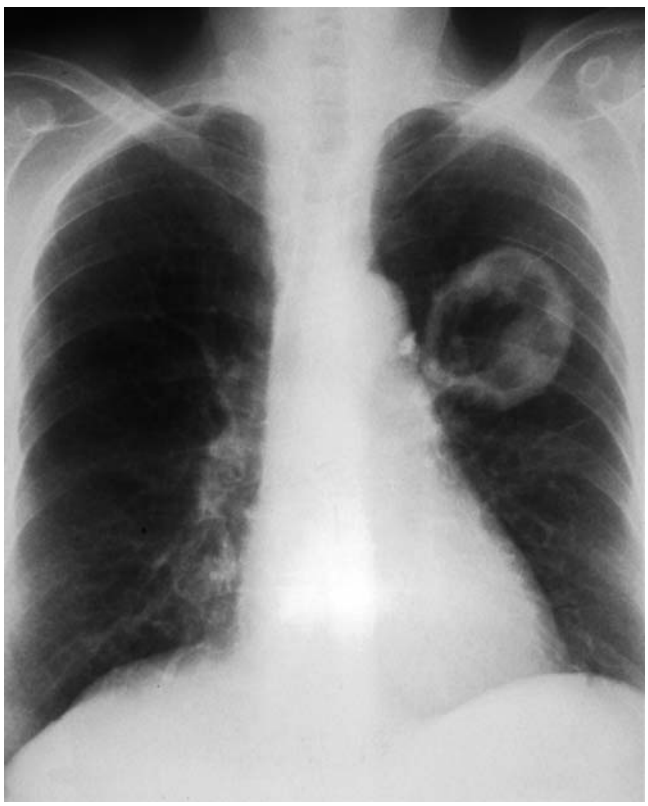

FIGURE 32.1 Posteroanterior radiograph of chest showing large cavitated squamous cell carcinoma in the left mid upper lung field. Note sharp contour of the lesion.

A.E. Fraire et al. (eds.), *Atlas of Neoplastic Pulmonary Disease*,
DOI 10.1007/978-0-387-89839-1_32,

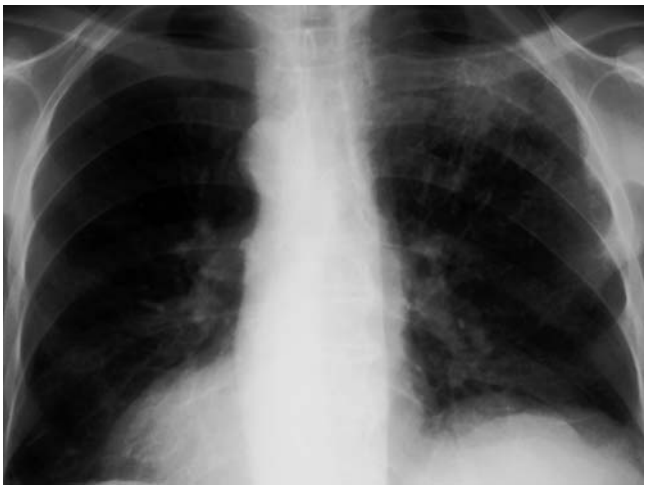

FIGURE 32.2 Posteroanterior radiograph of chest showing a non-cavitated opaque density in the left upper lung field. Note spiculated contour of the lesion.

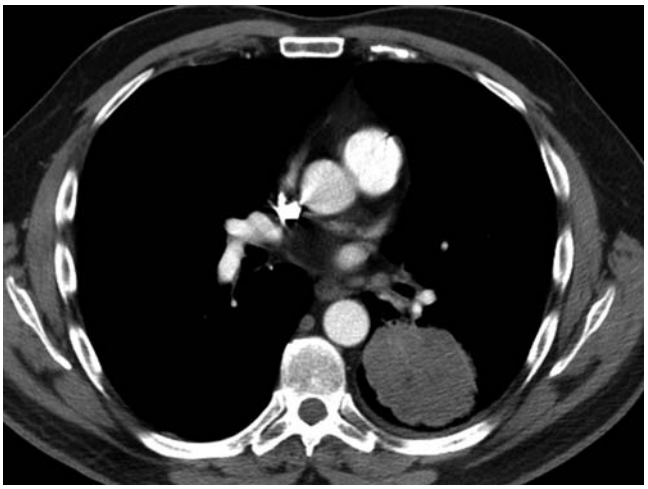

FIGURE 32.4 This CT of chest shows a squamous cell carcinoma involving the superior segment of the left lower lobe, with small areas of low density. The histopathology showed basaloid features.

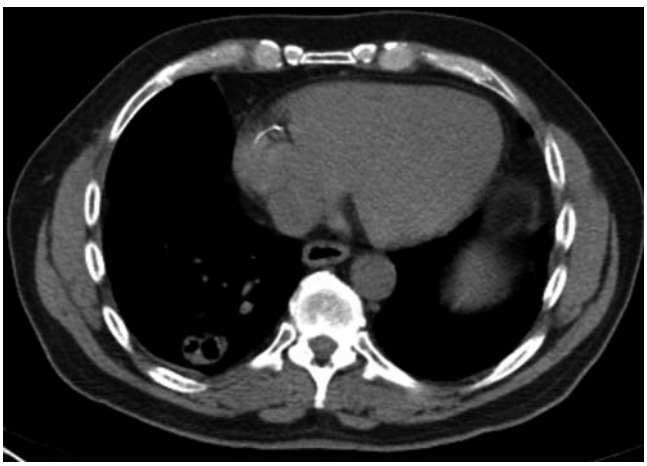

FIGURE 32.3 This CT of the chest shows a mass lesion of the posterior right lung with low-density material on the inside and a thick outer border. The histopathology showed a clear cell variant of squamous cell carcinoma.

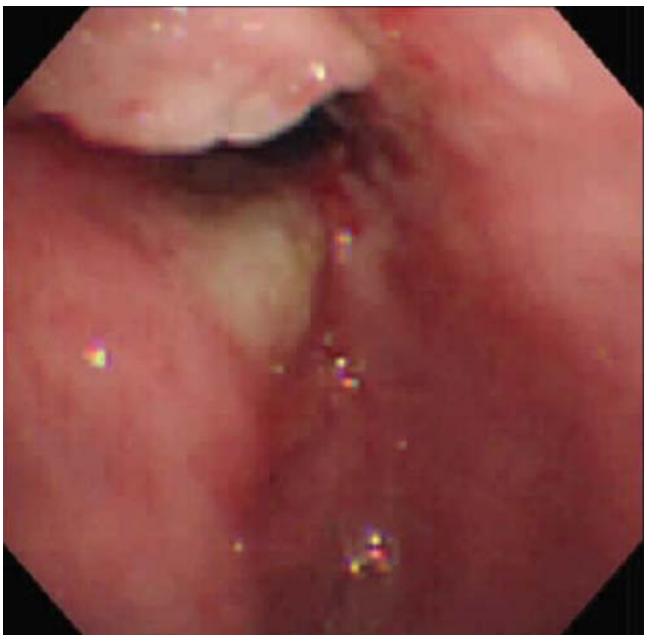

FIGURE 32.5 Bronchoscopic appearance of the entrance to the right middle lobe of a 60-year-old smoker with hemoptysis. The bronchus was completely obstructed. It was later re-opened with the help of an argon laser. Biopsy showed squamous cell carcinoma.

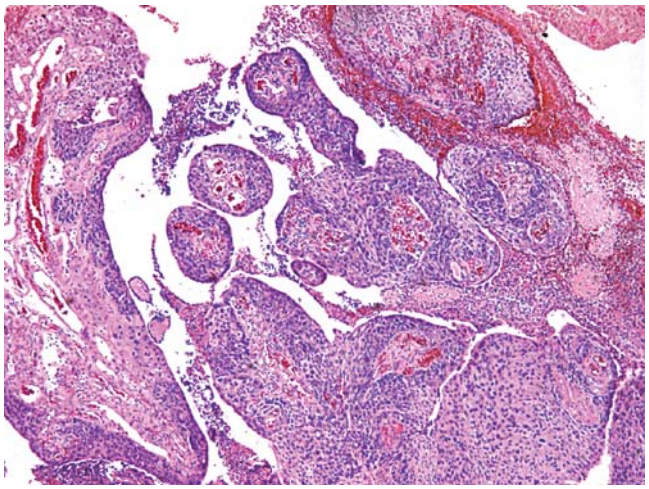

FIGURE 32.6 Histopathologic view of a squamous cell carcinoma with papillary features. Note fibrovascular cores lined by squamous cell carcinoma. Hematoxylin and eosin.

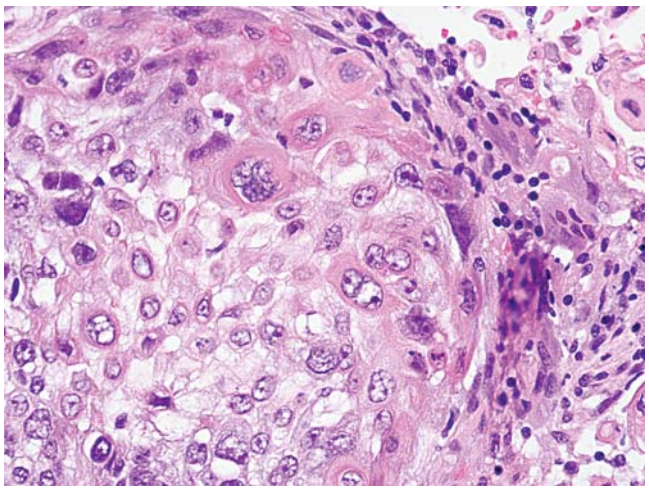

FIGURE 32.7 Histopathologic view of another squamous cell carcinoma with clear cell features. Hematoxylin and eosin.

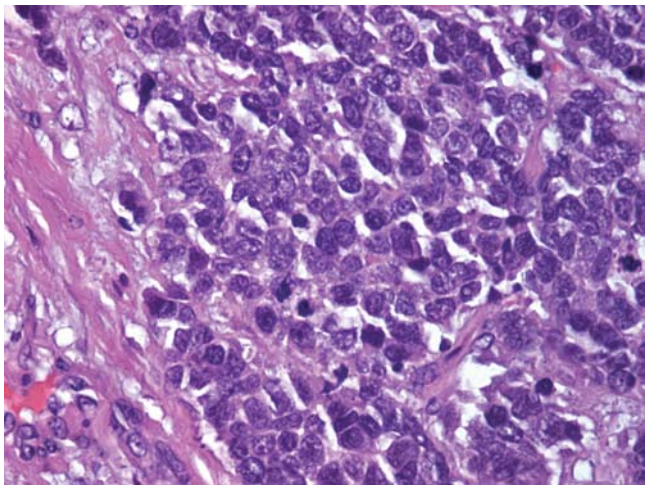

FIGURE 32.8 This small cell variant of squamous cell carcinoma can only be distinguished from true small cell carcinomas by means of immunohistochemical markers. Hematoxylin and eosin.

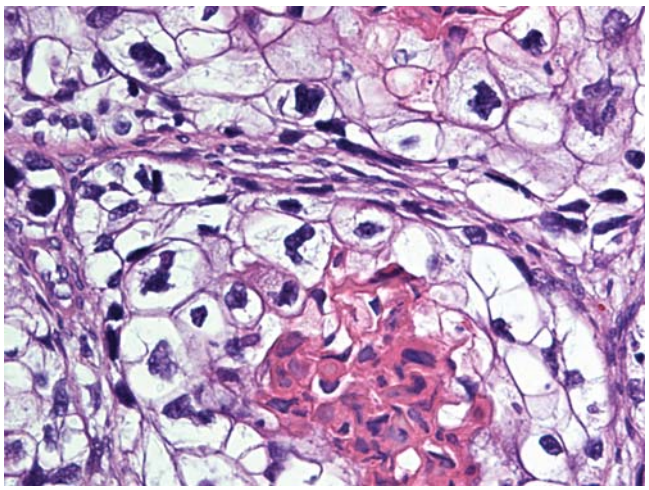

FIGURE 32.9 This squamous cell carcinoma shows cells with cytoplasmic clearing as well as groups of cells with features of keratinization. The keratinization helps to support the diagnosis. Hematoxylin and eosin.

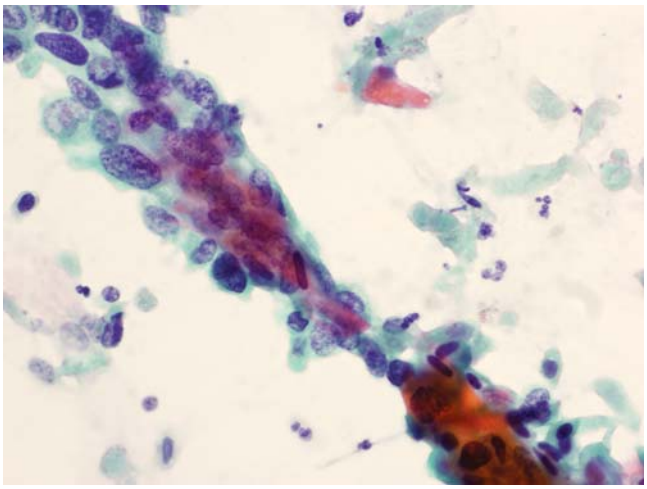

FIGURE 32.10 Squamous cell carcinoma, cytopathologic appearance in bronchial secretion. Note elongated cluster ("fish in a stream") of large cells with increased nuclear cytoplasmic ratio. Necrotic debris in the background. Papanicolaou stain.

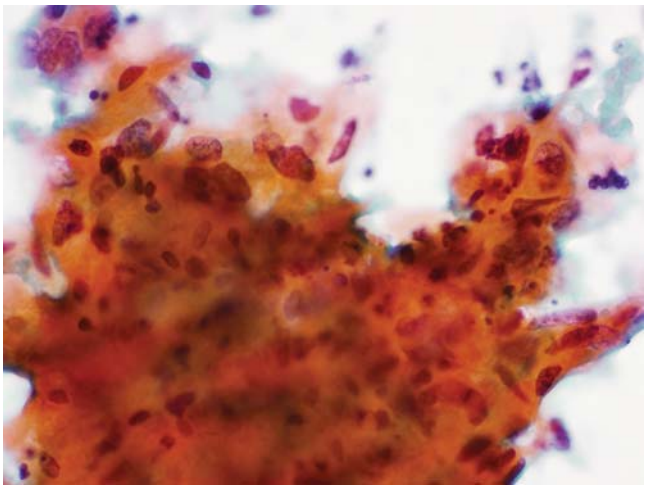

FIGURE 32.12 Squamous cell carcinoma, cytopathologic preparation showing a tri-dimensional cluster of large cells with bizarre nuclei and orangeophilic cytoplasm signifying keratinization. Papanicolaou stain.

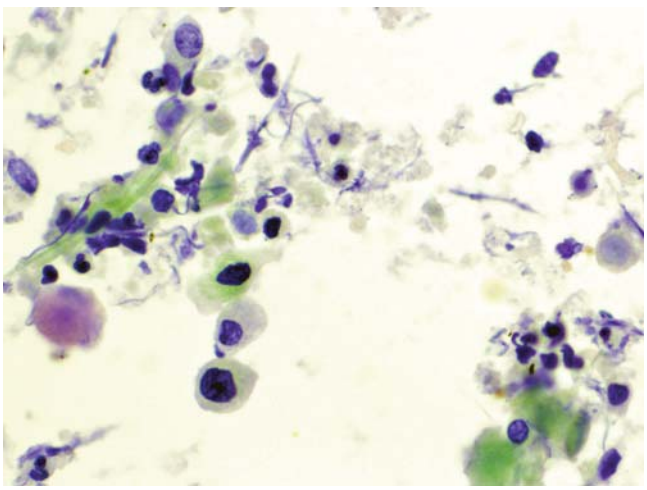

FIGURE 32.11 Squamous cell carcinoma, cytopathologic appearance in a bronchial wash. Note string-like arrangement of tumor cell showing classic "lump of coal" nuclei (very dense nuclear chromatin). Papanicolaou stain.

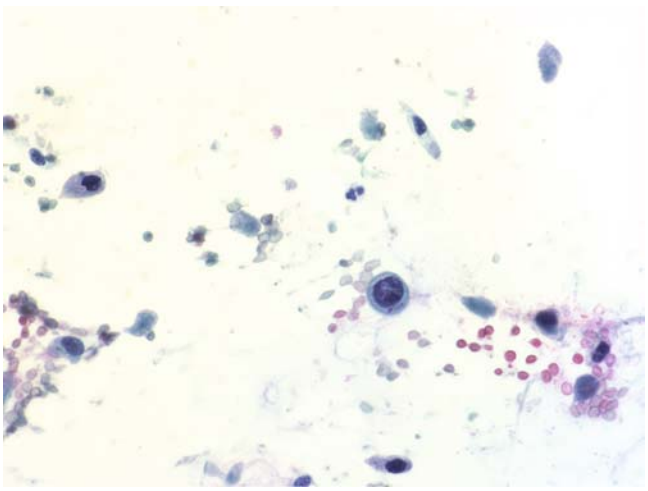

FIGURE 32.13 Squamous cell carcinoma. Cytopathologic preparation showing severely dysplastic cells with marked increase of the nuclear cytoplasmic ratio, nuclear hyperchromasia and nuclear membrane thickening. Papanicolaou stain. From Tomashefski et al, with permission from Springer (see chapter references for complete citation).

REFERENCES

- Bateson EM. The solitary circumscribed bronchogenic carcinoma. A radiological study of 100 cases. *Br J Radiol*. 1964;37:598–607.
- Dulmet-Brender E ,Jaubert F, Huchon G. Exophytic endobronchial epidermoid carcinoma. *Cancer*. 1986;57:1358–1364.
- Flieder DB, Hammar SP. Common non-small cell carcinomas and their variants. In: Tomashefski JF, Cagle PT, Farver CF, Fraire AE, eds. *Dail and Hammar's Pulmonary Pathology*, Vol II. New York, Berlin, Heidelberg: Springer; 2008:216–307.
- Moro D, Brichon PY, Brambilla E, Veale D, Labat F, Brambilla C. Basaloid bronchial carcinoma. A histologic group with a poor prognosis. *Cancer*. 1994;73:2734–2739.
- Ohori NP, Hoff ER. Ch 45. Cytopathology of pulmonary neoplasia. In: Tomashefski JF, Cagle PT, Farver CF, Fraire AE, eds. *Dail and Hammar's Pulmonary Pathology*. 3rd ed., Vol II. Springer: Berlin, Heidelberg, New York; 2008:767–795.

- Tomashefsky JF, Connors AF, Rosenthal ES, et al. Peripheral vs. central squamous cell carcinoma of the lung. A comparison of clinical features, histopathology and survival. *Arch Pathol Lab Med*. 1990;114:468–474.
- Wang BY, Gil J, Kaufman D, Gan L, Kohtz S, Burstein DE. P63 in pulmonary squamous neoplasms, and other pulmonary tumors. *Hum Pathol*. 2002;33:921–926.
- Zeren EH, Laga AC, Allen TC, et al. Squamous cell carcinoma, Part 3. In: Cagle PT, Editor-in-Chief. *Color Atlas and Text of Pulmonary Pathology*. 2nd ed. Philadelphia, Baltimore, New York: The Wolters Kluwer Co; 2008:42–45.

CHAPTER 33

Adenocarcinoma

Shanda Blackmon, Armin Ernst, Philip T. Cagle, Timothy C. Allen,
and Armando E. Fraire

Currently, adenocarcinoma ranks as the number one type of major lung cancer, constituting a significant proportion of all of the non-small cell lung cancers. In contrast to small cell and squamous cell lung cancers which are centrally located, most adenocarcinomas are peripheral, subpleural in location. The few that are central may be visualized endoscopically as endobronchial polyoid masses. Radiographically, adenocarcinomas usually present as a nodular subpleural mass of varying sizes and are often diagnosed as solitary pulmonary nodule. A common finding allowing the diagnosis in some cases is spiculations of the tumor nodules. Calcification does not occur except in rare cases associated with preexisting disease such as histoplasmosis. Cavitation in these tumors is unusual but does occur. The World Health Organization recognizes five microscopic subtypes of adenocarcinoma (acinar, papillary, bronchiolo-alveolar, solid with mucin production, and mixed) as well as five (rarer) variants [clear, fetal, colloid (mucinous), mucinous cystadenocarcinoma, and signet ring], but in reality most cases are mixed, containing varying proportions of the above-cited subtypes and variants. The cytopathology of these tumors reflect their microscopic morphology. High nuclear cytoplasmic ratio, cytoplasmic vacuolization, and prominent nucleoli are major cytopathologic features. Peripheral adenocarcinomas are readily accessible through transthoracic fine needle aspiration biopsy while the more centrally located variants can be diagnosed through endoscopy and examination of bronchial washings and brushings for cytopathologic evaluation.

FIGURE 33.1 CT scan of the chest. Note large peripherally located tumor mass with spiculated borders on the left lung. While peripheral in location, the mass did not reach the pleural surface. On biopsy the mass was proven to be a well-differentiated adenocarcinoma.

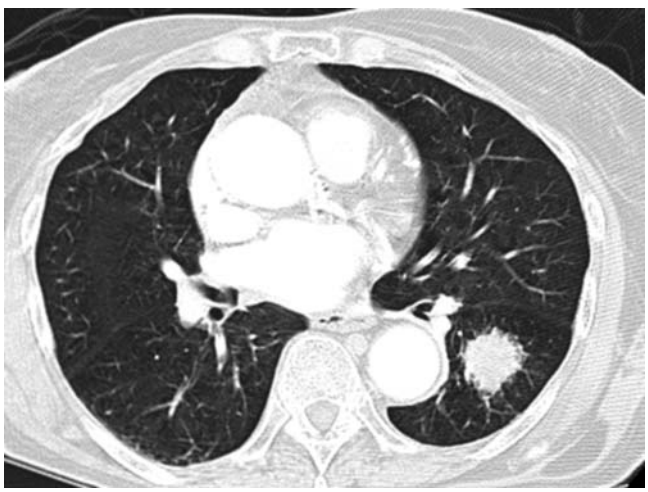

A.E. Fraire et al. (eds.), *Atlas of Neoplastic Pulmonary Disease*,
DOI 10.1007/978-0-387-89839-1_33, © Springer Science+Business Media, LLC 2010

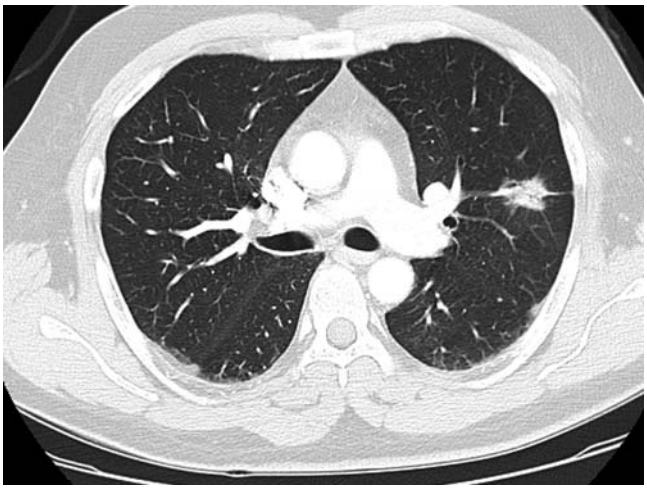

FIGURE 33.2 CT of chest. Note mass lesion presenting as a spiculated mass of the left upper lobe. Biopsy showed an acinar type of adenocarcinoma.

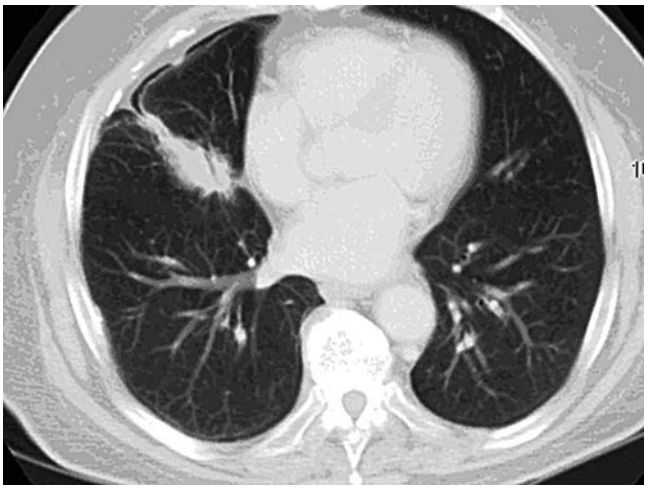

FIGURE 33.4 CT scan of the chest. Note diagonally oriented tumor mass along the oblique fissure of the right lung. Histopathologically, this was a solid type of adenocarcinoma with mucin production.

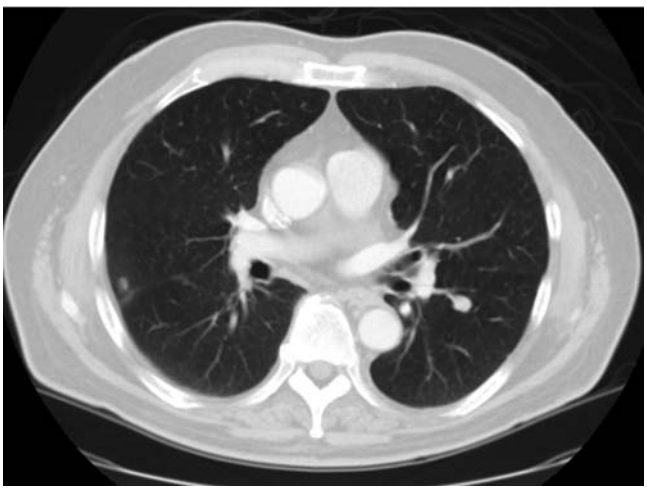

FIGURE 33.3 CT of chest. Note small round nodule in the left lower lobe, below the carina. Also an area of opacity in the minor fissure of the right lung, biopsy demonstrated adenocarcinoma, clear cell variant.

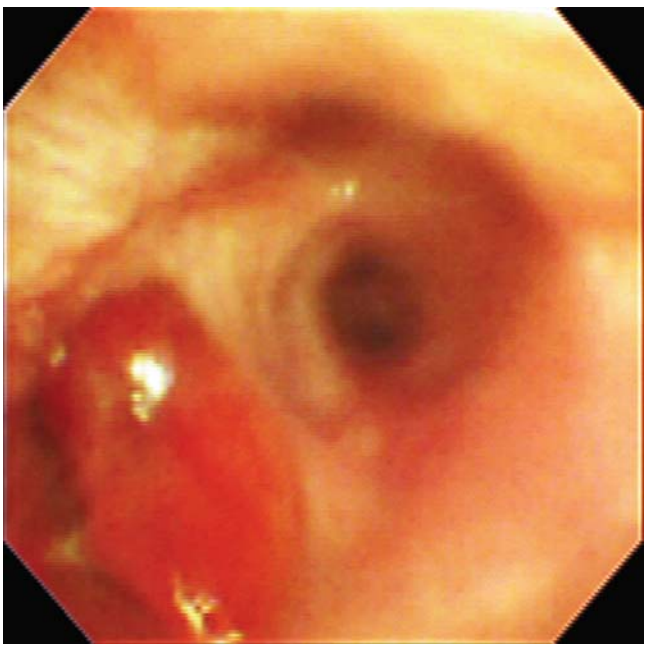

FIGURE 33.5 Bronchoscopic image of a partial right lower lobe obstruction with a fleshy appearing tumor. The 49-year-old male patient complained of intermittent hemoptysis. Biopsy confirmed adenocarcinoma.

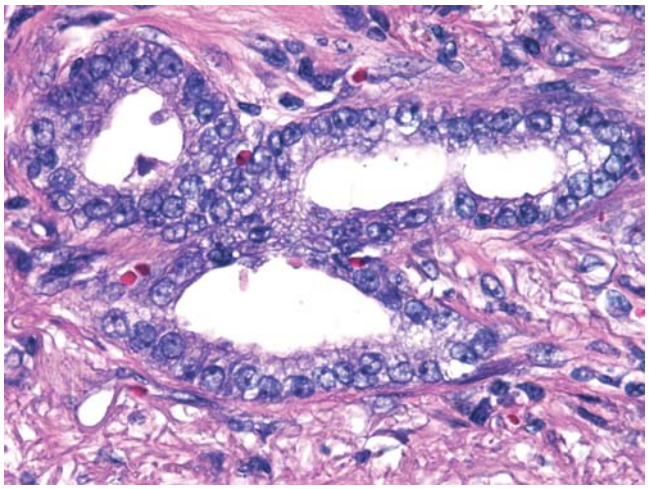

FIGURE 33.6 Adenocarcinoma, acinar-type, high-power microscopic view. Note acinar structure lined by large neoplastic cells and a background with a desmoplastic stroma. Hematoxylin and eosin.

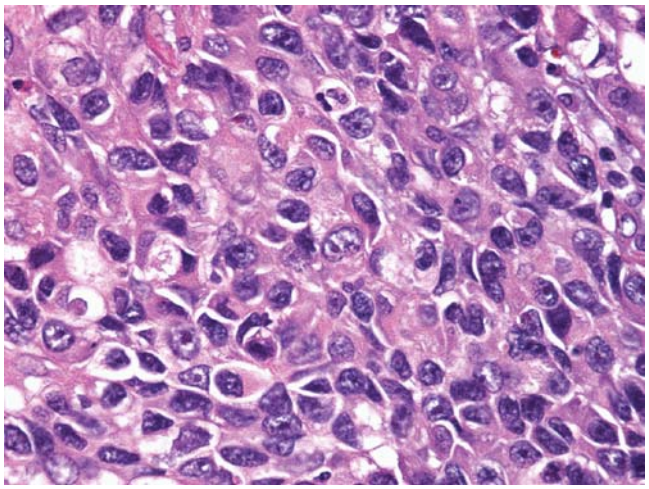

FIGURE 33.8 Adenocarcinoma, solid type with mucin production, high-power microscopic view. Note compact arrangement of large tumor cells with no acinar or papillary features. Hematoxylin and eosin.

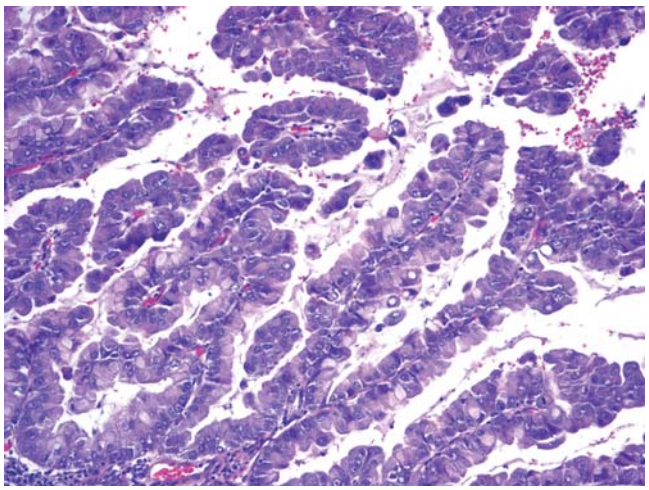

FIGURE 33.7 Adenocarcinoma, papillary-type, high-power microscopic view. Note multiple papillary fronds lined by columnar, focally mucinous cells. Hematoxylin and eosin.

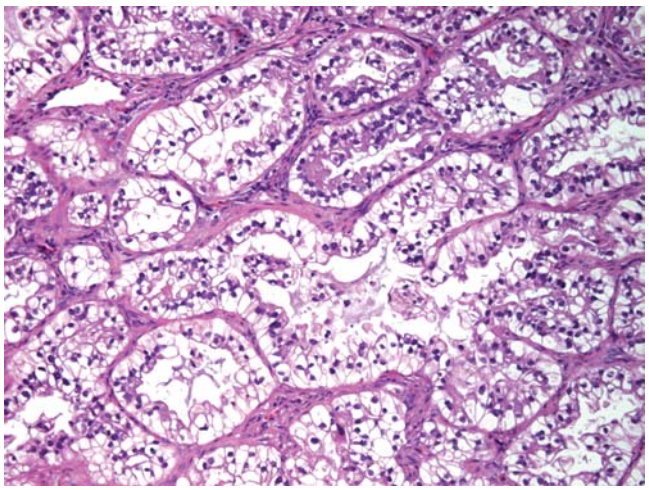

FIGURE 33.9 Adenocarcinoma, clear cell type. High-power microscopioc view. Note gland-like tubular spaces lined by cells with abundant clear (empty-looking) cytoplasm. Hematoxylin and eosin.

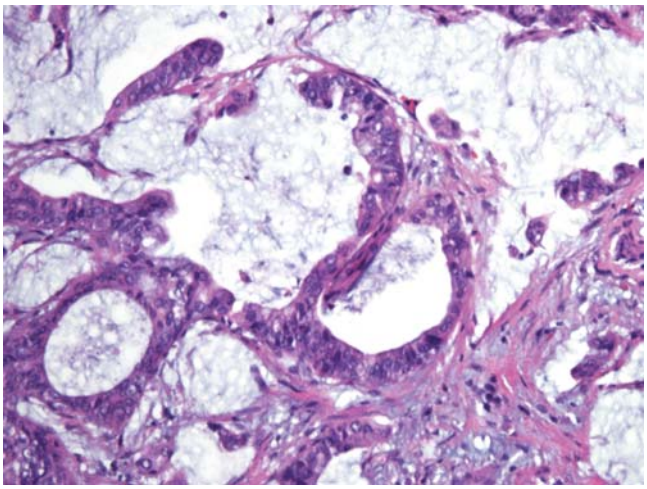

FIGURE 33.10 Adenocarcinoma colloid (mucinous) variant. High-power microscopic view showing mucin-filled cystic spaces lined by large hyperchromatic tumor cells. Hematoxylin and eosin.

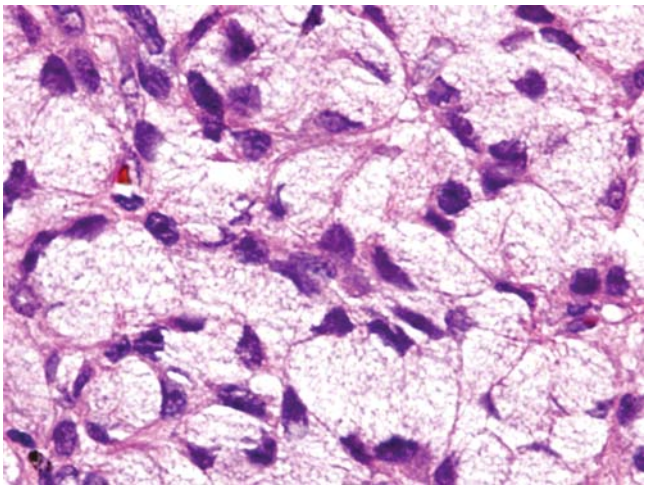

FIGURE 33.11 Adenocarcinoma, signet-ring cell type. High-power view showing clusters of large cells with abundant microvacuolated cytoplasm and small dark nuclei pushed to the periphery, hence the name signet-ring carcinoma. Hematoxylin and eosin.

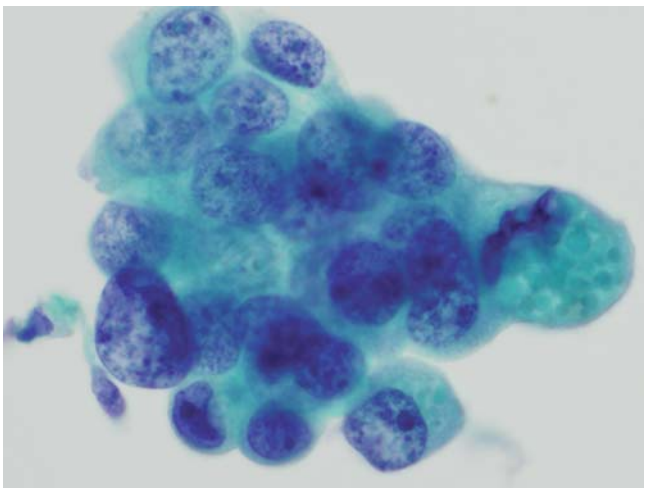

FIGURE 33.12 Adenocarcinoma, mucinous type. Cytopathologic appearance. Note group of large pleomorphic cells with high nuclear cytoplasmic ratio. Papanicolaou stain.

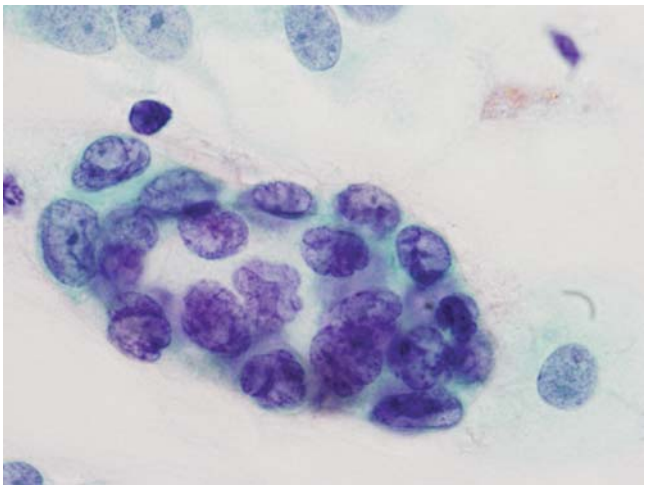

FIGURE 33.13 Cytopathologic view of adenocarcinoma, mucinous type from a patient with bronchioloalveolar carcinoma. It is difficult to separate conventional mucinous adenocarcinoma from mucinous bronchioloalveolar carcinoma on cytologic preparations alone. Papanicolaou stain.

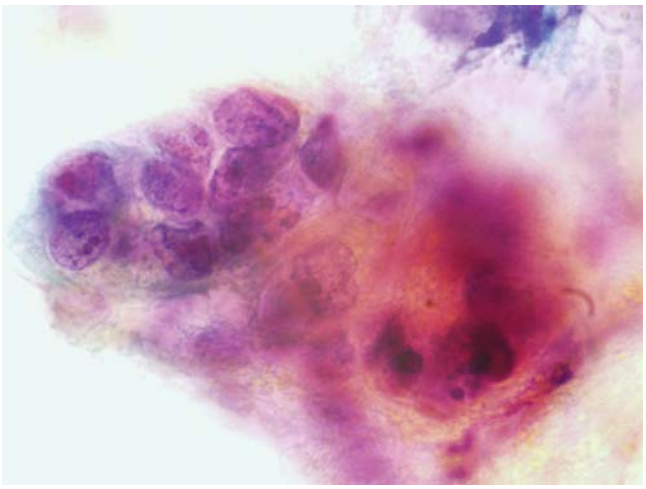

FIGURE 33.14 Adenocarcinoma. Cytopathologic appearance in a bronchial brush preparation. Note cluster of cells with large nuclei showing considerable variation in size and shape. Papanicolaou stain.

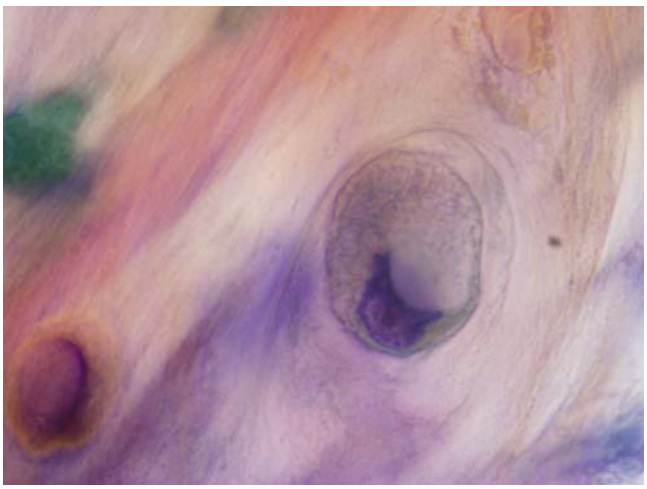

FIGURE 33.15 Adenocarcinoma, signet-ring type, high-power cytopathologic view. Note a large cell with mucin-filled cytoplasm and a distorted hyperchromatic nucleus pushed towards its periphery. Papanicolaou stain.

REFERENCES

- Bennett DE, Sasser WF, Ferguson T. Adenocarcinoma of the lung in men. A clinicopathologic study of 100 cases. *Cancer*. 1969;23:431–439.
- Cagle PT, Cohle SD, Grenberg SD. Natural history of pulmonary scar cancers. Clinical and pathologic implications. *Cancer*. 1985;56:2031–2035.
- Castro CY, Moran CA, Flieder DG, Suster S. Primary signet ring cell adenocarcinomas of the lung: a clinicopathologic study of 15 cases. *Histopathology*. 2001;39:397–401.
- Davison AM, Lowe JW, DaCosta P. Adenocarcinoma arising in a mucinous cystadenoma of the lung. *Thorax*. 1992;47:129–130.
- Graeme-Cook F, Mark EJ. Pulmonary mucinous cystic tumors of borderline malignancy. *Hum Pathol*. 1991;22:185–190.
- Hayashi H, Kitamura H, Nakatani Y, Inayama Y, Ito T. Primary signet-ring cell carcinoma of the lung: Histochemical and immunohistochemical characterization. *Hum Pathol*. 1999;30:378–383.
- Moran CA, Hochholzer L, Fishback N, Travis WD, Koss MN. Mucinous (so-called colloid) carcinomas of lung. *Mod Pathol*. 1992;5:634–638.
- Silver SA, Askin FB. True papillary carcinoma of the lung: a distinct clinicopathologic entity. *Am J Surg Pathol*. 1997;21:43–51.
- Valaitis J, Warren S, Gamble D. Increasing incidence of adenocarcinoma of the lung. *Cancer*. 1981;47:1042–1046.
- Vincent RG, Pickren JW, Lane WW, et al. The changing histopathology of lung cancer. A review of 1682 cases. *Cancer*. 1977;39:1647–1655.

CHAPTER 34

Large Cell Carcinoma

Armin Ernst, Philip T. Cagle, Timothy C. Allen, Dina R. Mody,
and Armando E. Fraire

This carcinoma represents about 10% of all lung cancers. Microscopically, its main feature is the high level of malignancy and lack of squamous or glandular features. However, on electron microscopy, features of either adenocarcinoma or squamous cell can be appreciated suggesting that large cell carcinomas are basically poorly differentiated adenocarcinomas or squamous cell carcinomas. Nonetheless, the clinical presentation and the radiographic appearance more closely resemble adenocarcinoma. The endoscopic appearance is not distinctive since most large cell carcinomas do not involve the proximal airways. Most present as fleshy hemorrhagic-looking masses such as those shown in this chapter.

Grossly, these tumors usually present as subpleural fleshy tumor masses with minimal or absent scarring. Currently, the WHO classification scheme of lung cancers recognizes several microscopic variants of large cell carcinoma: basaloid, clear cell, lymphoepithelial-like, and large cell neuroendocrine carcinoma (elsewhere in this atlas, we discuss large cell neuroendocrine carcinoma). With the exception of the basaloid variant, these carcinomas preferably occur at the periphery of the lung and are inaccessible to the bronchoscope but accessible by fine-needle transthoracic biopsy procedures. There are no specific cytologic features except that the neoplastic cells tend to be dispersed. The cytoplasm is moderate to abundant and nucleoli prominent, features that help to separate this tumor from small cell carcinoma on cytologic preparations.

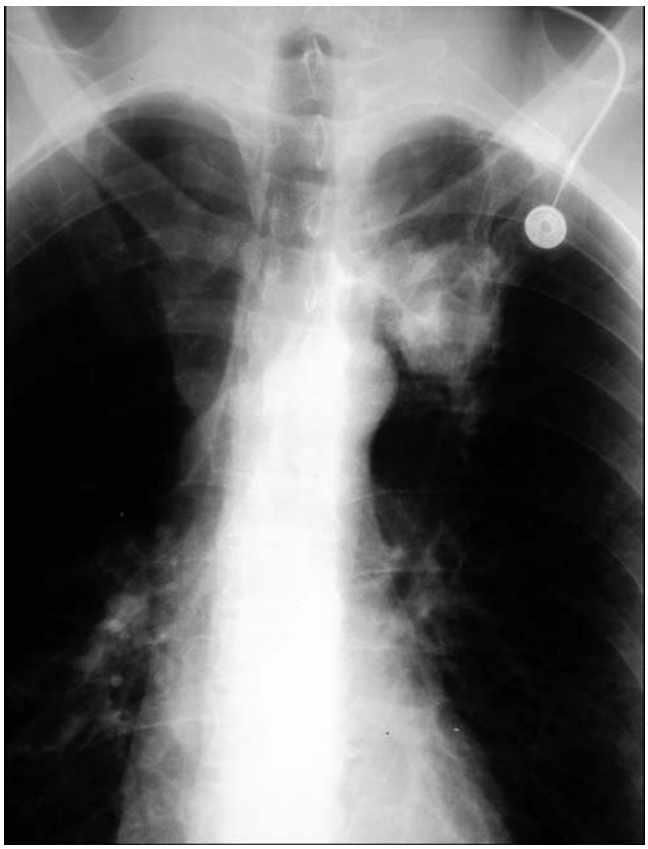

FIGURE 34.1 Chest radiograph of chest. Note large nodular density with relatively well-defined borders in the left upper lobe. Biopsy documented large cell carcinoma of lung.

A.E. Fraire et al. (eds.), *Atlas of Neoplastic Pulmonary Disease*,
DOI 10.1007/978-0-387-89839-1_34, © Springer Science+Business Media, LLC 2010

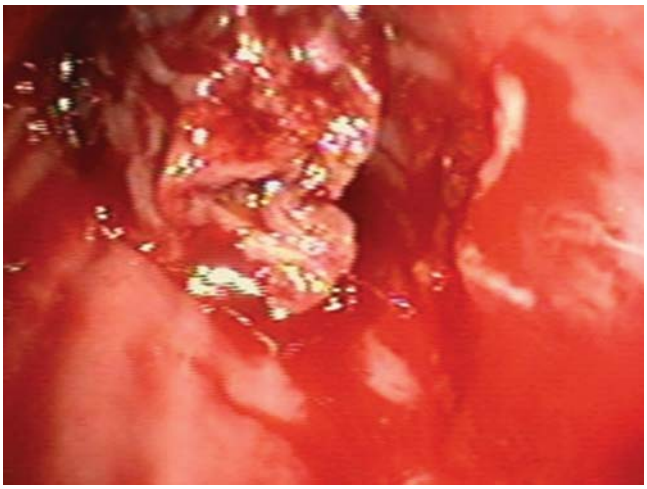

FIGURE 34.2 Large cell carcinoma. Bronchoscopic view of a lesion in the left main stem bronchus. Note diffuse bleeding at the surface of the tumor. The patient was a 68-year-old non-smoking man. Biopsy confirmed large cell carcinoma.

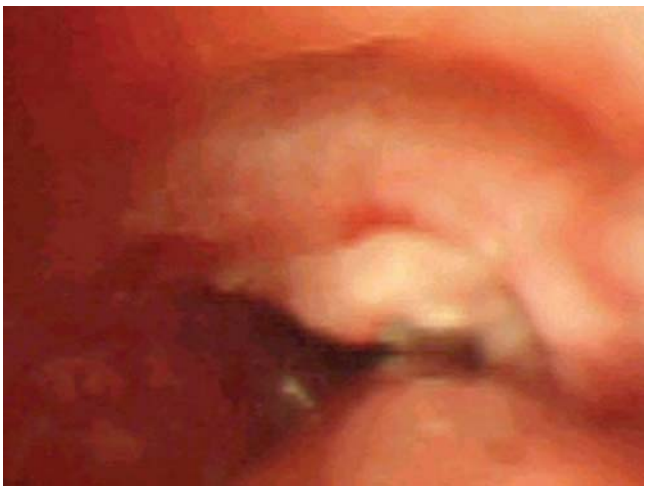

FIGURE 34.3 Large cell carcinoma. Bronchoscopic view of the right main stem bronchus of a 66-year-old woman with peripheral abnormalities on screening CT of the chest. Visible is a yellow tan necrotic mass at the roof of the bronchus. Biopsy showed a large cell carcinoma.

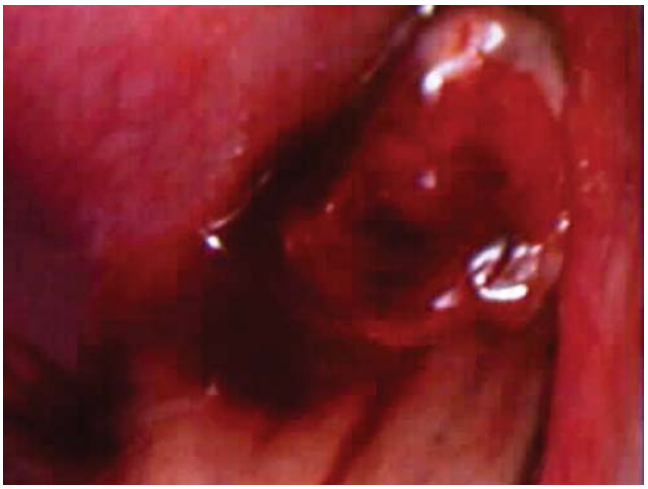

FIGURE 34.4 Biopsy proven large cell carcinoma. Bronchoscopic view of a lesion emanating from the right upper lobe.

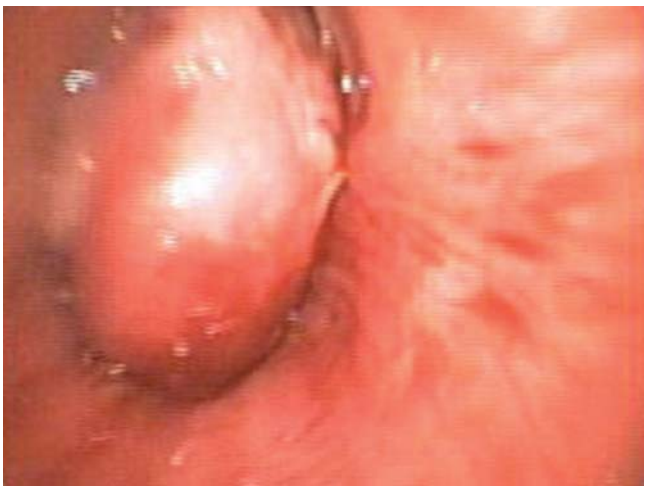

FIGURE 34.5 Large cell carcinoma. Bronchoscopic image of a completely obstructing mass in the left main stem bronchus of a 62-year-old man with recurrent left-sided pneumonia. Biopsy confirmed large cell carcinoma.

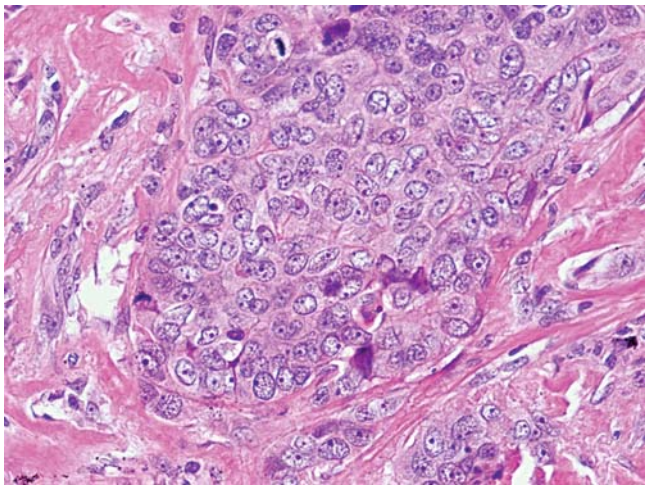

FIGURE 34.6 Large cell carcinoma, microscopic view. Note a nest of tumor cells with abundant cytoplasm, atypical nuclei, distinct nucleoli and some mitoses. Also note absence of acinar differentiation, keratinization, or intercellular bridges. Hematoxylin and eosin.

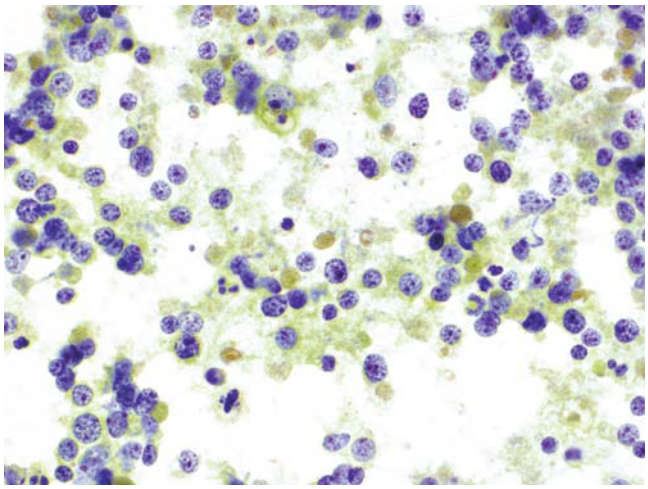

FIGURE 34.8 Large cell carcinoma; cytopathologic view. Note dispersed tumor cell population with predominance of larger cells. Few lymphocytes can be seen in the background. Papanicolaou stain.

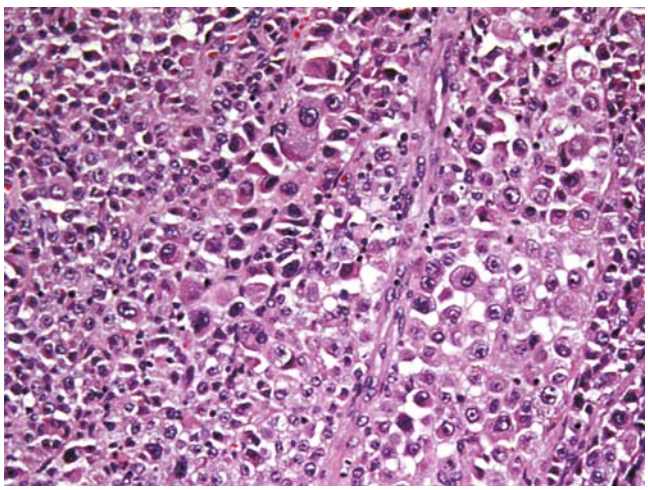

FIGURE 34.7 Large cell carcinoma, microscopic view showing large, plump cells with rhabdoid features. Hematoxylin and eosin.

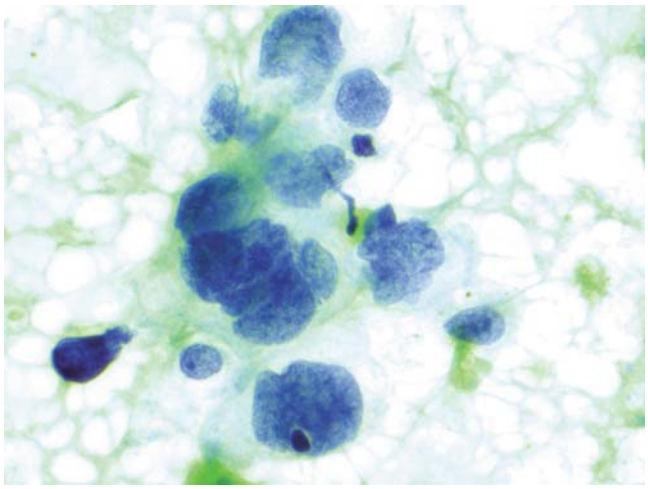

FIGURE 34.9 Large cell carcinoma; cytopathologic view. Closer high-power view showing a group of cells with very dense nuclear chromatin and lack of squamous or glandular features. FNA preparation; Papanicolaou stain.

REFERENCES

- Brambilla E, Pugatch B, Geisinger K, et al. Large cell carcinoma. In: Travis WD, Brambilla E, Müller-Hermelink HK, Harris CC, eds. *World Health Organization Classification of Tumours. Pathology and Genetics of Tumours of the Lung, Pleura, Thymus and Heart*. Lyon: IARC Press; 2004:45–52.
- Cavazza A, Colby TV, Tsokos M, Rush W, Travis WD. Lung tumors with a rhabdoid phenotype. *Am J Clin Pathol.* 1996;105:182–188.
- Churg A. The fine structure of large cell undifferentiated carcinoma of the lung. Evidence for its relation to squamous cell carcinomas and adenocarcinomas. *Hum Pathol.* 1978;9:143–156.
- Downey RS, Sewell CW, Mansour KA. Large cell carcinoma of the lung: a highly aggressive tumor with dismal prognosis. *Ann Thorac Surg*. 1989;47:806–808.
- Foroulis CN, Iliadis KH, Mauroudis PM, Kosmidis PA. Basaloid carcinoma, a rare primary lung neoplasm:

report of a case and review of the literature. *Lung Cancer*. 2002;35:335–338.
- Han AJ, Xiong M, Gu YY, Lin SX, Xiong M. Lymphoepithelioma-like carcinoma of the lung with a better prognosis. A clinicopathologic study of 32 cases. *Am J Clin Pathol*. 2001;115:841–850.
- Kim DJ, Kim KD, Shin DH, et al. Basaloid carcinoma of the lung: a really dismal histologic variant? *Ann Thorac Surg*. 2003;76:1833–1837.
- Rossi G, Marchioni A, Milani M, et al. TTF -1, cytokeratin 7, 34betaE12, and CD56/NCAM immunostaining in the subclassification of large cell carcinomas of the lung. *Am J Clin Pathol.* 2004;122:884–893.
- Shimazaki H, Aida S, Sato M, et al. Lung carcinoma with rhabdoid cells: a clinicopathological study and survival analysis of 14 cases. *Histopathology*. 2001;38:425–434.
- Sunday ME, Choi N, Spindel ER, Chin WW, Mark EJ. Gastrin-releasing peptide gene expression in small cell and large cell undifferentiated lung carcinomas. *Hum Pathol*. 1991;22:1030–1039.

CHAPTER 35

Small Cell Carcinoma

Armin Ernst, Shanda Blackmon, Philip T. Cagle, Timothy C. Allen,
Dina R. Mody, and Armando E. Fraire

Small cell carcinomas are highly malignant tumors composed of relatively small uniform cells with scant cytoplasm and stippled nuclear chromatin pattern. An ultrastructural hallmark of these tumors is the presence of membrane-bound, electron-dense granules that contain a variety of active peptide moieties. Small cell carcinomas occur in middle age and older individuals with a mean age of 59 years. Cough, hemoptysis and chest pain are symptoms associated with the development of tumor masses in the lung. On chest radiographs and computed tomography (CT), small cell carcinomas appear as hilar or perihilar masses, often in continuity with mediastinal lymphadenopathy and lobar collapse. A small percent of tumors are peripherally located and in these instances the radiographic presentation will be that of a solitary lung nodule. Positron Emission Tomography (PET) scanning is useful in patients with extensive disease and also in the determination of prognosis.

A submucosal infiltration pattern of the bronchial mucosa can be appreciated endoscopically which, when extensive, may result in luminal narrowing. In advanced cases, complete or near-complete bronchial obstruction will be seen. Another endoscopic presentation is that of multiple small nodules on the mucosal surface of the bronchus. These tumors tend to be centrally located presenting as bulky, gray white fleshy masses surrounding major bronchi, at times with endobronchial components. Their consistency is generally soft, reflecting the absence of desmoplasia. The tumor cells are densely packed, small, round to oval to spindle-shaped with little supporting stroma. Architectural patterns include nesting, trabeculations, peripheral palisading, and formation of rosettes. The tumor cells show very high nuclear cytoplasmic ratio and stippled nuclear chromatin patterns. Although referred to as small, the cells of small cell carcinoma are generally two to three times the size of red blood cells or small resting lymphocytes. The cytologic features of small cell carcinoma are distinctive. Characteristically, the cells are dark, pyknotic (india-ink dot), and show scant cytoplasm and nuclear molding. The nuclear chromatin shows the so-called salt and pepper pattern. Nucleoli are absent or are very small and inconspicuous. In sputum preparations, tumor cells may be found in rows, entrapped within strands of mucus but in Saccomano's preparations, the tumor cells tend to be dispersed. At times, a combination of larger neoplastic cells with squamous or glandular differentiation may be seen. Also, at times, a component of large cell undifferentiated carcinoma will be observed in tumors with mixed phenotypes. A necrotic background is frequently seen containing apoptotic bodies and/or granular debris.

A.E. Fraire et al. (eds.), *Atlas of Neoplastic Pulmonary Disease*,
DOI 10.1007/978-0-387-89839-1_35,

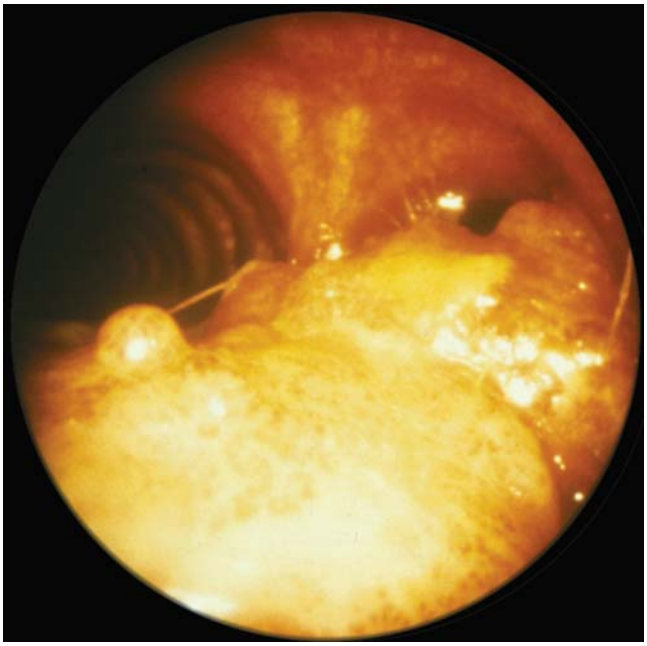

FIGURE 35.1 Small cell carcinoma. Endoscopic imageof distal trachea in a patient with hemoptysis. The posterior wall is diffusely infiltrated by tumor involving the main carina and extending into the right main stem bronchus. Biopsy showed small cell carcinoma.

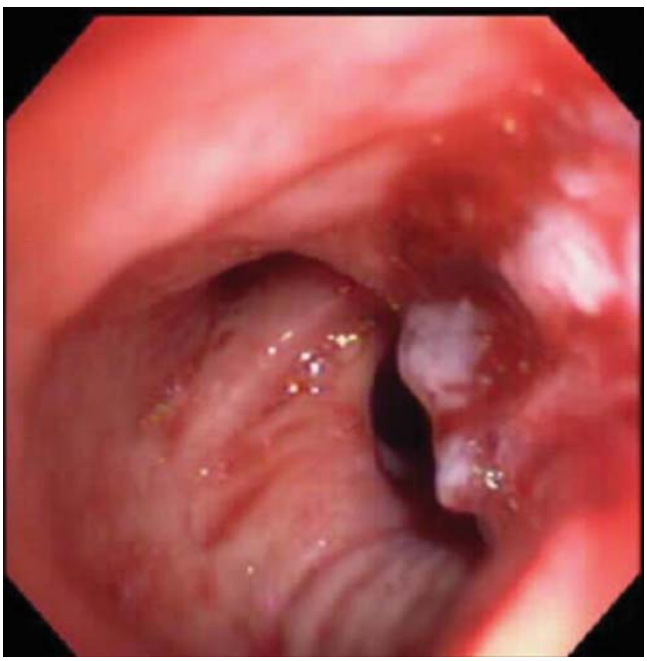

FIGURE 35.2 Small cell carcinoma. Endoscopic image of the bronchus intermedius of a 69-year-old man with right hilar lymphadenopathy. On biopsy, the mucosal lesions with erythematous background showed small cell carcinoma.

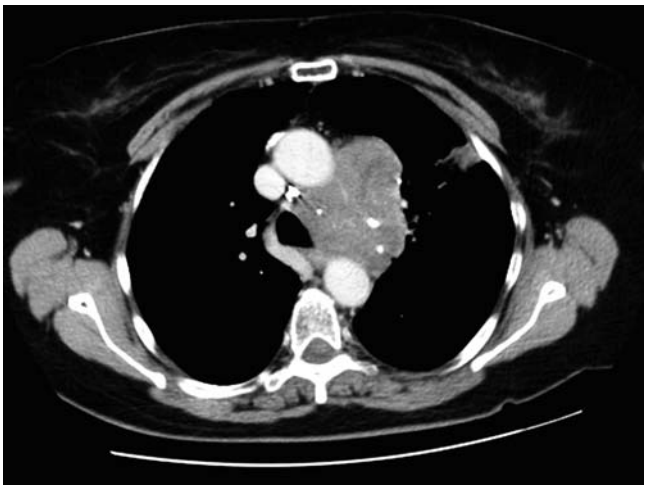

FIGURE 35.3 CT of chest from a patient with biopsy proven small cell carcinoma. Note large mediastinal mass next to the aorto-pulmonary window.

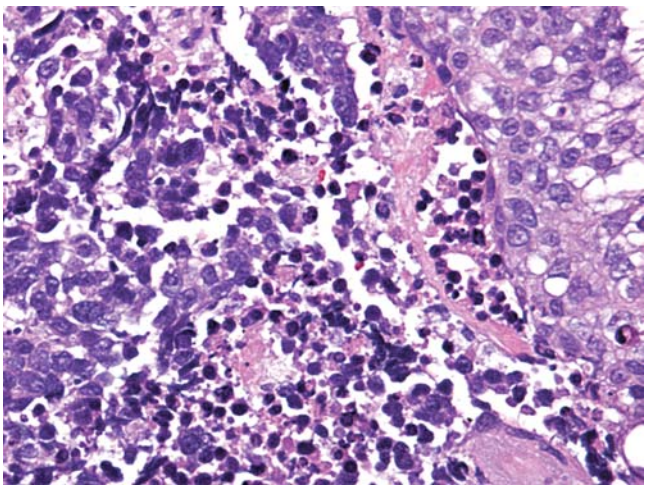

FIGURE 35.4 Small cell carcinoma. Classic variant, high-power view. Note population of cells with round to oval tumor cells showing scant cytoplasm. Hematoxylin and eosin.

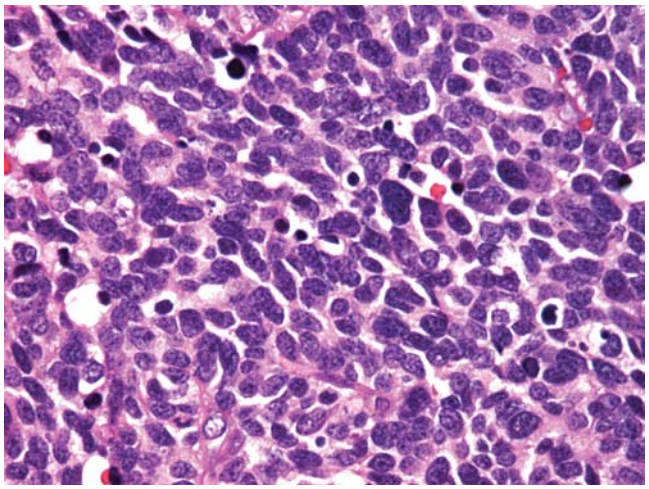

FIGURE 35.5 Small cell carcinoma. In this tumor, the cells tend to be more fusiform but retain the high nuclear cytoplasmic ratio feature. Hematoxylin and eosin.

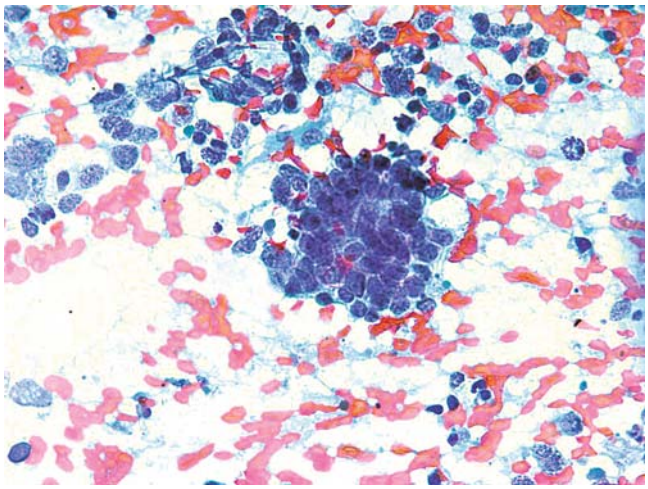

FIGURE 35.7 Small cell carcinoma – similar to Fig. 35.6, but in this instance, the tumor cells show a proteinaceous background. Papanicolaou stain.

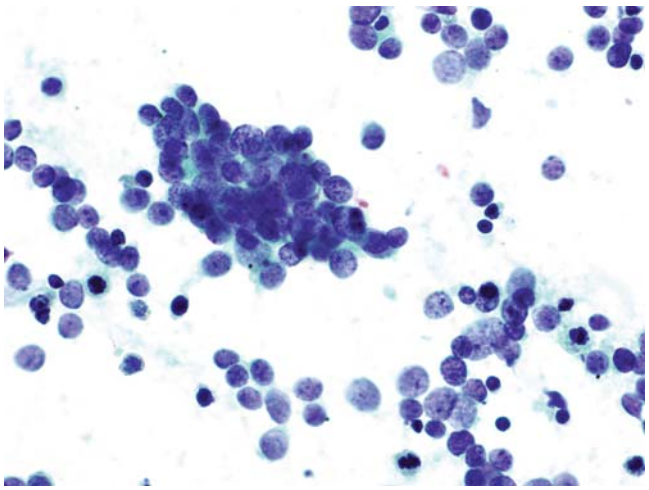

FIGURE 35.6 Small cell carcinoma. Cytologic appearance. Note cluster of small very dark cells showing scant cytoplasm. Papanicolaou stain.

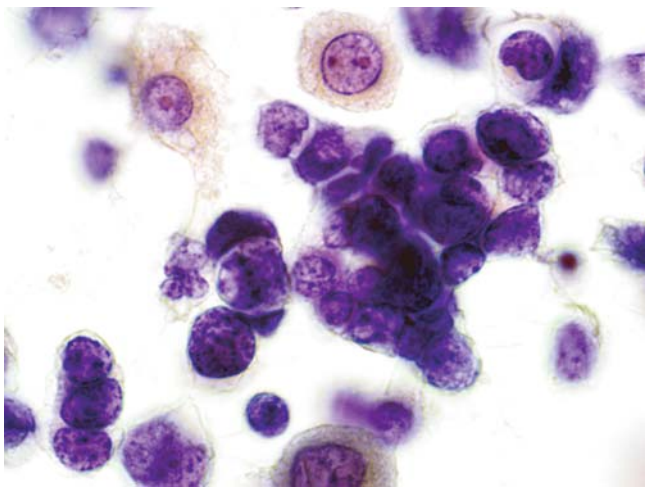

FIGURE 35.8 Small cell carcinoma. High-power view of a cytologic preparation at oil immersion. Note cells on center left with molding and other cells with very scant cytoplasm and hyperchromatic nuclei. Papanicolaou stain.

REFERENCES

- Devendro G. Small cell carcinoma. In: Duhamell DR, Harell JH, eds. *Clinical Atlas of Airway Diseases. Bronchoscopy, Radiology and Pathology*. Philadelphia: Elsevier Saunders; 2005:42–45.
- Fraire AE, Johnson EH, Yesner R, et al. Prognostic significance of histopathologic subtyping and stage in small cell lung cancer. *Human Pathol*. 1992;23: 520–528.
- Hirsch FR, Osterlind K, Hansen HH. The prognostic significance of histopathologic subtyping of small cell carcinoma of the lung according to the classification of the World Health Organization. A study of 375 consecutive patients. *Cancer*. 1983;52: 2144–2150.
- Johnston WW, Elson CE. Ch 14. Respiratory tract. In: Bibbo M, ed. *Comprehensive Cytopathology*. Philadelphia, London, Toronto: WB Saunders Co; 1991:320–398.
- Kato H, Konaka C, Ono J, Takahashi M, Hayata Y. Ch VI. Malignant tumor cells. In: *Cytology of the Lung: Techniques and Interpretation*. Tokyo- New York: Igaku-Shoin; 1983:75–131.
- Shore DF, Paneth M. Survival after resection of small cell carcinoma of the bronchus. *Thorax*. 1980;35: 819–822.
- Smit EF, Groen HJM, Timens W, Deboer WJ, Postmus PE. Surgical resection for small cell carcinoma of the lung – a retrospective study. *Thorax*. 1994;49: 20–22.

CHAPTER 36

Adenosquamous Carcinoma

Shanda Blackmon, Philip T. Cagle, Timothy C. Allen,
and Armando E. Fraire

This uncommon non-small cell variant of lung cancer is characterized by combined histopathologic features of squamous cell carcinoma and adenocarcinoma. Most patients have history of smoking and the clinical presentation is similar to that of other non-small cell carcinomas. A requirement for diagnosis is that each component represents at least 10% of the tumor substance. Furthermore, unequivocal evidence of squamous lineage consisting of squamous pearls, or cells with intercellular bridges plus unequivocal evidence of glandular differentiation consisting of acini, tubules, or papillary formations are required for definitive diagnosis. These tumors are almost always peripherally located and rarely accessible to the bronchoscope. High-grade mucoepidermoid carcinomas (MEC) must be differentiated from adenosquamous carcinomas. A helpful distinguishing feature of MEC is their central location.

The radiographic and gross appearances of the tumor are also non-distinctive and very similar to that of other non-small carcinomas. Cytologically, features of squamous differentiation such as cells with dense cytoplasm and well-defined borders, plus cells with mucin vacuoles may be present. Sputum preparations with tissue fragments may contain squamous pearls.

FIGURE 36.1 CT image of chest showing an adenosquamous carcinoma of the left lung. Note large peripherally located tumor mass which is very near to the chest wall.

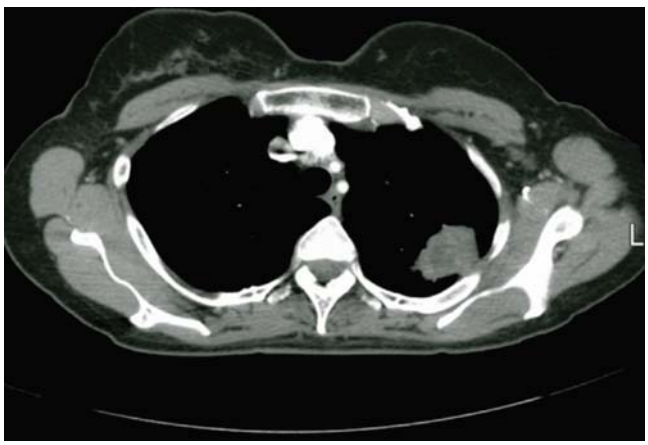

A.E. Fraire et al. (eds.), *Atlas of Neoplastic Pulmonary Disease*,
DOI 10.1007/978-0-387-89839-1_36,

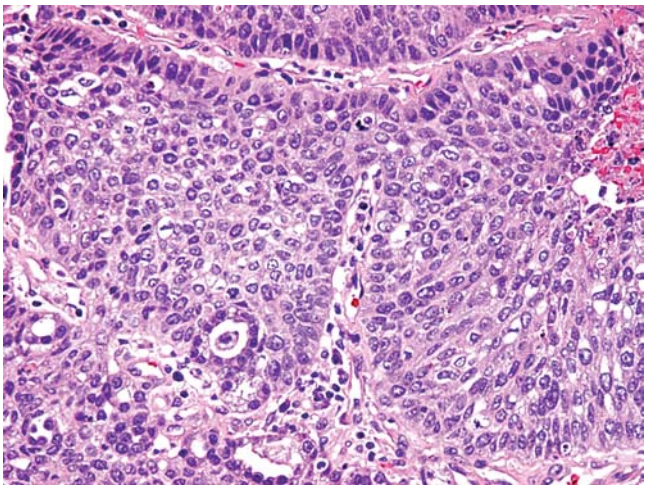

FIGURE 36.2 Adenosquamous carcinoma. Microscopic view. Note tumor cells with squamous cell differentiation. Focal necrosis on the far right upper corner and acinar structures on the left lower corner of the field. Hematoxylin and eosin.

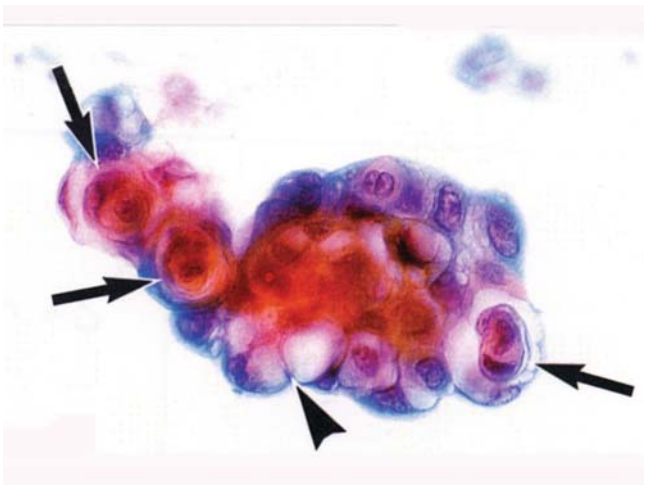

FIGURE 36.4 Cytopathologic appearance. Adenosquamous carcinoma. Tissue fragment recovered from a sputum sample. Note squamous pearl (*arrows*) and intracytoplasmic vacuoles indicative of mucin production (*arrow head*) (Courtesy of Dr. Sudha Kini, Henry Ford Hospital, Detroit, MI). With permission from Springer (see chapter references for complete citation).

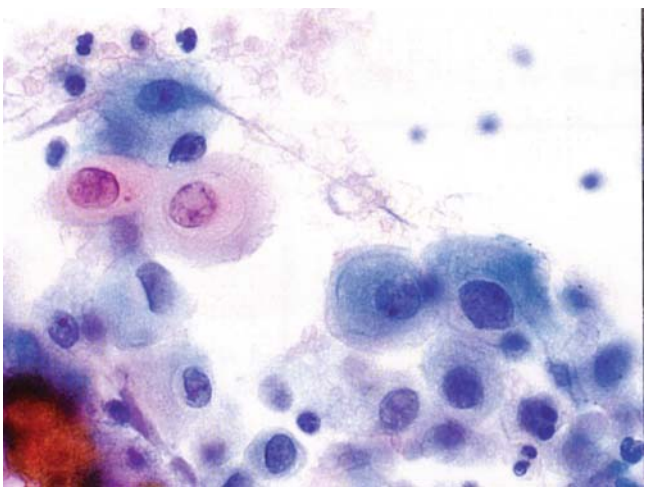

FIGURE 36.3 Cytopathologic appearance. Adenosquamous carcinoma showing larger squamous cells and small glandular cells. Papanicolaou stain (Courtesy of Dr. Sudha Kini, Henry Ford Hospital, Detroit, MI). With permission from Springer (see chapter references for complete citation).

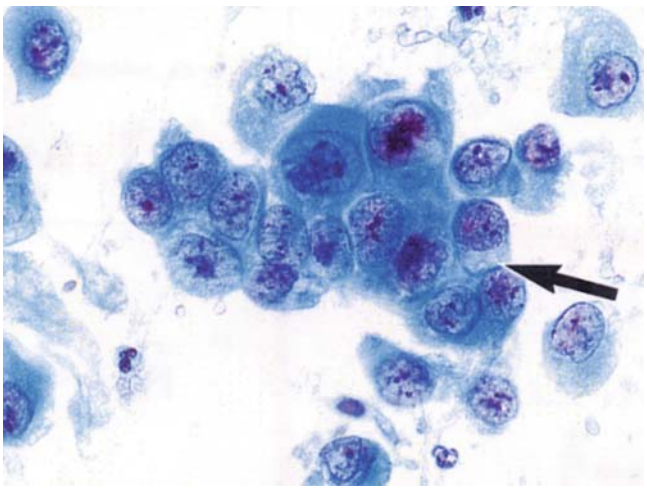

FIGURE 36.5 Cytopathologic appearance. Adenosquamous carcinoma. Cytologic bronchial brush preparation. Note cells with dense cytoplasm and well-defined borders suggestive of squamous differentiation (*arrow*) (Courtesy of Dr. Sudha Kini, Henry Ford Hospital, Detroit, MI). With permission from Springer (see chapter references for complete citation).

REFERENCES

- Brambilla E, Travis WD. Adenosquamous carcinoma. In: Travis WD, Brambilla E, Müller-Hermelink HK, Harris CC, eds. *World Health Organization Classification of Tumours. Pathology and Genetics of Tumours of the Lung, Pleura, Thymus and Heart.* Lyon: IARC Press; 2004:52–52.
- Ishida T, Kaneko S, Yokoyama H, Inoue T, Sugio K, Sugimachi K. Adenosquamous carcinoma of the lung: Clinicopathologic and immunohistochemical features. *Am J Clin Pathol*. 1992;97:678–685.
- Laga AC, Allen TC, Cagle PT. Adenosquamous carcinoma. In: Cagle PT, Editor-in-chief. *Color Atlas and Text of Pulmonary Pathology*. 2nd ed. Philadelphia, Baltimore New York: Wolter Kluwer; 2008:62–63.
- Kini SR, ed. *Color Atlas of Pulmonary Cytopathology. Adenosquamous Carcinoma*. New York, Berlin, Heidelberg: Springer-Verlag; 2002:264.
- Takamori S, Noguchi M, Morinaga S, et al. Clinicopathologic characteristics of adenosquamous carcinoma of the lung. *Cancer* (Philadelphia). 1991;67:649–654.
- Yousem SA. Pulmonary adenosquamous carcinomas with amyloid-like stroma. *Mod Pathol*. 1989;2:420–426.

CHAPTER 37

Bronchioloalveolar Carcinoma

Shanda Blackmon, Philip T. Cagle, Timothy C. Allen, Dina R. Mody, and Armando E. Fraire

This unique subtype of adenocarcinoma is primarily characterized by its distinctive architectural growth pattern. In this type of growth pattern, called lepidic pattern, the tumor cells spread along intact pre-existing alveolar walls. Mucinous, non-mucinous, and mixed variants are recognized. In addition to this architectural growth pattern, demonstration of vascular, pleural or stromal invasion is required for a definite diagnosis of bronchioloalveolar carcinoma. Current WHO criteria indicate that in the absence of invasion, this lesion is essentially an in-situ tumor.

A bronchioloalveolar pattern is often mixed with other major patterns of adenocarcinomatous growth such as acinar or papillary. The radiographic presentation of these tumors reflects their gross appearance. Grossly, these tumors may present as single nodules, multiple nodules, or in a diffuse pneumonic form. Recently, with the advent of screening programs, radiographic patterns of ground glass opacities are becoming more apparent. The clinical presentation is not different from that of other lung cancers, except in the case of the diffuse mucinous pneumonia-like tumors that may be associated with broncorrhea. The cytologic diagnosis of bronchioloalveolar carcinoma is difficult. The finding of tri-dimensional ball-like aggregates of strikingly similar tumor cells may be a clue for the cytopathologic diagnosis. These ball-like aggregates may have hobnailed outlines with no molding. Abundant mucus in the background is another clue for the diagnosis. Psammoma bodies may be seen.

FIGURE 37.1 CT scan of chest showing a spiculated lesion in the posterior aspect of the right lower lobe. Tissue examination showed a mucinous type of bronchioloalveolar adenocarcinoma.

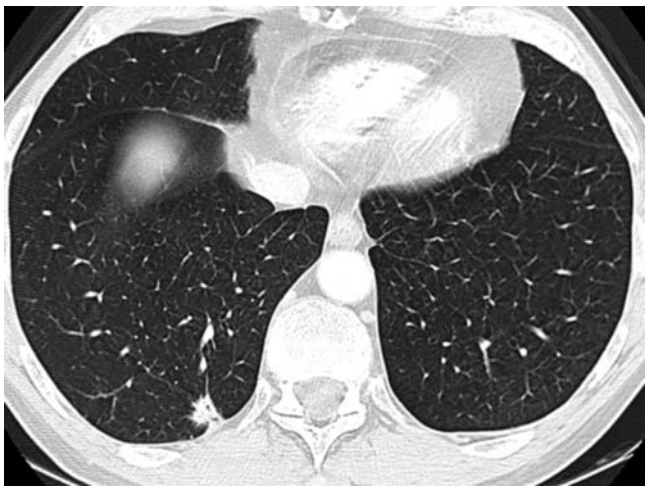

A.E. Fraire et al. (eds.), *Atlas of Neoplastic Pulmonary Disease*,
DOI 10.1007/978-0-387-89839-1_37, © Springer Science+Business Media, LLC 2010

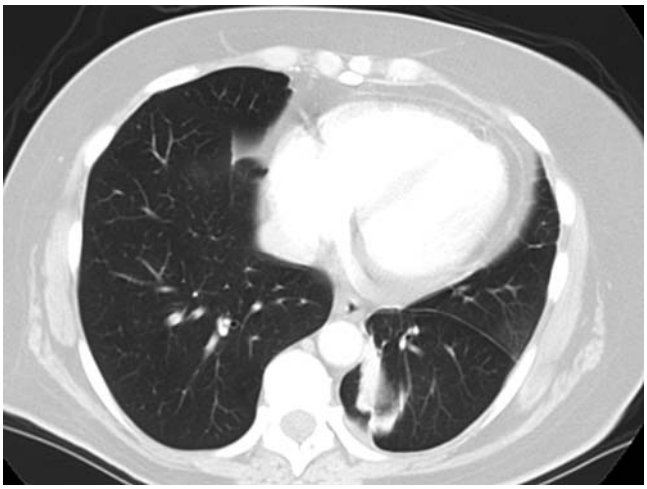

FIGURE 37.2 CT scan of chest showing ground glass opacity in the posterior segment of left lower lobe. Tissue examination showed a non-mucinous type of bronchioloalveolar carcinoma.

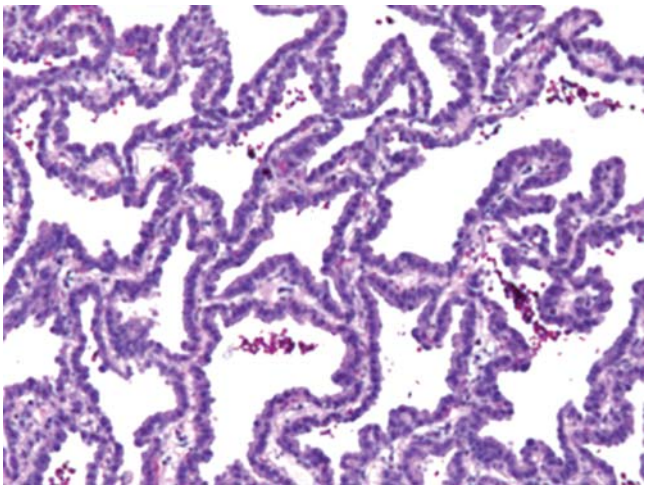

FIGURE 37.4 Bronchioloalveolar carcinoma, non-mucinous type. Microscopic view. Note slightly thickened, well-preserved alveolar walls lined by cuboidal non-mucinous tumor cells. Hematoxylin and eosin.

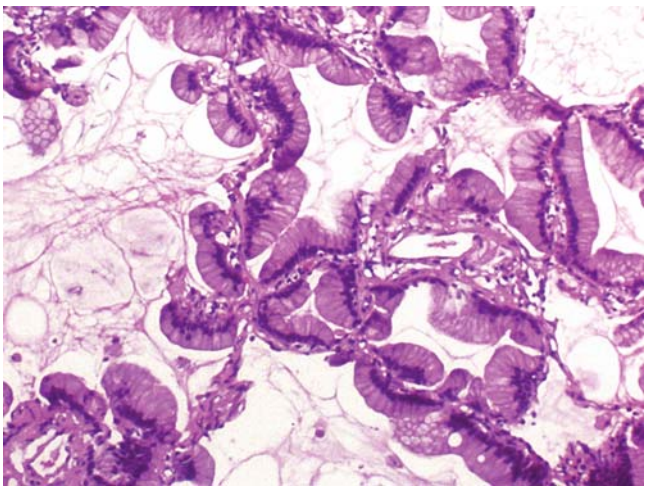

FIGURE 37.3 Bronchioloalveolar carcinoma mucinous type. Microscopic view. Note rows of tall columnar mucinous cells resting upon delicate strands of connective tissue representing a preserved alveolar network of the lung. Hematoxylin and eosin.

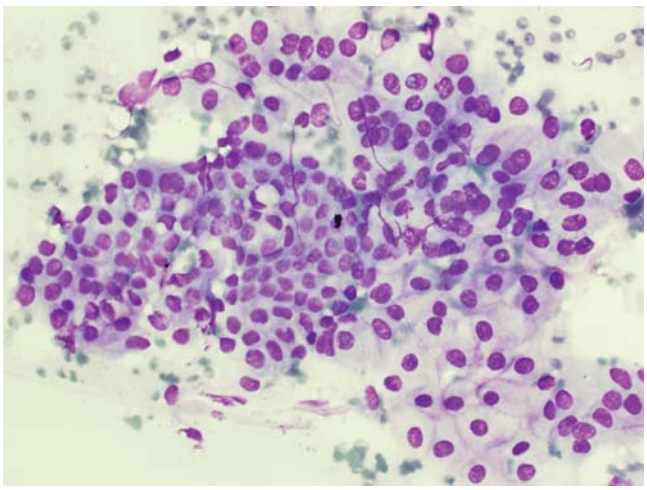

FIGURE 37.5 Bronchioloalveolar carcinoma. Cytopathologic adequacy evaluation of mucinous bronchioloalveolar carcinoma. Tri-dimensional cell groups with a honeycomb-like appearance on low magnification. Mild nuclear pleomorphism and finely vacuolated cytoplasmic mucin. Note also absence of terminal bars and cilia. Diff-Quik Stain.

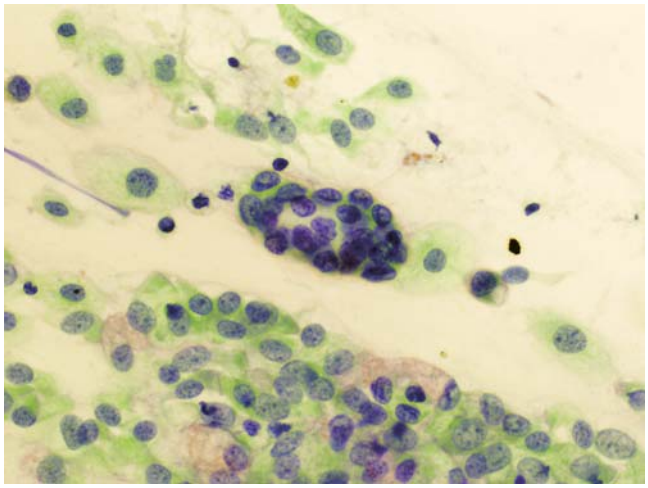

FIGURE 37.6 Bronchioloalveolar carcinoma; high-power view; cytopathologic features. Note cluster of cells nuclear contour irregularity, hyperchromasia, and chromatin clearing with nuclear holes from intranuclear cytoplasmic inclusions. Although the cells appear small compared to normal bronchial epithelial cells, the chromatinic characteristics are very different. Papanicolaou stain.

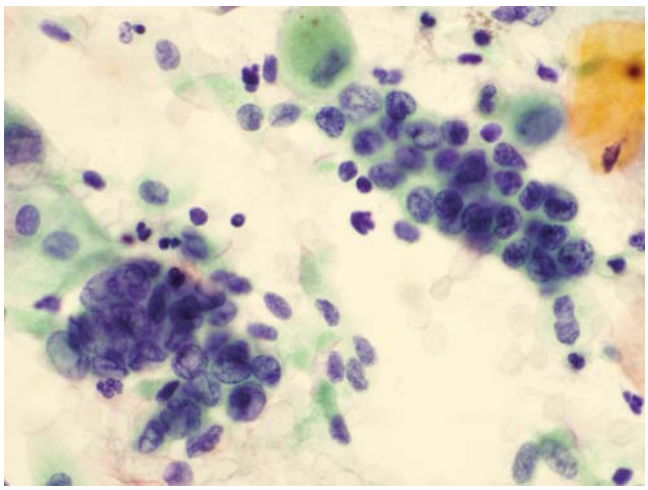

FIGURE 37.7 Bronchioloalveolar carcinoma; high-power view; cytopathologic features. Tri-dimensional microacinar structure with nuclear overlap and large nuclei compared to adjacent ciliated bronchial epithelial cells. Note intranuclear cytoplasmic inclusion (holes) which are fairly characteristic, when present. Papanicolaou stain.

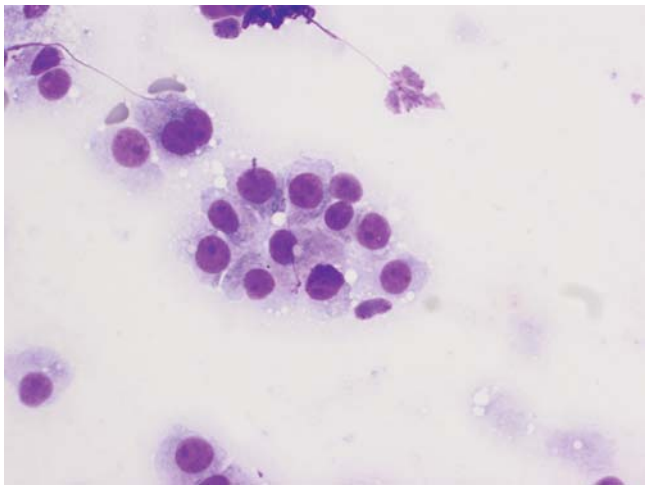

FIGURE 37.8 Bronchioloalveolar carcinoma; high-power cytopathologic view. Note centrally located group of cells show relatively bland-looking cells with high nuclear cytoplasmic ratio. Diff-Quick stain.

REFERENCES

- Colby TV, Koss MN, Travis WD. *Tumors of the Lower Respiratory Tract*. 3rd ed. Washington DC: Armed Forces Institute of Pathology; 1995.
- Colby TV, Noguchi M, Henschke C, et al. Adenocarcinoma. In: Travis WD, Brambilla E, Müller-Hermelink HK, Harris LC, eds. *WHO Classification of Tumours, Pathology and Genetics of Tumours of the Lung, Pleura, Thymus and Heart*. Lyon: IARC Press; 2004:35–44.
- Noguchi M, Morikawa A, Kawasaki M, et al. Small adenocarcinoma of the lung. histologic characteristics and prognosis. *Cancer*. 1995;75:2844–2852.
- Susuki K, Yokose T, Yoshida J, et al. Prognostic significance of the size of central fibrosis in peripheral adenocarcinoma of the lung. *Ann Thorac Surg*. 2000;69:893–897.
- Terasaki H, Niki T, Matsuno Y, et al. Lung adenocarcinoma with mixed bronchiolo-alveolar and invasive components: clinico-pathological features, sub-classification by extent of invasive foci and immunohistochemical characterization. *Am J Surg Pathol*. 2003;27:937–951.
- Yokose T, Susaki K, Nagai K, et al. Favorable and unfavorable morphological prognostic factors in peripheral adenocarcinoma of the lung 3 cm or less in diameter. *Lung Cancer*. 2000;29:197–204.

CHAPTER 38

Large Cell Neuroendocrine Carcinoma

Shanda Blackmon, Philip T. Cagle, Timothy C. Allen, Dina R. Mody, and Armando E. Fraire

In the current 2004 WHO Classification of Lung Tumors, large cell neuroendocrine carcinoma is listed as one of the four variants of large cell carcinoma. The other three are basaloid carcinoma, clear cell carcinoma, and lymphoepithelioma-like carcinoma. In this chapter, we discuss large cell neuroendocrine carcinoma.

Large cell neuroendocrine carcinomas are not common, representing only about 3% of all lung cancers. The majority are located near the periphery of the lung and are not accessible to the bronchoscope. Radiographically, they do not differ from other non-small cell lung cancers and are usually well defined with marked heterogeneous enhancement. Grossly, these tumors present as fleshy masses similar to other non-small cell carcinomas. Microscopically, they show features of neuroendocrine morphology, that is, nesting, palisading, trabeculation, and/or formation of rosette-like structures. Individual cells are larger than two to three times the size of resting lymphocytes, have a high nuclear cytoplasmic ratio and single or multiple nucleoli. They frequently show necrosis, which can be extensive. Mitotic activity in these tumors is high, with counts of 11 mitoses or more per 10 high-power fields being needed for diagnosis. Another requirement for diagnosis is immunoreactivity for at least one neuroendocrine marker, excluding neuron-specific enolase. Cytopathologic preparations such as those from transthoracic FNAs show features of high-grade carcinomas but seldom with architectural or cytopathologic features that would permit the diagnosis.

FIGURE 38.1 CT findings of neuroendocrine carcinoma. This CT shows a large oval-shaped tumor mass without spiculation, on the superior segment of the left lower lobe.

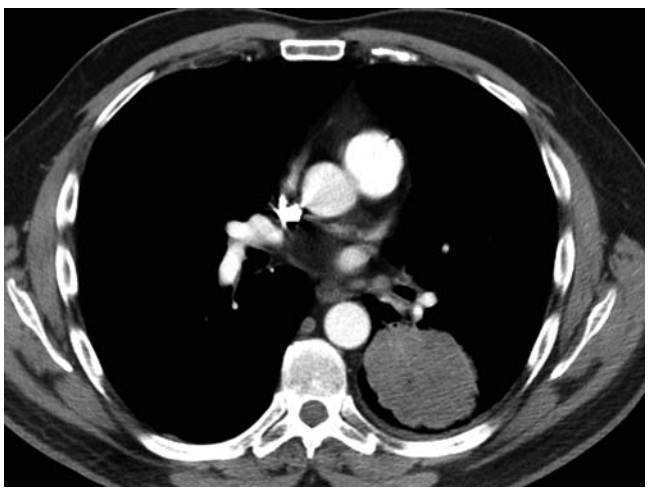

A.E. Fraire et al. (eds.), *Atlas of Neoplastic Pulmonary Disease*,
DOI 10.1007/978-0-387-89839-1_38,

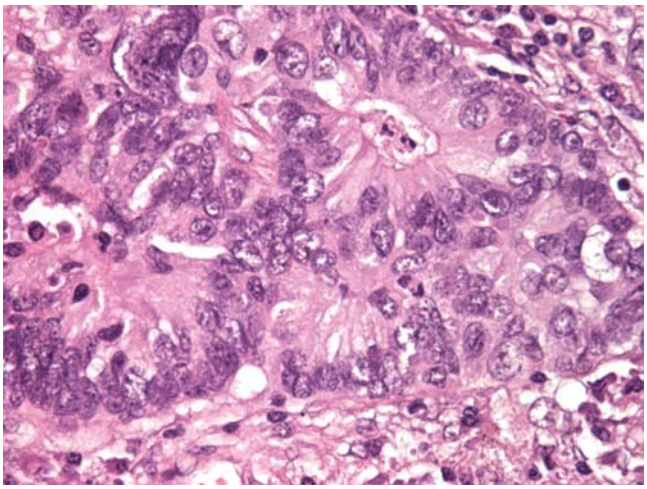

FIGURE 38.2 Large cell neuroendocrine carcinoma. Microscopic view. Nest of tumor cells with abundant cytoplasm, highly atypical nuclei and palisading of the outer rim of cells. Note absence of acinar differentiation, keratinization, or intercellular bridges. Hematoxylin and eosin.

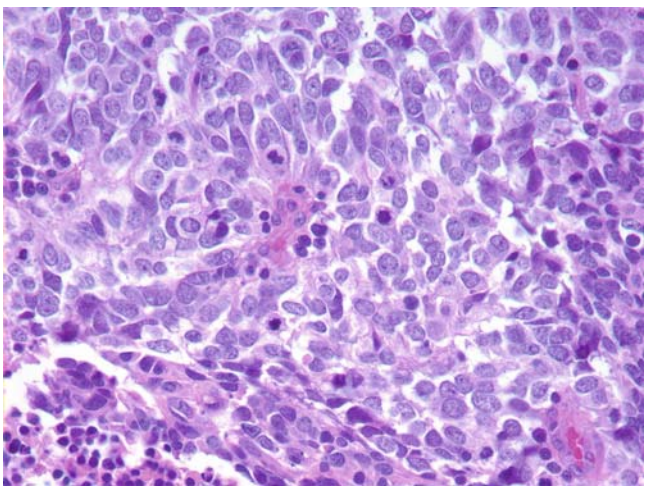

FIGURE 38.3 Histopathology of Large Cell Neuroendocrine Carcinoma, microscopic view. Note large pleomorphic tumor cells. The mitotic rate was brisk. Hematoxylin and eosin.

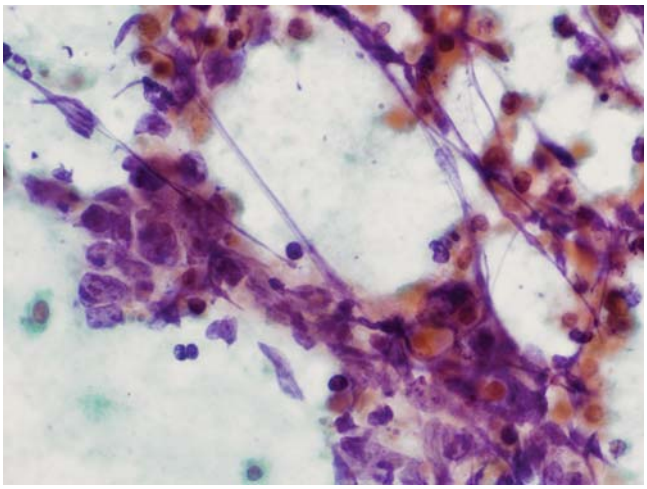

FIGURE 38.4 Cytopathology of large cell neuroendocrine carcinoma. Note similarity of cells to those shown in Fig. 38.3. However, in this preparation, it is not possible to diagnose neuroendocrine differentiation of the tumor cells. Diff Quick stain.

REFERENCES

- Brambilla E, Pugatch B, Geisinger K, et al. Large cell carcinoma. In: Travis WD, Brambilla E, Müller-Hermelink HK, Harris CC, eds. *World Health Organization of Tumours, Pathology and Genetics of Tumours of the Lung, Pleura, Thymus and Heart.* Lyon: IARC Press; 2004:45–52.
- Chong S, Lee KS, Chung MJ, et al. Neuroendocrine tumors of the lung: clinical, pathologic and imaging findings. *Radiographics*. 2006;26:41–57.
- Iyoda A, Hiroshima K, Toyozaki T, et al. Clinical characterization of pulmonary large cell neuroendocrine carcinoma and large cell carcinoma with neuroendocrine morphology. *Cancer*. 2001;91:1992–2000.
- Jung KJ, Lee KS, Han J, et al. Large cell neuroendocrine carcinoma of the lung: clinical, CT, and pathologic findings in 11 patients. *J Thorac Imaging*. 2001;16: 156–162.
- Oshiro Y, Kusumoto M, Matsuno Y, et al. CT findings of surgically resected large cell neuroendocrine carcinoma of the lung in 38 patients. *Am J Roentgenol*. 2004;182:87–91.
- Takei H, Asamura H, Maeshima A, et al. Large cell neuroendocrine carcinoma of the lung: a clinicopathologic study of eighty-seven cases. *J Thorac Cardiovasc Surg*. 2002;124:285–292.

CHAPTER 39

Sarcomatoid Carcinoma

Shanda Blackmon, Armin Ernst, Philip T. Cagle, Timothy C. Allen,
Dina R. Mody, and Armando E. Fraire

Sarcomatoid carcinomas are currently listed separately by the WHO as a distinct category of malignant lung tumors. This group of carcinomas encompass some epithelial pseudo sarcomatous carcinomas as well as tumors with true sarcomatous components such as carcinosarcoma. In this atlas we cover two variants of sarcomatoid carcinoma: Giant Cell Carcinoma and Spindle Cell Carcinoma. Both known to be fast growing, clinically aggressive tumors with a propensity to present in advanced stage and to have a rather poor prognosis. Their radiographic presentation is non specific and their cytopathologic features are not well defined, although identification of large bizarre strap cells in cytologic preparations can be a clue for the diagnosis. The histopathology of giant cell carcinoma is highly distinctive. It is made of highly pleomorphic mono or multinucleated giant cells lacking evidence of any squamous or glandular features. Typically, an important inflammatory component, usually neutrophilic, can be found within these tumors. Active migration of leukocytes into giant cells, a phenomenon known as emperipolesis is another important histopathologic feature of these tumors.

The spindle cell variant is composed of nests and fascicles of spindle shaped tumor cells with a high grade of malignancy and remarkable similarity to true sarcomas of the lung, except that the spindle cells are cytokeratin positive, supporting their epithelial nature. In cytologic preparations bizarre cells with dense hyperchromatic nuclei can be seen.

FIGURE 39.1 Sarcomatoid carcinoma. CT of chest showing large spiculated mass in the right upper lobe. Note extension of spiculations to chest wall.

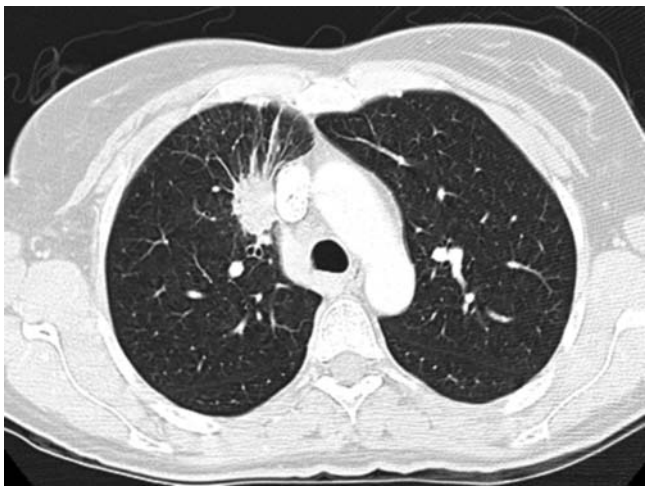

A.E. Fraire et al. (eds.), *Atlas of Neoplastic Pulmonary Disease*,
DOI 10.1007/978-0-387-89839-1_39,

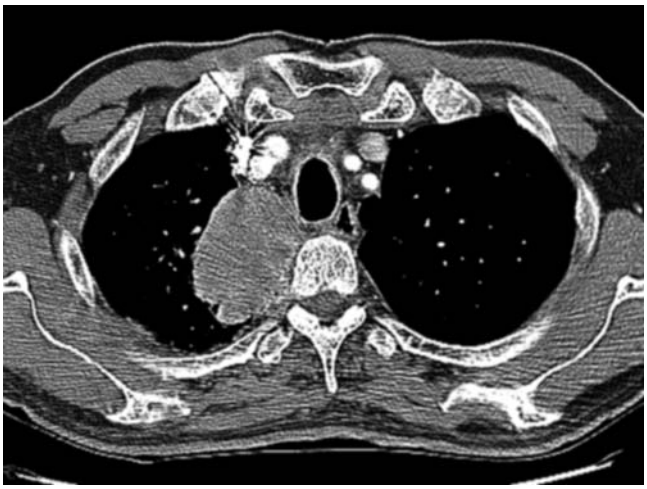

FIGURE 39.2 Sarcomatoid carcinoma. CT of chest showing a large right upper lobe paramediastinal mass, abutting on the adjacent vertebral body and the postero-lateral aspect of the trachea.

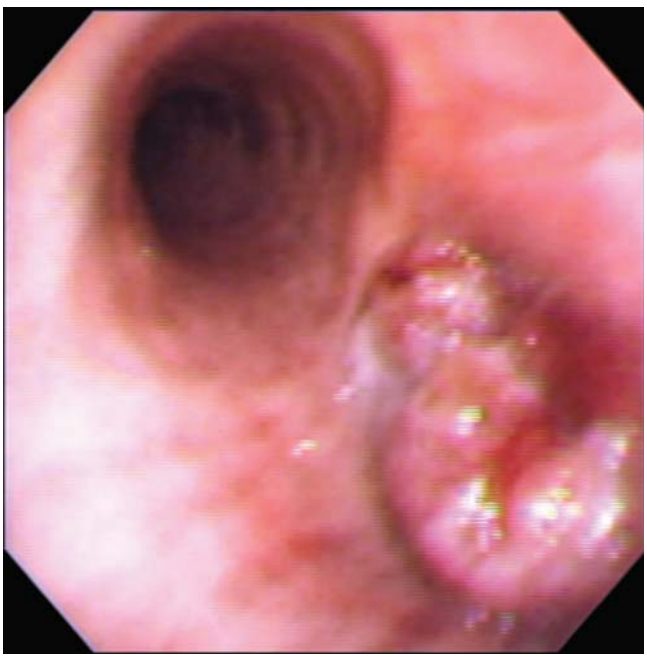

FIGURE 39.3 Sarcomatoid carcinoma. Bronchoscopic image of a fleshy lobulated mass in the right main stem bronchus. The patient was a 55 year old man. A biopsy showed pleomorphic carcinoma.

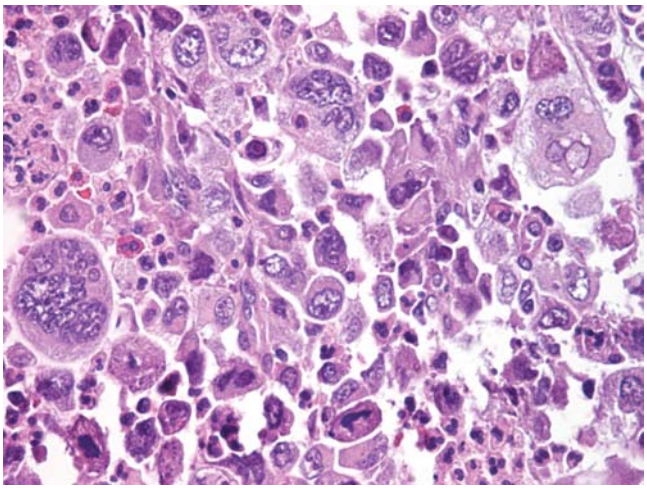

FIGURE 39.4 Sarcomatoid carcinoma. This high-power microscopic view of the giant cell variant of pleomorphic carcinoma shows prominent bizarre giant cells some with emperipolesis. Equally pleomorphic large cells dominate the field. Hematoxylin and eosin.

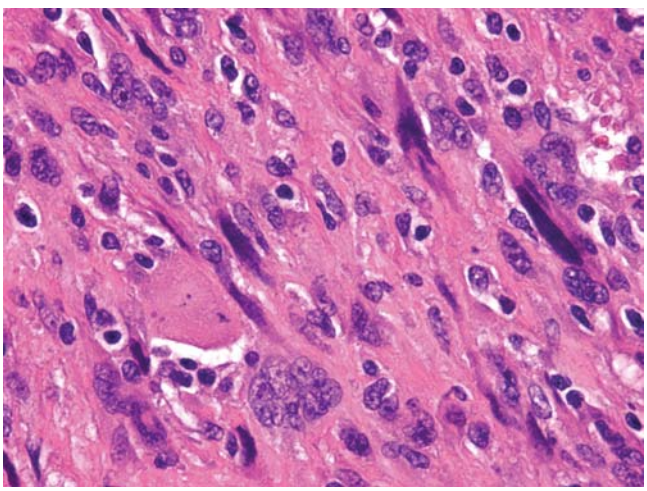

FIGURE 39.5 Sarcomatoid carcinoma. This high-power microscopic view of a spindle (sarcomatoid) cell variant of pleomorphic carcinoma displays large prominent spindle-shaped tumor cells. The background is a fibrous stroma. Hematoxylin and eosin.

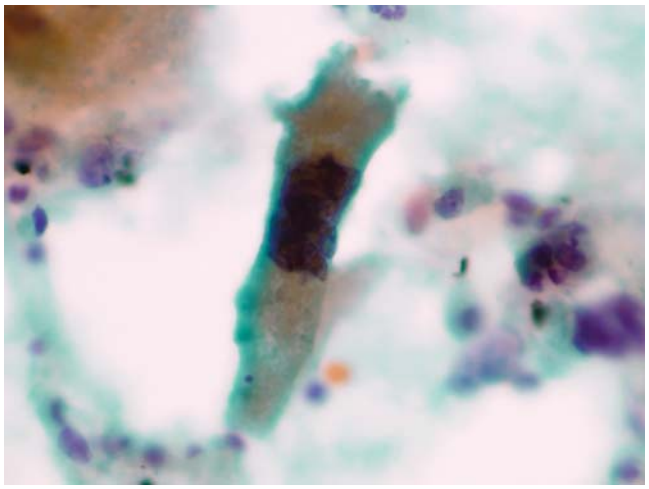

FIGURE 39.6 Sarcomatoid carcinoma. This bronchial wash cytopathologic preparation shows a very large bizarre strap cell with a square "lump of coal" nucleous. White blood cells are in the background. Papanicolaou stain.

REFERENCES

- Dacic S, Finkelstein SD, Sasatomi E, et al. Molecular pathogenesis of pulmonary carcinosarcoma as determined by microdissection-based allelotyping. *Am J Surg Pathol*. 2002;26:510–516.
- Holst VA, Finkelstein S, Colby TV, et al. P53 and K-ras mutational genotyping in pulmonary carcinosarcoma, spindle cell carcinoma, and pulmonary blastoma: Implications for histogenesis. *Am J Surg Pathol*. 1997;21:801–811.
- Koss MN, Hochholzer L, Frommelt RA. Carcino sarcomas of the lung – A clinicopathologic study of 66 patients. *Am J Surg Pathol*. 1999;23:1514–1526.
- Nash AD, Stout AP. Giant cell carcinoma of the lung. Report of 5 cases. *Cancer*. 1958;11:369–376.
- Pelosi G, Fraggetta F, Nappi O, et al. Pleomorphic carcinomas of the lung show a selective distribution of gene products involved in cell differentiation, cell cycle control, tumor growth, and tumor cell motility- A clinicopathologic and immunohistochemical study of 31 cases. *Am J Surg Pathol*. 2003;27:1203–1215.
- Rossi G, Cavazza A, Sturm N, et al. Pulmonary carcinomas with pleomorphic, sarcomatoid, or sarcomatous elements – A clinicopathologic and immunohistochemical study of 75 cases. *Am J Surg Pathol*. 2003;27:311–324.
- Wang N-S, Seemayer TA, Ahmed MN, Knaack J. Giant cell carcinoma of the lung. A light and electron microscopic study. *Hum Pathol*. 1976;7:3–16.
- Wick MR, Ritter JH, Humphrey PA. Sarcomatoid carcinomas of the lung: A clinicopathologic review. *Am J Clin Pathol*. 1997;108:40–53.

CHAPTER 40

Pulmonary Blastoma

Shanda Blackmon, Philip T. Cagle, Timothy C. Allen, Dina R. Mody, and Armando E. Fraire

A rare malignant tumor of the lung, pulmonary blastoma refers to peripherally located tumors of adult patients, variably composed of primitive ("fetal") adenocarcinomatous components, with or without an associated sarcomatoid component. This primitive fetal component recapitulates a phase in the embryonic development of the lung and this is the reason for this tumor being referred to as a blastoma, in a manner similar to the blastomas of the kidney and other anatomical sites. There is also a remarkable similarity of this primitive epithelium to secretory endometrium justifying the name "endometrioid" for these tumors. This tumor needs to be differentiated from pleuropulmonary blastoma of childhood, which is discussed elsewhere in this atlas, in the section of tumors of childhood.

Pulmonary blastomas of the adult are apt to achieve a large size and present radiographically as tumor masses nearly filling an entire hemithorax. The endoscopic and cytopathologic features of pulmonary blastomas have not been well characterized. In a cytologic preparation from our files, the tumor cells assumed a polygonal configuration showing angulated nuclei and abundant cytoplasm.

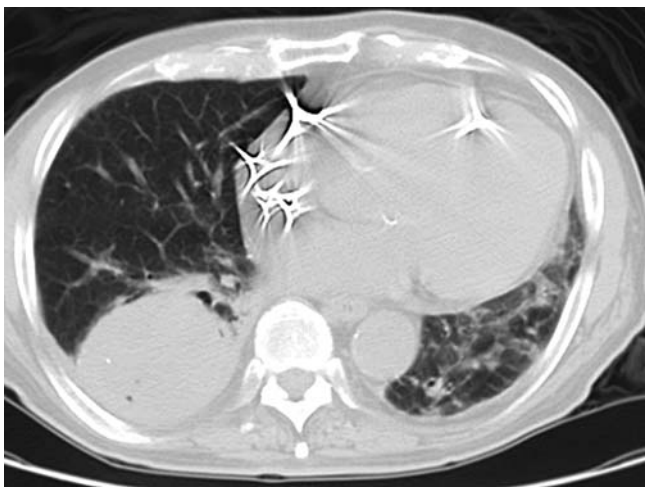

FIGURE 40.1 CT of chest. This rather large pulmonary blastoma occupies the superior segment of the right upper lobe in a patient with a pacemaker. Large size is a major feature of pulmonary blastomas.

A.E. Fraire et al. (eds.), *Atlas of Neoplastic Pulmonary Disease*,
DOI 10.1007/978-0-387-89839-1_40, © Springer Science+Business Media, LLC 2010

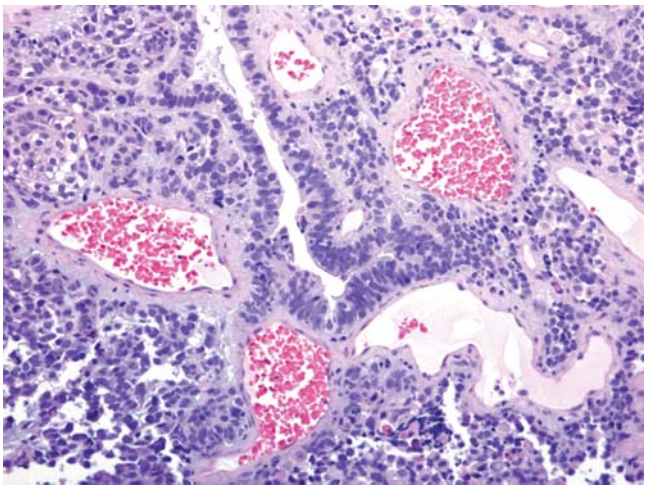

FIGURE 40.2 This high-power view of the histopathology of a pulmonary blastoma shows fetal type glands with an associated poorly differentiated sarcomatous component. Hematoxylin and eosin.

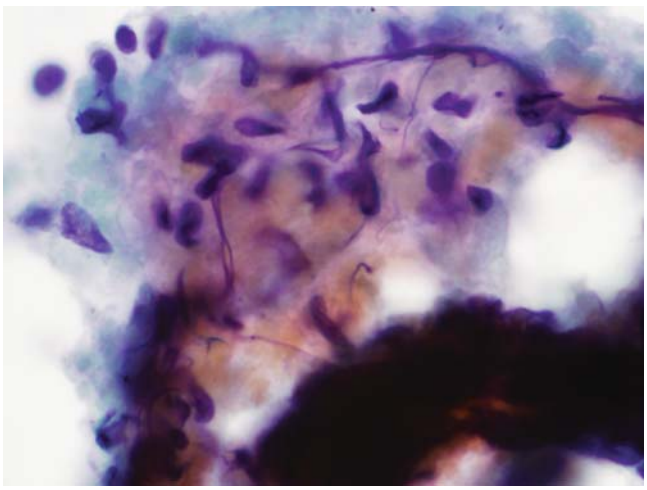

FIGURE 40.3 This cytopathologic preparation of a biphasic pulmonary blastoma shows large polygonally shaped atypical cells with dark angulated nuclei and abundant basophilic cytoplasm. Papanicolaou stain.

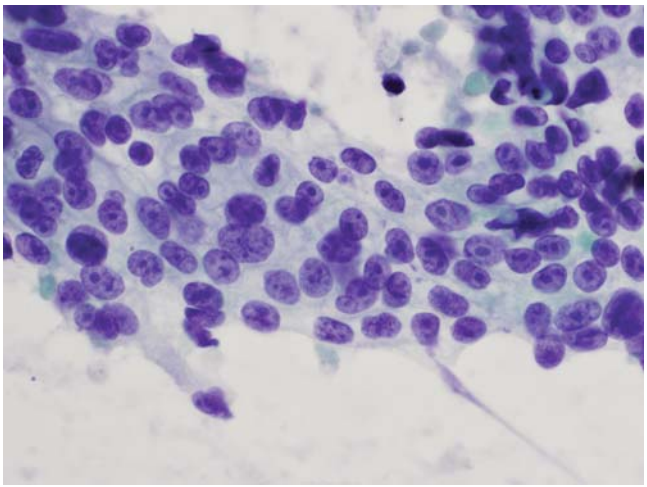

FIGURE 40.4 This additional cytopathologic view of the neoplasm shown in Fig. 40.3 shows more uniform epithelial cells arranged in sheets. Note focal nuclear crowding and overlapping. Papanicolaou stain.

REFERENCES

- Cohen M, Emms M, Kaschula ROC. Childhood pulmonary blastoma. A pleuropulmonary variant of the adult type pulmonary blastoma. *Pediatr Pathol.* 1991;11:382–391.
- Koss M, Hochholzer L, O'Leary T. Pulmonary blastomas. *Cancer.* 1991;67:2368–2381.
- Nakatani Y, Kitamura H, Inayama Y, et al. Pulmonary endodermal tumor resembling fetal lung. The optically clear nuclei is rich in biotin. *Am J Surg Pathol.* 1994;18:637–642.

CHAPTER 41

Metastatic Tumors

Shanda Blackmon, Armin Ernst, Dina R. Mody, and Armando E. Fraire

Metastatic tumors to the lung are extremely common. In fact, the lung ranks number one in terms of organs harboring metastatic diseases. Lung involvement in some autopsy series cite pulmonary involvement in up to 54% of the cases. Factors accounting for the high number of metastasis to the lungs include their rich capillary network and possibly a favorable "seed and soil" disposition inherent to pulmonary tissues. In relative order of frequency, metastatic tumors to the lung originate from carcinomas in the breast, colon, stomach, pancreas, kidney, prostate, liver, thyroid, adrenal, male genital tract, and the female genital tract. Sarcomas from bone, soft tissue, and visceral sites are prone to disseminate via the blood stream and frequently metastasize to the lungs. Melanomas also spread to lungs but not frequently. Rarely, a primary lung tumor will spread to involve both lungs closely mimicking metastatic disease. Despite extensive work up, some metastatic carcinomas can not be classified in regards to their site of origin. This occurs in a minority of cases.

Pulmonary metastasis can be parenchymal or endobronchial, solitary or multiple. The most common radiographic presentation is that of multiple well-defined nodules with or without cavitation. Very large metastatic tumors to the lung known as "cannon ball" metastasis can occur in a variety of setting, particularly in tumors from the kidneys. Endobronchial metastasis can be visualized via flexible bronchoscope but may be difficult to distinguish from primary tumors, unless sufficient evidence of previous malignancy is available for consideration in the differential diagnosis. Cytopathologic features of metastatic tumors closely resemble features seen in the primary tumors, for example, thyroid follicles in carcinomas from the thyroid or glandular structures with dirty necrosis, in tumors from the colon.

FIGURE 41.1 CT of chest showing a mass lesion, about 2.8 cm just anterior to the right lower lobe. Histopathology showed a tumor consistent with a colonic primary.

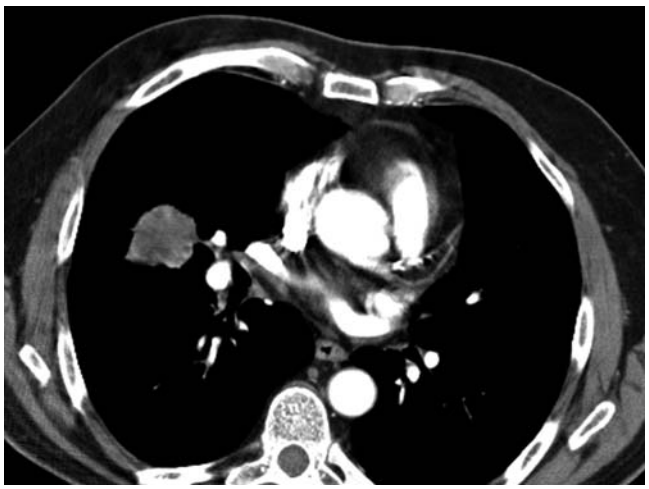

FIGURE 41.2 CT of chest. Note nodular density in right middle lobe. A biopsy showed metastatic renal cell carcinoma.

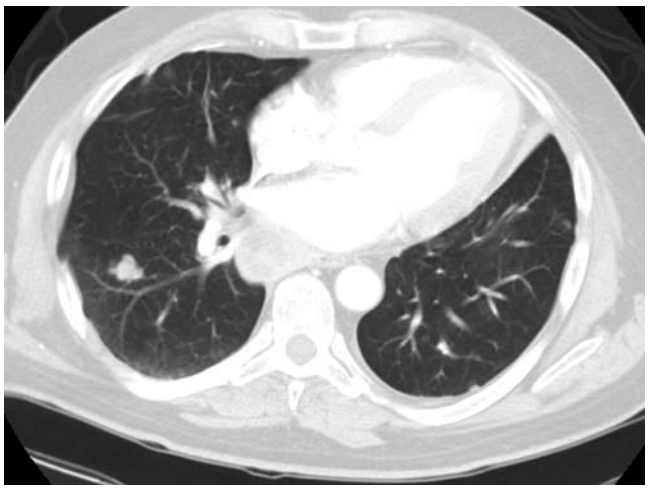

A.E. Fraire et al. (eds.), *Atlas of Neoplastic Pulmonary Disease*,
DOI 10.1007/978-0-387-89839-1_41,

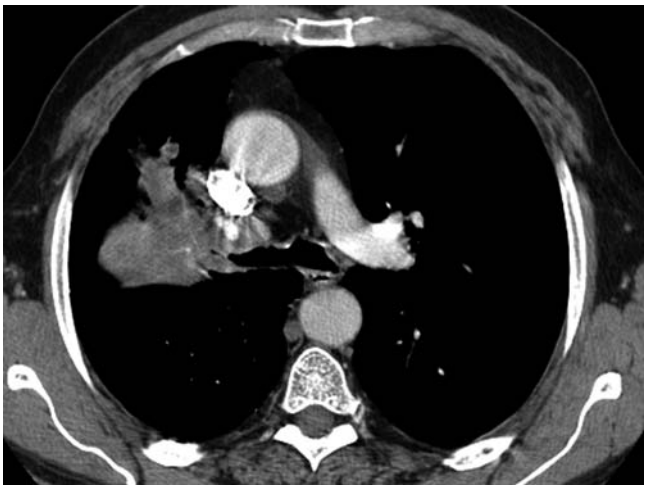

FIGURE 41.3 CT of chest showing large irregularly shaped mass lesion in the hilar area of the right upper lobe. Biopsy showed a metastatic salivary gland tumor.

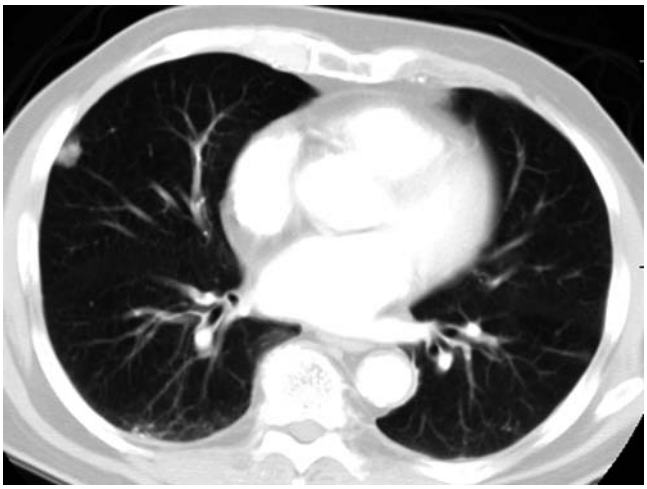

FIGURE 41.4 CT of chest showing a small subpleural density in the right middle lobe with a rounded outside border. Histopathology showed a metastatic malignant melanoma.

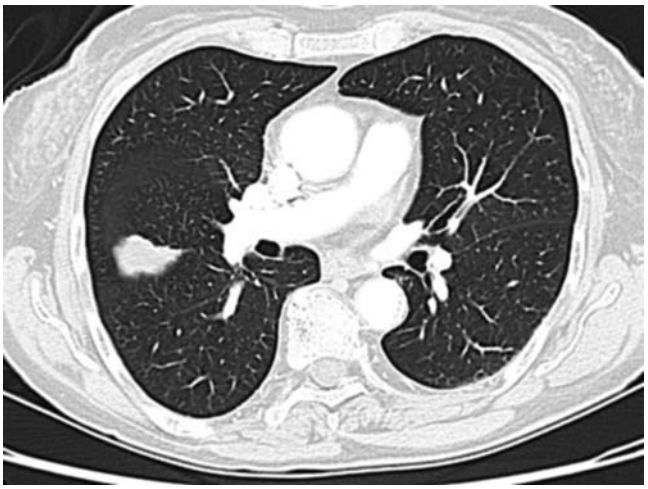

FIGURE 41.5 CT of chest showing a well-defined irregular density in the right middle lobe. Biopsy showed a metastatic leiomyosarcoma.

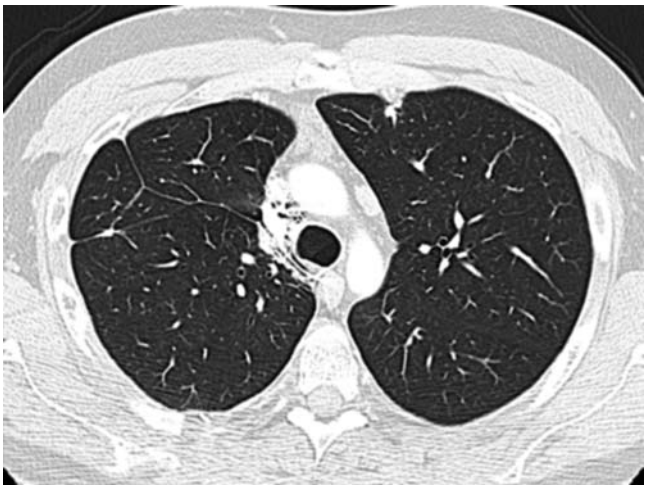

FIGURE 41.6 CT of chest showing a small pleural-based opacity in the left upper lobe. Biopsy showed a metastatic osteosarcoma.

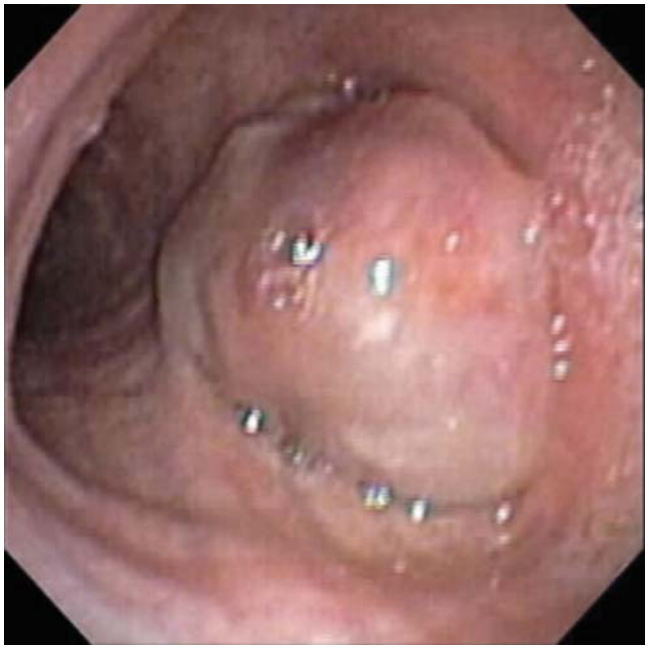

FIGURE 41.7 Bronchoscopic image of the right main stem bronchus of a 72-year-old male. Previously a chest radiograph obtained for shortness of breath had shown complete right lung atelectasis. A biopsy showed evidence of metastatic carcinoma of unknown origin.

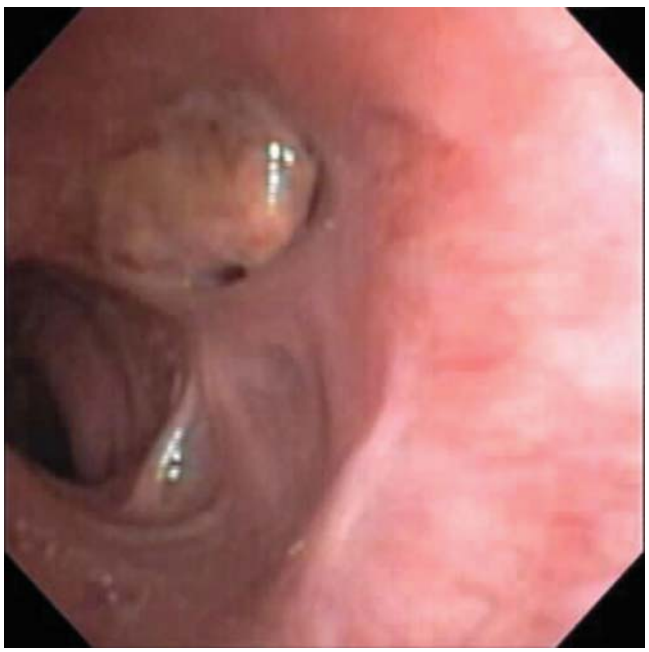

FIGURE 41.8 Bronchoscopic image of a lesion in the right lower lobe bronchus of a 79-year-old female. A chest radiograph showed segmental atelectasis. Biopsy could not elucidate the origin and the tumor was classified as metastatic carcinoma of unknown origin.

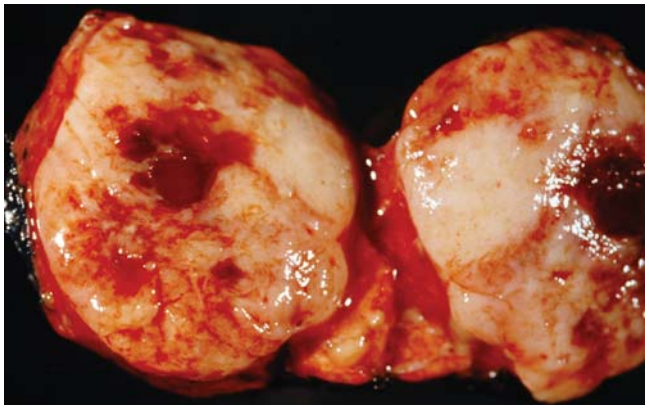

FIGURE 41.9 This metastatic renal cell carcinoma shows a gray white substance, focal hemorrhages, and well-defined borders (Courtesy of Dr. Eugene Mark, Massachusetts General Hospital, Boston, MA).

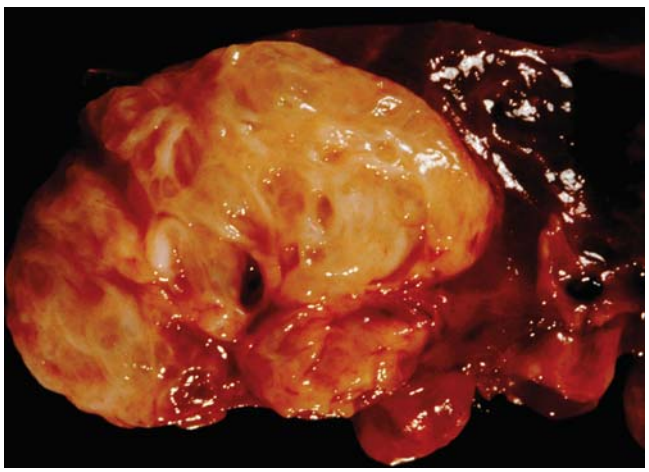

FIGURE 41.10 This metastatic germ cell tumor is made up of yellow tan substance. Hemorrhagic lung tissue is on the right (Courtesy of Dr. Eugene Mark, Massachusetts General Hospital, Boston, MA).

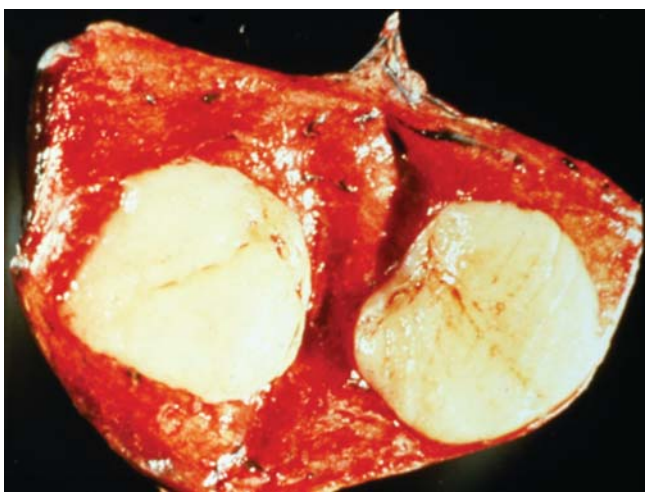

FIGURE 41.11 This mixed tumor of salivary gland metastatic to lung shows features similar to those found in primary tumors, namely well-defined borders and firm consistency (Courtesy of Dr. Eugene Mark, Massachusetts General Hospital, Boston, MA).

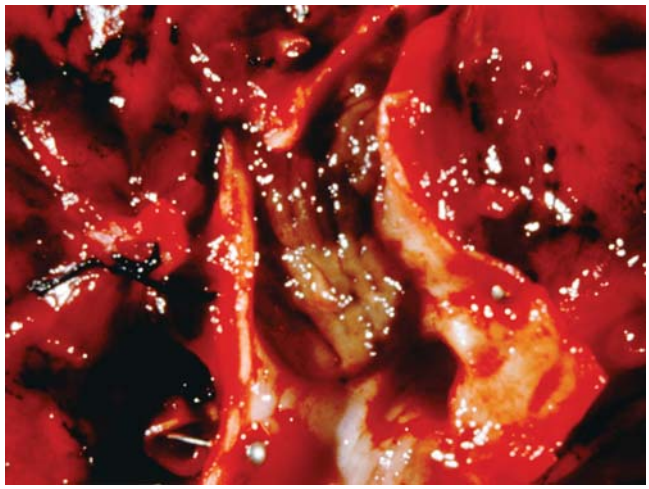

FIGURE 41.12 Endobronchial metastases from a melanoma. Note elongated tumor mass nearly occluding the airway lumen (Courtesy of Dr. Eugene Mark, Massachusetts General Hospital, Boston, MA).

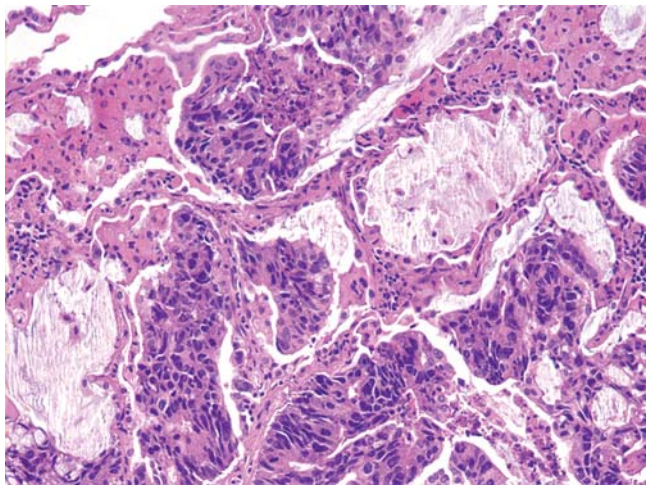

FIGURE 41.13 Metastatic carcinoma from colon; note dense groups of tumor cells with compressed lumina and pools of mucin. Hematoxylin and eosin.

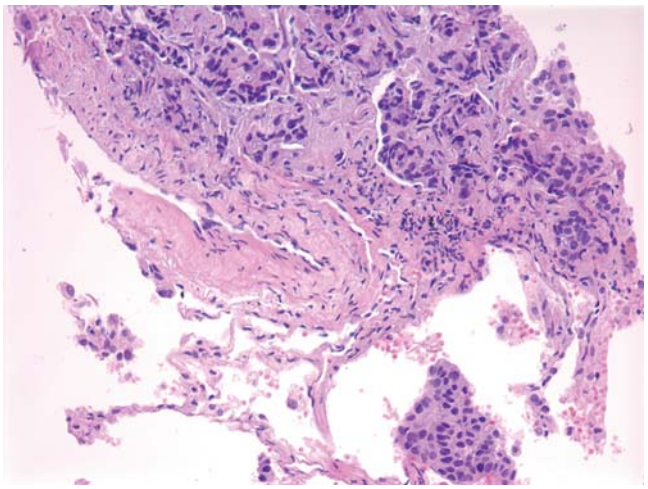

FIGURE 41.14 Transthoracic needle core biopsy showing metastatic carcinoma from breast. Note small nodular aggregates of tumor cells suggestive of a mammary origin. Hematoxylin and eosin.

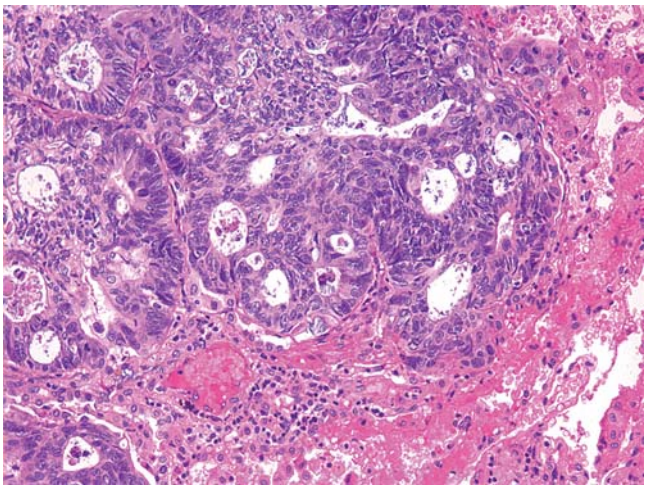

FIGURE 41.15 Metastatic carcinoma from colon. In contrast to the tumor shown in a preceding Figure, this tumor shows multiple widely open glandular lumina and no mucin pools. Hematoxylin and eosin.

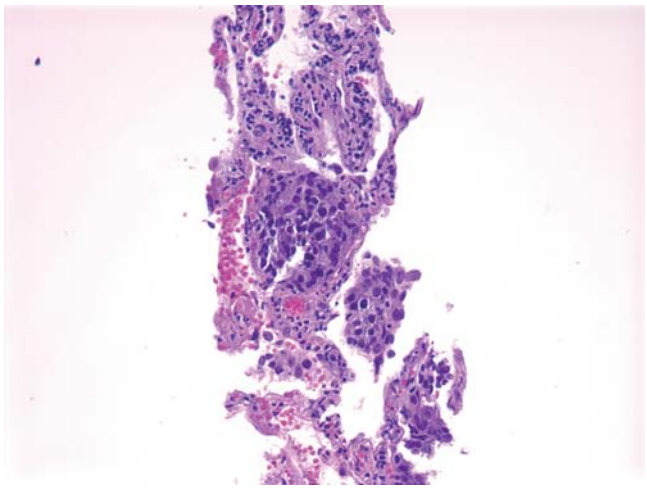

FIGURE 41.16 Poorly differentiated carcinoma metastatic to lung in a transthoracic needle core biopsy. The microscopic tumor morphology and immunostaining with a wide panel of markers did not help to identify the origin of this tumor. Hematoxylin and eosin.

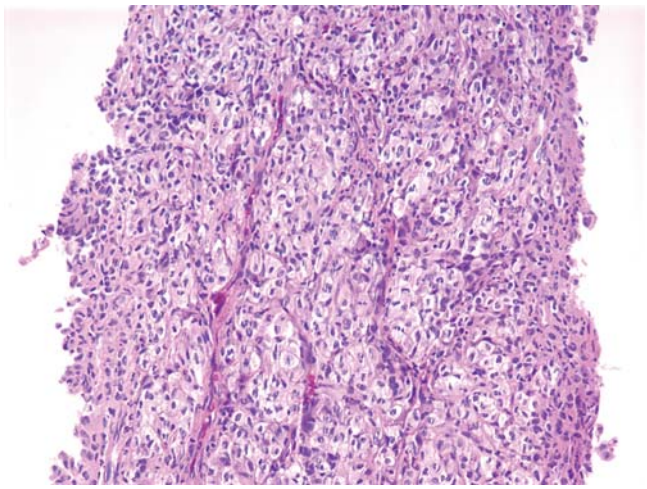

FIGURE 41.18 Metastatic renal cell carcinoma. Note nesting pattern and some cells showing cytoplasmic clearing. Hematoxylin and eosin.

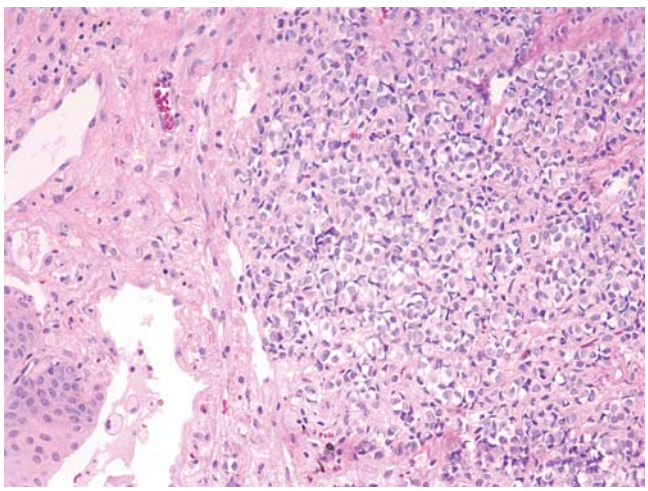

FIGURE 41.17 Metastatic carcinoma from breast. Tumor is on the right side, fibrosed tissue on the left. Hematoxylin and eosin.

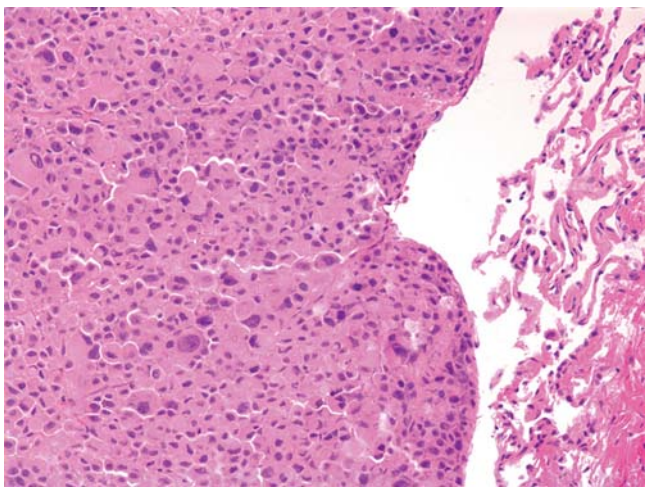

FIGURE 41.19 Metastatic melanoma to the lung. Tumor is on mid-center and left side of image. Note large cells with ample eosinophilic cytoplasm. Hematoxylin and eosin.

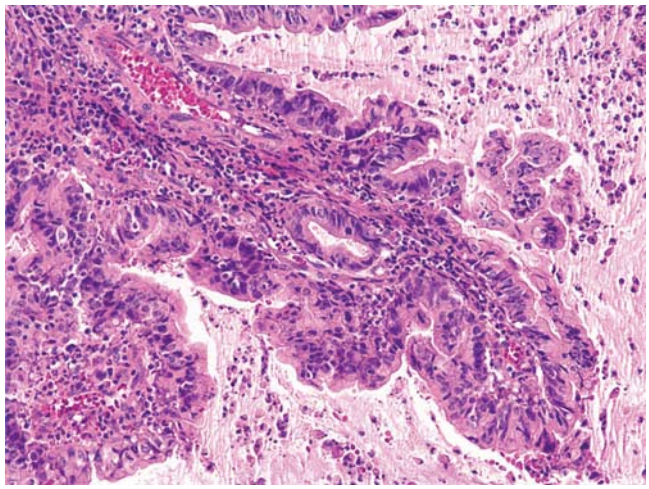

FIGURE 41.20 This cholangiocarcinoma metastatic to lung shows large spaces lined by tall columnar hyperchromatic cells. The adjacent connective tissue stroma is inflamed. Hematoxylin and eosin.

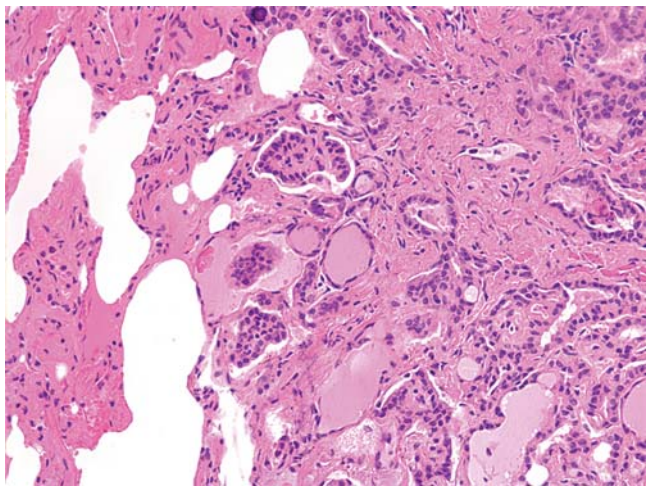

FIGURE 41.21 Metastatic follicular carcinoma from thyroid. Note recapitulation of thyroid follicular pattern in a fibrotic stroma. Hematoxylin and eosin.

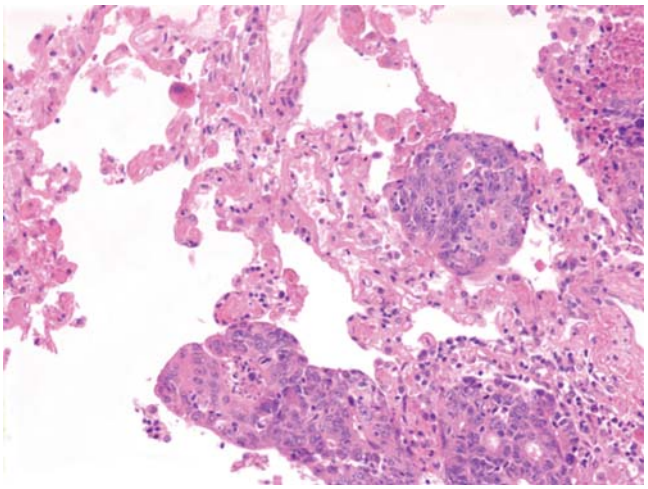

FIGURE 41.22 Another metastatic colonic carcinoma of lung. In this case, tumor is represented by at least three small ball-like aggregates of epithelial cells, some with open lumina. Hematoxylin and eosin.

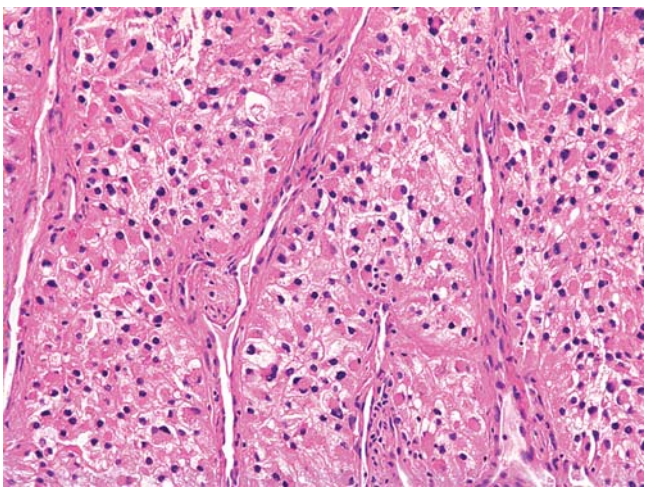

FIGURE 41.23 This is a metastatic carcinoma from the kidney. Note cells with abundant eosinophilic or clear cytoplasm corresponding to a renal cell carcinoma with oncocytic features. Hematoxylin and eosin.

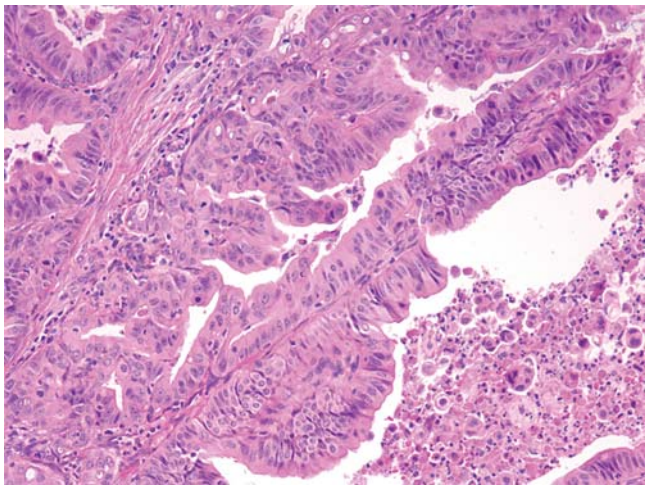

FIGURE 41.24 This metastatic carcinoma originated in the endometrium. Note papillary fronds with long, thin, and delicate fibrovascular cores. Hematoxylin and eosin.

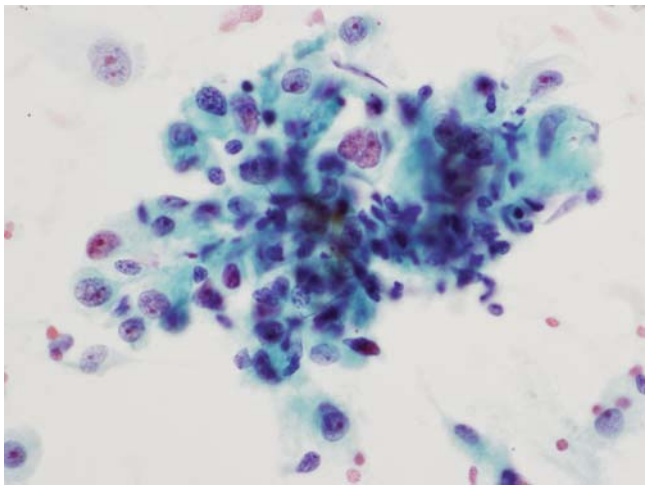

FIGURE 41.26 Cytopathologic preparation of metastatic renal cell carcinoma to the lung. Note rare larger cells with prominent nucleoli. Papanicolaou stain.

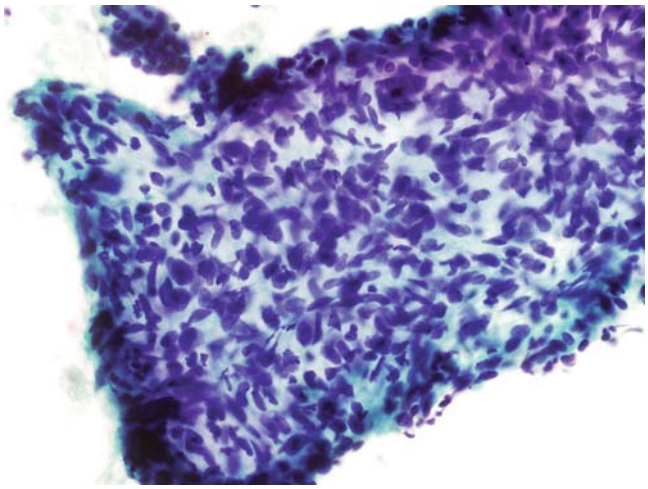

FIGURE 41.25 Cytopathologic preparation of a malignant fibrous histiocytoma metastatic to the lung. Note hypercellular cluster of cells with predominant spindle cell morphology. Papanicolaou stain.

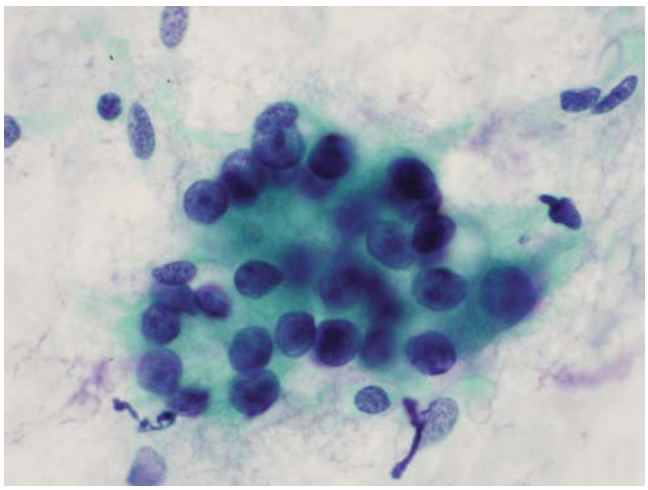

FIGURE 41.27 Cytopathologic preparation of a metastatic adenocarcinoma from the prostate. Note abortive glands and rare cells with prominent nucleoli. Papanicolaou stain.

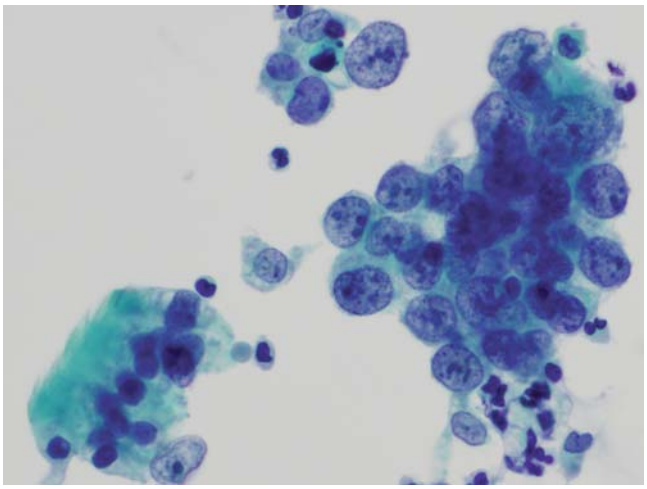

FIGURE 41.28 Cytopathologic preparation of adenocarcinoma from the parotid gland. Note epithelial phenotype of tumor cells and variation in cell size. A group of normal-looking ciliated bronchial epithelial cells is present in the left lower corner. Papanicolaou stain.

REFERENCES

- Askin FB. Something old? something new? Second primary or pulmonary metastasis in the patient with known extrathoracic carcinoma. *Am J Clin Pathol*. 1993;100:4–5.
- Bourke SJ, Henderson AF, Stevenson RD, et al. Endobronchial metastases simulating primary carcinoma of the lung. *Respir Med*. 1989;83: 151–152.
- Dail DH, Cagle PT, Marchevsky AM, Khoor A, Geisinger K. Metastases to the lung. In: Travis WD, Brambilla E, Müller-Hermelink HK, Harris CC, eds. *World Health Organization Classification of Tumours. Pathology and Genetics of Tumours of the Lung, Pleura, Thymus and Heart*. Lyon: IARC Press; 2004: 122–124.
- Dodd LG, Chai C, McAdams P, et al. Fine needle aspiration of osteogenic sarcoma metastatic to the lung. Report of four cases. *Acta Cytol*. 1998;42:754–758.
- Flint A, Lloyd RV. Colon carcinoma metastatic the lung: cytologic manifestations and distinction from primary pulmonary adenocarcinoma. *Acta Cytol*. 1992;36:230–235.
- Kerr VE, Cadman E. Pulmonary metastases in ovarian cancer. *Cancer*. 1985;56:770–776.
- Khaddami M. Cytologic diagnosis of metastatic malignant melanoma of the lung in sputum and bronchial washings. A case report. *Acta Cytol*. 1993;37: 403–408.
- Kini SR. Ch. 14. Thyroid carcinoma metastatic to other body sites. In: Kline TS, ed. *Thyroid, Guides to Clinical Aspiration Biopsy*. 2nd ed. New York: Igaku Shoin; 1996.
- Kumar J, Hancheran A, Ratnam SS. Pulmonary metastases in gestational trophoblastic disease. A review of 97 cases. *Br J Obstet Gynecol*. 1988;95:70–74.
- Levy H, Horak DA, Lewis MI. The value of bronchial washings and bronchoalveolar lavage in the diagnosis of lymphangitic carcinomatosis. *Chest*. 1985;87: 129–131.
- Lozowski MS, Mishriki Y, Epstein H. Metastatic malignant fibrous histiocytoma in lung examined by fine needle aspiration: case report and literature review. *Acta Cytol*. 1980;24:350–354.
- Kini SR, ed. *Color Atlas of Pulmonary Cytopathology*. New York, Berlin, Heidelberg: Springer Verlag; 2002:151–164.
- Rabb SS, Berg LC, Swanson PE, et al. Adenocarcinoma in the lung in patients with breast cancer, a prospective analysis of the discriminatory value of immunohistology. *Am J Clin Pathol*. 1993;100:27–35.
- Saleh HA, Masood S, Wynn G, et al. Unsuspected metastatic renal cell carcinoma diagnosed by fine needle aspiration biopsy. A report of four cases with immunocytochemical contributions. *Acta Cytol*. 1994;38:551–561.
- Veratraeten A, Saule MC, Wallaert B, et al. Metastatic prostatic adenocarcinoma diagnosed by bronchoalveolar lavage and tumor marker determination. *Eur Respir J*. 1991;4:1296–1298.
- Whitesell PL, Peters SG. Pulmonary manifestations of extrathoracic malignant lesions. *Mayo Clin Proc*. 1993;68:485–491.
- Zimmerman RI, Bibbo M. Fine needle aspiration diagnosis of a pulmonary metastasis from a cutaneous adenoid cystic carcinoma. A case report. *Acta Cytol*. 1998;42:367–370.

Subject Index

Note: The letter 'f' following the locators refer to figures in the text.

A.E. Fraire et al. (eds.), *Atlas of Neoplastic Pulmonary Disease*,
DOI 10.1007/978-0-387-89839-1,